University of Leicester

# Pharmacological Characterisation of Recombinant Vanilloid Receptors

**Patricia May Wah Lam**

**University Department of Cardiovascular Sciences**
**(Pharmacology and Therapeutics Group)**
**University of Leicester**

**Thesis Submitted for the Degree of Doctor of Philosophy**

**September 2005**





ProQuest LLC
789 East Eisenhower Parkway
P.O. Box 1346
Ann Arbor, MI 48106-1346

# Pharmacological characterisation of recombinant vanilloid receptors

Patricia May Wah Lam

TRPV1 is a non-selective, $Ca^{2+}$-permeable, ligand gated ion channel involved in pain transmission. TRPV1 is activated by capsaicin, noxious heat (~43°C), protons and more controversially by endocannabinoids. This thesis presents (1) a detailed pharmacological characterisation of human and rat TRPV1 expressed in non-neuronal cells (2) an assessment of endo- and exocannabinoid activity at these receptors and (3) the establishment and characterisation of the first neuronal TRPV1 expression system.

In HEK cells expressing human and rat isoforms of TRPV1, capsaicin, anandamide (an endocannabinoid), olvanil (a structural analogue of capsaicin) and ethanol displayed TRPV1 activity. In contrast, $\Delta^9$-THC (an exocannabinoid) did not. No significant difference occurred between human and rat with respect to capsaicin and anandamide activity at 22°C or 37°C. Anandamide displayed partial agonism relative to capsaicin at both temperatures at rat only. Anandamide was also an agonist at cannabinoid $CB_1$ receptors. Capsazepine, a competitive TRPV1 antagonist, inhibited capsaicin, olvanil and anandamide responses; was not temperature-dependent but displayed a 6-fold higher potency at human TRPV1.

The first neuronal model to express recombinant human TRPV1 was produced by sub-cloning and transfection into the neuroblastoma SH-SY5Y cell-line, a more physiologically relevant system. Pharmacological characterisation confirmed expression of TRPV1 with comparable pharmacology to non-neuronal models in this thesis. For example, capsaicin $pEC_{50}$/capsazepine $pK_B$ in HEK (human TRPV1) and SH-SY5Y were 6.77/6.75 and 6.63/7.44 respectively. In SH-SY5Y cells, the agonist resiniferatoxin displayed the highest potency ($pEC_{50}$ 9.03). Iodo-RTX, an antagonist, revealed a higher affinity than capsazepine. Capsaicin-mediated increases in intracellular calcium ($pEC_{50}$ 6.63) in SH-SY5Y cells were sufficient to sustain [$^3$H]noradrenaline release ($pEC_{50}$ 9.21). In a perfusion system, it was shown that the two events were temporally linked.

Overall, these findings have:

1. expanded current knowledge of TRPV1 pharmacology
2. established a neuronal model for further studies, especially TRPV1 desensitisation

## Acknowledgements

Well, where do I begin to thank people during my PhD? First and foremost is Dave Lambert, my excellent and humourous supervisor and a scientist whom I very much admire. He gave me an opportunity, which I originally thought I'd never survive but has since been such a rompiballe!

I'd like to thank Darren Smart for his supervision and advice and also Shaun McNulty's support. I'm also very grateful to Graham Smith and Davina Owen for technical support at GlaxoSmithKline. Also, I'd like to acknowledge Prof Tobin and John McDonald, from CPP, for technical support and advice during my cloning work. I am also grateful to the British Journal of Anaesthesia for funding my project and GlaxoSmithKline for material costs.

Thankyou to everyone, past and present in the Department of Anaesthesia for your support, in particular Prof Rowbotham, Dr Thompson, Christine, Nicola, Ed (see you in HK?), Paulie, TimXL (worlds best tea-boy), Chris (Manamana!), Lynn, Wei, Jim (thankyou for lunchtime treats), Masato, Massimo, Elena, Jack, John1 (remember, to thine own self be true), John2, Mie, Kat, Fariha, Emer, James and anyone else I've missed off my list.

Also, thanks to Emmy who set forth the wheel in motion. She recommended me as a PhD candidate but also mentioned that I was a "minx" to my colleagues, which was met with much confusion and intrigue.

Time spent during my PhD was definitely an international affair and I'd like to extend my gratitude to Tiago, Gaby, Dolores, Cristina, Elena, Roberto, JP and anyone else I've forgotten to include. I will always look back fondly on the carnival parties, football and all the fun and shenanigans we had.

A massive thanks to the following who kept me typing and for being great buddies: Splata (see you in Splott), Jasmin/Frodo (rock on!), Sara, Nik the Bubble (see you in Cyprus), Phuong, Si, DJ Rob F (Medici music maestro) as well as Gillian, Ray and Beryl from LOROS. Thanks also to Jo (Radio 1) for the live lounge sessions, Beethoven, Aretha Franklin, Jeff Buckley (RIP), Marios (great late-night curries albeit bad service), Orange Tree/O Bar (cocktails galore), big sis' M and little bro' Mickey for keeping my spirits high. I can't forget my considerate, understanding housemates – Shantaz and Kaj (and Dev) for putting up with me working odd hours and my thesis fatigue syndrome. Thanks!

Last but not least, I am forever indebted to my wonderful, loving parents who strived so hard to give me the chance to shine.

*Knowing is not enough; we must apply.*

*Willing is not enough; we must do.*

Goethe

## TABLE OF CONTENTS

## List of Figures

## List of Tables

## List of Abbrevations

| | |
|---|---|
| AMT | Anandamide membrane transporter |
| ASIC | Acid-sensitive ion channel |
| BSA | Bovine serum albumin |
| $CB_1$ | Cannabinoid receptor type 1 |
| CHO | Chinese hamster ovary |
| CGRP | Calcitonin gene-related peptide |
| CLSM | Confocal laser scanning microscopy |
| CNS | Central nervous system |
| DAG | Diacylglycerol |
| DMSO | Dimethylsulphoxide |
| DRG | Dorsal root ganglion |
| DTT | Dithiothreitol |
| $EC_{50}$ | Effective concentration producing a half-maximal response |
| $EC_{80}$ | Effective concentration producing 80% of the maximal response |
| EDTA | Ethylenediaminetetraacetic acid |
| EGTA | Ethylene glycol bis(2-aminoethyl ether)-N,N,N'N'-tetraacetic acid |
| FAAH | Fatty acid amide hydrolase |
| FLIPR | Fluorometric imaging plate reader |
| Fluo-3AM | Fluo-3 acetoxymethyl ester |
| Fura-2AM | Fura-2 acetoxymethyl ester |
| GDP | Guanosine diphosphate |
| GTP | Guanosine triphosphate |
| HEK | Human embryonic kidney |
| HEPES | N-(2-Hydroxyethyl)piperazine-N'-(2-ethanesulphonic acid) |
| IASP | International Association for the Study of Pain |
| $K_B$ | Equilibrium dissociation constant of a competitive reversible antagonist |
| $K_i$ | Inhibition constant of a drug |
| NA | Noradrenaline |
| NADA | N-arachidonoyl-dopamine |
| NO | Nitric oxide |
| NRM | Nucleus raphe magnus |
| NRPG | Nucleus reticularis paragigantocellularis |
| NSAID | Nonsteroidal anti-inflammatory drug |
| NSB | Non-specific binding |
| PAG | Periaqueductal grey |
| PKA | Protein kinase A |
| PKC | Protein kinase C |
| PNS | Peripheral nervous system |
| PUFA | Polyunsaturated fatty acid |
| RTX | Resiniferatoxin |
| SG | Substantia gelatinosa |
| $\Delta^9$-THC | $\Delta^9$-Tetrahydrocannabinol |
| TRP | Transient receptor potential channel |
| TRPV1 | Vanilloid receptor subtype 1 |
| VSCC | Voltage-sensitive calcium channel |

# 1 INTRODUCTION

Pain is a universal experience and a disabling accompaniment of many clinical conditions such that pain control is one of the most important applications in therapeutics. Recent cloning and subsequent investigation of the vanilloid receptor (TRPV1) has revealed that it is a "molecular integrator" of noxious stimuli and a promising candidate in analgesic research and development (Cortright *et al.*, 2004).

## 1.1 The Physiology of Pain

The International Association for the Study of Pain (IASP) defined pain as "an unpleasant sensory and emotional experience associated with actual or potential tissue damage, or described in terms of such damage" (Merskey, 1986). This definition highlights the duality of pain as a physiological and psychological experience. In other words, pain is a physiological event that is dependent upon subjective recognition, in that, without psychological awareness, pain cannot exist. Pain is generally considered as a warning signal of actual or perceived tissue damage, which nevertheless, can occur in the absence of tissue damage, even though the experience may be described as if the damage had occurred.

Two types of pain are described:

1. Acute – actual or potential physiological harm is signalled and this type of pain stops prior to complete healing, a process that may take a few days or weeks.
2. Chronic – previously defined as pain that persisted beyond the normal time of healing, that is, longer than 3-6 months. However, the IASP (Merskey *et al.*, 1994) concluded that this definition on the basis of a time interval and evidence of healing was inadequate. Physiological changes may contribute to the experience of many chronic pains, for example, phantom limb pain, in addition to recurrent episodic pains, which include migraine. Normal healing has not occurred for chronic cases associated with rheumatoid arthritis or metastatic carcinomas. Also, changes in the central nervous system (CNS) due to injury may prolong and maintain pain long after the expected period of healing. In addition, chronic pain is associated with hyperalgesia, which is defined as increased pain associated with mild, noxious stimuli. Other pain types include allodynia which is pain elicited by non-noxious stimuli (Rang *et al.*, 2000).

The distinctions between acute and chronic pain have important implications for pain assessment and intervention. While acute pain signals tissue damage, chronic pain is markedly dissociated from tissue damage and associated with considerable suffering, psychological, behavioural and environmental changes.

Physiologically, pain can be divided into two separate phenomena (Hawthorn *et al.*, 1999):

1. Nociceptive or physiological pain – nociceptive pain results from intense or potentially damaging stimuli, for example, a pinprick or inflammatory pain. This pain is produced by stimulation of specialised pain-sensitive receptors: nociceptors, which are aptly named as nociceptive derives from the Latin word *nocere* "to hurt".
2. Pathological pain – produced where changes occur in response to disease or trauma and low intensity or normally innocuous stimuli (Woolf, 1991). Often this occurs after nerve (termed neuropathic or neurogenic) or tissue damage and is not a single entity as several mechanisms underlie pathological pain. It is characterised by a disruption of normal mechanisms so that the pain occurs in the absence of an obvious stimulus, in response to innocuous stimulus, and in a prolonged or exaggerated fashion to noxious stimuli.

Nociception is a complex series of events that occur between a site of active tissue damage and the perception of noxious stimuli while in contrast this is termed algesia in humans as this includes an affective emotional component. Nociception and algesia comprise of 4 processes (Fine *et al.*, 1998):

1. Transduction: noxious stimuli are translated into electrical activity at the sensory endings of nociceptors.
2. Transmission: impulses are propagated from the nociceptors to the CNS.
3. Modulation: nociceptive transmissions are modified by a number of neural influences *via* peripheral nerves or in the CNS.
4. Perception: the brain perceives the sensation.

### *1.1.1 Transduction*

The neurone or nerve cell is the basic component of the nervous system and neurones exist in a variety of forms and sizes. However, specific physical features are common to most neurones. These particular elements include a cell body (soma) from which extends a

single nerve process called an axon and a variable number of branching processes called dendrites; see Figure 1.1 for a detailed pictorial representation.

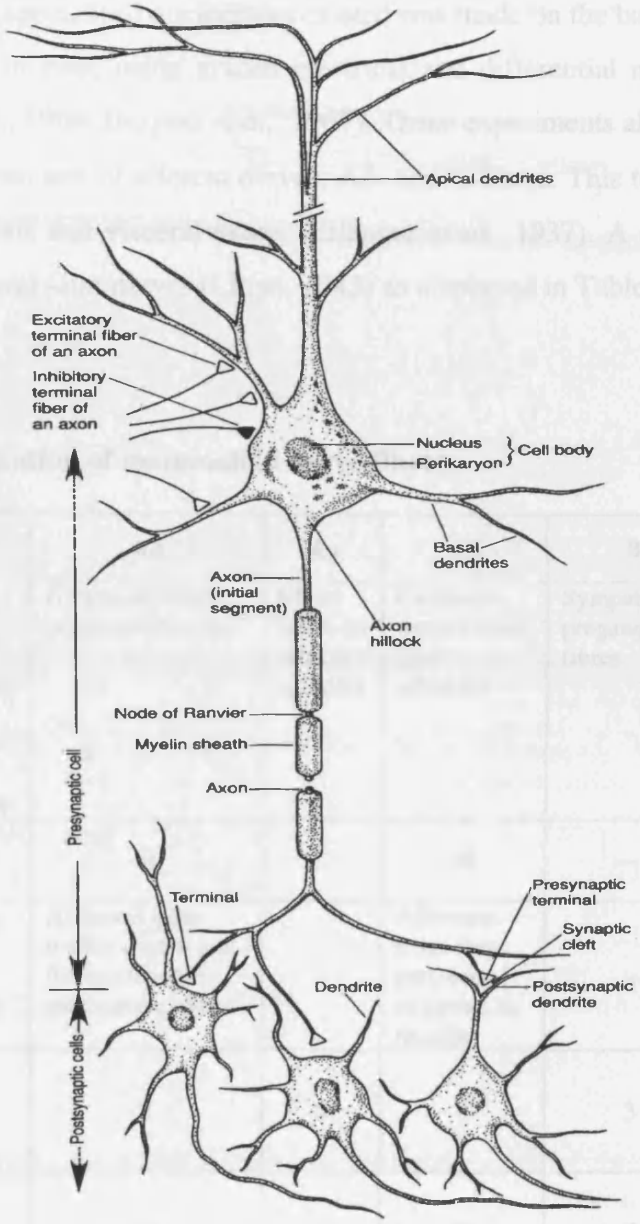


**Figure 1.1 The main features of a vertebrate neurone**

*The cell body gives rise to two types of processes – dendrites and axons. Axons vary in length with some extending more than 1 metre. Most axons in the CNS are very thin compared with the diameter of the cell body. The axon hillock, the region of the cell body where the axon emerges, is where the action potential is initiated. Many axons are insulated by a fatty myelin sheath, which is interrupted at regular intervals by the Nodes of Ranvier. Branches of one neurone (the presynaptic neurone) form synaptic connections with the dendrites or cell body of another neurone (the postsynaptic cell). The branches of the axon of one neurone may form synapses with as many as 1000 other neurones. Reproduced from Principles of neural science (Kandel, 1991).*

Nociceptive receptors or nociceptors are free nerve endings that show a wide distribution. They respond to various noxious stimuli: chemical, thermal and mechanical, transmitting this information *via* sensory afferent fibres to the CNS (Rang *et al.*, 2000).

The inference that specialised nociceptors existed was made on the basis of experiments on peripheral nerves in man, using graded electrical and differential nerve blocks (Adrian, 1931; Bessou *et al.*, 1969; Burgess *et al.*, 1967). These experiments also indicated that pain was signalled by two sets of afferent nerves; Aδ- and C-fibres. This terminology is used in relation to cutaneous and visceral axons (Erlanger *et al.*, 1937). A different terminology applies to muscle and joint nerves (Lloyd, 1943) as displayed in Table 1.1.

**Table 1.1 Classification of mammalian nerve fibres**

| | **Aα** | **Aβ** | **Aγ** | **Aδ** | **B** | **C** |
|---|---|---|---|---|---|---|
| Fibre Type (Erlanger & Gasser 1937) and function | Primary muscle spindle afferents, motor fibres to motor neurones | Cutaneous touch, pressure afferents | Motor fibres to muscle spindles | Cutaneous temperature, pain afferents | Sympathetic preganglionic fibres | Cutaneous pain afferents (unmyelinated); sympathetic postganglionic fibres |
| Group (Lloyd 1943) and function | I | II | – | III | – | IV |
| | Primary muscle spindle afferents | Afferents from tendon organs and from cutaneous mechanoreceptors | – | Afferents from deep pressure receptors in muscle | – | Unmyelinated nerve fibres |
| Average fibre diameter (μm) | 15 | 8 | 6 | 3 | 3 | 0.5 |
| Average conduction velocity (m/s) | 95 | 50 | 20 | 15 | 7 | 1 |

The cell bodies of nociceptors, akin to most primary afferent neurones, exist in one of three locations (Snider *et al.*, 1998):

1. Dorsal root ganglia; innervates the trunk, limbs and viscera and projects centrally to the spinal cord dorsal horn (Figure 1.2).
2. Trigeminal ganglia; innervates the head, oral cavity and neck and projects centrally to the brain stem trigeminal nucleus.
3. Nodose ganglia; peripheral terminals innervate visceral tissues and central terminals project to the floor of the fourth ventricle.

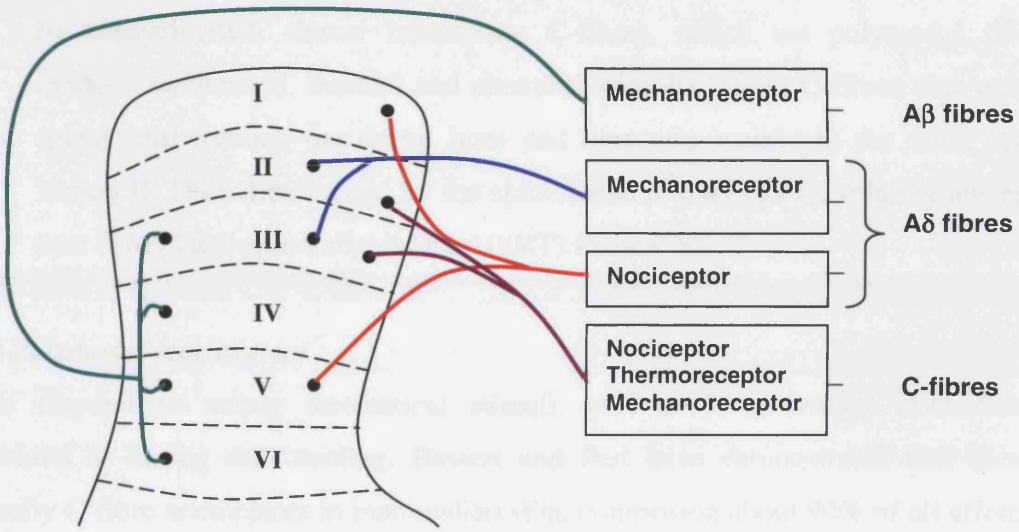


**Figure 1.2 Termination of afferent fibres in the dorsal horn of the spinal cord**
*Spinal afferent nociceptive fibres enter the spinal cord via the dorsal roots and terminate in the grey matter in the dorsal horn. Projection pathways arise from Laminae I and V and lead to the thalamus.*

As mentioned, nociceptors can be located among two types of primary afferent neurones, C- and Aδ-fibres. C-fibre nociceptors are small-diameter, unmyelinated, slowly conducting axons with small-diameter bodies. In contrast, Aδ fibre nociceptors are medium-diameter,

lightly myelinated peripheral axons whose conduction velocities are intermediate between those of C-fibres and the rapidly conducting, large diameter Aβ-fibres (Harper *et al.*, 1985).

Two different types of nociceptive (noxious) stimuli are perceived as pain (Fine *et al.*, 1998):

1. Somatic pain – an intense, localised sharp or stinging sensation. This is mediated by fast-conducting lightly myelinated Aδ fibres, which have a high threshold (that is, require a strong mechanical stimulus) and enter into the spinal cord through the dorsal horn where they terminate mostly in lamina I.
2. Visceral pain – a diffuse, dull, aching or burning sensation. This type is mediated by unmyelinated, slower conducting C-fibres, which are polymodal (that is, mediate mechanical, thermal and chemical stimuli). These C-fibres also enter the spinal cord through the dorsal horn and terminate mainly in the outer layer of lamina II. They then ascend by the spinothalamic tract (STT), spinomesencephalic tract (SMT) and spinoreticular tract (SRT) to the CNS.

### *1.1.2 Polymodal Nociceptors*

These respond to strong mechanical stimuli, noxious heat, irritant chemicals and sometimes to strong skin cooling. Bessou and Perl have demonstrated that these are generally C-fibre nociceptors in mammalian skin, comprising about 90% of all afferent C-fibres (Bessou *et al.*, 1969). Since most studies of nociceptors have involved the use of mechanical or heat stimuli, the terminology of AMH and CMH is used to refer to A-fibre mechano-heat-sensitive nociceptors and C-fibre mechano-heat-sensitive nocicepters respectively (Meyer *et al.*, 1994).

By comparison, the chemosensitivity of C-polymodal nociceptors has not been studied as intensively. They can be excited by potassium, histamine, serotonin (5-hydroxytryptamine), bradykinin, capsaicin, mustard oil, acetylcholine and dilute acids, by various methods (topical, intradermal and arterial injections). These chemicals act on nociceptors by altering the conductance of ion channels in the cell membrane and causing depolarisation. This can result in sensitisation of the nociceptors, producing an increased responsiveness to stimulation (Rang *et al.*, 1991).

Cold nociceptors, transmitting along C-fibres, have been reported in the monkey (LaMotte *et al.*, 1982) and in humans (Campero *et al.*, 1996). These respond strongly to prolonged cooling of the skin by ice and weakly to strong pressure, but are not responsive to heat. Cutaneous Aδ nociceptors also respond to temperatures below 0°C (Simone *et al.*, 1997). Cold pain is thought to be mediated by nociceptors located in cutaneous veins (Klement *et al.*, 1992), see Table 1.4.

## 1.2 Transmission and Modulation

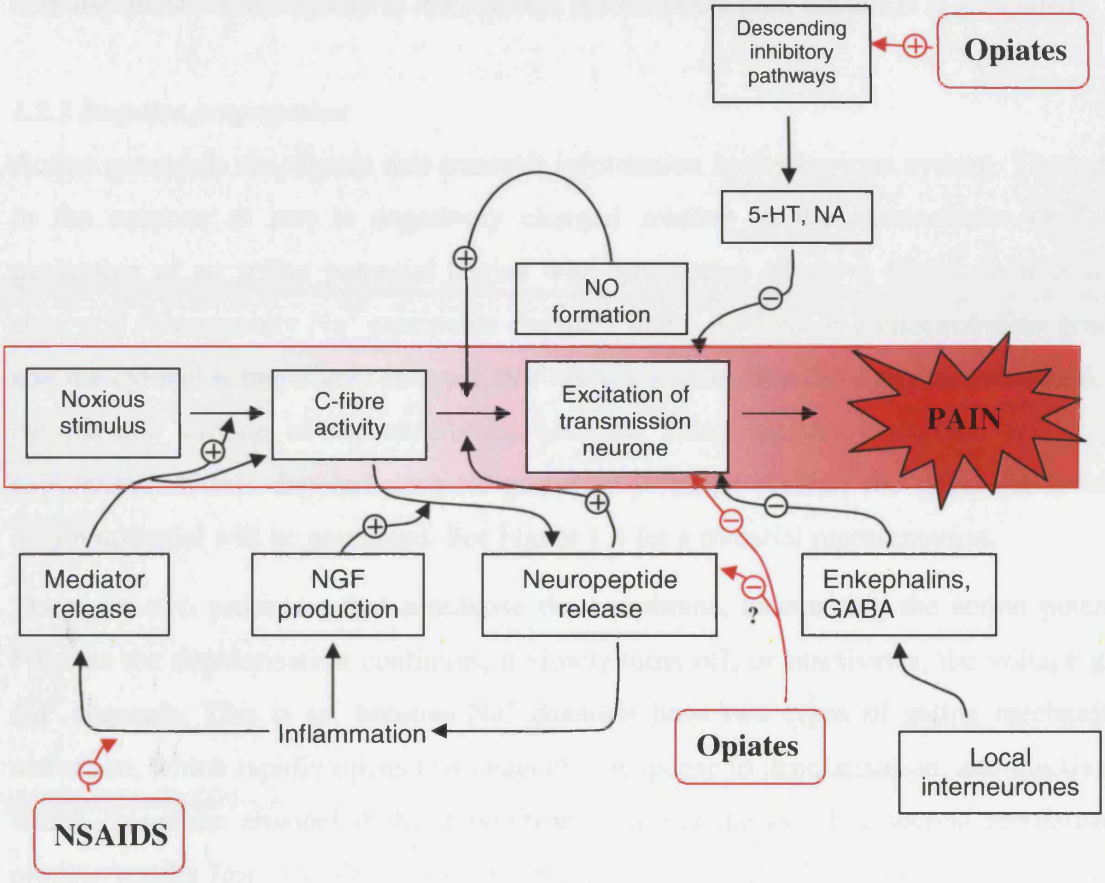


**Figure 1.3 Summary of modulatory mechanisms in the nociceptive pathway**
*NA – noradrenaline; NGF – nerve growth factor; GABA –γ-aminobutyric acid; NSAIDS – non-steroidal anti-inflammatory drugs; NO – nitric oxide. (Illustration was adapted from Rang et al., 2003).*

Pain transmission involves peripheral and central mechanisms. The former is initiated when nociceptors are activated by noxious stimuli. Tissue damage produces the release of chemical mediators such as prostaglandins and bradykinin that activate nociceptors. In response to activation, neuropeptides, such as substance P, may also be released from primary afferent neurones into the local extracellular fluid increasing pain sensation (Figure 1.3). Substance P can cause neurogenic inflammation by inducing mast cell degranulation. Nerve growth factor, produced by peripheral tissues in inflammation, can increase chemosensitivity of nociceptors and is thought to be involved in hyperalgesia. Nociceptors can then conduct electrical signals to the spinal cord. Central transmission involves pain being transmitted from primary afferent axons to the spinal cord dorsal horn, then the thalamus and finally to the cerebral cortex where pain sensation is generated.

### *1.2.1 Impulse propagation*

Action potentials are signals that transmit information in the nervous system. The cytosol in the neurone at rest is negatively charged relative to the extracellular fluid. The generation of an action potential begins with stimulation of nerve fibres, such as in the skin, and subsequently $Na^+$ permeable channels open. As there is a concentration gradient and the cytosol is negatively charged, $Na^+$ ions enter the fibre through these channels. The cytoplasmic surface of the membrane becomes more negatively charged and is now depolarised. If this depolarisation or generator potential reaches the threshold level, an action potential will be generated. See Figure 1.4 for a pictorial representation.

There are two processes that repolarise the membrane, terminating the action potential. First, as the depolarisation continues, it slowly turns off, or inactivates, the voltage gated $Na^+$ channels. This is so, because $Na^+$ channels have two types of gating mechanisms: activation, which rapidly opens that channel in response to depolarisation, and inactivation which closes the channel if the depolarisation is maintained. The second repolarisation process results from the delayed opening of voltage-gated $K^+$ channels. As $K^+$ channels begin to open, $K^+$ efflux increases. The delayed increase in $K^+$ efflux combined with a decrease in $Na^+$ influx to produce a net efflux of positive charge from the cell, which continues until the cell has repolarised to its resting value. Note that this process results in a wave of depolarisation/repolarisation that can propagate all over the surface of the axon. Once the depolarisation/repolarisation wave reaches the axon terminal it turns on the

mechanisms of synaptic transmission which results in the necessary communication between nerve cells (Bear *et al.*, 2001).

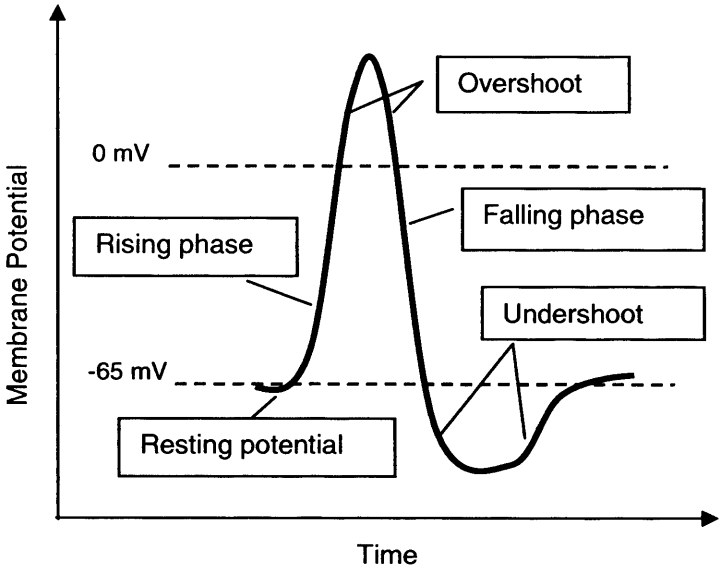


**Figure 1.4 The generation of an action potential**
*The action potential can be split into different phases. Initially, the neurone is at rest at which a resting potential at around -65 mV can be measured. The rising phase ensues due to rapid depolarisation of the membrane. Overshoot is reached when the inside of the neurone is positively charged relative to the outside. The falling phase relates to rapid repolarisation while the final part is undershoot.*

### *1.2.2 Synaptic transmission*

Neural signals are transferred between neurones at contact sites called synapses. A synapse is defined as the specialised junction where an axon terminal contacts another neurone or cell type. The normal direction of information flow is from the axon terminal to the target neurone. Thus, the axon terminal is presynaptic while the target neurone is postsynaptic. The process of transferring the neural signal at a synapse is known as synaptic transmission. Two types of synapses exist: electrical and chemical. Electrical synapses occur at gap junctions and are bi-directional, that is, the electrical transmission can occur in both directions (Bear *et al.*, 2001).

The majority of synaptic transmission in the human CNS occurs *via* chemical synapses. Different varieties of chemical synapses exist both within and outside of the CNS where the latter are known as neuroeffector junctions but specific structural features are common to all. In constrast to electrical synapses, the presynaptic and postsynaptic membranes in chemical synapses are separated by a synaptic cleft that is 20-50 nm wide. The axon terminal contains synaptic vesicles, small membrane-enclosed spheres that store neurotransmitter, the chemical used to communicate with the postsynaptic neurone. Many axon terminals contain secretory granules that are larger vesicles. The amino acid and amine neurotransmitters are stored in and released from synaptic vesicles while for peptide neurotransmitters, this occurs in secretory granules. On the presynaptic side, both the membrane and proteins protruding into the cytoplasm of the terminal along the intracellular face of the membrane are sites of neurotransmitter release. The protein accumulated in and just under the postsynaptic membrane is called the postsynaptic density (Bear *et al.*, 2001). This area contains the neurotransmitter receptors, which convert the intercellular signal (neurotransmitter) into an intracellular signal (a change in membrane potential or a chemical change) in the postsynaptic cell. Neurotransmitters can be grouped as shown in Table 1.2.

**Table 1.2 Examples of neurotransmitters**

| Amino acids | Biogenic amines | Neuropeptides | Other |
|---|---|---|---|
| Aspartate | Dopamine | Gastrin releasing peptide | Nitric oxide |
| GABA | Noradrenaline | Gastrin | |
| Glutamate | Adrenaline | Insulin | |
| Glycine | Serotonin | Neurohypophyseals e.g. vasopressin, oxytocin | |
| | Histamine | Neuropeptide Y | |
| | Acetylcholine | Opioids e.g. dynorphin, endorphin, enkephalins | |
| | | Tachykinins e.g. substance P | |

*Neurotransmitters can be grouped under the above headings as shown in the table. Biogenic amines are produced endogenously in the human body. Neuropeptides are typically larger in size than the amino acids and this group is relatively large. Nitric oxide is not a typical neurotransmitter, which has led to speculation over the definition of a neurotransmitter (Rang et al., 2003).*

The neurotransmitter is synthesised by the neurone and stored in vesicles at the axon terminal. When the action potential reaches the axon terminal, it causes the fusion of synaptic vesicles with the presynaptic membrane. This releases neurotransmitter molecules into the synaptic cleft where they diffuse across the cleft and bind to receptors on the postsynaptic cell. The activated receptors cause changes in the activity of the postsynaptic neurone. The neurotransmitter molecules are released from the receptors and undergo reuptake into the presynaptic axon terminal or are enzymatically degraded in the synaptic cleft (Augustine *et al.*, 1999). A summary of this is displayed in Figure 1.5.

### *1.2.3 Neurotransmitter receptors*

There are four major receptor superfamilies which are summarised in Table 1.3 (Rang *et al.*, 2003). They vary in terms of molecular structure and their transduction mechanisms and produce a variety of cellular effects. Ligand-gated ion channels and G-protein-coupled receptors are considered further.

**Table 1.3 The four receptor superfamilies**

| | Ligand-gated ion channels | G-protein-coupled receptors | Kinase-linked receptors | Nuclear receptors |
|---|---|---|---|---|
| **Location** | Membrane | Membrane | Membrane | Intracellular |
| **Effector** | Ion channel | Channel or membrane | Enzyme | Gene transcription |
| **Coupling** | Direct | G-protein | Direct | *Via* DNA |
| **Examples** | Nicotinic acetylcholine receptor | Muscarinic acetylcholine receptor | Insulin, growth factor, cytokine receptors | Steroid, thyroid hormone receptors |
| **Structure** | Oligomeric assembly of subunits surrounding a central pore | Monomeric (occasionally dimeric) structure comprising 7 transmembrane helices | Single transmembrane helix linking extracellular receptor domain to intracellular kinase domain | Monomeric structure with separate receptor and DNA-binding domains |
| **Time for response** | Milliseconds | Seconds | Hours | Hours/days |

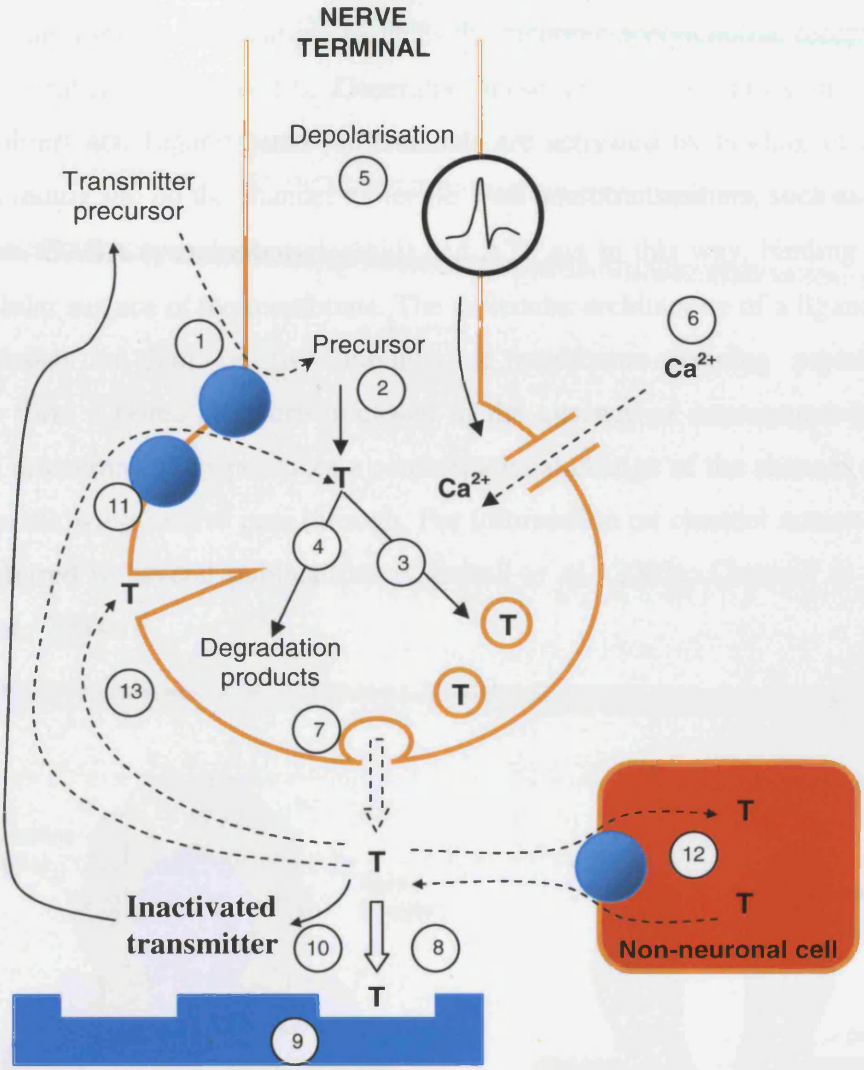


**Figure 1.5 Summary of synaptic transmission for amine and amino acid transmitters**
*In order: 1. uptake of transmitter precursors; 2. synthesis of transmitter; 3. storage of transmitter in vesicles; 4. degradation of excess transmitter; 5. depolarisation; 6. influx of $Ca^{2+}$ in response to depolarisation; 7. release of transmitter by exocytosis; 8. diffusion to postsynaptic membrane; 9. interaction with postsynaptic receptors; 10. inactivation of receptors; 11. reuptake of transmitter or degradation products by nerve terminals; 12. uptake of transmitter by non-neuronal cells; 13. interaction with presynaptic receptors. Peptide mediators differ in that they may be synthesised and packaged in the cell body rather than in the terminals. (Figure was adapted from Rang et al., 2003).*

### *1.2.4 Ligand-gated ion channels*

Commonly called ionotropic receptors, these are membrane proteins with a similar structure to other ion channels but incorporating a ligand-binding (receptor) site, usually in the extracellular domain. An example includes the nicotinic acetylcholine receptor with its structure illustrated in Figure 1.6. Generally, these are the receptors on which fast neurotransmitters act. Ligand-gated ion channels are activated by binding of a chemical ligand to a binding site on the channel molecule. Fast neurotransmitters, such as glutamate, acetylcholine, GABA (γ-aminobutyric acid) and ATP act in this way, binding to sites on the extracellular surface of the membrane. The molecular architecture of a ligand-gated ion channel consists of four or five subunits of membrane-spanning proteins, which collectively form a pore. The pore is closed in the absence of neurotransmitter but the presence of neurotransmitter produces a conformational change of the channel causing the pore to open allowing ions to pass through. For information on channel nomenclature, the reader is referred to several publications (Catterall *et al.*, 2003a; Catterall *et al.*, 2003b; Gutman *et al.*, 2003).

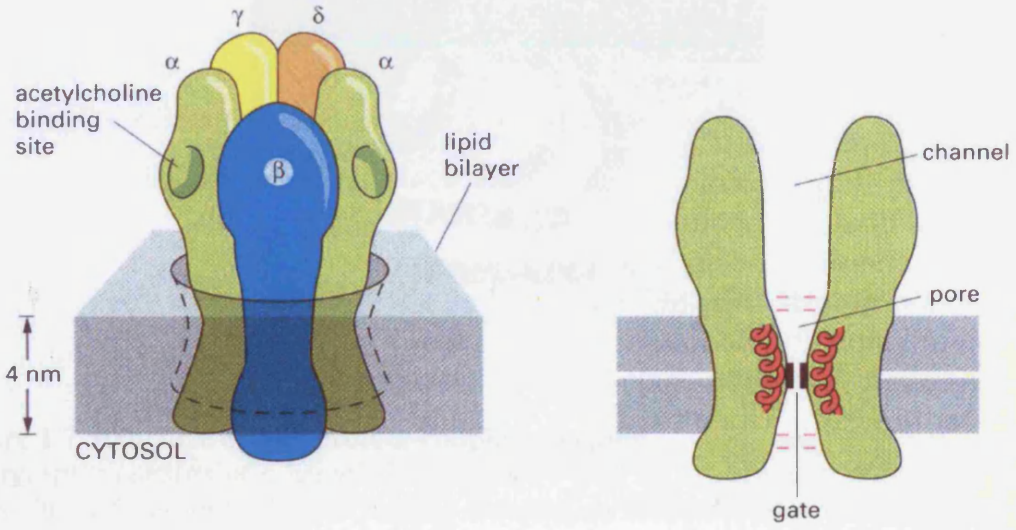


**Figure 1.6 Structure of the nicotinic acetylcholine receptor**
*The receptor is composed of five subunits surrounding a transmembrane pore, lined by α-helices forming a gate. When the ligand acetylcholine binds to the receptor, the helices pull the gate open allowing the influx of cations. Figure from Alberts and co-authors* (Alberts *et al.*, 1994).

### *1.2.5 G-protein-coupled receptors (GPCRs)*

This is the largest family of receptors, also termed metabotropic, with a seven-transmembrane spanning topology (see Figure 1.7). Examples range from adrenoceptors, dopamine receptors to the cannabinoid receptors. They are coupled to intracellular effector systems *via* a trimeric G-protein. G-protein activation is pictorially represented in Figure 1.8. For further interest, the reader is referred to several publications (Baldwin, 1994; Neer, 1995).

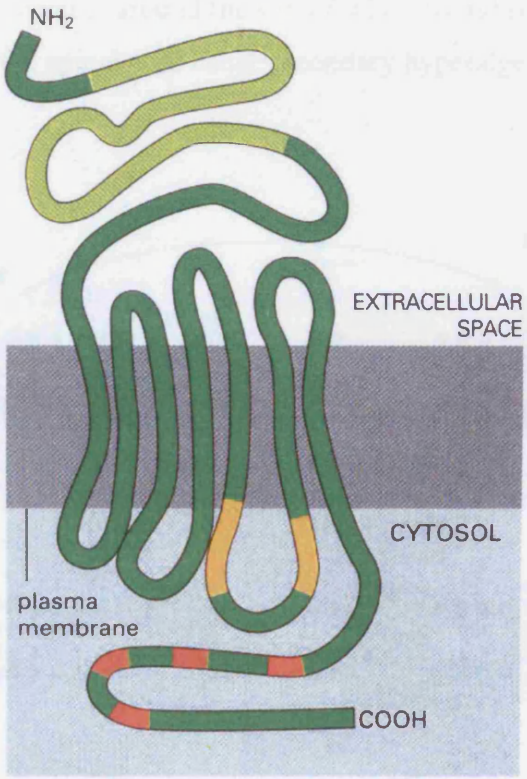


**Figure 1.7 Structure of a G-protein-coupled receptor**
*The receptor consists of a heptahelical structure with an extracellular N-terminal and an intracellular C-terminal. Ligand binding domains are located on the N-terminal side (light green) and in the transmembrane section while G-protein coupling occurs intracellularly (orange sections) on the C-terminal side. The red intracellular parts are sites of phosphorylation during receptor regulation. Figure from Alberts and co-authors (Alberts et al., 1994).*

### *1.2.6 Common peripherial mediators of pain and hyperalgesia*

Hyperalgesia can be further defined as primary hyperalgesia and secondary hyperalgesia. The former occurs within the damaged tissue while the latter refers to tissues, surrounding

the damaged area, which can become sensitised. A number of chemicals are able to sensitise nerve endings to noxious stimuli of which examples include bradykinin, prostaglandins and substance P. Prostaglandins can increase the sensitivity of nociceptors. Aspirin and other nonsteroidal anti-inflammatory drugs (NSAIDs) are effective against hyperalgesia as they inhibit the enzymes required for prostaglandin synthesis. Substance P, a peptide, is synthesised by nociceptors. Activation of a one branch of a nociceptor axon can lead to the secretion of substance P by the other branches of that axon. The effects of substance P include vasodilation and the release of histamine from mast cells. Both sensitisation of other nociceptors around the site of injury by substance P and amplification of nociceptive output in the spinal cord cause secondary hyperalgesia (Bear *et al.*, 2001).

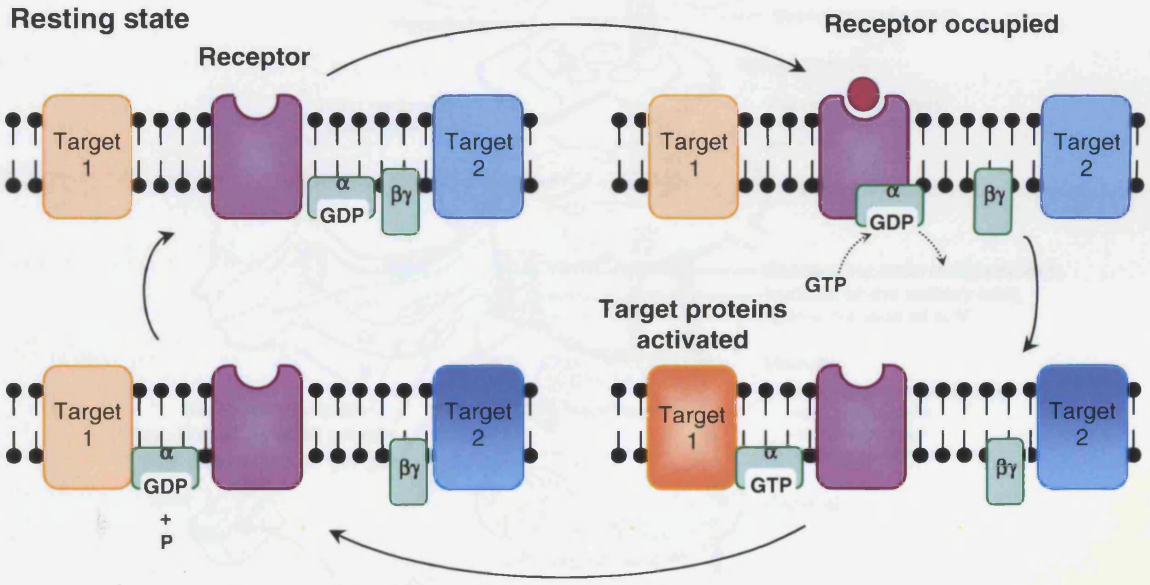


**Figure 1.8 G-protein activation**
*The G-protein consists of three subunits (α, β, γ), which are anchored to the membrane through lipid residues. Coupling of the α-subunit to an agonist-occupied receptor causes the bound GDP to exchange with intracellular GTP; the α-GTP complex then dissociates from the receptor and from the βγ-subunit complex and interacts with a target protein (target 1, which may be an enzyme such as adenylate cyclase or an ion channel). The βγ-complex may also activate a target protein (target 2). The GTPase activity of the α-subunit is increased when the target protein is bound, leading to hydrolysis of the bound GTP to GDP, whereupon the α-subunit reunites with the βγ-complex.*

### *1.2.7 Ascending Pathways*

Anatomically, the nervous system comprises the CNS and the peripheral nervous system (PNS). The CNS consists of the brain and spinal cord and the PNS consists of the cranial and spinal nerves and the structures that emanate from them.

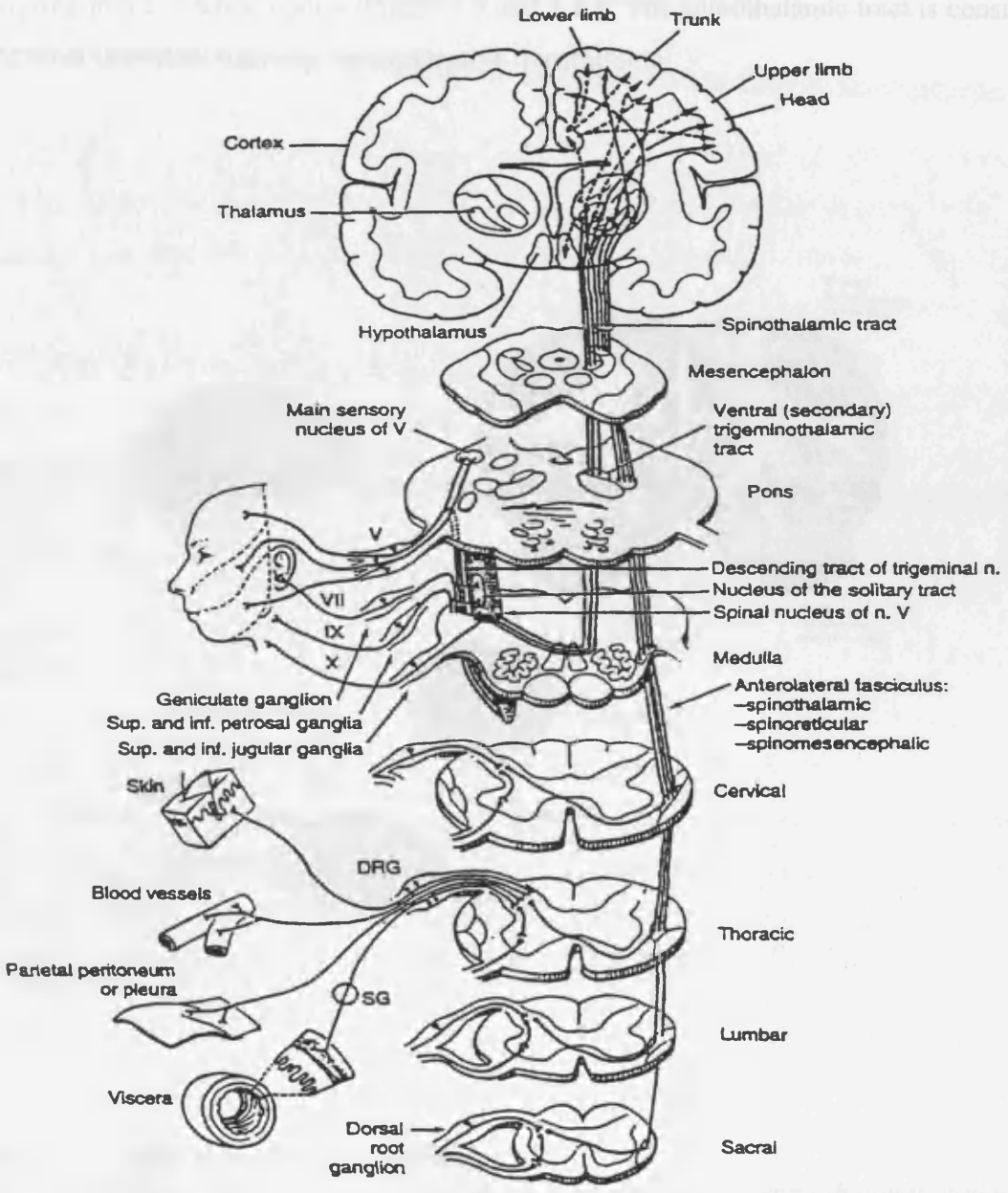


**Figure 1.9 Ascending nociceptive pathways**
*Pathways shown lead from the periphery via autonomic and somatic primary afferents. DRG – dorsal root ganglion; inf. – inferior; n. – nerve; SG – sympathetic ganglion; sup. – superior; (Bonica, 1990).*

Transmission of afferent (sensory) input is initiated by activation of peripheral receptors with subsequent depolarisation of their axons. These axons relay information to their cell bodies generally located in the dorsal root ganglion (DRG). Central axonal processes of these first-order neurones synapse in the dorsal horn, where sensory input is modulated. Information travels contralaterally *via* ascending columns such as the anterolateral funiculus and posterior columns to synapse in the reticular system and the thalamus, finally arriving in the cerebral cortex (Figure 1.9 and 1.10). The spinothalamic tract is considered the most important pathway for nociceptive transmission.

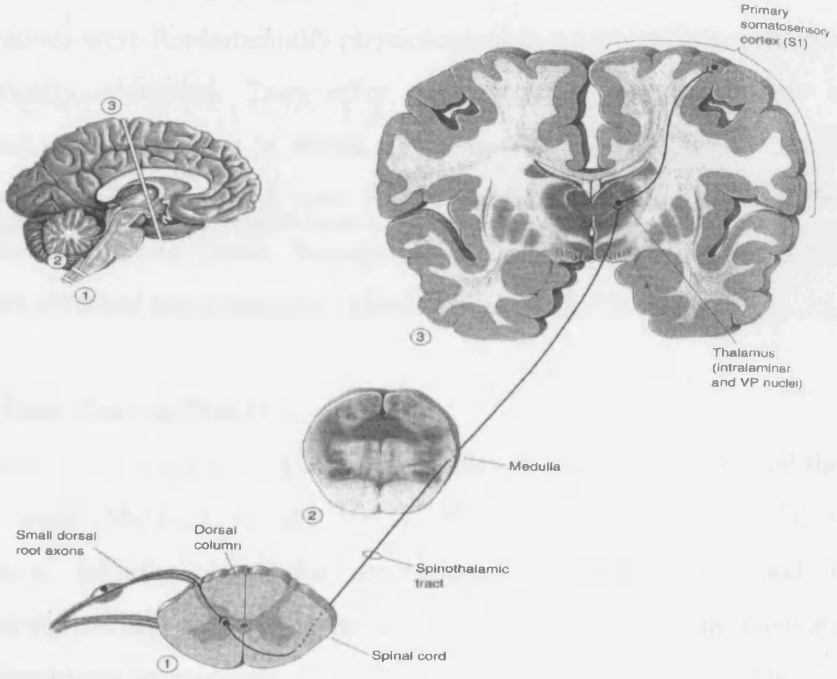


**Figure 1.10 The spinothalamic pathway**
*Information regarding pain and temperature is relayed by the spinothalamic pathway to the brain (Bear et al., 2001).*

### *1.2.8 Theories of Nociception*

For centuries there has been sustained endeavour to develop a philosophical and scientific understanding of the nature of pain. Early civilisations proposed various explanations including the influences of gods, the intrusion of magical fluids, the frustration of desire and deficiency or excess in the circulation of Qi. Since the French philosopher René Descartes introduced his Cartesian theory in 1664, there has been a gradual evolution in the understanding of pain. Descartes' theory led to two significant hypotheses in the 19$^{th}$ century: the specificity theory (Schiff, 1859) and the intensity (summation) theory (Erb, 1895) as described by Main and Spanswick (Main *et al.*, 2000). The former concept considers pain to be a specific sensation, which was independent of other sensations. The latter theory postulated that touch was experienced as a painful sensation only after a certain threshold following intense stimulation. However, both of these theories and their later derivatives were fundamentally physiological in nature and the perception of pain was not specifically addressed. They offer an inadequate simplistic view between tissue damage and pain perception in which any tissue damage initiated a sequence of neural events that inevitably produced pain. Neither of these theories explain the occurrence of pain in the absence of tissue damage or variation in pain between individuals with (apparently) identical tissue damage (Main *et al.*, 2000).

### *1.2.9 The Gate Control Theory*

A major innovation occurred in 1965 when Melzack and Wall introduced their gate control theory of pain (Melzack *et al.*, 1965). This has stood the test of time and was revolutionary; initially about the mechanisms of transmission and modulation of nociceptive signals and secondly, pain was acknowledged as a dual phenomenon resulting from the interaction between physiological and psychological events (Dickenson, 2002).

The gate control theory postulated that spinal "gates", in the dorsal horn at each segmental level in the spinal cord, determine whether heat, pain or touch impulses were transmitted to the brain. Successful transmission through the gate was affected not only by the intensity of the stimulation and competing local stimuli, but also by descending impulses from the brain. In contrast to Descartes' model that displayed a one-way system of transmitting information from the periphery, there is continual modulation of information from the periphery.

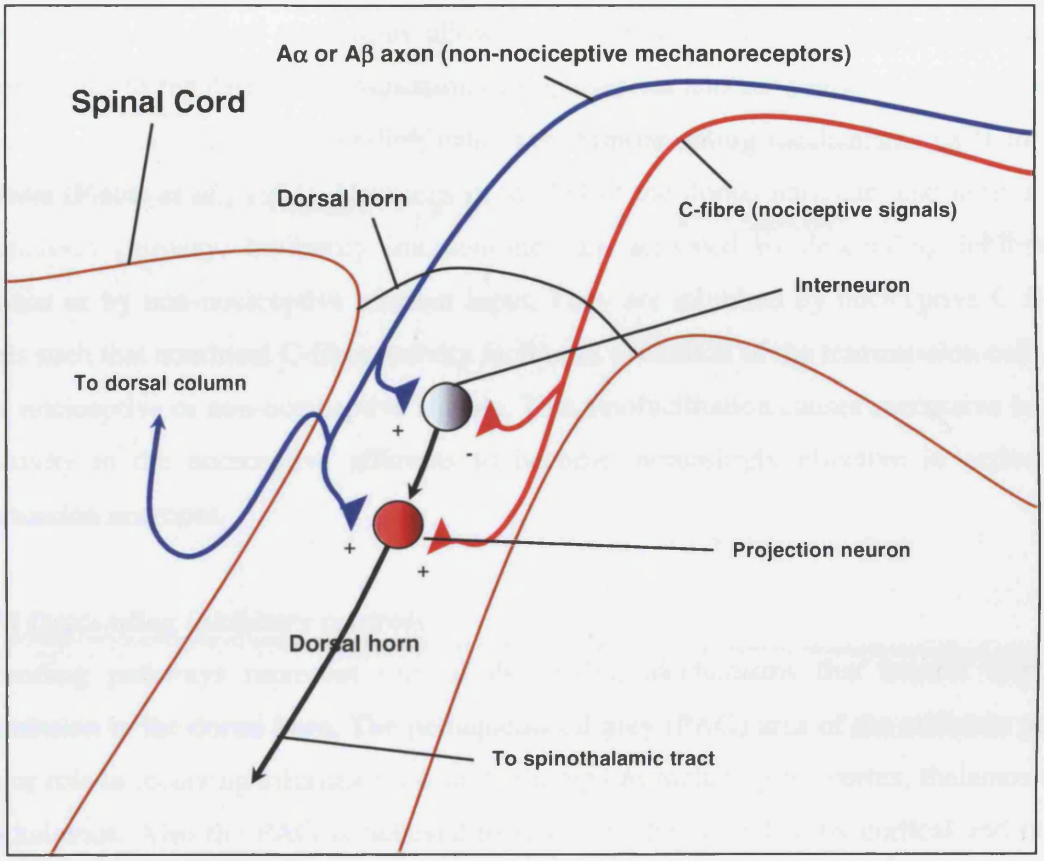


**Figure 1.11 Gate control theory**
*Certain neurones in the dorsal horn, which project an axon up the spinothalamic tract, are excited (+) by both large diameter sensory axons and unmyelinated pain axons. The projection neurone is also inhibited (-) by an interneurone (in the substantia gelatinosa). The interneurone can simultaneously be excited (+) by the sensory and inhibited (-) by the pain axons. Thus, information from the pain axon alone maximally excites the projection neurone relaying nociceptive signals to the brain. In contrast, high activity in the mechanoreceptive axon activates the interneurone and inhibits nociceptive signals.*

Substantia gelatinosa (SG) cells, in Lamina II of the dorsal horn, are short inhibitory interneurones projecting to Lamina I and V and they control transmission at the first synapse of the nociceptive pathway (Figure 1.11), between the primary afferent fibres and spinothalamic tract transmission neurones. SG cells respond to the activity of afferent fibres entering the spinal cord (thus allowing the arrival of impulses *via* one group of afferent fibres to regulate the transmission of impulses *via* another pathway. Also SG cells respond to the activity of descending pathways. Similar gating mechanisms exist in the thalamus (Fields *et al.*, 1994). Neurones in the SG of the dorsal horn can also inhibit the transmission pathway. Inhibitory interneurones are activated by descending inhibitory neurones or by non-nociceptive afferent input. They are inhibited by nociceptive C-fibre signals such that continual C-fibre activity facilitates excitation of the transmission cells by either nociceptive or non-nociceptive signals. This autofacilitation causes successive bursts of activity in the nociceptive afferents to become increasingly effective in activating transmission neurones.

### *1.2.10 Descending inhibitory controls*

Descending pathways represent one of the gating mechanisms that control impulse transmission in the dorsal horn. The periaqueductal grey (PAG) area of the midbrain plays a major role in receiving information from brain regions including the cortex, thalamus and hypothalamus. Also the PAG is believed to represent the site whereby cortical and other inputs act to control the nociceptive "gate" in the dorsal horn. Reynolds electrically stimulated the PAG of rat brain and this resulted in antinociception with non-painful sensations being unaffected (Reynolds, 1969).

The nucleus raphe magnus (NRM), located in the medulla, is the main neuronal pathway in descending antinociception and is activated by PAG stimulation. This pathway descends *via* fibres in the dorsolateral funiculus of the spinal cord, which form synaptic connections on dorsal horn interneurones (Figure 1.12). The NRM receives an input from spinothalamic neurones *via* the adjacent nucleus reticularis paragigantocellularis (NRPG). This system may be part of a regulatory feedback loop whereby transmission through the dorsal horn is controlled according to the amount of activity reaching the thalamus (Rang *et al.*, 2000).

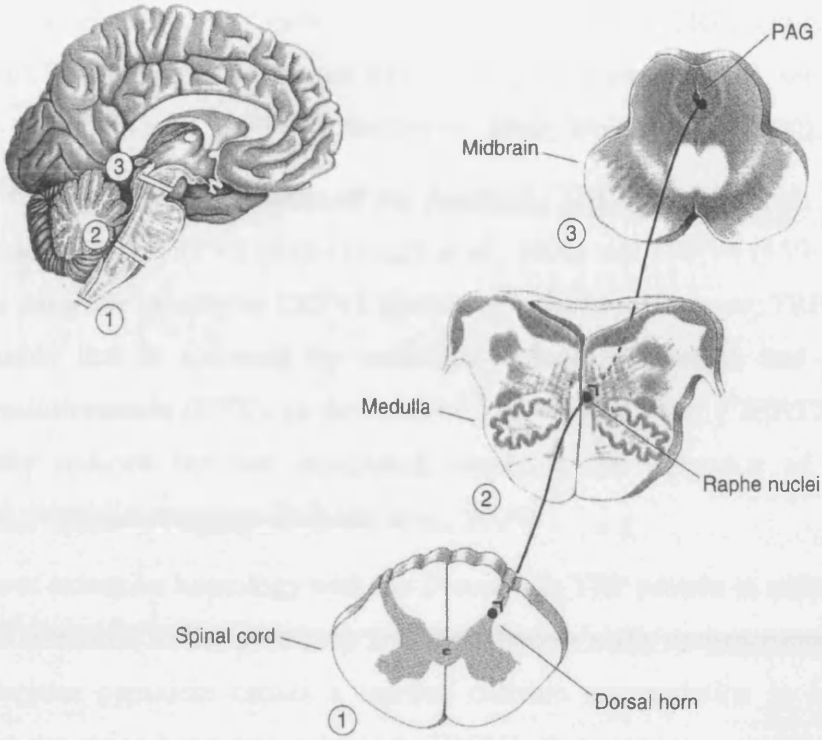


**Figure 1.12 Descending pain inhibitory pathways**
*The PAG of the midbrain can influence the raphe nuclei in the medulla and subsequently modulate the flow of nociceptive information through the dorsal horns of the spinal cord (Bear et al., 2001).*

## 1.3 Perception of pain

This is a personal and subjective experience in humans and is described as algesia. This event varies tremendously between individuals despite similar stimuli. Pain can be influenced by cognitive, mental and environmental factors. In animals, perception of pain and the related psychology is not understood or known and the term nociception is employed to describe pain in this case (Bear *et al.*, 2001). Perception is not considered further but the reader is referred to the following publications by Craig and Weisenberg (Craig, 1994; Weisenberg, 1994).

## 1.4 TRP channels

The transient receptor potential (TRP) channel superfamily consists of three main subfamilies most closely related to the TRP protein orginally discovered in *Drosophila*: TRPC (C for classical or canonical), TRPV (V for vanilloid), TRPM (M for melastatin-related). The other categories, more distantly related, include TRPP (Polycystic Kidney Disease-type), TRPN and TRPML and TRPA (ankyrin repeat channel), see Table 1.4 and Figure 1.13 (Clapham *et al.*, 2003; Montell *et al.*, 2002; Walker *et al.*, 2000).

The TRPV family currently consists of six members, TRPV1–6 of which TRPV2 (49%) (Caterina *et al.*, 1999), TRPV3 (43%) (Smith *et al.*, 2002) and TRPV4 (45%) (Nilius *et al.*, 2004) share sequence identity to TRPV1 (shown in brackets). However, TRPV1 is the only family member that is activated by vanilloids including capsaicin and its ultrapotent analogue, resiniferatoxin (RTX). In the brain of TRPV1-null mice, [$^3$H]RTX binding sites are markedly reduced but not eliminated, implying the existence of other, as yet unidentified, vanilloid receptors (Roberts *et al.*, 2004).

TRPV1 shares extensive homology with the *Drosophila* TRP protein in retina; however the similarity is restricted to the pore-loop and the adjacent sixth transmembrane segment in TRPV1. Because capsaicin causes a marked calcium accumulation in rat retina, it is possible that the retina has a site, related to TRPV1, that recognises vanilloids. OSM-9, a novel protein similar to rat TRPV1, plays a role in olfaction, mechanosensation and olfactory adaptation in *Caenorhabditis elegans*. However, OSM-9 is not activated by capsaicin which suggests that vanilloid isoforms did occur early during evolution and also, capsaicin recognition is a later addition to TRPV1 (Jordt *et al.*, 2002; Szallasi *et al.*, 1999b).

## Table 1.4 Overview of the TRP family

| Family | Proposed Name of Channel | Channel | Number of amino acids | Expression Pattern | Cloned from the following species | Regulation | Possible function |
|---|---|---|---|---|---|---|---|
| TRPC | | TRP | 1275 | Photoreceptors of *Drosophila*; antenna of *Drosophila* during development | *Drosophila*, *Calliphora* | PUFAs? $Ca^{2+}$ | Light-activated channel |
| | | TRPL | 1124 | Photoreceptors of *Drosophila* | *Drosophila* | PUFAs? DAG? | Light-activated channel |
| | | TRPγ | 1128 | Photoreceptors of *Drosophila* | *Drosophila* | | Light-activated channel subunit |
| | TRPC1 | TRP1 | 759 (β-Isoform) 793 (α-Isoform) 778 (*Xenopus*) | Brain, ovary, heart, testes (change during development) | *Xenopus*, mouse, rat, bovine, human | SOC | |
| | TRPC2 | TRP2 | 1172 (Mouse) | Bovine: testes, spleen, liver; mouse:testes; rat: vomeronasal organ | Bovine, rat, mouse | SOC? $InsP_3$ | Pheromone, acrosomal reaction |
| | TRPC3 | TRP3 | 848 (Human) 836 (Mouse) | Brain mainly and in low levels in intestine, prostate, lung, placenta, testis | Human, rat, mouse | DAG, SOC? | Neurotrophin-activated channel |
| | TRPC4 | TRP4 | 974 (Mouse) | Brain, adrenal, liver, lung, heart, spleen, kidney, testis, uterus, aorta | Bovine, rat, mouse | SOC? PLC | Vasorelaxation |
| | TRPC5 | TRP5 | 975 (Mouse) 974 (Rabbit) | Brain, olfactory bulb | Rabbit, Mouse | SOC? PLC | |
| | TRPC6 | TRP6 | 929 (Rat) 930 (Mouse) | Brain, lung, ovary | Rat, mouse, rabbit | DAG | |
| | TRPC7 | TRP7 | 862 | Heart, lung, eye and in low levels in brain, spleen, testes | Mouse | DAG | |
| TRPV | OSM-9 | | 937 | Olfactory, mechanosensory and osmosensory neurones | *C. elegans* | | Osmoreception, olfaction |
| | TRPV1 | VR1 | 828 (Rat) | Dorsal root ganglia, trigeminal and nodose sensory ganglia | Human, mouse, rat | Capsaicin, pH<5.9, noxious heat (>43°C), phorbols, lipids, anandamide? Inhibited by capsazepine, ruthenium red, iodo-resiniferatoxin | Thermal and inflammatory pain |
| | TRPV2 | VRL-1 | 761 (VRL-1 in Rat) | Sensory ganglia, spinal cord, spleen, lung, brain, intestine, vas deferens | Human, mouse, rat | Noxious heat (>53°C). Inhibited by Ruthenium red | High temperature pain |
| | | GRC | 756 | Spleen, lung, brain | Mouse | Regulated by IGF-1. Inhibited by Ruthenium red | Growth factor regulated channel |
| | TRPV3 | VRL3 | 790 | Dorsal root ganglion, trigeminal ganglion, spinal cord, brain, skin, tongue | Human | Temperature-sensitive at ~ 37°C | |
| | TRPV4 | VRL-2 (OTRPC4, VR-OAC, TRP12) | 871 | Kidney, heart, liver | Mouse | Osmolarity, mechanosensitive? Inhibited by Ruthenium red, econazole, $Cu^{2+}$, $Pb^{2+}$, $Cd^{2+}$, $Mg^{2+}$, $Gd^{3+}$, $La^{3+}$ | Osmosensory transduction |
| | TRPV5 | ECaC1 | 730 | Intestine, kidney, placenta | Rabbit | Constitutively active (activity increased by low $[Ca^{2+}]_i$). Antagonised by elevated $[Ca^{2+}]_i$ | |
| | | CaT2 | 723 | Kidney | Rat | | |
| | TRPV6 | ECaC2 (CaT1) | 727 | Intestine, brain, thymus, adrenal gland | Rat | Constitutively active (activity increased by low $[Ca^{2+}]_i$) and store depletion. Antagonised by elevated $[Ca^{2+}]_i$ | $Ca^{2+}$ absorption in intestine |
| | | CaT-L | 725 | Placenta, exocrine pancreas, salivary gland, prostate cancer | Human | | |

| | | | | | | | |
|---|---|---|---|---|---|---|---|
| TRPM | TRPM1 | Melastatin | | Melanocytes | | Translocation? | |
| | TRPM2 | TRPC7<br>LTRPC2 | 1503 | Brain, bone marrow, spleen, heart, leukocytes, liver, lung, kidney, prostate, testis, skeletal muscle, ubiquitous | Human | ADP-ribose, NAD, redox | |
| | TRPM3 | KIAA1616<br>LTRPC3 | | | | | |
| | TRPM4 | LTRPC4 | | | | | |
| | TRPM5 | MTR1<br>LTRPC5 | | Ubiquitous | | | |
| | TRPM6 | Chak2 | | | | | |
| | TRPM7 | TRP-PLIK<br>LTRPC7 | 1862 | Brain, haematopoietic cells | Mouse | Phosphorylation, reduction in Mg-ATP | Channel linked to cellular metabolism |
| | TRPM8 | TRP-p8<br>CMR1 | | Prostate, primary tumours, peripheral nervous system | | Menthol, icilin, cold (<26°C) | |
| TRPP | | Polycystin-2 | 968 | Kidney | Human | | |
| | | PCL | 805 | Kidney | Mouse | $Ca^{2+}$ | |
| TRPML | | Mucolipin-1 | 580 | Ubiquitous | Human | | |
| TRPN | | NOMPC | 1619 | *Drosophila* bristles | *Drosophila* | | |
| TRPA | TRPA1 | ANKTM1 | | | | | Cold temperature pain |

*Abbreviations: PUFAs (Polyunsaturated fatty acids), DAG (Diacylglycerol), SOC (Store-operated channel), $InsP_3$ (Inositol 1,4,5-trisphosphate), PLC (Phospholipase C).*

*Information from the following sources: (Clapham et al., 2001; Gunthorpe et al., 2002; McKemy, 2005; Minke et al., 2002; Montell et al., 2002; Nilius et al., 2005; Smith et al., 2002; Xu et al., 2002).*

As well as TRPV1 and its homologue TRPV2, which respond to high noxious temperatures, the receptor TRPM8 was cloned and identified recently to be the "cold menthol receptor". Agonists include menthol and icilin. In addition, a distant relation, TRPA1 or ANKTM1, has also been proposed to be a detector of noxious cold temperatures in nociceptive afferents as TRPA1 RNA transcripts have been found in nociceptive afferents which express TRPV1. Also, mTRPA1-expressing Chinese hamster ovary (CHO) cells elicited non-selective cation currents at an aggregate threshold of approximately 17°C (McKemy, 2005; Peier *et al.*, 2002). However, controversy arose over TRPA1's proposed function as a detector of cold temperatures after TRPA1-expressing HEK293 or *Xenopus* oocytes did not display cold-activation of TRPA1 currents (Jordt *et al.*, 2004). Instead, TRPA1 was activated by isothiocynates, found in wasabi and yellow mustard, as well as other pungent substances found in ginger and clove oil (Bandell *et al.*, 2004; Jordt *et al.*, 2004). Furthermore, TRPA1 is thought to be involved in inflammatory hypersensitivity (McKemy, 2005).

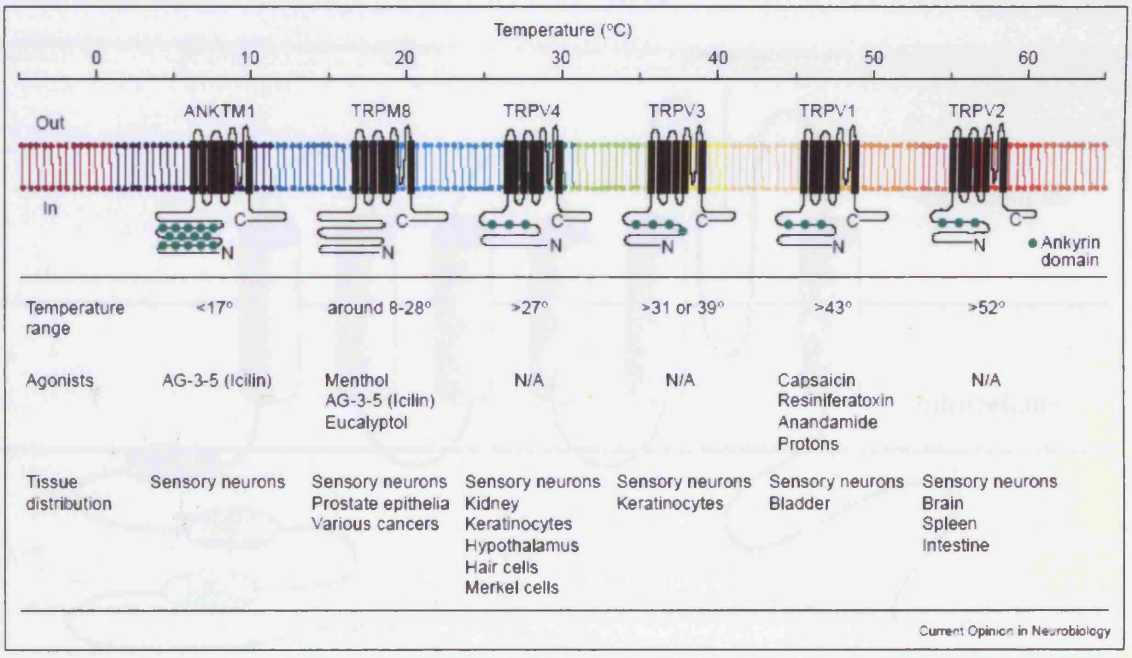


**Figure 1.13 Summary illustration of known thermosensory channels**
*Image from Jordt and co-authors (Jordt et al., 2003).*

## 1.5 The TRP subfamily member TRPV1

Caterina and colleagues transfected eukaryotic cells with pools of a rat cDNA library and utilised calcium imaging to identify those cells that responded to capsaicin. Once a positive

pool was found, it was divided into smaller pools until they had isolated a single cDNA encoding the capsaicin-gated channel. They named this the vanilloid receptor-1 (VR1) (Caterina *et al.*, 1997). However, the nomenclature has since been updated and the receptor is currently known as TRPV1 (Clapham *et al.*, 2003). The rat TRPV1 (rTRPV1) cDNA contains an open reading frame of 2514 nucleotides and encodes a protein of 838 amino acids with a molecular mass of 95 kDa. At the N-terminus, TRPV1 has three ankyrin repeat domains and the carboxyl terminus has no recognisable motifs (Figure 1.14). The predicted membrane topology of TRPV1 features six transmembrane domains and a possible pore-loop between the fifth and the sixth membrane-spanning regions (Caterina *et al.*, 1997).

TRPV1 is thought to form a homo- or heterotetrameric channel with a pore, however evidence is scarce. Immunoprecipitation studies of differently tagged TRPV1 subunits in heterologous expression systems and DRG neurones favour the formation of homo-tetramers (Kedei *et al.*, 2001).

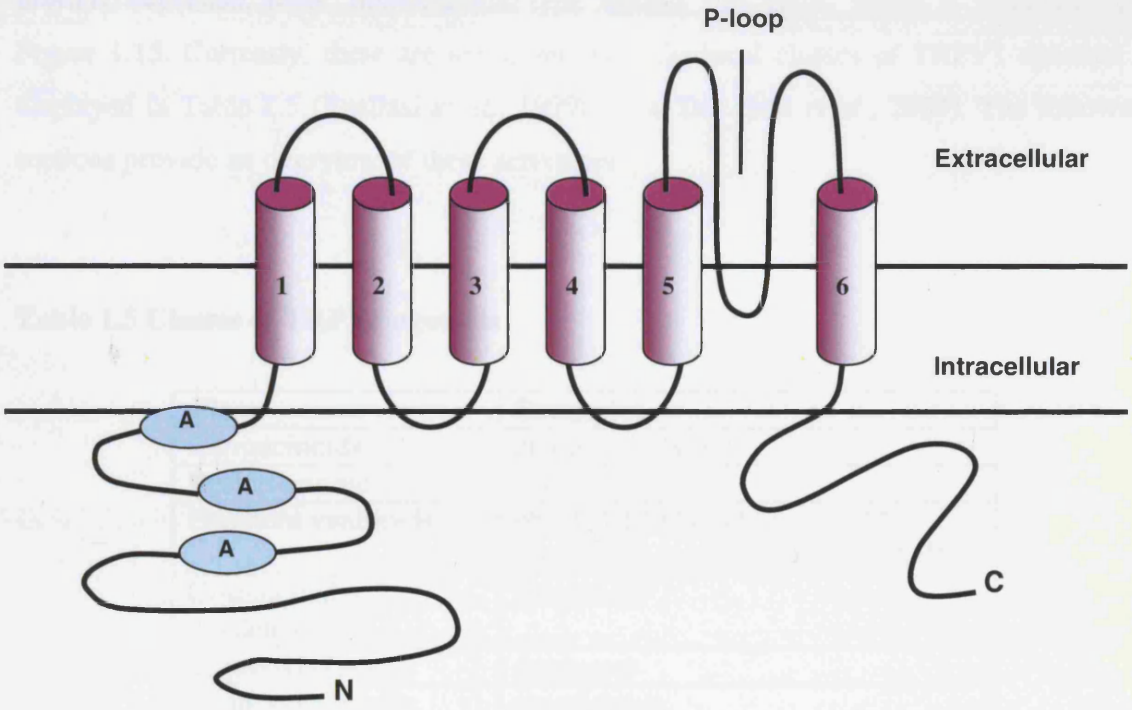


**Figure 1.14 Predicted topology of a TRPV1 subunit**
*TRPV1 consists of six transmembrane domains with three ankyrin repeat domains at the N-terminal. TRPV1 is thought to be tetrameric with a channel pore allowing the influx of sodium and calcium ions.*

More recently, GlaxoSmithKline (Hayes *et al.*, 2000) cloned human vanilloid receptor-1 (hTRPV1) cDNA which was expressed in *Xenopus* oocytes and human embryonic kidney (HEK293) cells. The cDNA contains a 2517 bp open reading frame with 839 amino acids and 92% homology to rTRPV1. In 2001, McIntyre *et al.* and Cortright *et al.*, also cloned hTRPV1 cDNA which encoded a 839 amino acid protein which was expressed in *Xenopus* oocytes and CHO cells and displayed a 85% identity to rTRPV1 (Cabral *et al.*, 2001; Cortright *et al.*, 2001; McIntyre *et al.*, 2001). Generally, hTRPV1 is highly expressed in human DRG neurones, particularly the small to medium diameter cells, with relatively low levels in a variety of brain regions such as the cerebellum and hippocampus (Hayes *et al.*, 2000). Expression was also found in peripheral tissues including the kidney, pancreas and bladder. These results agree with findings from rTRPV1 expression profiles (Sanchez *et al.*, 2001).

### 1.6 Activators of TRPV1

TRPV1 is a complex receptor in that it has many activators including noxious heat, protons, capsaicin, RTX, non-vanilloid-type ligands and lipids, which is summarised in Figure 1.15. Currently, there are seven reported chemical classes of TRPV1 agonists as displayed in Table 1.5 (Szallasi *et al.*, 1999b; Van Der Stelt *et al.*, 2004). The following sections provide an overview of these activators.

**Table 1.5 Classes of TRPV1 agonists**

| Class | Examples |
|---|---|
| Capsaicinoids | capsaicin, olvanil |
| Resiniferanoids | resiniferatoxin |
| Phorboid vanilloids | phorbol 12-phenyl-acetate, 13-acetate, 20-homovanillate (PPAHV) |
| Unsaturated dialdehydes | isovelleral |
| Triprenyl phenols | scutigeral |
| Endocannabinoids | anandamide |
| Eicosanoids | 12- and 15-(*S*)-hydroperoxyeicosatetraenoic acids, 5- and 15-(*S*)-hydroxyeicosatetraenoic acids, leukotriene $B_4$ |

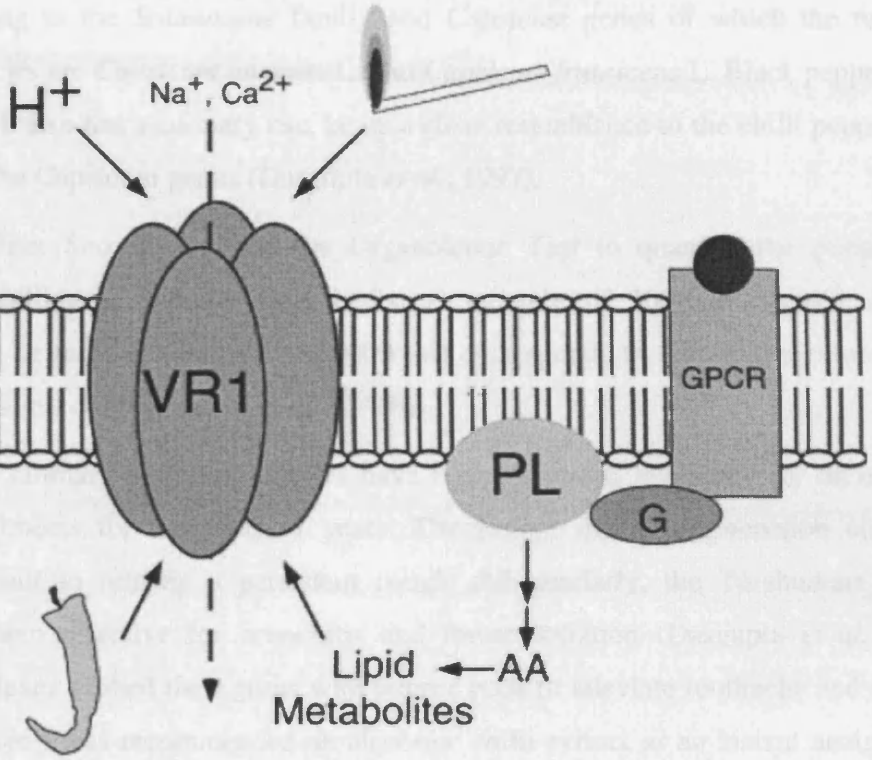


**Figure 1.15 Summary of TRPV1 activators**
*TRPV1 or VR1 subunits are predicted to cluster as a tetramer containing a pore for cationic influx, regulated by multiple pain-producing stimuli. Membrane-permeant second messengers, such as lipid metabolites, may modulate nociceptor activity. Abbreviations: AA=arachidonic acid; G=heterotrimeric G-protein; GPCR=G-protein-coupled receptor; PL=phospholipase. Capsaicin and noxious heat are represented by pepper and flame respectively. Figure obtained from Caterina and Julius (Caterina et al., 2001).*

### *1.6.1 Historical background on capsaicin*

"Hot" peppers or chillies are consumed daily by approximately a quarter of the world's population (Szallasi *et al.*, 1999b). Chillies were cultivated by the inhabitants of the Tamaulipas mountains in Mexico as early as 5000 BC. Christopher Columbus was believed to have introduced chillies to the Old World, that is, Europe and with the aid of Portuguese explorers the culinary use of chillies spread to India (Dasgupta *et al.*, 1997).

Chillies belong to the *Solanaceae* family and *Capsicum* genus of which the two most common species are *Capsicum annuum* L. and *Capsicum frutescens* L. Black pepper, *Piper nigrum*, which also has a culinary use, bears a close resemblance to the chilli pepper but is unrelated to the Capsicum genus (Dasgupta *et al.*, 1997).

In 1912, Wilbur Scoville devised the Organoleptic Test to quantify the pungency or hotness of chillies in Scoville Heat Units. A measure of 300-600 Scoville Units is considered to be mild in contrast to 350000 that corresponds to that of the extremely hot Mexican habanero chilli (Szallasi *et al.*, 1999b).

Besides their culinary purposes, chillies have been exploited medically for an extensive variety of ailments for hundreds of years. The Aztecs drank a concoction containing chillies and salt to remedy a persistent cough and similarly, the Tarahumara Indians considered them effective for bronchitis and throat irritation (Dasgupta *et al.*, 1997). Native Americans rubbed their gums with pepper pods to alleviate toothache and in 1850, the Dublin Free Press recommended an alcoholic chilli extract as an instant analgesic for sore teeth (Szallasi *et al.*, 1999b).

Chilli peppers have also been employed for defence, which is illustrated by the Incas burning dried chillies to temporarily blind invading Spaniards. Today, pepper sprays are widely available to law enforcement officials and the general public for self-defence in the United States (Szallasi *et al.*, 1999b).

Capsaicin, the pungent component in chillies, was isolated by Thresh in 1846 who predicted that the structures of capsaicin and vanillin were closely related. Högyes (1878) proposed that an extract of *Capsicum*, acts selectively on sensory neurones to promote a sensation of pain and trigger heat loss through sweating (Szallasi *et al.*, 1999b). In 1919, Nelson determined the chemical structure of capsaicin to be an acylamide derivative of homovanillic acid, 8-methyl-N-vanillyl-6-nonenamide (Nelson, 1919). Capsaicin possesses a (homo)vanillyl group as a structural motif and thus is also termed a vanilloid. Little more

was learned about capsaicin until Janscó demonstrated that capsaicin not only activates sensory neurones but also renders animals resistant to painful stimuli by exerting a long-term sensory receptor-blocking action called desensitisation (Jancso *et al.*, 1967). Consequently, capsaicin sensitivity has proven to be an extremely useful functional marker for sensory neurones that detect unpleasant or painful (noxious) stimuli (Szallasi *et al.*, 1999b).

### *1.6.2 Capsaicin-sensitive primary afferent neurones*

Capsaicin sensitivity is considered to be a principal pharmacological trait of a major subpopulation of nociceptive sensory neurones, the somata of which are located in DRG, trigeminal and nodose ganglia (Holzer, 1991). Most capsaicin-sensitive nociceptors are C-fibres (Jancso *et al.*, 1977; Szolcsanyi, 1977) and are peptidergic and non-peptidergic (Holzer, 1991) but a small population consists of Aδ fibres (Nagy *et al.*, 1983). Unsurprisingly, the skin, cornea and mucous membranes of the mouth are rich in capsaicin-sensitive neurones. Additionally, capsaicin-sensitive neurones innervate the muscles, joints and visceral organs in the cardiovascular, respiratory and genitourinary systems (Caterina *et al.*, 2001). Visceral capsaicin-sensitive neurones are implicated in both reflex autonomic responses to the conscious perception of visceral discomfort and to visceral stimuli including changes in blood flow, heart rate or respiratory rate (Ness *et al.*, 1990). Some neurones in the preoptic hypothalamus have been reported to exhibit capsaicin sensitivity. It has been proposed that these cells represent "warm" receptors involved in the regulation of core body temperature (Hori, 1984; Jancso-Gabor *et al.*, 1970).

### *1.6.3 Capsaicin effects on sensory neurones*

For decades, capsaicin has been utilised to identify pain-sensitive neurones and to investigate the role of this class of neurone in the healthy organism or their contribution to disease states. Excitation, desensitisation and neurotoxicity are the characteristic effects of capsaicin. Capsaicin excitation results in the depolarisation of sensory neurones by the influx of sodium and calcium ions (Caterina *et al.*, 2001) and vanilloid-sensitive neurones transmit noxious information (perceived as pain or itching) to the CNS (afferent function). Peripheral terminals of these neurones release proinflammatory neuropeptides (efferent function), which are thought to be involved in initiating the cascade of neurogenic inflammation (Szallasi *et al.*, 1999b). Among sensory neuropeptides, the tachykinin

substance P displays the best correlation with vanilloid sensitivity (Holzer, 1991). As some small diameter sensory neurones are polymodal nociceptors, neurones with Aδ-fibres may function as mechanoheat-sensitive nociceptors. Thus, vanilloid-sensitive neurones are heterogeneous morphologically, neurochemically and functionally and they encompass several subclasses of DRG neurones (Szallasi *et al.*, 1999b).

The algogenic substance bradykinin is able to recruit intermediate-size neurones (240-320 $\mu m^2$), normally unresponsive to capsaicin, to respond to vanilloids. This illustrates that vanilloid sensitivity is a plastic property of DRG neurones (Stucky *et al.*, 2001). Consequently, the number of nociceptors that innervate inflamed tissue increases and may play an important role in the development of inflammatory hyperalgesia (Szallasi *et al.*, 1999b).

Vanilloid-sensitive neurones are also activated by a variety of chemical stimuli in which some of these compounds, including histamine and bradykinin, have their own receptors. Others including xylene and mustard oil are thought to function in a non-receptor-mediated manner, possibly by perturbing membranes (Jancso *et al.*, 1968).

### *1.6.4 Capsaicin effects in whole animals*

In adult rats small systemic capsaicin doses cause an initial excitation of sensory neurones followed by desensitisation while larger doses produce depletion of C-fibres (Winter *et al.*, 1995). The degree of capsaicin neurotoxicity is high in neonatal rats (Scadding, 1980) resulting in a loss of more than half the C-fibres whereas the loss was relatively minor in adult rats (Jancso *et al.*, 1985). Large capsaicin doses applied to neonatal rats were neurotoxic and sensitivity to noxious stimuli was often permanent. In adult rats that were treated neonatally with capsaicin, analgesia to noxious mechanical, chemical stimuli, or both were observed. In contrast, the responses to a thermal challenge were not consistent, with some reports of an increase in thermal nociceptive thresholds and in others there was no change. Similarly in mice, significant analgesia to chemical but not thermal stimuli occurred. On the contrary, capsaicin administered locally revealed a reduction, an increase or no effect on nociceptive thresholds in rats. The variability in results was thought to be contributed by differences in application and could affect the rate and extent of skin penetration (Winter *et al.*, 1995).

Capsaicin sensitivity varies between species; in particular, birds do not display capsaicin sensitivity while guinea pigs are extremely sensitive. This could be to deter particular

animals such as mammals, from ingesting the plant while birds are probably insensitive in order to disperse seeds. The described sensitivity was shown in acute toxicity studies (Glinsukon *et al.*, 1980) and was also discussed by Jordt and coworkers who cloned chicken TRPV1 from DRG. They found that the avian receptor was activated by noxious heat and protons but not by capsaicin and AEA. As previously mentioned, this suggests that capsaicin and AEA activation was a more recent acquisition to TRPV1's characteristics (Jordt *et al.*, 2002).

### *1.6.5 Resiniferatoxin*

The latex of the Moroccan cactus-like plant, *Euphorbia resinifera*, contains an extremely irritant constituent. It was only in 1975 that this compound was isolated and named resiniferatoxin (RTX) (Hergenhahn *et al.*, 1975). RTX shares structural features of two classes of natural irritants; phorbol esters and capsaicinoids. Recently, RTX has been identified as a potent capsaicin agonist at TRPV1. Although RTX did bind to PKC, this low-affinity interaction could not explain its extreme pungency. Like capsaicin, RTX is termed a vanilloid as it possesses a (homo)vanillyl group as a structural motif essential for bioactivity despite differences in the rest of the molecule (Figure 1.16) (Szallasi *et al.*, 1999b). RTX's ultrapotency predicted the existence of high-affinity specific [$^3$H]RTX binding in rat DRG membranes and this was demonstrated by Szallasi and Blumberg in 1990 (Szallasi *et al.*, 1990). Importantly, this was the first firm evidence for the existence of a vanilloid binding site (Szallasi *et al.*, 1999b). RTX's potency as an agonist is several thousand-fold higher than capsaicin in rat DRG neurones (Acs *et al.*, 1996) but was only a few-fold more potent in investigations on recombinant TRPV1 (Caterina *et al.*, 1997; Jerman *et al.*, 2000). In addition, RTX is non-pungent in contrast to capsaicin, thus RTX is considered an attractive candidate in the pain clinic.

An analogue of RTX called PPAHV was originally synthesised with the aim of producing a less pungent therapeutic drug in comparison to capsaicin. PPAHV is slightly pungent with anti-nociceptive and anti-inflammatory properties and is equipotent with capsaicin in binding to rat DRG (Appendino *et al.*, 1996). Later investigations on recombinant rat and human TRPV1 expressed in HEK293 cells revealed PPAHV as a full agonist at rat (Jerman *et al.*, 2000) but either no activity (McIntyre *et al.*, 2001) or reduced potency at human was reported (Smart *et al.*, 2001). This suggests that there is a difference in the agonist binding site between species. Like capsaicin, PPAHV is capable of causing desensitisation against

neurogenic inflammation in adult rats. However, unlike capsaicin, PPAHV is unable to produce a hypothermic response which again suggests differences in action (Appendino *et al.*, 1996).

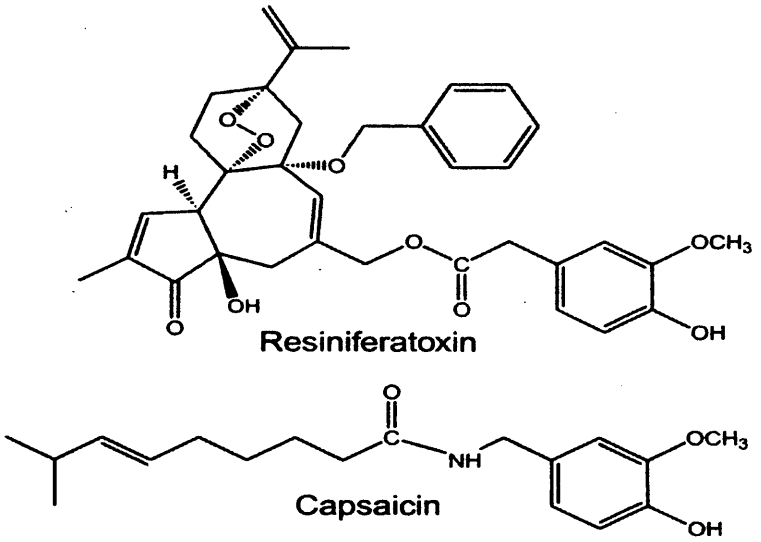


**Figure 1.16 Chemical structures of capsaicin and resiniferatoxin**

### *1.6.6 Non-vanilloid type activators*

Naturally-occuring compounds such as sesquiterpene unsaturated dialdehydes (polygodial and warburganal) are pungent and appear to stimulate sensory neurones in a vanilloid receptor-mediated fashion (Sterner *et al.*, 1999). Polygodial also displays anti-allergic and anti-inflammatory effects and blocks tachykinin NK-2 receptors, which suggests that these tachykinin receptors are involved in these effects (Tratsk *et al.*, 1997).

Like capsaicin, the fungal terpenoid unsaturated dialdehyde isovelleral causes protective eye-wiping movements in the rat upon intraocular instillation (Szallasi *et al.*, 1996b). However, isovelleral was inactive but interestingly displayed competitive antagonism against capsaicin- and RTX-stimulated calcium responses at both recombinant rat and human TRPV1 (Jerman *et al.*, 2000; Smart *et al.*, 2001). This suggests that isovelleral's activities are not necessarily vanilloid-mediated despite showing similar effects to capsaicin in rat sensory neurones (Szallasi *et al.*, 1996b).

The most commonly known triprenyl phenol is scutigeral, a non-pungent compound found in *Albatrellus ovinus* mushrooms. Scutigeral induced calcium uptake by rat DRG neurones,

could be blocked by both capsazepine and ruthenium red (Szallasi *et al.*, 1999a). In constrast, scutigeral was inactive at recombinant human TRPV1 expressed in HEK293 cells (Smart *et al.*, 2001).

The eicosanoids, 12- and 15-(*S*)-hydroperoxyeicosatetraenoic acids (12S- and 15S-HPETE), are derived from arachidonic acid. 12S-HPETE is produced endogenously in sensory neurones following stimulation with bradykinin and this suggests this eicosanoid plays a role in inflammatory pain (Shin *et al.*, 2002). These metabolites have demonstrated vanilloid activity comparable to capsaicin in neonatal rat DRG neurones (Hwang *et al.*, 2000). As these compounds are highly unstable, pharmacological data (*in vivo* or *ex vivo*) on TRPV1-mediated responses relating to hyperalgesia are currently unavailable.

### *1.6.7 Heat*

It is a fact that TRPV1 functions as a molecular transducer of noxious thermal stimuli *in vivo* based on observations of heterologous non-neuronal systems. Whereas numerous proteins, including receptors and channels, display structural or activity modifications as a function of temperature, TRPV1's thermal response is related to nociception. TRPV1 is only gated by temperatures exceeding ~43°C up to ~49°C (Tominaga *et al.*, 1998), a threshold matching that of heat-evoked pain responses in humans and animals or heat-evoked electrophysiological responses in primary afferent nerve fibres or cultured sensory neurones (Cesare *et al.*, 1996; LaMotte *et al.*, 1978; Raja *et al.*, 1999).

Sensitivity to capsaicin and noxious heat are also well correlated among small-diameter sensory neurones in culture (Kirschstein *et al.*, 1999; Nagy *et al.*, 1999a; Nagy *et al.*, 1999b). Also, TRPV1 and native heat-evoked currents share a number of properties, including similar current-voltage relationships, selective permeability to cations (Cesare *et al.*, 1996; Nagy *et al.*, 1999b; Reichling *et al.*, 1997) and in some reports, sensitivity to vanilloid receptor antagonists (Kirschstein *et al.*, 1999). The correlation between sensitivity to heat and capsaicin support a direct relationship between TRPV1 expression and heat sensitivity in human TRPV1-transfected HEK293 cells ($HEK293_{hTRPV1}$). Capsaicin and heat responses also exhibit cross-desensitisation and the vanilloid receptor antagonists, capsazepine and ruthenium red diminish both capsaicin- and heat-evoked currents. Also, both responses are characterised by relatively high permeability to calcium ions and outwardly rectifying current-voltage relationships. Capsaicin or heat evoked single channel currents in excised membrane patches from $HEK293_{TRPV1}$ cells and sensory

neurones, demonstrated that activation does not require diffusable cytoplasmic second messengers (Tominaga *et al.*, 1998). Modifying capsaicin potency or thermal activation thresholds *via* site-specific mutations in TRPV1 expressed in heterologous cells, supply further evidence that TRPV1 transduces responses to both these stimuli (Jordt *et al.*, 2000).

However, discrepancies between native heat- and vanilloid-evoked responses have been reported, including differences in relative permeability to calcium and sodium ions (Cesare *et al.*, 1996; Nagy *et al.*, 1999b) and sensitivity to vanilloid receptor antagonists (Nagy *et al.*, 1999b; Reichling *et al.*, 1997) which suggests that vanilloids and heat activate TRPV1 through overlapping but separate mechanisms. Also, the amplitudes of the capsaicin- and heat-evoked responses among individual sensory neurones are not well correlated, contrary to the expected responses at the same channel. In addition, capsaicin- and heat-evoked responses displayed poor co-sensitivity in membrane patches excised from cultured rat sensory neurones despite that most patches were sensitive to capsaicin or heat (Nagy *et al.*, 1999b).

Consequently, Nagy and Rang proposed that functional isoforms of TRPV1 resulting from alternative RNA splicing, post-translational modification or association with other cellular proteins could respond to capsaicin and heat (Nagy *et al.*, 1999b). Unfortunately, these issues have not been resolved.

Expression of multiple forms of heat-activated channels in individual sensory neurones that differ in their biophysical or pharmacological properties may explain some of the above discrepancies. This is illustrated by a TRPV1 homologue: vanilloid receptor-like 1 (VRL-1 or TRPV2), which is insensitive to capsaicin or protons but responds to high threshold heat stimuli (>50°C) (Caterina *et al.*, 1999). This threshold is similar to that for a subset of medium- to large-diameter sensory neurones in culture and for some thin myelinated (Aδ) nociceptors *in vivo*. TRPV2 expression within rat and mouse sensory ganglia is generally restricted to neurones with these same anatomical properties. Caterina and Julius proposed that TRPV2 detects the "high-threshold" thermal sensitivity of this subset of nociceptors while TRPV1 distinguishes moderate-intensity heat stimuli in small-diameter, unmyelinated (C-fibre) nociceptors. However, their proposal is generally based on correlative evidence, due to lack of selective and potent pharmacological agents to investigate vanilloid receptors *in vivo* (Caterina *et al.*, 2001).

### *1.6.8 Protons*

Infection, inflammation or ischaemia generate an array of chemical mediators that activate or sensitise nociceptor terminals to elicit pain and promote tenderness at the site of tissue injury (Levine *et al.*, 1994). Protons play a role in this pro-algesic response, reducing the extracellular pH below the physiological norm. In cultured sensory neurones, extracellular protons elicit both transient and sustained excitatory responses, the latter of which is thought to account for persistent pain associated with local tissue acidosis (Bevan *et al.*, 1994). Protons or low pH can modulate the activity of various receptors and ion channels expressed by primary afferent nociceptors, including acid-sensitive ion channels (ASICs) of the degenerin family (Waldmann *et al.*, 1997b), ATP-gated channels (Li *et al.*, 1997) and vanilloid receptors (Caterina *et al.*, 1997). It is unknown which, if any, of these contribute to acid-evoked pain, however, electrophysiological and genetic studies of native and cloned vanilloid receptors imply that they function significantly in mediating sustained proton responses *in vivo* (Caterina *et al.*, 2001). In both TRPV1-expressing mammalian cells and *Xenopus* oocytes, moderately acidic conditions can enhance capsaicin-evoked responses by increasing agonist potency ($EC_{50}$ of 90 nM at pH 7.4 versus 36 nM at pH 6.4) without altering efficacy (Caterina *et al.*, 1997; Jordt *et al.*, 2000; Tominaga *et al.*, 1998). Significantly, extracellular protons also potentiate heat-activated currents (Tominaga *et al.*, 1998). In TRPV1-expressing oocytes or HEK293 cells, temperature response curves revealed that a decrease in extracellular pH creates distinctly larger inward currents at temperatures that are noxious to mammals (>43°C). In addition, heat sensitisation occurs whereby the threshold for channel activation is significantly decreased allowing substantial currents to occur at temperatures as low as 35°C, conditions under which the channel is normally closed. This increase of TRPV1 thermal responsiveness by protons resembles the increase in nociceptor thermal sensitivity associated with inflammation (Handwerker *et al.*, 1991). In both cases, a major decrease in the threshold for heat-evoked responses occurs and an increase in response levels results at temperatures above the initial pain threshold. Crucially, TRPV1 displays dynamic modulation of heat-evoked currents between pH 6-8, a sensitivity range that matches the degree of local acidosis achieved during most types of tissue injury, for example, sunburn injuries (Jordt *et al.*, 2000).

It is unknown whether these proton-evoked responses result from a decrease in the channel's thermal response threshold or involve additional processes. However, proton-evoked channel activation and proton-mediated potentiation can be functionally uncoupled

as suggested by structure-function studies (Jordt *et al.*, 2000). Also, extracellular protons are believed to increase the probability of channel opening (Baumann *et al.*, 2000; Tominaga *et al.*, 1998). Acidic solutions induced ionic currents when applied to outside-out, but not inside-out, membrane patches excised from $HEK293_{TRPV1}$ cells. This implies that protons interact with an extracellular site(s) on the channel complex (Tominaga *et al.*, 1998). Possible TRPV1 sites for such interactions include two glutamate residues at positions 600 and 648, located by site-directed mutational analysis (Jordt *et al.*, 2000). The former residue is positioned between the putative fifth transmembrane domain and the pore loop. Introduction of neutral or positive residues at this site increased capsaicin or heat responses of TRPV1-expressing cells. For example, E600Q mutant (neutral charged residue) channels produced a >10-fold increase in sensitivity to capsaicin (no change in efficacy) while E600K (postively charged residue) mutants revealed a significant decrease in thermal activation threshold (30-32°C). In contrast, introduction of a more acidic residue (E600D) decreased sensitivity to capsaicin and heat. Hence, position 600 appears important in determining the pH sensitivity range of channel activation by noxious stimuli. Site 648 (located in the putative third extracellular loop) in oocyte mutants produced insensitivity to low pH (4.0) activation while sensitivity to capsaicin, heat and proton-mediated potentiation of these stimuli remained intact (Jordt *et al.*, 2000).

### *1.6.9 Lipids*

Interestingly, various lipid-derived second messengers, including arachidonic acid, structurally resemble capsaicin suggesting that TRPV1 may be activated by an endogenous ligand of this type (Figure 1.17). Currently, controversy exists over TRPV1 activation or alteration of TRPV1 sensitivity to other stimuli by endogenous capsaicin-like ligands.

One favourable argument comes from *in vitro* ocular phototransduction studies in the fruit fly, *Drosophila*, in which its TRP channels can be activated by polyunsaturated fatty acids (PUFAs) including arachidonic and linoleic acid (Chyb *et al.*, 1999). Also, heterologously expressed mammalian TRPC3 and TRPC6 channels can be activated by DAG, further implicating lipids as potential *in vivo* regulators of TRP channel function (Hofmann *et al.*, 1999).

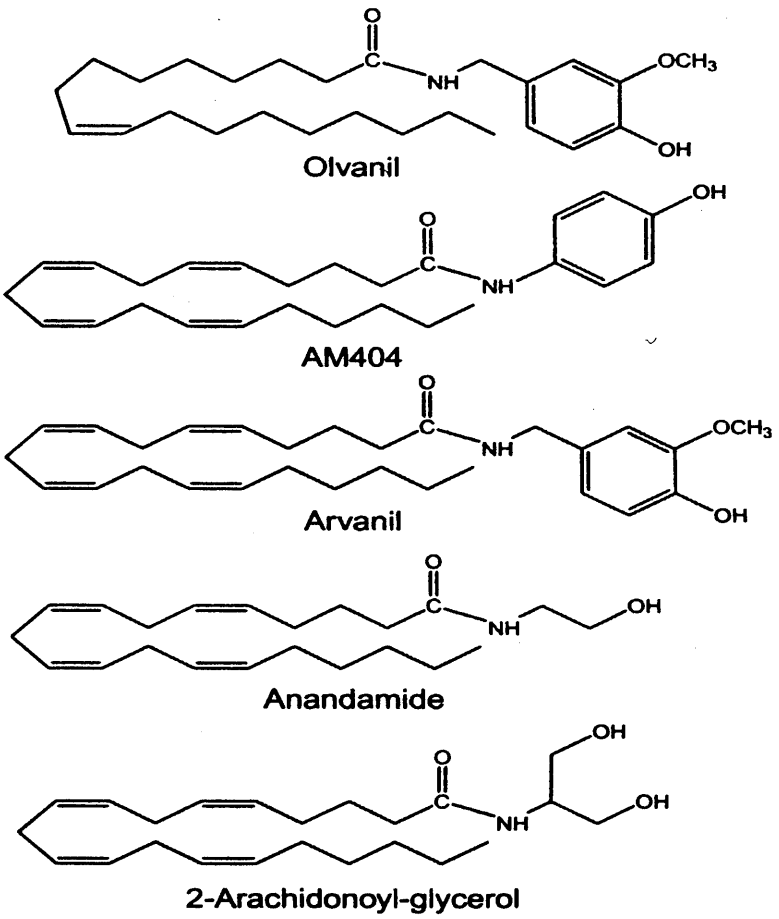


**Figure 1.17 Chemical structures of potential lipid TRPV1 ligands**

Additional evidence comes from structural and functional connections between cannabinoid and vanilloid receptor pharmacology. For example, synthetic vanilloid receptor ligands, such as olvanil or other long-chain *N*-acyl-vanillyl amides, bear structural similarity to the endogenous cannabinoid receptor agonist anandamide (arachidonylethanolamide), also abbreviated as AEA. Olvanil also resembles AM404, a synthetic AEA transport inhibitor and both block reuptake of AEA into cells (Beltramo *et*

*al.*, 1999; Melck *et al.*, 1999). This suggests that some cannabinoid receptor ligands may interact with vanilloid receptors (Zygmunt *et al.*, 2000; Zygmunt *et al.*, 1999). These compounds are significantly less potent than capsaicin and elicit responses with somewhat slower kinetics but both evoke outwardly rectifying, nonselective cationic currents in HEK293 cells or *Xenopus* oocytes expressing TRPV1. These responses appear to be specific because they are inhibited by capsazepine but not by cannabinoid receptor antagonists and a number of other synthetic or endogenous cannabinoid receptor agonists have little or no effect on TRPV1 function.

AEA is able to activate TRPV1 in both native and recombinant expression systems, however, AEA is relatively less potent than capsaicin and displays differences in efficacy depending on the cell and assay type. This has led to questions over whether or not AEA is the endogenous ligand at TRPV1 (Van Der Stelt *et al.*, 2004). PUFAs or structurally related metabolites are produced *in vivo* through enzymatic cleavage of membrane lipids and their access to receptors within the same or adjacent cells may occur with significantly higher efficiency, particularly if much of the action is confined to the hydrophobic environment of the bilayer. Also, under inflammatory conditions, AEA and other lipid messengers may be released from macrophages and endothelial cells into a confined intercellular space such that the local concentrations of these compounds maybe sufficiently high enough to activate TRPV1 (Caterina *et al.*, 2001).

AEA produces analgesia with potency in the nanomolar range and inhibits release of calcitonin gene-related peptide (CGRP) in the skin through its actions at cannabinoid receptors. These findings have led some to argue that AEA exerts its actions on sensory neurones *via* cannabinoid receptors alone, without the involvement of vanilloid receptors (Szolcsanyi, 2000). However, AEA may interact with TRPV1 to produce physiological effects that are distinct from those mediated *via* cannabinoid receptors. AEA was found to produce vasodilation *via* interaction with sensory neurones containing TRPV1. AEA-evoked vasodilation was sensitive to the TRPV1 antagonist capsazepine but not to the $CB_1$ antagonist SR141716A. Other endogenous $CB_1$ agonists, including 2-arachidonoylglycerol, could not mimic the action of AEA (Zygmunt *et al.*, 1999). In addition, AEA mediates other non-$CB_1$ effects in transgenic mice lacking $CB_1$ where cannabimimetic activity was retained (Di Marzo *et al.*, 2000).

### *1.6.10 Ethanol*

Trevisani and colleagues noted the common observation that alcohol induces a 'burning' sensation in patients with oesophagitis and skin wounds and examined the effects of ethanol on the TRPV1 receptor. Ethanol (0.1-3%) enhanced the response of TRPV1 to agonists, such as capsaicin, and potentiated the activating effects of protons, AEA, and heat, as measured by calcium influx. Ethanol also reduced the temperature activation threshold of TRPV1 and induced tachykinin-dependent plasma extravasation *via* TRPV1 activation. These findings supported a role of TRPV1 receptors in visceral pain and inflammation aggravated by alcohol (Trevisani *et al.*, 2002).

## 1.7 Binding site of TRPV1

TRPV1 is a polymodal detector of noxious thermal and chemical stimuli including capsaicin, heat (~43°C) and low pH/protons. However, the site of activation is controversial. Previously, capsaicin was thought to bind to an extracellular site on TRPV1 but recently, the site has been argued to be at an intracellular domain. Observations of a significant delay between capsaicin addition and activation suggest slow diffusion or a membrane partition process prior to TRPV1 binding. Acid and heat stimuli exhibited no delay in gating currents but activation by all three stimuli produced a relatively slow increase to peak (Davis *et al.*, 2000; Gunthorpe *et al.*, 2000). Also, patch clamp studies applying a capsaicin analogue, DA-5018, to the inner surface of the membrane patch in cultured TRPV1-expressing primary sensory neurones or oocytes elicited a current. TRPV1 was only activated intracellularly in a concentration-dependent manner. Oocyte expression of a N-terminal splice variant of rat TRPV1 (rTRPV1) lacking the majority of the intracellular N-teminal, was unresponsive to capsaicin (Schumacher *et al.*, 2000). Furthermore, as capsaicin, capsazepine and RTX are lipid soluble compounds and are able to permeate the cell membrane, this encourages the argument for an intracellular site.

Capsaicin can activate TRPV1 when applied to either side of an excised membrane patch, which is consistent with the idea that vanilloids can permeate the lipid bilayer to mediate their effects (Caterina *et al.*, 1997). Recent electrophysiological studies utilising hydrophilic capsaicin derivatives suggest that vanilloids interact with an intracellular site on TRPV1 but specific ligand binding domains have not been mapped (Jung *et al.*, 1999). In addition, Vyklicky and colleagues suggested that there is at least one extracellular site,

as well as the intracellular site, which both need to be occupied to activate the channel (Vyklicky *et al.*, 2003).

Although capsazepine blocks the actions of both capsaicin and AEA, it is unknown whether these compounds compete for binding to the same site. While capsaicin potency is enhanced under moderately acidic (pH 6.4) conditions (Caterina *et al.*, 1997; Tominaga *et al.*, 1998), this appears not to be the case for AEA (Smart *et al.*, 2000a). This suggests that these agonists interact with TRPV1 in different ways.

## 1.8 Antagonists

To date, only one antagonist, capsazepine (Figure 1.18), has been extensively investigated (Bevan *et al.*, 1992). Capsazepine was developed for the investigation of structure-activity requirements for vanilloid-like activity (Walpole *et al.*, 1994). Capsazepine competitively inhibits vanilloid responses. In addition, capsazepine competes for specific RTX binding sites in a competitive manner (Bevan *et al.*, 1992). The utility of capsazepine is however, limited by its moderate and variable potency (see later for further information) and is nonspecific in that it antagonises voltage-sensitive calcium channels (VSCCs) (Docherty *et al.*, 1997) and nicotinic receptors (Liu *et al.*, 1997).

Efforts have been directed at the development of novel antagonists and this has resulted in the potent rTRPV1 antagonist, 5'-iodo-resiniferatoxin (iodo-RTX), Figure 1.18. Iodo-RTX was found to inhibit capsaicin-induced membrane currents in *Xenopus* oocytes expressing rTRPV1 and was also forty-fold more potent than capsazepine. Intrathecal administration of iodo-RTX blocked the acute pain response to capsaicin injections in *in vivo* murine studies (Wahl *et al.*, 2001). Wang and colleagues designed rTRPV1 antagonists, KJM429 and JYL1421 (Figure 1.18), in which the latter was sixty-fold more potent than capsazepine. Studies were performed in a recombinant CHO cell system and both antagonists blocked the action of capsaicin, heat and protons (Wang *et al.*, 2002).

One approach for novel analgesics includes desensitisation of C-fibre sensory neurones in which TRPV1 antagonists can complement this strategy. Because of the long desensitisation period after TRPV1 agonist treatment, antagonists may be useful when short-term inhibition of TRPV1 is required.

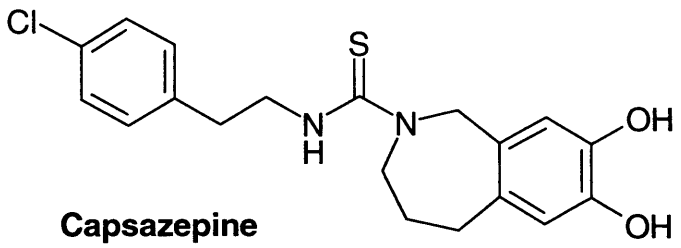


**Capsazepine**

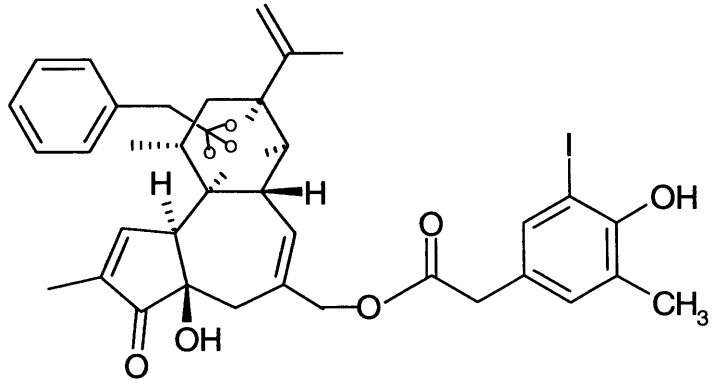


**Iodo-RTX**

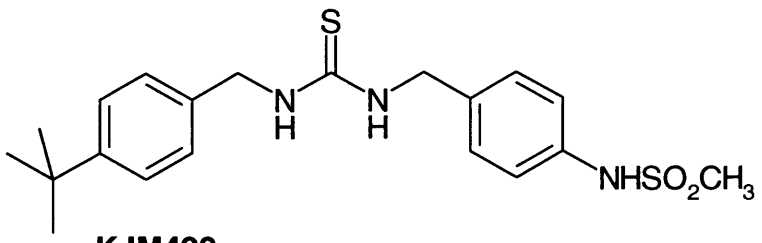


**KJM429**

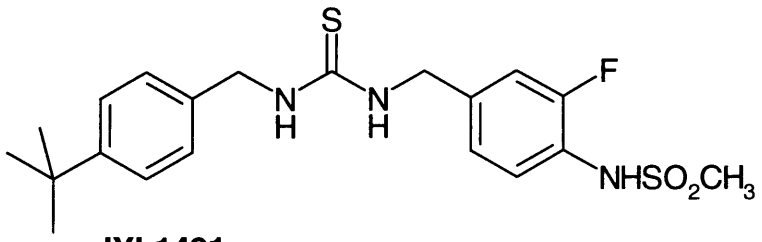


**JYL1421**

**Figure 1.18 Examples of TRPV1 antagonists**

## 1.9 Genetic Analysis of TRPV1

The studies described above present a strong argument for the involvement of TRPV1 not only in the actions of vanilloid compounds but also in sensory responses to noxious heat, acid stimuli and possibly endogenous lipids. One direct approach utilises "knockout" mice in which the TRPV1 gene is disrupted (Caterina *et al.*, 2000; Davis *et al.*, 2000). Despite the absence of TRPV1, sensory ganglion development (as assessed by the presence of several histological markers) is apparently unaltered in these animals. Functionally, however, disruption of the TRPV1 gene produces a range of specific defects related to nociception as described below.

*Deficits in cellular physiology and acute nociception*

Neurones from the DRG of TRPV1-null mice displayed no vanilloid-evoked electrophysiological responses either in culture or in sensory nerve fibres innervating an excised patch of skin. These mice displayed significant reductions in paw licking and neurogenic inflammation evoked by intraplantar injection of either capsaicin or RTX. Sensory neurones of the trigeminal system also depend on TRPV1 for vanilloid responsiveness: whereas wild-type mice avoided the consumption of capsaicin-containing water, littermates lacking TRPV1 exhibited no such aversion. Moreover, TRPV1-null mice failed to exhibit hypothermia observed in wild-type mice after subcutaneous injection of capsaicin. These data show that TRPV1 is required for transducing the nociceptive, inflammatory and hypothermic effects of vanilloid compounds.

The participation of TRPV1 in proton-evoked nociceptive responses is supported by data from *in vitro* assays. Whereas 30% of cultured wild-type DRG neurones displayed large, sustained current responses after exposure to acidic media, <7% of neurones from TRPV1-null mice displayed such responses. These results were mirrored in skin nerve preparations, in which the absence of TRPV1 resulted in a ~90% reduction in the number of acid-sensitive C-fibre nociceptors. Thus, the residual proton-evoked responses in TRPV1-null mouse C-fibres are possibly mediated by members of the ASIC family (Chen *et al.*, 1998; Lingueglia *et al.*, 1997; Waldmann *et al.*, 1997a; Waldmann *et al.*, 1997b). These proteins are part of a superfamily of channels that includes the amiloride-sensitive epithelial sodium channels, peptide-gated ion channels from snails and degenerins. At least four genes encoding ASIC subtypes have been identified of which many are expressed in sensory afferent neurones (Kellenberger *et al.*, 2002).

## 1.10 Capsaicin and the clinic

Currently, capsaicin solutions and creams can be applied topically for a variety of human pain disorders and are beneficial. The rationale is based on the principle of desensitisation caused by repeated application of capsaicin. The efficacy of capsaicin in treating pain seems to be related to its ability to deplete substance P from local sensory terminals. Minimal systemic absorption occurs after topical application (single or repeated) of effective local concentrations of the drug and no permanent damage to tissues is known to occur in the adult. Capsaicin is effective in controlling spinal detrusor hyperreflexia, a condition in which the micturition reflex is disrupted by spinal cord injury or neurological disorders, such as multiple sclerosis. Capsaicin is utilised by desensitising capsaicin-sensitive C-fibres involved in the micturition reflex, thus reducing the urge to void unnecessarily at low bladder volumes (Szallasi *et al.*, 1999b). Other diseases treated include non-allergic (vasomotor) rhinitis, notalgia paraesthetica and others as shown in Table 1.6.

**Table 1.6 Current clinical uses for topical capsaicin**
Adapted from (Szallasi *et al.*, 1999b).

| Type | Clinical conditions |
|---|---|
| Low concentration (0.025% or 0.075%) for pain relief | Postherpetic neuralgia<br>Diabetic neuropathy<br>Postmastectomy pain syndrome<br>Stump pain<br>Reflex sympathetic dystrophy<br>Trigeminal neuralgia<br>Oral neuropathic pain<br>Osteoarthritis<br>Rheumatoid arthritis<br>Fibromyalgia<br>Guillain-Barré syndrome<br>Meralgia paraesthetica<br>Burning mouth syndrome |
| High-concentration capsaicin creams (10%) to improve pain | Intractable pain due to bilateral peripheral neuropathy |
| Capsaicin creams to relieve itch | Psoriasis<br>Haemodialysis<br>Aquagenic pruritus<br>Vulvar vestibulitis<br>Notalgia paraesthetica<br>Brachioradial pruritus<br>Lichen simplex chronicus |
| Intranasal capsaicin drops (10 mM) | Cluster headache<br>Vasomotor rhinitis<br>Perennial allergic rhinitis |
| Intravesical capsaicin solution (10 mM) | Bladder hypersensitivity<br>Spinal detrusor hyperreflexia |

Therapeutically, capsaicin could be utilised as a non-narcotic analgesic to reduce cancer pain and in particular, neuropathic pain syndromes as the latter are insensitive to traditional pain-killers such as opiates (Szallasi *et al.*, 1996a). Various clinical trials using capsaicin have been undertaken of which some have been summarised in Table 1.7. Two recent developments include a capsaicin product ALGRX 4975 produced by the pharmaceutical company AlgoRX. This product is currently undergoing Phase II clinical development. NeurogesX, Inc. is developing a localised, high concentration capsaicin dermal patch. Their product, NGX-4010, is a synthetic trans-form of capsaicin and is being studied in Phase II and III trials for diabetic neuropathy and HIV-related neuropathy respectively.

**Table 1.7 Capsaicin clinical trials**

| Condition | Route of Administration | Analgesia | Reference |
|---|---|---|---|
| Diabetic neuropathy | Topical | Yes<br>No | (The Capsaicin Study Group, 1991)<br>(Chad *et al.*, 1990) |
| Polyneuropathy | Topical | No | (Low *et al.*, 1995) |
| Post-herpetic neuropathy | Topical | Yes<br>No | (Bernstein *et al.*, 1989)<br>(Watson *et al.*, 1993) |
| Post-trauma neuropathic pain musculoskeletal, post-surgical pain, | Intravenous | | AlgoRX |
| Diabetic neuropathy, post-herpetic neuropathy | Topical | | NeurogesX, Inc. |

Recently Mason performed a meta-analysis of 16 papers in order to review the efficacy and safety of topically applied capsaicin for chronic pain from neuropathic or musculoskeletal disorders, a summary is displayed in Table 1.8. They concluded that capsaicin had poor to moderate efficacy and that it may be useful as an additional or sole therapy for patients who are unresponsive or intolerant to other treatments (Mason *et al.*, 2004).

Capsaicin use in the clinic has been hindered for the following reasons:

1. Topical application, in sufficient doses for complete desensitisation, is difficult due to the initial irritation.
2. Animal and human vanilloid receptors differ in their ligand-binding properties. Capsaicin-sensitive neurones mediate different biological responses in humans and animals, thus extrapolation from animal to human studies should be made with caution.

The ultrapotent capsaicin analog RTX is undergoing clinical trials and has four major advantages over capsaicin:

1. Due to its ultrapotency, RTX may be used at a lower concentration. RTX is ultrapotent for the vanilloid receptor-mediated, desired actions of capsaicin only, but not for its receptor-unrelated side effects.
2. Desensitisation is favoured over irritation, which is the main factor limiting the therapeutic use of capsaicin.
3. RTX has a wider therapeutic range in which a full desensitisation to pain or neurogenic inflammation may be achieved by a single dose, without excessive toxicity.
4. Unlike capsaicin, RTX not only suppresses chemogenic pain, but is effective against noxious heat-evoked pain in normal rats or cold-evoked pain in animals with spinal cord injury.

However, as RTX activates PKC and is structurally similar to phorbol esters, well-known tumour promotors, there is a theoretical risk of tumourigenesis with the use of RTX.

**Table 1.8 Reviewed meta-analysis of capsaicin treatment**
Data were obtained from a recent published review (Mason *et al.*, 2004).

Estimates of efficacy and harm from meta-analysis of randomised controlled trials of capsaicin for treatment of chronic pain associated with neuropathic or musculoskeletal conditions

| Characteristic | No of trials | No of patients | No (%) responding to intervention | | Relative benefit (95% CI)* | Number needed to treat (95% CI)† |
|---|---|---|---|---|---|---|
| | | | Treatment | Placebo | | |
| Efficacy | | | | | | |
| Musculoskeletal pain: | | | | | | |
| At four weeks | 3 | 368 | 70/186 | 46/182 | 1.5 (1.1 to 2.0) | 8.1 (4.6 to 24) |
| Neuropathic pain: | | | | | | |
| At four weeks | 4 | 313 | 91/159 | 64/154 | 1.4 (1.1 to 1.7) | 6.4 (3.8 to 21) |
| At eight weeks | 6 | 656 | 197/331 | 126/325 | 1.4 (1.2 to 1.7) | 5.7 (4.0 to 10) |
| By outcome type: | | | | | | |
| Undefined improvement | 4 | 532 | 179/268 | 128/264 | 1.4 (1.2 to 1.6) | 5.5 (3.6 to 10) |
| Global or percentage pain reduction | 2 | 124 | 18/63 | 8/61 | 2.1 (0.99 to 4.3) | 6.5 (3.4 to 89) |
| By trial size: | | | | | | |
| <40 patients | 2 | 57 | 20/30 | 8/27 | 2.3 (1.2 to 4.2) | 2.7 (1.6 to 7.7) |
| ≥40 patients | 4 | 599 | 177/301 | 126/298 | 1.4 (1.2 to 1.6) | 6.3 (4.2 to 13) |
| Harm | | | | | | |
| Musculoskeletal pain: | | | | | | |
| Local adverse events at four weeks | 3 | 190 | 46/98 | 9/92 | 5.0 (2.6 to 9.6) | 2.6 (2.0 to 3.6) |
| Withdrawals at four weeks‡ | 4 | 398 | 19/203 | 6/195 | 2.5 (1.1 to 5.6) | 16.0 (9.1 to 63) |
| Neuropathic pain | | | | | | |
| Local adverse events at eight weeks | 4 | 300 | 69/154 | 26/146 | 3.2 (2.2 to 4.6) | 2.5 (2.0 to 3.3) |
| Withdrawals at eight weeks‡ | 5 | 503 | 40/253 | 6/250 | 5.5 (2.6 to 12) | 7.5 (5.5 to 12) |
| Combined | | | | | | |
| Local adverse events | 7 | 490 | 127/252 | 35/238 | 3.6 (2.6 to 5.0) | 2.5 (2.1 to 3.1) |
| Withdrawals‡ | 9 | 901 | 59/456 | 12/445 | 4.0 (2.3 to 6.8) | 9.8 (7.3 to 15) |

*Relative risks (95% confidence intervals) for harm.
†Numbers needed to harm (95% confidence intervals) for harm.
‡Related to adverse events.

## 1.11 Aims

There are two main themes to this thesis using a "recombinant receptor strategy" and $[Ca^{2+}]_i$ measurements:

- To perform a comparison of human and rat TRPV1 isoforms in the commonly available expression system (Human Embryonic Kidney; HEK). For this part of the work there are two questions:
  1. Are there differences in potency of the agonists capsaicin, anandamide (AEA) and olvanil and the antagonist capsazepine in $HEK293_{rTRPV1}$ and $HEK293_{hTRPV1}$ cells. Previous experiments have been performed with the FLIPR at room temperature so experiments will be performed at 22°C and the physiological temperature of 37°C.
  2. The endocannabinoid AEA structurally resembles capsaicin and has been found to activate TRPV1. It is unclear whether the major psychoactive exocannabinoid $\Delta^9$-THC (Pertwee, 2001) displays TRPV1 activity. This will be investigated.

- TRPV1 receptors are located on nociceptive afferents and as such the commonly used HEK expression system is highly unphysiological. The cellular background of a kidney cell and a neurone are vastly different. An easy to grow human neuroblastoma cell line, SH-SY5Y has been selected to transfect the human TRPV1 using a number of available strategies. There are two further questions to this section of the work:
  1. Does the hTRPV1 expressed in SH-SY5Y cells display the same pharmacology to $HEK293_{hTRPV1}$? A range of agonists and antagonists will be examined in both FLIPR and simple cuvette-based assays
  2. Are SH-SY5Y cells are capable of the release of noradrenaline? As TRPV1 is $Ca^{2+}$-permeable it is hypothesised that the increase in $[Ca^{2+}]_i$ produced by activation is able to evoke noradrenaline release. This will be studied in simple monolayer culture and using a new perfusion system with which noradrenaline release and $[Ca^{2+}]_i$ can be measured simultaneously.

# 2 MATERIALS & METHODS

## 2.1 Materials

### *2.1.1 Suppliers*

List of suppliers are displayed alphabetically below:

*Amersham Biosciences UK Ltd. (UK)*: l-[7,8-$^{3}$H]Noradrenaline

*Amersham Pharmacia Biotech (USA)*: GFX Micro Plasmid Prep Kit

*BDH Laboratory Supplies (Poole, Dorset BH15 1TO, UK)*: Triton X-100

*Citifluor Ltd. (UK)*: Antifade

*Costar (UK)*: 96-Well black plates for FLIPR assays

*Clontech Laboratories, Inc. (USA)*: NucleoBond plasmid purification kit

*Fisher Chemicals (Leicestershire, UK)*: Folin's reagent, D-glucose, perchloric acid, scintillation fluid – "HiSafe3" and OptiPhase Safe, Trypsin/EDTA Sodium chloride, Sodium hydroxide, Whatman G/F B filters

*Flowgen Bioscience Ltd. (Nottingham, UK):* Seakem ME Agarose

*GlaxoSmithKline (Essex, UK)*: SB-366791 antagonist

*Hayman Ltd. (Witham, Essex CM8 3YE, UK):* Ethanol (Ethyl alcohol)

*Invitrogen (Scotland)*: Foetal bovine serum, Fungizone, L-Glutamine, Penecillin/Streptomycin

*Life Technologies*: SOC media

*Millipore (Bellerica, MA, USA)*: Ultrafree DA-Amicon columns

*Molecular Probes (Oregon, USA)*: Alexa Fluor 466 goat anti-rabbit IgG antibody

*New England Biolabs (MA, USA)*: *Bam*HI, *Bst*XI, *Eco*RV, Ligase (T4), Ligase buffer (T4)

*PerkinElmer Life Sciences, Inc. (549 Albany Street, Boston, MA, USA)*: GTPγ[$^{35}$S]

*Roche Diagnostics (East Sussex, UK)*: *Hpa*I, Restriction enzyme buffers

*Sigma Chemical Co. (Fancy Road, Poole, Dorset, UK)*: Anandamide (N-arachidonoylethanolamine), ATP (Adenosine triphosphate), Bacitracin, bovine serum albumin (BSA), Capsaicin (8-methyl-N-vanillyl-6-nonenamide), Capsazepine (N-[2-(4-Chlorophenyl)ethyl]-1,3,4,5-tetrahydro-7,8-dihydroxy-2H-2-benzazepine-2-carbothioamide), DMSO (Dimethyl sulphoxide), DTT (Dithiothreitol), EGTA (ethylene glycol bis(2-aminoethyl ether)-N,N,N'N'-tetraacetic acid), Fura-2AM (Fura-2 acetoxymethyl ester), GTPγS, Sigmacote, $\Delta^{9}$-THC ($\Delta^{9}$-Tetrahydrocannabinol)

*Teflabs (Texas, USA)*: Fluo-3AM

*Tocris (Bristol, UK)*: All the FLIPR test compounds

*USB (Ohio, USA)*: HEPES (N-(2-Hydroxyethyl)piperazine-N'-(2-ethanesulphonic acid)

### *2.1.2 Cells*

*HEK293 cells*: Recombinant $HEK293_{rTRPV1}$ and $HEK293_{hTRPV1}$ cells were kindly donated by GlaxoSmithKline (Essex, UK).

*SH-SY5Y cells:* Undifferentiated SH-SY5Y human neuroblastoma cells were obtained from Dr. J. Biedler, Memorial Sloane-Kettering Institute for Cancer Research, Rye, NY, USA.

## 2.2 Pharmacological principles and terms

An agonist is able to bind to a receptor, activate it and produce a pharmacological response or effect. The concentration of a drug at which it is effective can be termed potency. For an agonist, potency can be defined by the $pEC_{50}$ value, that is, calculating the negative logarithm of the molar concentration of agonist producing 50% of the maximum response ($EC_{50}$). See Figure 2.1 for a pictorial representation of this.

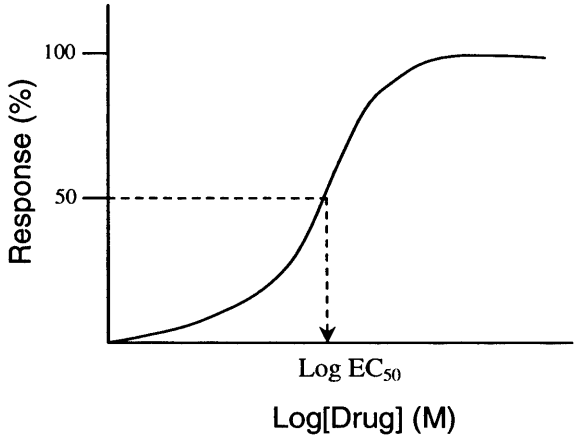


**Figure 2.1 A concentration response graph**
*A semi-log concentration curve is sigmoidal. The log $EC_{50}$ can be read off the graph after obtaining the value relating to 50% of the maximum response (depicted by dashed arrow).*

Efficacy, as a term, was coined by Stephenson to describe the way in which agonists vary in the response they produce despite occupying the same number of receptors (Stephenson, 1956). High-efficacy agonists produce maximal response while occupying a relatively low proportion of receptors. Partial agonists are not able to produce the maximal response regardless of how high the agonist concentration is applied. For further information, the reader is referred to a publication by Colquhoun (Colquhoun, 1998).

An antagonist is able to attenuate the effect of an agonist and this action can be competitive or non-competitive. The former describes when an antagonist binds to a region of the receptor in common with an agonist and binding is reversible or surmountable. Increasing the concentration of agonist, thereby shifting the equilibrium and increasing the proportion

of receptors that the agonist occupies may overcome the effects of a competitive antagonist. The concentration response curve will be shifted to the right with no change in the maximum response.

Non-competitive antagonists bind to an allosteric site on the receptor or an associated ion channel and no amount of agonist can fully overcome the effect once it has been established (insurmountable). The slope and the response seen in the concentration response curve will be reduced. For a review on insurmountable antagonism, the reader is referred to Vauquelin and co-workers (Vauquelin *et al.*, 2002).

As a measure of the potency of a competitive antagonist, $pK_B$ can be used. This is the negative logarithm of the molar concentration, which at equilibrium would occupy 50% of the receptors in the absence of an agonist. In an experiment in which a single concentration of antagonist has caused a parallel shift of the agonist concentration-response curve, an apparent $pK_B$ value can be calculated using the Gaddum-Schild equation assuming a slope of unity:

$$pK_B = -\log\left(\frac{EC_{50antagonist}}{EC_{50control}} - 1\right) \div [Antagonist]$$

Using a Schild analysis, a $pA_2$ value can be calculated (Arunlakshana *et al.*, 1959). With a minimum of three concentrations of an antagonist, a Schild plot of log (concentration ratio – 1) against log (antagonist concentration) can be plotted. The concentration ratio is the concentration of agonist producing a response that is usually 50% of the maximum in the presence of an antagonist, divided by the concentration producing identical response in the absence of antagonist.

If the line on the Schild plot is extrapolated to intercept the log[antagonist] axis, the resulting intercept depicts the $pA_2$ value if the Schild slope is equal to 1 (Figure 2.2). The $pA_2$ is a measure of the potency of an antagonist. It is the negative logarithm of the molar concentration of antagonist that would produce a 2-fold shift in the concentration-response curve for an agonist. Theoretically, the $pA_2$ would be equal to the $pK_B$.

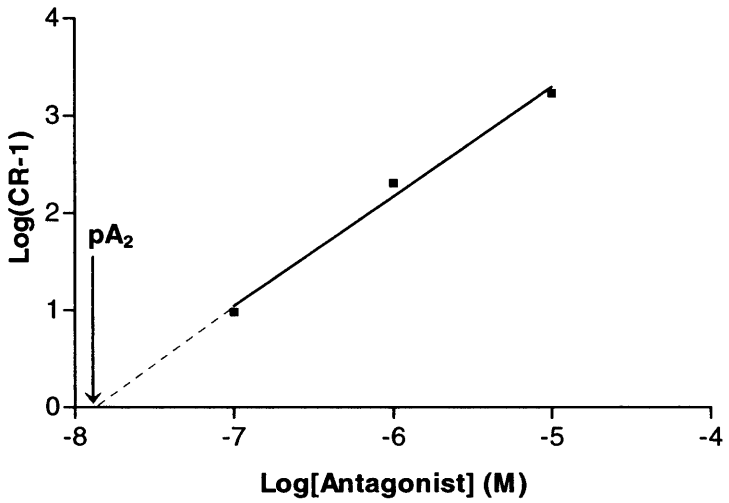


**Figure 2.2 A Schild plot**
*Typical data plotted with log (concentration ratio – 1) or log (CR-1) on the Y-axis against the log of the antagonist concentration on the x-axis. Extrapolating the line (dotted) so that log (CR-1)=0 produces the value for the $pA_2$.*

In addition, competition assays can be performed using a single concentration of ligand. The concentration of competing antagonist, which decreases the agonist response by 50%, is the $IC_{50}$ value. This enables the inhibition constant, that is, the $pK_i$, to be calculated using the Cheng-Prusoff equation (Cheng *et al.*, 1973) and the $EC_{50}$ of the agonist. In this thesis, the fixed concentration of the agonist (L) utilised was its $EC_{80}$ value (effective concentration that produces 80% of the maximum response).

$$pK_i = -\log\left(\frac{IC_{50}}{1+([L]/EC_{50})}\right)$$

The $pK_i$ can be defined as the negative logarithm of the molar concentration of antagonist in a competition assay that would occupy 50% of the receptors if no agonist were present. The $pK_i$ of an antagonist would theoretically equal the $pK_B$ at the same receptor (and therefore also the $pA_2$).

## 2.3 Preparation of buffers and solutions

*Krebs/HEPES*

143 mM NaCl; 11.7 mM glucose, 10 mM HEPES, 4.7 mM KCl, 1.2 mM $KH_2PO_4$, 1.2 mM $MgSO_4$ and 2.6 mM $CaCl_2$ were dissolved in distilled $H_2O$ and the pH was adjusted to 7.4 with 10 M NaOH.

In static cultures for [$^3$H]noradrenaline (NA) release measurements, Krebs/HEPES buffer was supplemented with 0.2 mM pargyline final concentration and 0.0175 g L-ascorbic acid/500 ml buffer to prevent uptake and autooxidation of catechols.

*Tyrodes Buffer (prepared in-house at GlaxoSmithkline)*

145 mM NaCl; 2.5 mM KCl;10 mM HEPES; 10 mM glucose; 1.2 mM $MgCl_2$ and 1.5 mM $CaCl_2$ were dissolved in Ultrapure deionised $H_2O$ and the pH was adjusted to 7.4 with 1 M NaOH.

*Harvest buffer*

154 mM NaCl; 10 mM HEPES and 1.71 mM EDTA were dissolved in distilled $H_2O$. The pH was adjusted to 7.4 with 10 M NaOH.

*EDTA stock solution*

A 0.5 M stock solution was prepared by dissolving EDTA in distilled $H_2O$. The pH was adjusted to 8.0 with 10 M NaOH and the solution was autoclaved before use.

*TAE buffer*

A 1 l 50 x buffer stock solution was prepared by dissolving 242 g Tris Base, 57.1 ml glacial acetic acid, 100 ml 0.5 M EDTA solution in distilled $H_2O$ and autoclaved before use. This was diluted to a 1 x working solution with final concentrations of 40 mM Tris Base, 20 mM acetic acid and 1 mM EDTA in distilled $H_2O$ when preparing agarose gels.

*Running Buffer*

This was prepared by diluting the TAE buffer stock to a 1 x buffer stock in sterile distilled $H_2O$. 0.02% (v/v) Ethidium bromide was added to the buffer and mixed thoroughly.

*Triton X-100*

A 4% Triton X-100 solution was prepared by dissolving in warmed distilled $H_2O$.

*EGTA*

EGTA was dissolved in 1 ml of 10 M NaOH followed by 9 ml of distilled $H_2O$ to produce a final concentration of 90 mM.

*Perchloric Acid*

A 70% stock was diluted in distilled $H_2O$ to make a final concentration of 0.4 M.

*GTPγ[$^{35}$S] Buffers*

The following listed GTPγ[$^{35}$S] buffers were prepared by dissolving the appropriate constituents in distilled $H_2O$ and the pH was adjusted to 7.4 with NaOH:

GTPγ[$^{35}$S] Reconstitution: 50 mM Tris-HCl, 10 mM DTT

GTPγ[$^{35}$S] Homogenising: 50 mM Tris-HCl, 0.2 mM EGTA

GTPγ[$^{35}$S] Assay: 50 mM Tris-HCl, 0.2 mM EGTA, 100 mM NaCl, 1 mM $MgCl_2$

## 2.4 Preparation of agonists, antagonists and fura-2AM

*Fluorimetry*: 10 mM stocks of capsaicin and AEA were prepared in DMSO and further diluted in Krebs/HEPES buffer for the former and a mix of Krebs/HEPES buffer and DMSO for the latter (due to high insolubility of AEA) when required. A 10 mM stock of capsazepine was prepared in DMSO and further diluted in Krebs/HEPES buffer. A 10 mM stock of $\Delta^9$-THC was prepared in ethanol and further diluted in ethanol on ice when required. A 1 mM stock of fura-2AM was prepared in DMSO and aliquoted. Appropriate controls were always included.

*GTPγ[$^{35}$S] Assay*: 10 mM capsaicin, AEA and $\Delta^9$-THC stocks were diluted in DMSO due to buffer incompatibility.

Solvent controls were used as appropriate. All stocks were stored at -20°C and dilutions of the stocks were prepared fresh on the day of experimentation.

*[$^3$H]NA release experiments:* A 2 M Pargyline stock was prepared in distilled $H_2O$, aliquoted and stored at -20°C.

## 2.5 Experimental locations

As this project was performed in collaboration with GlaxoSmithKline (Harlow, Essex), all experiments in relation to FLIPR, electroporation with Nucleofector were performed onsite at GlaxoSmithkline. GlaxoSmithkline provided the reagents/materials/equipment for FLIPR and CEDEX.

## 2.6 Cell culture

$HEK293_{hTRPV1}$ and $HEK293_{rTRPV1}$ cells were maintained in minimal essential media (MEM) supplemented with 10% foetal calf serum, 0.2 mM L-glutamine, 2.5 μg/ml fungizone, 100 IU/ml penicillin and 100 μg/ml streptomycin at 37°C in 5% $CO_2$/air. Cells were passaged with trypsin/EDTA when required and used when confluent.

SH-SY5Y human neuroblastoma cells; wild-type cells were cultured in MEM supplemented with 10% foetal calf serum, 2 mM L-glutamine, 2.5 μg/ml fungizone, 100 IU/ml penicillin and 100 μg/ml streptomycin at 37°C in 5% $CO_2$/air. $SH\text{-}SY5Y_{hTRPV1}$ cells

were cultured as before except 300 µg/ml hygromycin B was added. Cells were passaged with trypsin/EDTA when required and used when confluent.

## 2.7 Fluorimetric measurement of intracellular free calcium: Theory

Fura-2 is one of the most popular fluorescent $Ca^{2+}$ indicators used today. The $Ca^{2+}$ binding property of this indicator is formed by the presence of a tetracarboxylic acid core as found in EGTA, a $Ca^{2+}$ chelator. In low or free $Ca^{2+}$ conditions, fura-2 displays a broad excitation spectrum between 300 and 400 nm with a peak at approximately 370 nm as shown in Figure 2.3.

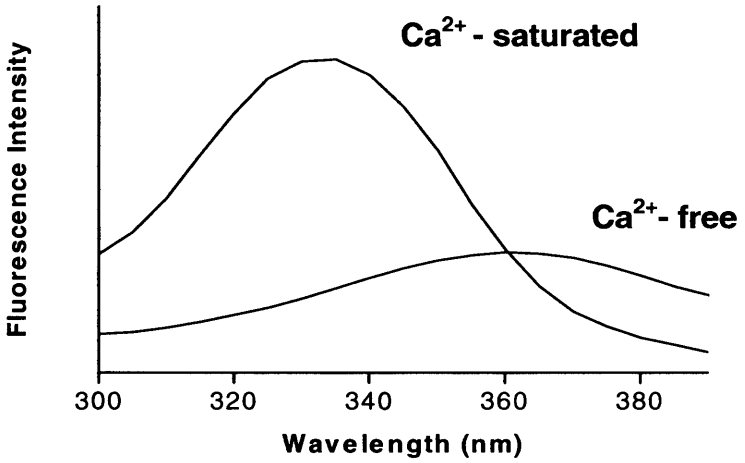


**Figure 2.3 $Ca^{2+}$ - saturated and $Ca^{2+}$ - free excitation spectra of fura-2**
*High $Ca^{2+}$ conditions produce a peak in the excitation spectrum unlike in low $Ca^{2+}$ conditions where a broad spectrum results. The isobestic or isoemissive point is located where the spectra coincide at 360 nm.*

Upon $Ca^{2+}$ binding, the excitation peak increases in intensity and shifts further in the UV range. As a consequence of these spectra, fura-2 is a dual excitation $Ca^{2+}$ indicator and if the dye is excited at 340 nm with an emission at 510 nm, $Ca^{2+}$ binding produces an increase in fluorescence, whereas a decrease in the fluorescent signal is observed when the dye is excited at 380 nm as displayed in Figure 2.4.

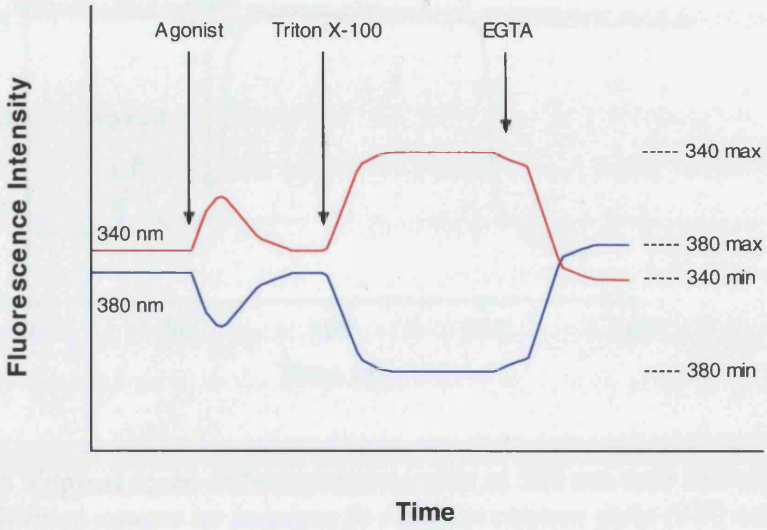


**Figure 2.4 Fluorescence intensities obtained during fura-2 experiments**
*During excitation at 340 nm and 380 nm, the addition of an agonist will increase the fluorescence intensity at 340 nm and decrease the fluorescence intensity at 380 nm. Addition of Triton X-100 results in maximum fluorescence at 340 nm and minimum fluorescence at 380 nm. Addition of EGTA gives minimum fluorescence at 340 nm and maximum fluorescence at 380 nm.*

When the dye is excited in quick succession at 340 nm and 380 nm, a ratio of the respective emission signals can be used to monitor $[Ca^{2+}]_i$ (Figure 2.5). The ratio signal is not dependent on dye concentration, illumination intensity or optical pathlength.

As fura-2 free acid is charged and thus cannot permeate lipid membranes, fura-2 supplied as an acetoxymethyl ester (fura-2AM) was used for lipophilic properties to permeate the cell membrane. When the cells are loaded with fura-2AM, the carboxylic acid groups of

the dye are cleaved by the cellular esterases and consequently the dye becomes trapped within the cells.

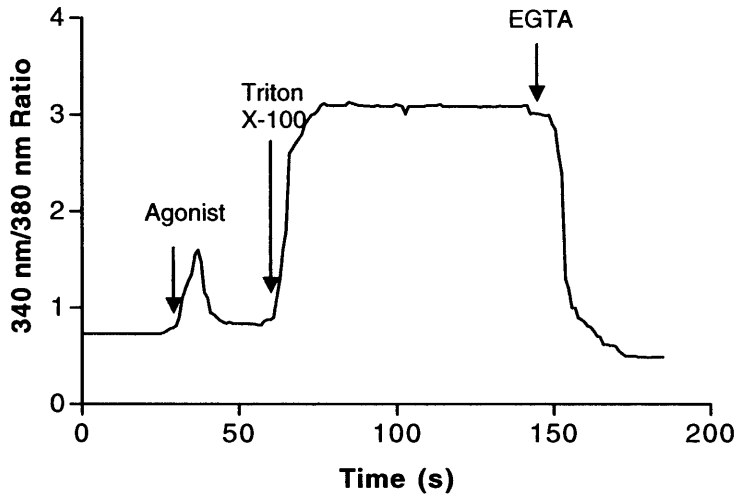


**Figure 2.5 Typical trace of fluorescence ratio at 340 nm and 380 nm**
*Agonist addition causes an increase in the fluorescence ratio (340 nm:380 nm). Triton X-100 produces the maximum ratio while EGTA decreases the ratio to the minimum.*

The effects on $[Ca^{2+}]_i$ at specific receptors are measured with a spectrofluorimeter. $[Ca^{2+}]_i$ is calculated from the fluorimetric ratios (340 nm:380 nm) at dual excitation and the following calibration equation (Grynkiewicz *et al.*, 1985):

$$[Ca^{2+}]_i = K_d \left[\frac{R - R_{min}}{R_{max} - R}\right] \times \left[\frac{F_{380\,max}}{F_{380\,min}}\right]$$

F = fluorescence intensity

$K_d$ = equilibrium dissociation constant of $Ca^{2+}$ for fura-2

R = F ratio ($F_{340\,nm}/F_{380\,nm}$)

$R_{min}$ = ($F_{340\,nm}/F_{380\,nm}$) formed at minimum $Ca^{2+}$ concentration (EGTA)

$R_{max}$ = ($F_{340\,nm}/F_{380\,nm}$) formed at maximum $Ca^{2+}$ concentration (Triton X-100)

$F_{380\,max}/F_{380\,min}$ = F ratio (380 nm) at minimum and saturated $Ca^{2+}$ concentration

### *2.7.1 Fluorimetric measurement of intracellular free calcium: Methodology*

Cells were detached, washed twice with and suspended in Krebs/HEPES buffer. Suspensions were loaded with a final concentration of 5 μM fura-2AM for 30 min at 37°C to allow fura-2AM to permeate the lipid bilayer of the cells. The cells were resuspended again in Krebs/HEPES buffer and then loaded fura-2AM was de-esterified for 20 min at room temperature in the dark. The cells were resuspended in Krebs/HEPES buffer and stored on ice until required.

A quartz cuvette containing a small magnetic flea stirrer was placed in a Perkin-Elmer LS50B spectrofluorimeter. 1.8 ml of warmed Krebs/HEPES buffer was pipetted into the cuvette followed by the addition of 200 μl cells. The temperature of the cuvette was maintained by external circulating pipes connected to a water bath which was heated two degrees above the desired temperature to compensate for intermediate cooling in the pipes. The temperature was confirmed using a thermocouple thermometer. The cells were allowed to heat up to the required temperature for 2 min prior to the addition of agonists. The antagonist capsazepine was pre-incubated for 10 min prior to the addition of agonist. Fluorescence emission was measured at 510 nm with excitation at 340 nm and 380 nm with the spectrofluorimeter using the FLDM program.

$R_{max}$ and $R_{min}$ were obtained with Triton X-100 and EGTA respectively and intracellular free calcium $[Ca^{2+}]_i$ was calculated according to Grynkiewicz (Grynkiewicz *et al.*, 1985) and $K_d$ values were 145 nM and 225 nM at 22°C and 37°C respectively (Simpson, 1999).

### *2.7.2 Measurement of $[Ca^{2+}]_i$ using the FLIPR*

In contrast to cuvette-based fluorimetry, the Fluorimetric Imaging Plate Reader (FLIPR) is a device that screens high-throughput numbers of samples. The FLIPR allows simultaneous stimulation and measurement of release of $[Ca^{2+}]_i$ from 96 samples (Figure 2.6). An operator controls a computerised 96-well pipettor to dispense liquids and perform dilutions. The FLIPR uses a 6 W argon ion laser to produce discrete spectral lines spaced from approximately 350-530 nm. The laser is set at a particular wavelength depending on which fluorescent calcium indicator is selected. The laser simultaneously illuminates the cells in the 96-well plate. A cooled charge couple device (CCD) camera records an image of each well. If necessary, images can be updated once per second for the measurement of rapid calcium responses. CCD data is converted to digital data and transferred to a computer (Sullivan *et al.*, 1999).

**Figure 2.6 The FLIPR 96 system**
*FLIPR models are supplied by Molecular Devices as a high-throughput screening instrument.*

Agonist-induced receptor activation was detected as an increase in fluorescence by means of multiple time-resolved images from individual wells. Functional antagonism is indicated by a suppression of agonist-induced increase in fluorescence. In each case the fluorescence changes are indicative of alterations in cytoplasmic calcium concentration. By means of concentration response curves, functional potencies were determined using standard pharmacological analysis as in Section 2.2.

### *2.7.3 Fluo-3*

Besides fura-2 which can be classified as a ratiometric $Ca^{2+}$ indicator, nonratiometric indicators are also available and include fluo-3 and rhod-2. Fluo-3 is a visible-wavelength excitation fluorescent indicator compared to fura-2 which is an ultraviolet-wavelength excitation fluorescent indicator. Fluo-3 was synthesised from BAPTA by combination with a fluorescein-like structure. The absorption and emission peaks of fluo-3 are 506 and 526 nm respectively. Fura-2 is not suitable for use in flow cytometry or confocal laser scanning microscopy (CLSM) because it is difficult to change the excitation wavelength quickly. However, this is not a problem for fluo-3 and this dye is a popular choice for these applications. In *in vitro* conditions, the $K_d$ of fluo-3 is relatively higher than that of fura-2, at approximately 400 nM (22°C, pH 7.0-7.5) and hence has a lower $Ca^{2+}$ binding affinity than fura-2. Fluo-3 is also available in an acetoxymethyl ester form (fluo-3AM) for cellular esterases to de-esterify and therefore trap the dye within the cells. Unlike fura-2, fluo-3

does not display a shift in its absorption or emission spectra upon binding $Ca^{2+}$, thus factors including differences in pathlength and volumes have to be considered when using fluo-3 (Takahashi *et al.*, 1999).

### *2.7.4 FLIPR assay*

Clonal cells expressing human or otherwise recombinant and/or native receptors were seeded into black-walled clear-base 96-well plates at a density of 25000 cells/well overnight in MEM supplemented as previously mentioned but excluded the antibiotic hygromycin B. This was followed by incubating the cells in MEM containing the cytoplasmic $Ca^{2+}$ indicator, Fluo-3AM (4 μM) at 25°C for 2 h. The cells were washed with and finally cultured in, Tyrodes's buffer and 1.5 mM $CaCl_2$ before being incubated for 20 min at 25°C with either buffer (alone) or buffer containing various antagonists. The plates were then placed in a FLIPR (Molecular Devices, California, USA) and illuminated by a 6 W argon laser to monitor cell fluorescence ($\lambda_{EX}$ = 488 nm, $\lambda_{EM}$ = 540 nm) before and after the addition of various agonists (Schroeder *et al.*, 1996).

## 2.8 GTPγ[$^{35}$S] Assay

The GTPγ[$^{35}$S] assay is an effective functional assay of G-protein coupled receptor activity, especially $G_i$. This assay compared activity between exo- and endo-cannabinoids and assessed the activity for olvanil, a structural analogue of capsaicin, which is also structurally similar to the endocannabinoid AEA. Ligand binding to a G-protein coupled receptor alters the receptors conformation to allow interaction with its G-protein. This interaction leads to the exchange of GDP for GTP. A radiolabelled, stable analogue of GTP, GTPγ[$^{35}$S] is used to measure the exchange of GDP for GTPγ[$^{35}$S] obtained by different ligands. Since the conformation of a receptor is not fixed but exists instead in a state of flux, there will be some background activation of G-proteins *via* non-ligand bound receptors. Background basal (total) is performed in the absence of ligand and the presence of GTPγ[$^{35}$S]. Non-specific binding (NSB) is assessed after saturation with unlabelled GTPγS. Finally, stimulated binding of the G-protein is measured in the presence of the ligand and is calculated from the difference with NSB.

### *2.8.1 Membrane preparation*

All test tubes and similar containers were treated with Sigmacote 48 h prior to the assay to prevent AEA and $\Delta^9$-THC adhering to the container surfaces by coating them with a covalently-bound silane layer.

Rats were killed by pre-stunning followed by cervical dislocation. Cerebella, which are rich in $CB_1$ receptors (Pertwee, 2001), were dissected from the brains of female Wistar rats (rat weight, 250 g each) were homogenised in homogenisation buffer using an Ultra Turrax homogeniser for 10 s followed by six consecutive bursts. Membrane fractions were collected *via* centrifugation at 20375 g for 10 min at 4°C followed by successive homogenisation and centrifugation for a total of three times. The total membrane fraction was finally resuspended in an appropriate volume of buffer with subsequent protein determination and ultimately stored at -70°C.

### *2.8.2 Protein assay (Lowry)*

The membrane fraction protein concentration was determined using the method of Lowry (Lowry, 1951). BSA protein standards at set concentrations of 0, 50, 100, 150, 200, 250 µg protein/ml were prepared in 0.1 M NaOH. Samples of unknown protein concentration were diluted in 0.1 M NaOH. 0.5 ml volumes of standards and samples were incubated for 10 min at room temperature in 2.5 ml of a solution consisting of A ($NaHCO_3$ in 0.1M NaOH), B (1% $CuSO_4$) and C (2% $Na^+$ $K^+$ tartrate) mixed to the ratio 100:1:1. 0.25 ml of Folin's reagent (previously diluted 1 in 4 in distilled $H_2O$) was then added to each tube, vortexed and incubated at room temperature for a further 30 min. Absorbance at 750 nm for the standards and samples was determined using a Corning 259 spectrophotometer. Linear regression of the known BSA protein concentrations was used to produce a standard curve from which sample protein concentrations were determined (Figure 2.7).

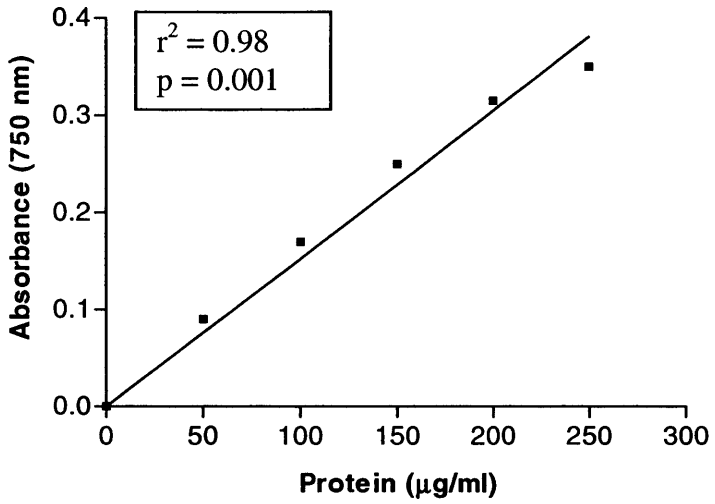


**Figure 2.7 A typical standard protein concentration curve**

### *2.8.3 GTPγ[$^{35}$S] binding assay*

GTPγ[$^{35}$S] binding was performed according to methodology described by Berger and colleagues with modifications (Berger *et al.*, 2000). All test tubes were treated with Sigmacote prior to experimenting to reduce ligand adherence (especially $\Delta^9$-THC) to regular (non-quartz) glassware. Rat cerebellar membranes were prepared as described in section 2.8.1. 20 µg of membranes were incubated in 0.5 ml volumes of buffer containing 50 mM Tris, 0.2 mM EGTA, 1 mM $MgCl_2$, 100 mM NaCl, 1% BSA, 100 µM GDP, 20 µl drug to be tested and ~150 pM GTPγ[$^{35}$S]. The reaction was incubated for 1 h at 30°C with gentle shaking and terminated by filtration through Whatman GF/B filters using a Brandel-harvester. Non-specific binding was determined in the presence of 10 µM GTPγS. Bound radioactivity was extracted for 8 h in 4.5 ml Optiphase "safe" scintillation fluid before assessing radioactivity by scintillation spectroscopy. Counts were measured and recorded as dpm (disintegrations per minute) by a Packard 1900 TR liquid scintillation analyser.

## 2.9 Measurement of [$^3$H]NA release

### *2.9.1 Static Cultures*

Monolayers of wild-type SH-SY5Y and SH-SY5Y$_{hTRPV1}$ cells were grown in 12-well multitrays (Section 2.6) until they were confluent on the day of experimentation. Cell culture media was aspirated from each well followed by a gentle 1 ml wash with pre-warmed Krebs/HEPES buffer per well. Cells were incubated for 1 h with 0.5 ml of 2

μCi/ml [$^3$H]NA (previously diluted in Krebs/HEPES buffer) in the 37°C waterbath. The monolayers were post-incubated for 15 min in 0.5 ml fresh Krebs/HEPES buffer in the 37°C waterbath. This post-incubation was repeated twice more. The agonist capsaicin (10 mM stock) was diluted in Krebs/HEPES buffer and incubated in a waterbath. When necessary, a 100 mM $K^+$ control was prepared by replacing the required $Na^+$ concentration with an appropriate amount of $K^+$ in the Krebs/HEPES buffer. After the last cell incubation in Krebs/HEPES, 0.5ml volumes of agonist or buffer were quickly pipetted onto the cells. The trays were incubated in the water bath for 3 min at 37°C. The tray was immediately placed on ice. Well contents were quickly transferred into pre-cooled Eppendorf tubes on ice. The Eppendorf tubes were briefly centrifuged for 30 s. 250 μl supernatant was transferred into fresh Eppendorf tubes and 1 ml Optiphase "safe" scint fluid (aqueous) was dispensed into each Eppendorf. Each Eppendorf was shaken to thoroughly mix the contents. 0.5 ml 0.4 M perchloric acid (PCA) was added to each well on the tray to digest the cells and this was incubated at room temperature for 30 min. 250 μl liquid from each well was transferred into labelled Eppendorf tubes and 1ml Optiphase "safe" scint fluid (aqueous) was added to each tube. The Eppendorf tubes were shaken vigorously to thoroughly mix the contents. A [$^3$H]NA standard control was prepared by adding 250 μl of 2 μCi/ml [$^3$H]NA (previously diluted in Krebs/HEPES buffer) to 1 ml Optiphase "safe" scint fluid (aqueous) and shaken. Counts were measured and recorded as dpm (disintegrations per minute) by a Packard 1900 TR liquid scintillation analyzer.

### *2.9.2 Simultaneous measurement of $[Ca^{2+}]_i$ and [$^3$H]NA release*

A sterile custom-made cylindrical glass enclosure was sealed onto a sterile glass coverslip (45 $mm^2$) with vaseline. This was used to contain and grow SH-SY5Y human neuroblastoma cells to maximum confluency in MEM plus supplements (as detailed in Section 2.6). The cells were loaded with 1 μCi of [$^3$H]NA and a final concentration of 5 μM fura-2AM in 1 ml cell culture media for 1 h in a 37°C cell culture incubator. Then, the liquid was discarded and the glass enclosure was carefully prised off the coverslip. The loaded cells were placed in a custom-made perfusion chamber, which was maintained at 37°C as illustrated in Figure 2.8. This incubation period was also sufficient for complete de-esterification of the AM ester group attached to fura-2. The chamber was inserted into a Perkin Elmer LS50B fluorimeter and was perfused at 1.37 ml/min with pre-warmed Krebs/HEPES buffer. After 1 min, 1 ml of 1 x $10^{-7}$ M capsaicin was perfused followed by

pre-warmed Krebs/HEPES buffer. Fluorescence emission was measured at 510 nm with excitation at 340 nm and 380 nm using the FLDM program. Simultaneous [$^3$H]NA release was collected *via* perfusate fractions (a volume of 840 µl each). The [$^3$H]NA released was measured from 0.25 ml aliquots from each perfusate fraction using Optiphase "safe" scintillation fluid.

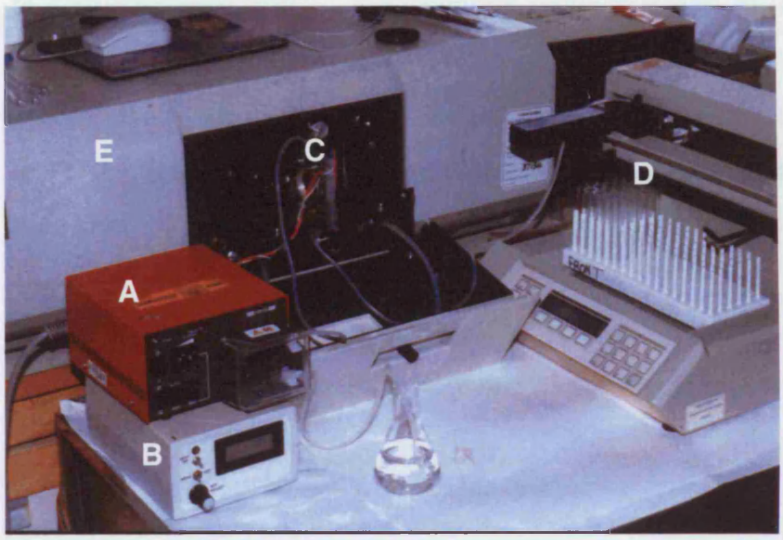


Key:

A: pump

B: temperature controller

C: perfusion chamber

D: fraction collector

E: fluorimeter

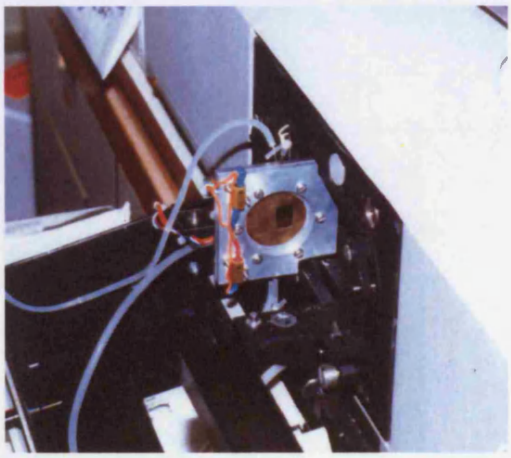

**Figure 2.8 Perfusion chamber**

## 2.10 Data Analysis

Generally, cuvette-based fluorimetric data were calculated as $\Delta[Ca^{2+}]_i$ (maximum $[Ca^{2+}]_i$ minus basal $[Ca^{2+}]_i$) unless otherwise stated. FLIPR data were calculated as peak fluorescence intensity (FI) minus basal FI and displayed as fluorescence intensity units (FIU). Data are presented as mean±SEM of (n) experiments or as single representative fluorimetric traces (from n experiments). Fluorimetric data were analysed using GRAPHPAD PRISM (V3.0) by non-linear regression curve fitting unless otherwise stated to derive potency ($pEC_{50}$, concentration producing 50% of the maximum response, $E_{max}$) and efficacy. GTPγ[$^{35}$S] data were expressed as stimulation factor (agonist stimulated specific binding/basal specific binding) and analysed using GRAPHPAD PRISM (V3.0). In some capsazepine inhibition studies, data were normalised to the maximum response produced by capsaicin alone and apparent $pK_B$ values (antagonist potency) were calculated, see Section 2.2.

Where appropriate, data were analysed with ANOVA and paired/unpaired t-tests with post-hoc corrections and differences were considered significant when $p \leq 0.05$.

# 3 BASIC PHARMACOLOGICAL CHARACTERISATION OF RAT & HUMAN TRPV1 EXPRESSED IN HEK293 CELLS

## 3.1 Introduction

TRPV1 is a ligand-gated ion channel whose activation by capsaicin increases intracellular calcium ($[Ca^{2+}]_i$). Capsaicin, the pungent vanilloid component in chilli peppers, is the classic agonist at TRPV1 on C-fibres and a small population of Aδ-fibres. Depolarisation of the sensory nerves involves the influx of sodium and calcium ions with the generated action potential perceived as pain. Paradoxically, sustained application of capsaicin induces analgesia, which is likely to result from a chemical denervation.

In addition, the endocannabinoid AEA structurally resembles both capsaicin and olvanil and has been found to activate TRPV1 *in vitro*. Controversially, it is thought that AEA may interact with vanilloid receptors *in vivo* leading to receptor desensitisation and analgesia. Olvanil has complex interactions with the cannabinoid system, in that it potentiates the agonist activity of endogenous cannabinoids by inhibiting the reuptake of AEA. Olvanil is a more potent reuptake inhibitor than AM404, of which the latter is commonly used for this purpose. (Janusz *et al.*, 1993). Olvanil is also a $CB_1$ agonist, but does not bind to $CB_2$ receptors or inhibit fatty acid amide hydrolase (FAAH), an inactivator of AEA. The overall activity of olvanil in most models is that of an analgesic, but it is unclear how these effects are mediated by TRPV1, the $CB_1$ receptor, or other components of the endogenous pain sensation system. (Di Marzo *et al.*, 1998).

Since TRPV1 was first cloned, pharmacological differences have been noted between recombinant TRPV1 and endogenous TRPV1 expressed in DRG. For example, the potencies of capsaicin and AEA were higher in $HEK293_{rTRPV1}$ relative to DRG cultures. Differences in AEA efficacy between the $HEK293_{rTRPV1}$ relative to DRG cultures have been reported (Jerman *et al.*, 2002).

In addition, few characterisation studies have compared recombinant rat and human TRPV1 which makes it difficult to extrapolate data to an *in vitro* model comparable to an *in vivo* situation (McIntyre *et al.*, 2001; Smart *et al.*, 2001).

The exocannabinoid $\Delta^9$-Tetrahydrocannabinol ($\Delta^9$-THC), the major psychoactive compound from the maurijuana plant (*Cannabis sativa*), binds to $CB_1$ located in mammalian brain. Although endocannabinoid effects have been investigated at TRPV1, $\Delta^9$-THC has not been investigated for TRPV1 activation. Despite the opposing effects

mediated by $CB_1$ and TRPV1 receptors, that is, $CB_1$ promotes antinociceptive effects while TRPV1 causes nociception, controversy in the literature concerns the classification and roles of TRPV1 and $CB_1$ receptors and whether they are subdivisions of a superfamily.

## 3.2 Aims

Using recombinant human (h) and rat (r) TRPV1 receptors expressed in HEK293 cells, the following basic investigations will be made:

- $[Ca^{2+}]_i$ measurements will be used to compare the differences in affinity of the TRPV1 antagonist capsazepine against capsaicin and AEA in both TRPV1 species.
- Temperature-dependent effects of capsaicin and AEA will be investigated. Standard FLIPR screening utilises the fixed temperature of 25°C and other non-FLIPR studies have used 22°C. A temperature of 22°C will be compared with a physiological temperature of 37°C.
- The exocannabinoid $\Delta^9$-THC will be investigated for TRPV1 activation. If $\Delta^9$-THC produces an $[Ca^{2+}]_i$ response, this exocannabinoid will be examined for agonistic properties.

## 3.3 Results

### *3.3.1 Temporal profiles*

*Capsaicin*: the methods used to perform these studies are described in Chapter 2, Section 2.7.1. Capsaicin produced a time- (Figure 3.1) and concentration- (Figure 3.4, Table 3.1) dependent increase in $[Ca^{2+}]_i$. Figure 3.1 displays typical traces in response to varying concentrations of capsaicin in $HEK293_{rTRPV1}$ and $HEK293_{hTRPV1}$ cells at 22°C and 37°C. Addition of capsaicin at 60 s caused a rapid (~40 s) elevation in $[Ca^{2+}]_i$ and this reached a maximum at around 10 μM capsaicin. $[Ca^{2+}]_i$ response in $HEK293_{hTRPV1}$ was greater than in $HEK293_{rTRPV1}$ and probably this is suggestive of higher expression in the former cell-line. In the $HEK293_{hTRPV1}$ cells the response was biphasic in nature with this profile being less pronounced at the lower (22°C) temperature. Once the maximal $[Ca^{2+}]_i$ response was achieved, there was a gradual decrease. Overall, there was some variability in $[Ca^{2+}]_i$ responses between receptor species and temperatures; in $HEK293_{rTRPV1}$, $\Delta[Ca^{2+}]_i$ ranged from 79-90 nM and 146-198 nM at 22°C and 37°C respectively with 10 μM capsaicin. In $HEK293_{hTRPV1}$, $\Delta[Ca^{2+}]_i$ ranged from 188-475 nM and 488-1046 nM at 22°C and 37°C respectively.

*AEA*: the methods used to carry out these studies are described in Chapter 2, Section 2.7.1. Typical traces displayed a time-dependent increase in $[Ca^{2+}]_i$ in response to different concentrations of AEA in $HEK293_{rTRPV1}$ and $HEK293_{hTRPV1}$ cells at 22°C and 37°C (Figure 3.2). AEA produced a concentration-dependent increase in $[Ca^{2+}]_i$ as shown in Figure 3.4 with $pEC_{50}$ and $E_{max}$ values displayed in Table 3.1. Addition of AEA at 60 s caused a rapid (~40 s) elevation in $[Ca^{2+}]_i$ and this reached a maximum at approximately 10 μM AEA. Like capsaicin, AEA's $[Ca^{2+}]_i$ response in $HEK293_{hTRPV1}$ was greater than in $HEK293_{rTRPV1}$ and this could be due to higher expression in the former cell-line. In the $HEK293_{hTRPV1}$ cells the response was generally biphasic in nature at the higher concentrations (for example, at 10 μM) with this profile being less pronounced at the lower (22°C) temperature. After the maximal $[Ca^{2+}]_i$ response was achieved, there was a steady decline in response. Overall, there was some variability in $[Ca^{2+}]_i$ responses between receptor species and temperatures; in $HEK293_{rTRPV1}$, $\Delta[Ca^{2+}]_i$ ranged from 17-23 nM and 18-63 nM at 22°C and 37°C respectively with 10 μM AEA. In $HEK293_{hTRPV1}$, $\Delta[Ca^{2+}]_i$ ranged from 217-282 nM and 302-567 nM at 22°C and 37°C respectively.

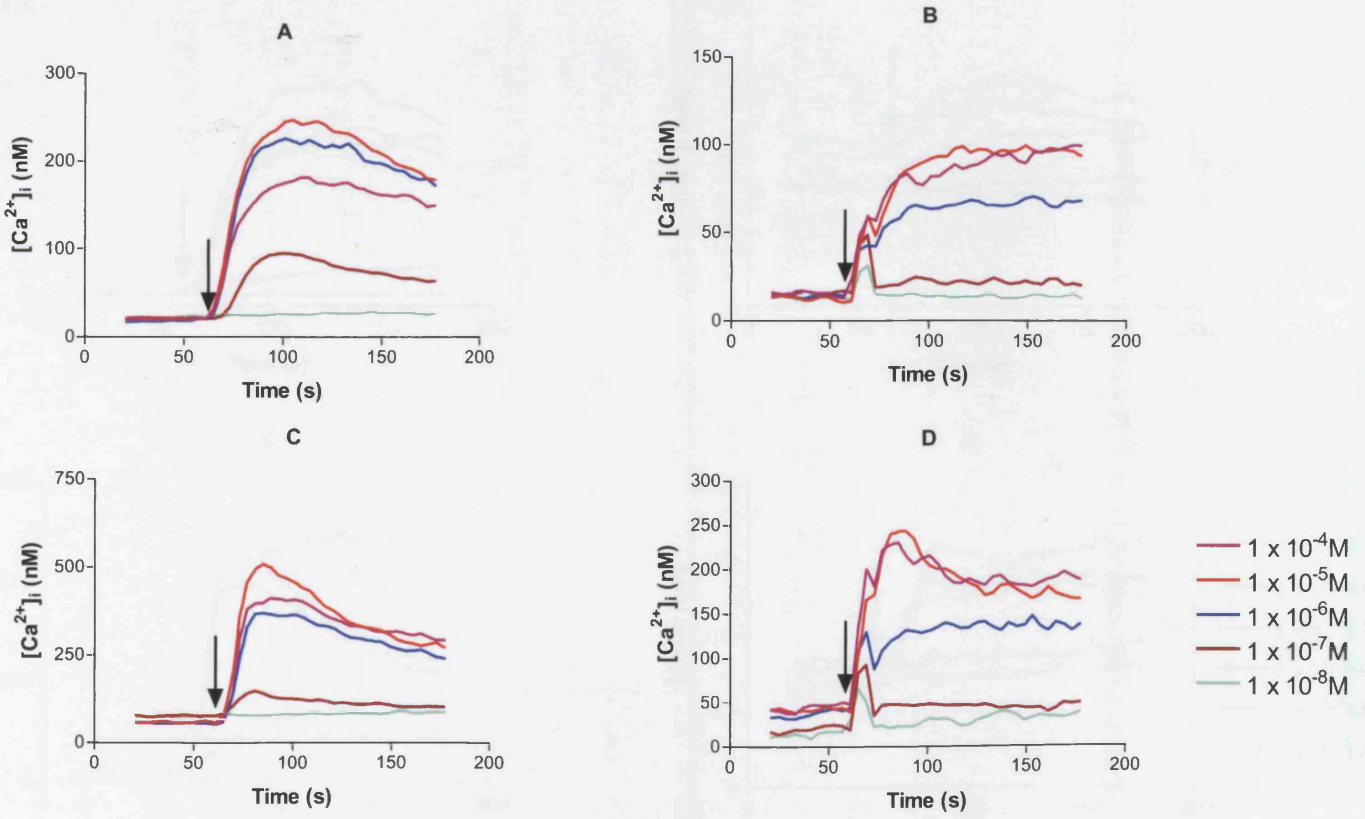


**Figure 3.1 Typical traces obtained from fluorimetric measurements in capsaicin concentration response curves**
*22℃: (A) hTRPV1 and (B) rTRPV1, 37℃: (C) hTRPV1 and (D) rTRPV1. Arrows indicate the addition of capsaicin at 60 s. Data are from single representative experiments as shown in Table 3.1.*

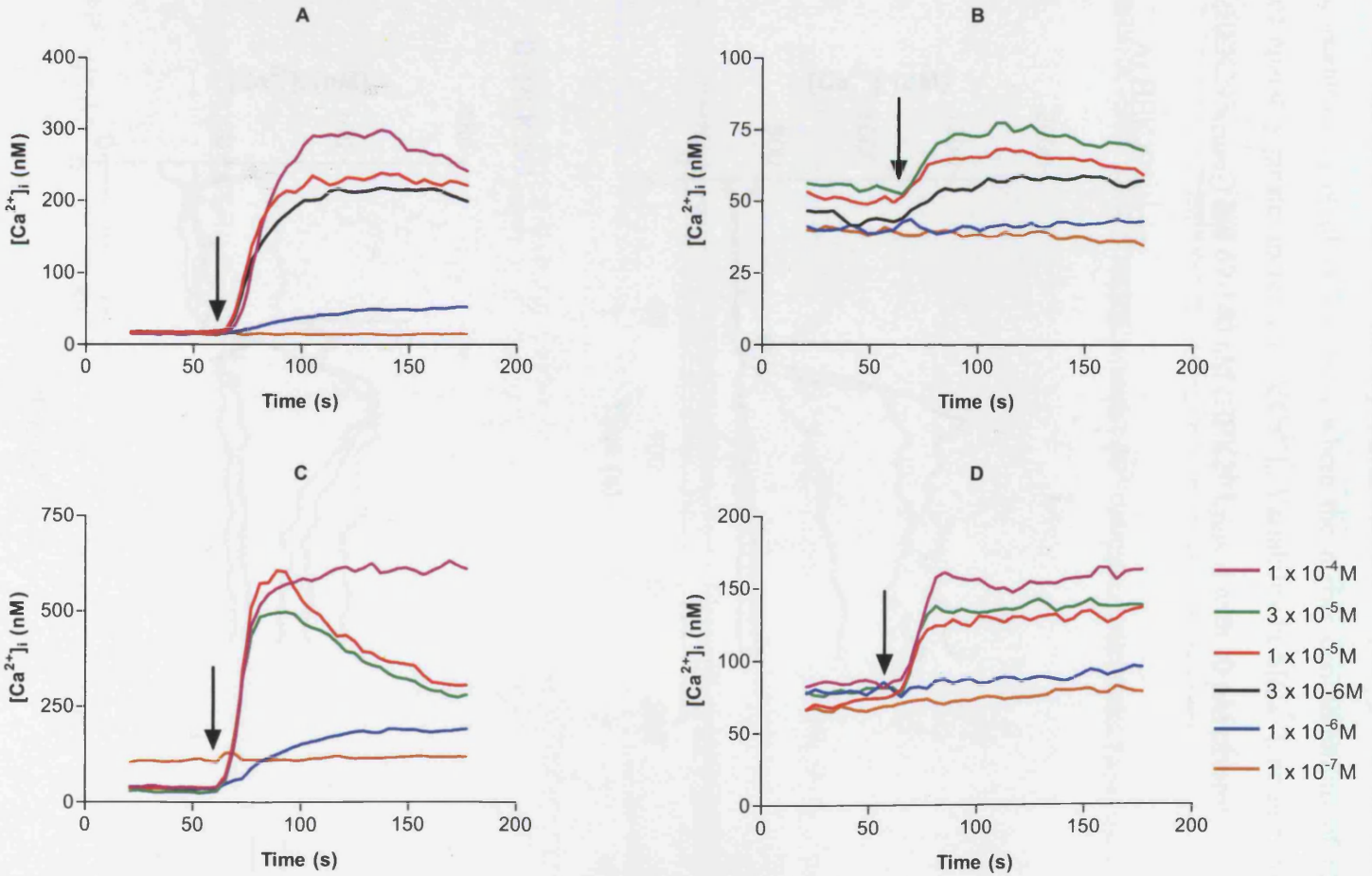


**Figure 3.2 Typical traces obtained from fluorimetric measurements in AEA concentration response curves**

*22℃: (A) hTRPV1 and (B) rTRPV1, 37℃: (C) hTRPV1 and (D) rTRPV1. Arrows indicate the addition of AEA at 60 s. Data are from single representative experiments as shown in Table 3.1.*

*Olvanil*: Figure 3.3 displays typical traces, showing the change in $[Ca^{2+}]_i$ levels in response to varying concentrations of olvanil in $HEK293_{hTRPV1}$ and $HEK293_{rTRPV1}$ respectively at 37°C. The traces show a time-dependent increase in $[Ca^{2+}]_i$ with the addition of different concentrations of olvanil at 60 s where the higher concentrations of olvanil produce a comparably greater increase in $\Delta[Ca^{2+}]_i$. Variability in $\Delta[Ca^{2+}]_i$ ranged from 639-1053 nM ($HEK293_{hTRPV1}$) and 69-140 nM ($HEK293_{rTRPV1}$) with 10 µM olvanil.

A) $HEK293_{hTRPV1}$

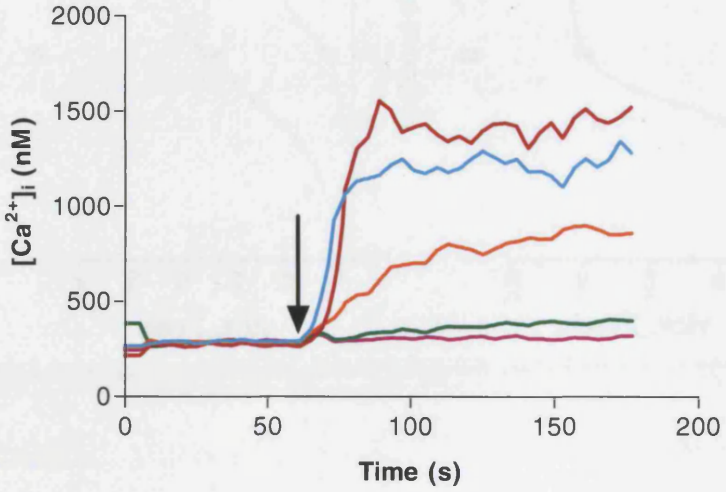


B) $HEK293_{rTRPV1}$

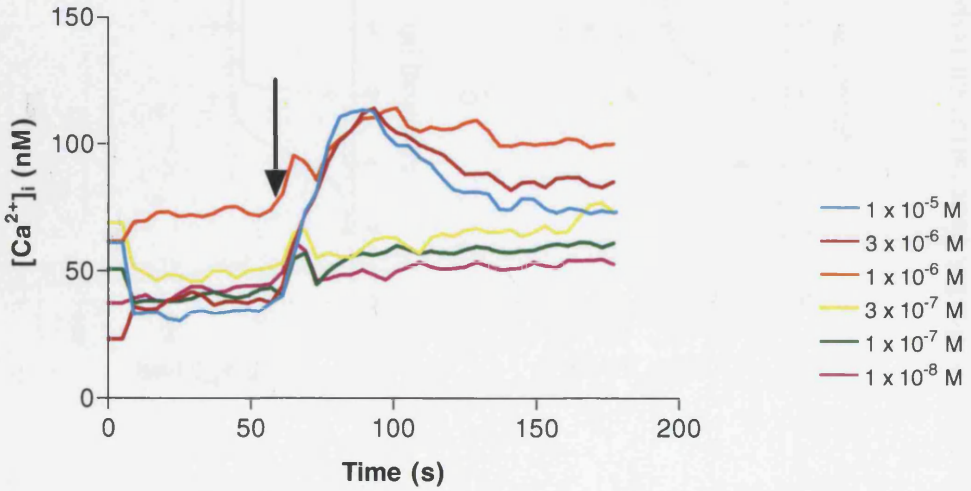


**Figure 3.3 Temporal profiles for varying concentrations of olvanil at rTRPV1 and hTRPV1 at 37°C**

*Each trace represents the $[Ca^{2+}]_i$ response obtained at different agonist concentrations, added at 60 s as indicated by the arrows.*

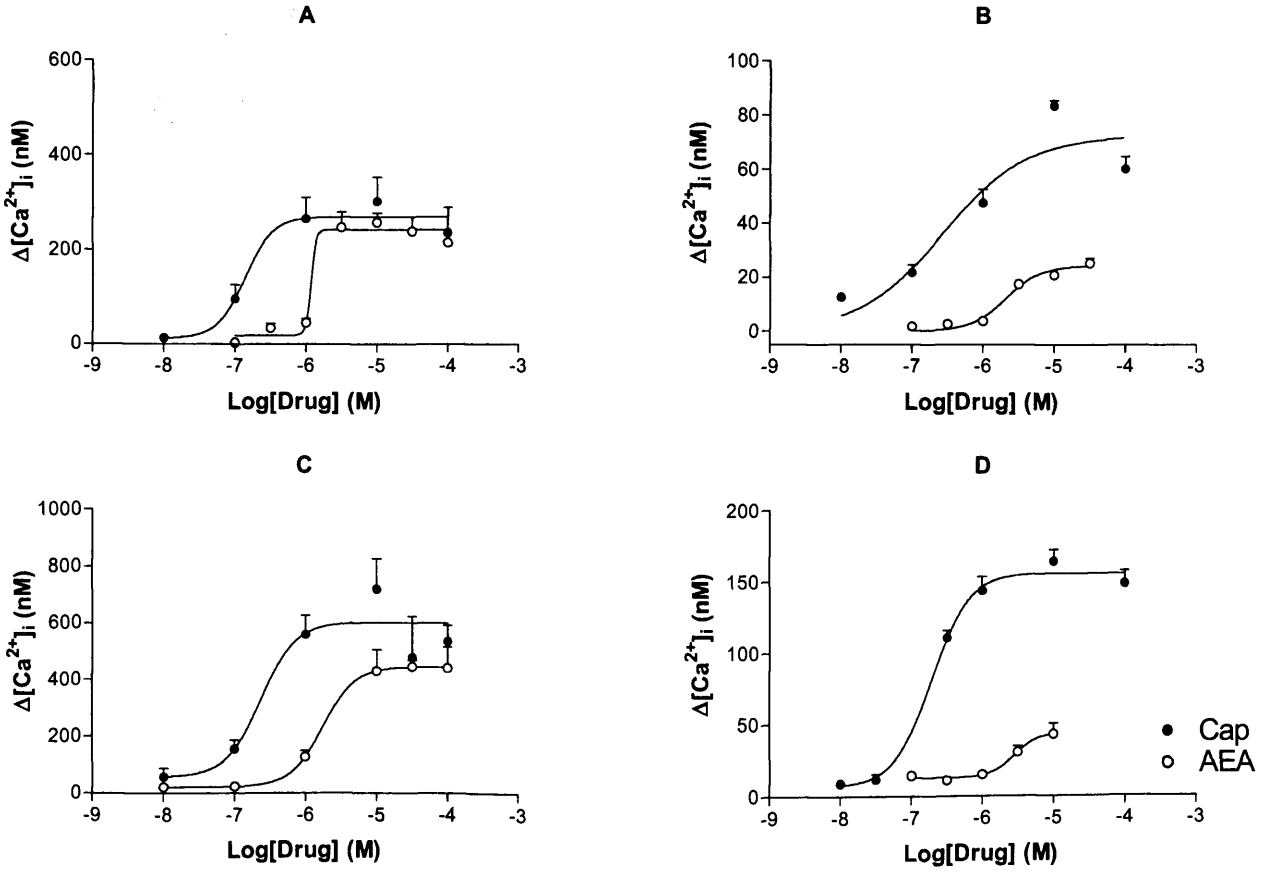


**Figure 3.4 Capsaicin and AEA concentration response curves**

*At 22 ℃ (A) hTRPV1 and (B) rTRPV1; at 37 ℃ (C) hTRPV1 and (D) rTRPV1. Cap=capsaicin, AEA=anandamide and data are mean±SEM (n=3-7).*

### *3.3.3 Effect of Olvanil on HEK293$_{hTRPV1}$ and HEK293$_{rTRPV1}$*

The activity of olvanil was compared with capsaicin at human (h) and rat (r) TRPV1 isoforms expressed HEK293 cells (Figure 3.5). Mean $pEC_{50}$ ranges for capsaicin and olvanil are displayed in Table 3.2.

A) hTRPV1

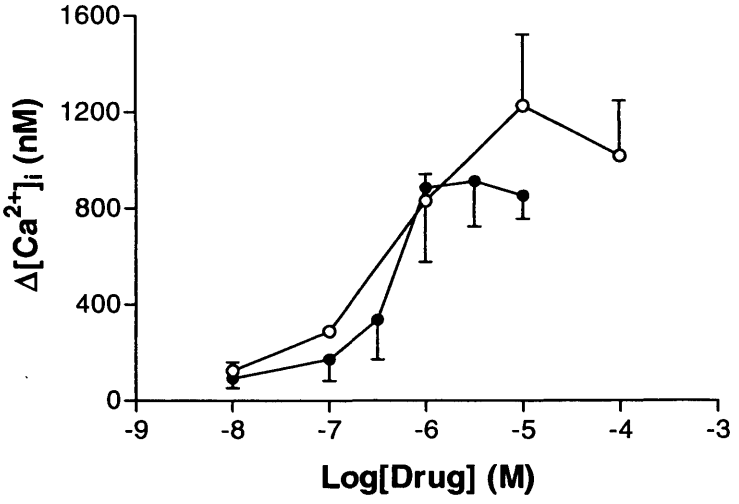


B) rTRPV1

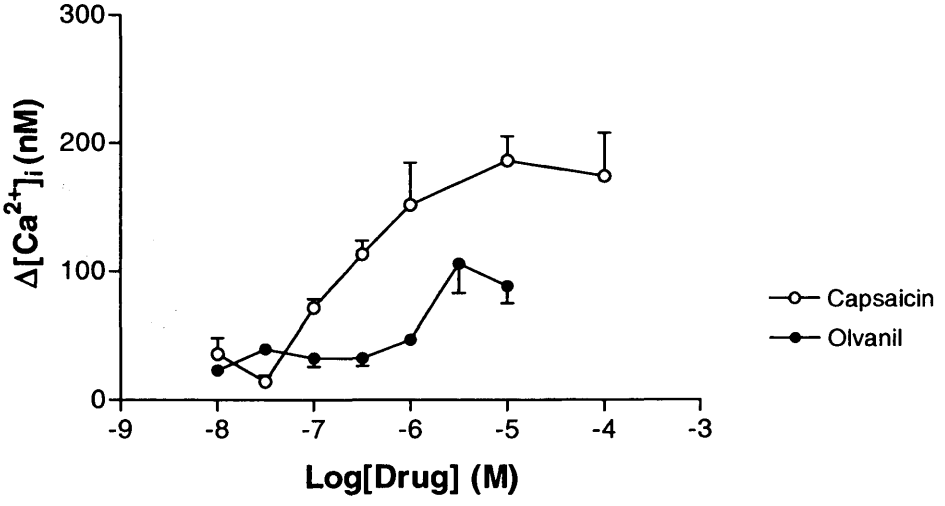


**Figure 3.5 Comparison of capsaicin and olvanil at hTRPV1 and rTRPV1 expressed in HEK293 cells at 37°C**

*Data presented as mean±SEM, n=5 for all except for olvanil at hTRPV1where n=4*

From Figure 3.5 and Table 3.2 of mean $pEC_{50}$ ranges, it is evident that there is no species difference in $pEC_{50}$ for capsaicin (included as a control reference) or olvanil. The reduced efficacy suggests partial agonism for olvanil at rTRPV1.

**Table 3.2 Mean $pEC_{50}$ range obtained from the respective concentration response curves of capsaicin and olvanil in hTRPV1 and rTRPV1**

| | Mean $pEC_{50}$±SEM | |
|---|---|---|
| | **hTRPV1** | **rTRPV1** |
| Capsaicin | 6.70±0.19 | 6.86±0.17 |
| Olvanil | 6.33±0.22 | 5.91±0.10* |

**p=0.0013 compared to capsaicin at rTRPV1, Capsaicin and olvanil in rTRPV1, unpaired t-test, n=5 for all except hTRPV1 olvanil where n=4*

**Inhibition studies**

***3.3.4 Capsaicin***

Since a large variance in $[Ca^{2+}]_i$ levels, including the maximum was found between flasks of cells the following data have been normalised (except where stated).

**Table 3.3 Effect of capsazepine on capsaicin response at rTRPV1 and hTRPV1 at 22°C and 37°C**

| | 22°C | | | 37°C | | |
|---|---|---|---|---|---|---|
| | **$pEC_{50}$ (Ctrl)** | **$pEC_{50}$ (+Cpz)** | **$pK_B$** | **$pEC_{50}$ (Ctrl)** | **$pEC_{50}$ (+Cpz)** | **$pK_B$** |
| **rTRPV1** | 6.34±0.09 | 4.88±0.10 | 5.98±0.09 | 6.02±0.07 | 4.50±0.15 | 6.02±0.10 |
| **hTRPV1** | 6.73±0.15 | 4.49±0.16 | 6.76±0.25* | 6.45±0.05* | 4.22±0.05 | 6.75±0.04* |
| **rTRPV1/hTRPV1** | | | 6.0 | | | 5.4 |

*(Ctrl=control; Cpz=Capsazepine) Data are mean±SEM (n=3-4) at 22°C and 37°C and compared with unpaired t-test. $pEC_{50}$ was significantly different at rTRPV1 at 22°C than at 37°C (p=0.03). *$pEC_{50}$ was significantly higher at hTRPV1 than at rTRPV1 at 37°C (p=0.002). $pK_B$ at hTRPV1 was significantly higher than at rTRPV1 (p=0.02 and 0.004 at 22°C and 37°C respectively). There was no difference in the $pK_B$ at rTRPV1 (p=0.76) or hTRPV1 (p=0.95) at either temperature.*

Capsazepine (30 μM) competitively antagonised the capsaicin mediated increase in $[Ca^{2+}]_i$ in $HEK293_{hTRPV1}$ and $HEK293_{rTRPV1}$ at 22°C and 37°C, Figure 3.6 yielding $pK_B$ values as shown in Table 3.3. Capsazepine alone was inactive. Capsazepine was approximately six-fold more potent at hTRPV1 than rTRPV1.

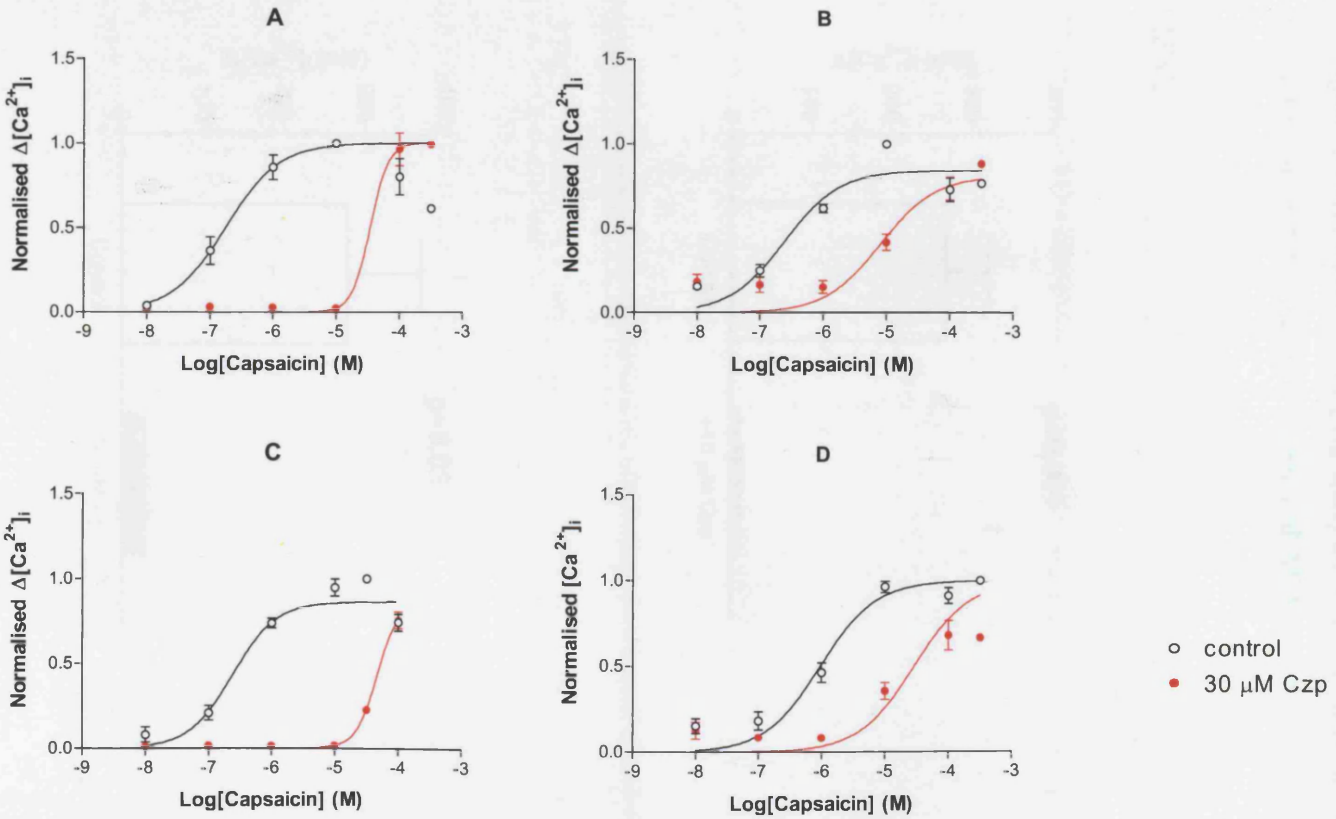


**Figure 3.6 Capsaicin concentration response curves are shifted to the right by capsazepine at 22°C and 37°C at rat and human TRPV1**

*Capsazepine (Czp, 30 μM) produced a rightward shift in the concentration response curve to capsaicin indicative of competitive antagonism. Data (mean±SEM, n=3-4) are normalised to the maximum capsaicin (Cap) response in each individual experiment. At 22℃ (A) hTRPV1 and (B) rTRPV1, at 37℃ (C) hTRPV1 and (D) rTRPV1.*

### *3.3.5 AEA*

Capsazepine (10 μM) inhibited the AEA response at 22°C and 37°C at hTRPV1 as shown in Figure 3.7. However, a full $pK_B$ analysis with capsazepine could not be performed due to relative insolubility and low potency of AEA.

22°C:

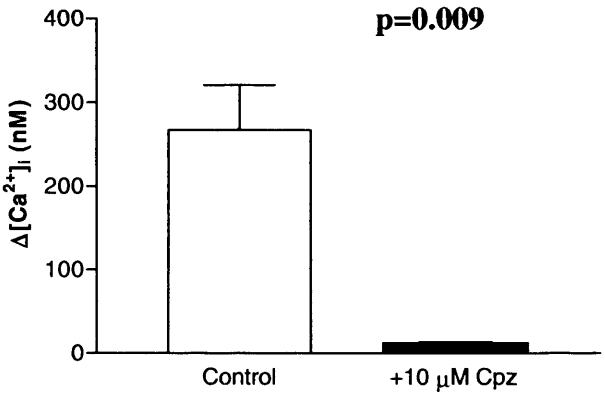


37°C:

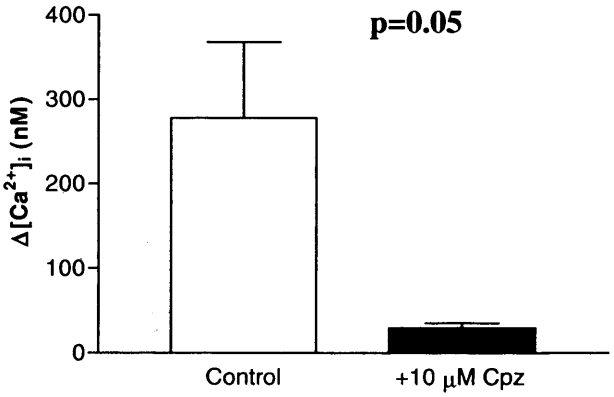


**Figure 3.7 Effect of 10 μM capsazepine on 3 μM AEA at 22°C and 37°C**
*Capsazepine (Cpz) inhibited AEA response in terms of mean $\Delta[Ca^{2+}]_i \pm$SEM at both temperatures in $HEK293_{hTRPV1}$ cells. AEA concentration chosen was approximately 80% of $E_{max}$ from AEA concentration response curves in Figure 3.4. Data was n=3 at both 22 ℃ and 37 ℃.*

### *3.3.6 Olvanil*

Capsazepine also inhibited the response to olvanil in both $HEK293_{hTRPV1}$ (Figure 3.8) and $HEK293_{rTRPV1}$ (Figure 3.9) at 37°C. The degree of inhibition was greater at hTRPV1 than that in rTRPV1.

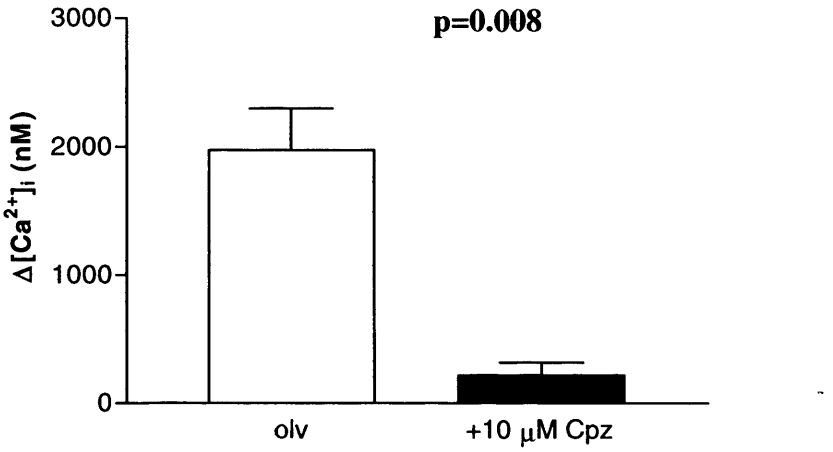


**Figure 3.8 10 μM Capsazepine inhibited the response produced by 1 μM olvanil at hTRPV1 at 37°C**
*Data (n=3) are mean±SEM, olv=olvanil and Cpz=capsazepine*

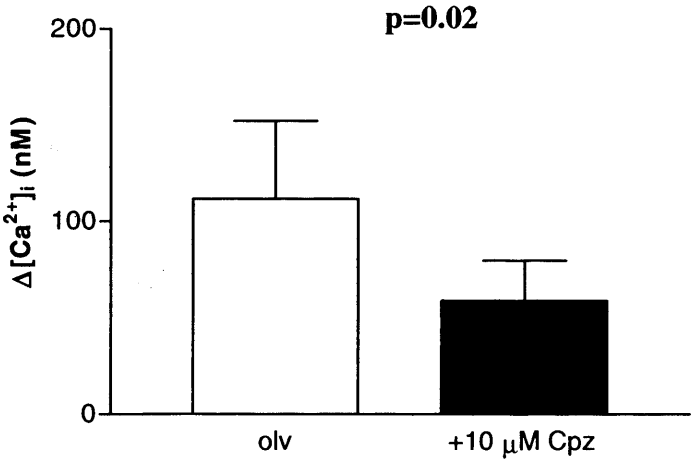


**Figure 3.9 Effect of 10 μM capsazepine on the response due to 1 μM olvanil at rTRPV1 at 37°C**
*Data (n=3) are mean±SEM, olv=olvanil and Cpz=capsazepine*

### *3.3.7 Effects of the exocannabinoid, $\Delta^9$-THC at hTRPV1*

Figure 3.10 displays typical $[Ca^{2+}]_i$ traces in $HEK293_{hTRPV1}$ cells at 37°C, using methodology described in Section 2.7.1. Initially drug solvent effects were investigated (Figure 3.10A). Following addition of 170 mM (20 µl) ethanol (solvent for $\Delta^9$-THC) at 60 s, $[Ca^{2+}]_i$ increased which peaked at approximately 85 s. At maximum $[Ca^{2+}]_i$, 20 µl DMSO (solvent for capsazepine) was added and a gradual decrease in $[Ca^{2+}]_i$ to basal was observed. When 30 µM capsazepine was added at maximum $[Ca^{2+}]_i$, a prompt decrease in $[Ca^{2+}]_i$ to basal resulted. The change in $[Ca^{2+}]_i$ ($\Delta[Ca^{2+}]_i$) was calculated to be 106 nM (control) and 100 nM (capsazepine addition).

Next, the active drug effects were examined (Figure 3.10B). Two typical $[Ca^{2+}]_i$ traces in $HEK293_{hTRPV1}$ cells at 37°C, to which 100 µM $\Delta^9$-THC (20 µl) was added at 60 s. Both traces displayed similar increases in $[Ca^{2+}]_i$ and peaked at approximately 90 s with values of 170 nM and 152 nM. The addition of 20 µl DMSO at maximum $[Ca^{2+}]_i$ resulted in a gradual decrease in $[Ca^{2+}]_i$ to basal. In comparison, addition of 30 µM capsazepine at maximum $[Ca^{2+}]_i$ produced a sharper decline in $[Ca^{2+}]_i$ to basal. The $\Delta[Ca^{2+}]_i$ was similar to the solvent experiments with 100 nM (control) and 98 nM (capsazepine addition).

The ethanol effect was probed further and appeared concentration-dependent. However, the response failed to saturate despite using concentrations up to 1.5 M, Figure 3.10C.

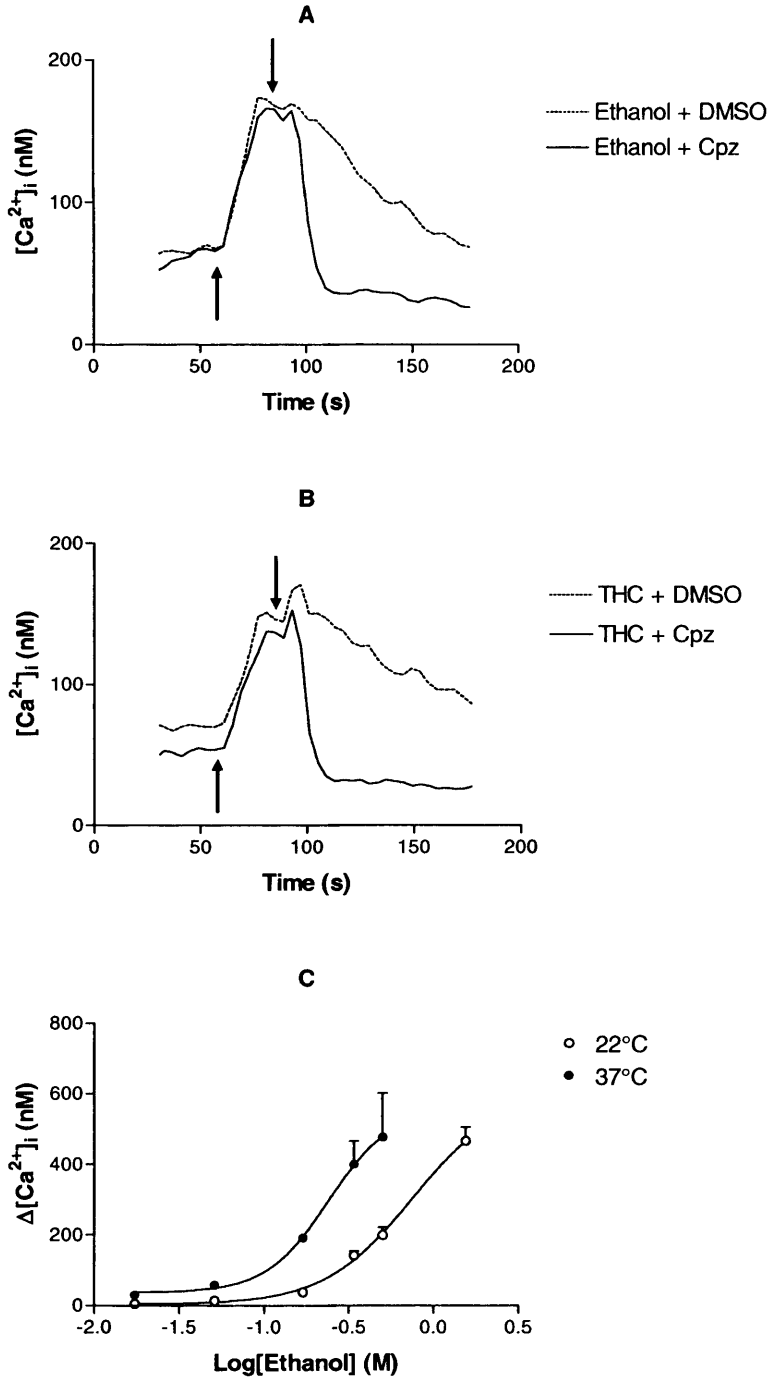


**Figure 3.10 Effect of ethanol and $\Delta^9$-THC on $[Ca^{2+}]_i$ at hTRPV1 at 37°C**

*(A) Ethanol (170 mM) and (B) $\Delta^9$-THC (100 μM) addition (indicated by the initial arrows), produced a capsazepine (Czp) sensitive increase in $[Ca^{2+}]_i$. Capsazepine or DMSO (addition shown by latter arrow, 30 μM capsazepine in DMSO to 0.3% v/v final). (C) Ethanol concentration response at hTRPV1 at 22℃ (n=4) and 37℃ (n=5), data are mean±SEM.*

### *3.3.8 Comparison of $\Delta^9$-THC and ethanol with capsaicin and AEA*

Figure 3.11 shows $[Ca^{2+}]_i$ response in $HEK293_{hTRPV1}$ cells at 37°C to ethanol, $\Delta^9$-THC, capsaicin and AEA measured fluorimetrically as in Section 2.7.1. The largest response, approximately 600 nM, was produced by capsaicin and AEA. Statistical analysis using ANOVA, comparing capsaicin, AEA, $\Delta^9$-THC and ethanol, displayed an overall significant difference ($p<0.001$, ANOVA) in $[Ca^{2+}]_i$ response. However, there was no difference between ethanol and $\Delta^9$-THC ($p>0.05$) or capsaicin and AEA ($p>0.05$).

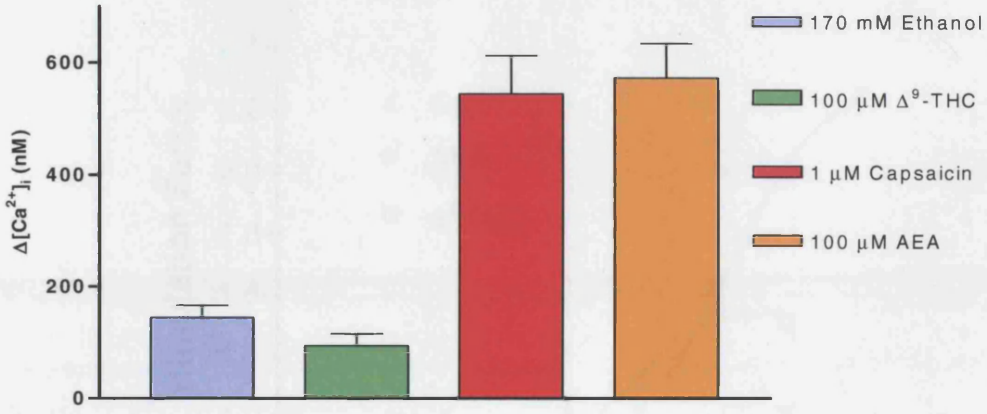


**Figure 3.11 $[Ca^{2+}]_i$ response of $HEK293_{hTRPV1}$ cells at 37°C to various compounds**
*$\Delta[Ca^{2+}]_i$ was determined by subtracting the basal from peak fluorimetric measurements of $[Ca^{2+}]_i$. AEA and capsaicin produced the greatest response while ethanol and $\Delta^9$-THC produced the lowest response. ANOVA analysis displayed $p<0.001$ in comparing ethanol, $\Delta^9$-THC, capsaicin and AEA. T-test with Bonferroni correction verified that there was no significant difference ($p>0.05$) in $[Ca^{2+}]_i$ response between ethanol and $\Delta^9$-THC. Data are mean±SEM ($n=6$-9).*

### *3.3.9 GTPγ[$^{35}$S] Experiments*

These were performed in order to determine the activity of the various agonists, AEA, $\Delta^9$-THC and capsaicin, at rat $CB_1$ receptor in cerebellar membranes (Section 2.8). The assay involved the addition of these compounds to stimulate the incorporation of GTPγ[$^{35}$S] into the G protein relative to basal. This is displayed as stimulation factor (Figure 3.12). AEA

and $\Delta^9$-THC produced a concentration-dependent stimulation that was saturable. Corresponding $pEC_{50}$ and $E_{max}$ values were 5.79±0.09 and 7.10±0.13 ($p<0.05$) and 2.29±0.06 and 1.54±0.04 ($p<0.05$) respectively while capsaicin failed to stimulate GTPγ[$^{35}$S] binding.

$\Delta^9$-THC was a partial agonist relative to AEA in this system and the relative intrinsic activity (α) was 0.41. The $pEC_{50}$ value of AEA at $CB_1$ is in agreement ($p>0.05$) with that at hTRPV1 ($pEC_{50}$ displayed in brackets); 22°C (5.82) and 37°C (5.84); at rTRPV1, 22°C (5.66) and 37°C (5.55).

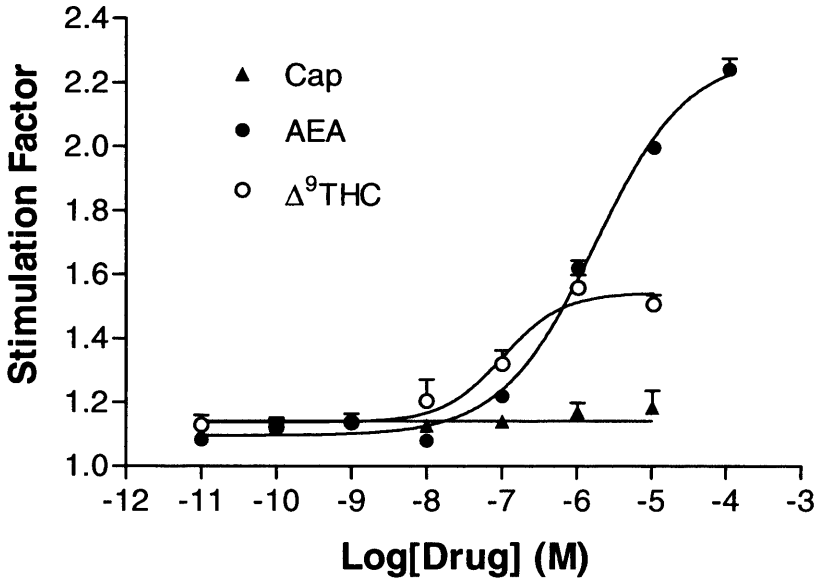


**Figure 3.12 GTPγ[$^{35}$S] assay showing effects of AEA, $\Delta^9$-THC and capsaicin at $CB_1$ in rat cerebellar membranes**
*Data are mean±SEM (n=3) and expressed as stimulation factor (agonist stimulated specific binding relative to basal specific binding).*

Due to the structural similarities of AEA and olvanil and AEA's agonist activity at the $CB_1$ receptor, olvanil response was examined at the $CB_1$ receptor (Figure 3.13). AEA, used as positive control, exhibited a stimulation factor greater than 1, relating to the activation of $CB_1$ receptor. SR141716A, a classic $CB_1$ antagonist, inhibited the AEA response at the $CB_1$ receptor. Interestingly, the degree of inhibition resulted in a relatively low stimulation factor compared to capsaicin and AEA. In comparison to the initial GTPγ[$^{35}$S] binding experiment (Figure 3.12), AEA stimulated a relatively lower binding which could be due

to a reduced expression of $CB_1$. As expected, capsaicin failed to stimulate GTPγ[$^{35}$S] binding. Under the same assay system olvanil does not display activity at $CB_1$ receptors.

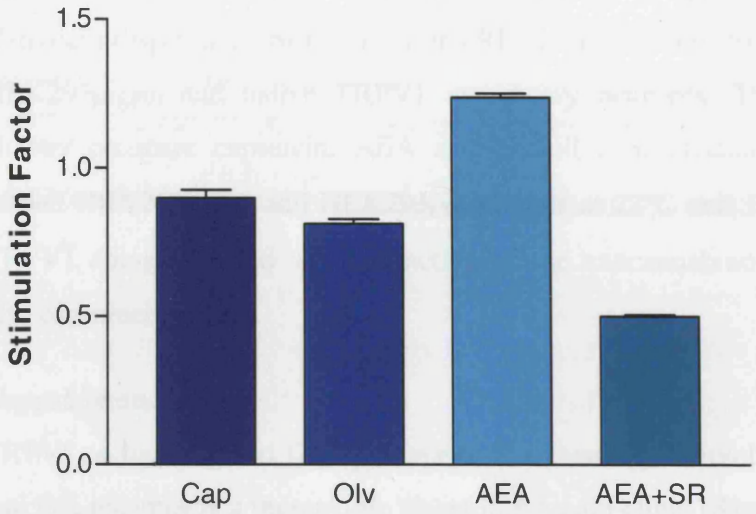


**Figure 3.13 GTPγ[$^{35}$S] assay showing the effects of capsaicin, olvanil and AEA on the $CB_1$ receptor, in rat cerebellar membranes, n=3**

*10 μM Olvanil (Olv) and 10 μM capsaicin (Cap) produced no effect, while 10 μM AEA activated $CB_1$ with inhibition of AEA activation by 10 μM of the antagonist SR141716A (SR). Data are mean±SEM (n=3).*

## 3.4 Discussion

*General comments*

TRPV1, a ligand-gated, $Ca^{2+}$ permeable ion channel represents an important member of the TRP receptor family that is linked to nociceptive signalling (Szallasi *et al.*, 1999b). Capsaicin displays agonist activity at TRPV1 expressed in recombinant $HEK293_{rTRPV1}$ and $HEK293_{hTRPV1}$ and native TRPV1 in sensory neurones. The studies described in this chapter compare capsaicin, AEA and olvanil concentration response curves in fura-2 loaded $HEK293_{rTRPV1}$ and $HEK293_{hTRPV1}$ cells at 22°C and 37°C. The pharmacology of a TRPV1 antagonist and any interaction of the exocannabinoid $\Delta^9$-THC with TRPV1 are also examined.

*Capsaicin and AEA*

TRPV1, a ligand-gated $Ca^{2+}$ permeable ion channel, is involved in nociceptive signalling and this receptor is a therapeutic target in the pain clinic (Szallasi *et al.*, 1999b). Capsaicin and AEA are agonists at recombinant rat and human TRPV1 receptors (Jerman *et al.*, 2000; Smart *et al.*, 2000b; Smart *et al.*, 2001; Sprague *et al.*, 2001) and native TRPV1 in sensory neurones (Caterina *et al.*, 1997; Jerman *et al.*, 2002). The capsaicin response at recombinant rat and human TRPV1 receptors was examined at 22°C and 37°C (two commonly used experimental temperatures). There was a temperature-dependent increase in maximum response (with no significant change in potency) to capsaicin at both receptors. However, it has been previously reported for recombinant $HEK293_{rTRPV1}$ cells that the potency decreased with increasing temperature although the temperature reached 50°C, a temperature that would of itself activate TRPV1 (Sprague *et al.*, 2001). There is currently no explanation for this discrepancy. At rTRPV1, the $pEC_{50}$ value reported here of 6.56 at 22°C was lower than recently reported (Jerman *et al.*, 2000; Sprague *et al.*, 2001) in transfected HEK293 cells. However, at 37°C, the $pEC_{50}$ values were in good agreement (Sprague *et al.*, 2001). At hTRPV1, $pEC_{50}$ values reported here were 6.88 and 6.77 at 22°C and 37°C respectively and these were in reasonable agreement with those determined from FLIPR-based calcium assays at 25°C (Smart *et al.*, 2000a; Smart *et al.*, 2001) in $HEK293_{hTRPV1}$. Species differences for capsaicin have not been reported in other studies (Jerman *et al.*, 2000; Smart *et al.*, 2000a; Smart *et al.*, 2001). At higher capsaicin concentration (100 μM), there was an apparent decline in $Ca^{2+}$ response, which may result from an acute desensitisation process.

The endocannabinoid, AEA, activates not only the $CB_1$ receptor (Calignano *et al.*, 1998) but also TRPV1 (Zygmunt *et al.*, 1999). The AEA response at 22°C at hTRPV1 ($pEC_{50}$ 5.82) is consistent with reported values of 5.6 (Smart *et al.*, 2001), 5.95 (Smart *et al.*, 2000a) and 5.69 (Sprague *et al.*, 2001). No difference in potency was observed for AEA response at hTRPV1 or rTRPV1 with increasing temperature but there was an increase in maximum response, consistent with changes observed for capsaicin. Reports differ in classifying AEA as either a partial (Zygmunt *et al.*, 1999) or full agonist at recombinant TRPV1 (Smart *et al.*, 2000a) and this may be due to species or expression differences. AEA partial and full agonism at rTRPV1 and hTRPV1 respectively has also been reported by Ralevic and co-workers (Ralevic *et al.*, 2001). As more receptors are present in cells expressing the human clone it may be suspected that higher expression coupled with the possible introduction of a receptor reserve increases relative intrinsic activity. However studies on recombinant rat and human TRPV1 have shown that AEA is a full agonist whilst in rat DRG, it was difficult to ascertain due to solubility issues (Jerman *et al.*, 2002; Smart *et al.*, 2000a).

*Olvanil*

Both capsaicin and olvanil increased $[Ca^{2+}]_i$ in hTRPV1 and rTRPV1 in a concentration-dependent manner. During the course of this study, $pEC_{50}$ data relating to responses due to olvanil, displayed some variability. On the whole, the differences between the responses were small and could be accounted for by cell batch variation as exhibited by the observed variation in $[Ca^{2+}]_i$. A species difference was observed in terms of the degree of response obtained between batches and between the recombinant human and rat isoforms; with the maximum response in hTRPV1 cells being much larger than that of rTRPV1 expressing cells. In terms of potency, no species difference was observed for capsaicin and olvanil. However, a significant difference was observed in the activation of the rTRPV1 receptor by capsaicin and olvanil. A $pEC_{50}$ value of 6.86 was obtained with capsaicin whereas the value estimated with olvanil was 5.91. Olvanil appears to be less efficacious than capsaicin in rTRPV1, suggesting partial agonism although it has been reported to be a full agonist (Jerman *et al.*, 2000).

It is clear that the $pEC_{50}$ values reported in the literature indicate that both capsaicin and olvanil are generally more potent than those obtained in the present study (see Table 3.4). One possible reason for this discrepancy maybe due to the use of different experimental

procedures. For instance, in the paper by Ralevic and colleagues (Ralevic *et al.*, 2001), the technique employed to measure the change in $[Ca^{2+}]_i$ was FLIPR; to monitor cell fluorescence (Sullivan *et al.*, 1999) before and after the addition of the agonist whereas in this thesis chapter, $[Ca^{2+}]_i$ changes were measured with a LS50B spectrofluorimeter. Also, the FLIPR assay system is maintained at a temperature of 25°C whereas the cells were equilibrated to 37°C in this chapter's experiments. See Chapter 5 for experiments using olvanil at hTRPV1 expressed in SH-SY5Y cells.

**Table 3.4 Comparison of reported $pEC_{50}$ values for capsaicin and olvanil**

| Cells | Technique Used | $pEC_{50}$ Value | | Reference |
|---|---|---|---|---|
| | | Capsaicin | Olvanil | |
| $HEK293_{hTRPV1}$ | Measuring $[Ca^{2+}]_i$ using FLIPR | 7.10±0.06 | 7.73±0.05 | (Ralevic *et al.*, 2001) |
| $HEK293_{rTRPV1}$ | | 7.79±0.13 | 8.09±0.09 | (Ralevic *et al.*, 2001) |
| $HEK293_{rTRPV1}$ | | 8.25±0.11 | 8.37±0.04 | (Jerman *et al.*, 2002) |
| Rat DRG | | 7.45±0.10 | 7.55±0.07 | (Jerman *et al.*, 2002) |

*Olvanil GTPγ[$^{35}$S] Experiments*

GTPγ[$^{35}$S] assays were performed in order to compare $CB_1$ activity of olvanil and capsaicin with that of the endocannabinoid AEA. With the GTPγ[$^{35}$S] assay, a stimulation factor greater than 1 is indicative of receptor activation. Interestingly, the results possibly indicate inverse agonism by the antagonist SR141716A, which matched suggestions in the literature that SR141716A displays inverse agonism at $CB_1$ (MacLennan *et al.*, 1998). Since olvanil shares structural similarities with AEA, it maybe expected that it exhibits agonism at $CB_1$. However, this was not found to be the case. The GTPγ[$^{35}$S] assay is not subject to a high level of upstream signal amplification and hence olvanil does not display $CB_1$ activity in this assay. Contrary to the findings of this study, Di Marzo and colleagues reported activation of the $CB_1$ receptor by the vanilloid olvanil. They reported an inhibition of forskolin-induced cAMP formation *via* the activation of the $CB_1$ receptor in a cAMP

assay, see Figure 3.14 (Di Marzo *et al.*, 1998). The cAMP assay is a much more responsive means of testing activity and has a greater amplification. Hence the finding that olvanil is a $CB_1$ agonist.

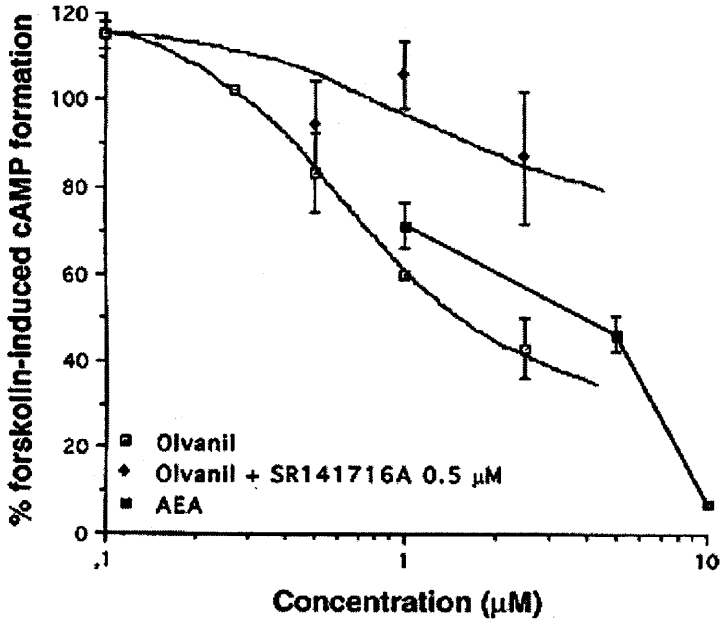


**Figure 3.14 Inhibition of forskolin induced cAMP formation as a result of $CB_1$ activation by olvanil.**
*Figure taken from paper by Di Marzo (Di Marzo et al., 1998).*

*Capsazepine studies*

Capsazepine is a competitive antagonist at TRPV1 (Walpole *et al.*, 1994). Competitive antagonism was displayed at both rTRPV1 and hTRPV1 at 22°C and 37°C with this molecule. Capsazepine potency was not temperature-dependent at TRPV1, as confirmed by others (Nagy *et al.*, 1999b), but there was an approximate six-fold increase in capsazepine potency for hTRPV1 compared to rTRPV1. This difference is consistent with that reported by McIntyre and co-workers (McIntyre *et al.*, 2001). Values of $pK_B$ for this antagonist have proved highly variable. For example in FLIPR-based assays, this varied from 6.58 to 7.31 in $HEK293_{hTRPV1}$ cells (Smart *et al.*, 2000a; Smart *et al.*, 2001) and 7.52 in $HEK293_{rTRPV1}$ (Jerman *et al.*, 2000). Other reports include values of 6.04 in guinea-pig trachea, 5.12 in guinea-pig bronchi (sensory neurones) and 6.65 at rTRPV1 transfected

CHO cells (Belvisi *et al.*, 1992; Ellis *et al.*, 1994; McIntyre *et al.*, 2001). See Table 3.5 for variation in reported capsazepine $pK_B$ values. The reason for these differences is unclear.

**Table 3.5 Wide-range of reported capsazepine $pK_B$ values**

| Cells | Temp (°C) | [Capsazepine] | [Capsaicin] | $pK_B$ | Reference |
|---|---|---|---|---|---|
| $HEK293_{hTRPV1}$ | 25 | 0.1 μM-10 μM | 100 nM | 6.58 | (Smart *et al.*, 2001) |
| $HEK293_{rTRPV1}$ | 25 | 0.1 nM-10 μM | 100 nM | 7.52 | (Jerman *et al.*, 2000) |
| Guinea pig bronchi (sensory neurones) | RT? | 1 μM-1 mM | $10^{-8} - 10^{-4}$ M | 5.12 | (Belvisi *et al.*, 1992) |
| Guinea pig trachea | 37 | 10 μM | 1-10000 nM | 6.04 | (Ellis *et al.*, 1994) |
| $CHO_{rTRPV1}$ | RT | 1 nM-30 μM | 0.35 μM | 6.65 | (McIntyre *et al.*, 2001) |

*$CHO_{rTRPV1}$ - rTRPV1 recombinantly expressed in chinese hamster ovary cells, RT - room temperature*

It has been shown that capsazepine inhibited the $[Ca^{2+}]_i$ response produced by AEA at 22°C and 37°C. Low AEA potency in conjunction with poor chemical insolubility in aqueous systems posed difficulties in obtaining a complete $pK_B$ analysis of AEA inhibition by capsazepine.

Capsazepine was shown to inhibit olvanil-mediated responses in both human and rat recombinant cells although full $pK_B$ analysis could not be performed because similar to AEA, olvanil possesses poor chemical insolubility in aqueous systems. In addition, inhibition at rTRPV1 was minimal but this is probably due to the low level of response exhibited by these cell batches.

*Investigation of exocannabinoid activity at TRPV1*

The exocannabinoid $\Delta^9$-THC activates $CB_1$ receptors, however, only endo- rather than exocannabinoid activity at TRPV1 has been extensively examined. Experiments were performed to determine whether $\Delta^9$-THC was able to activate TRPV1 in a similar fashion to that of the endocannabinoid AEA. $\Delta^9$-THC produced elevated $[Ca^{2+}]_i$ levels but subsequent investigations with an ethanol control attributed this effect to ethanol alone. These results are supported by ethanol activity at TRPV1 reported by Trevisani and colleagues (Trevisani *et al.*, 2002). Capsaicin, AEA, protons and heat can potentiate the modulation of TRPV1 activity by ethanol. Also, the threshold for heat activation of TRPV1 dropped from 42°C to 34°C. Ethanol was found to increase the potency and

efficacy of capsaicin and caused the release of substance P from central and peripheral terminals of capsaicin-sensitive nociceptors on C- and Aδ-fibres. Release of substance P is related to pain sensation and ethanol can lower the threshold of TRPV1 to body temperature, thus the data provided an explanation for the burning pain sensed by patients with oesophagitis after consuming alcoholic beverages (Trevisani *et al.*, 2002). These data indicate that endo- rather than exocannabinoids are TRPV1 activators.

GTPγ[$^{35}$S] binding assay was employed to act (i) as a positive control for $\Delta^9$-THC activity and (ii) to allow a comparison of AEA potency at $CB_1$ and TRPV1 to be made. Both AEA and $\Delta^9$-THC activated the $CB_1$ receptor. AEA displayed a lower potency than a previously reported $pEC_{50}$ value of 6.56 while the potency of $\Delta^9$-THC was consistent with the literature (Kearn *et al.*, 1999). The data demonstrated that $\Delta^9$-THC was a partial agonist relative to AEA. As expected, capsaicin had no effect at the $CB_1$ receptor.

Speculation exists over whether AEA or other similar unidentified lipid compounds are endogenous ligands at TRPV1. It has been clearly demonstrated that AEA is active at both TRPV1 and $CB_1$. It has been known for some time that TRPV1 receptors mediate vasodilation, in arterial vessels, produced in response to AEA (Zygmunt *et al.*, 1999). In summary, capsaicin activates TRPV1, $\Delta^9$-THC activates $CB_1$ and AEA activates both receptors. Thus it could be suggested that $CB_1$ and TRPV1 may respectively be metabotropic and ionotropic members of a family of receptors.

# 4 SUBCLONING &TRANSFECTION OF HUMAN TRPV1 IN SH-SY5Y CELLS

## 4.1 Introduction

The vanilloid receptor and signal transduction of noxious stimuli remained elusive for many years until Caterina cloned rat TRPV1 from DRG, thus providing a tool for molecular and pharmacological study (Caterina *et al.*, 1997). This has instigated further cloning studies including those from GlaxoSmithKline who cloned human TRPV1 (hTRPV1) cDNA, expressed in *Xenopus* oocytes and HEK293 cells. The cDNA contained a 2517 bp open reading frame with 839 amino acids and 92% homology to the rat isoform (Hayes *et al.*, 2000). In 2001, Cortright *et al.*, and McIntyre *et al.* cloned hTRPV1 cDNA encoding a 839 amino acid protein which was expressed in *Xenopus* oocytes and CHO cells with 85% identity to rTRPV1 (Cortright *et al.*, 2001; McIntyre *et al.*, 2001). To date, recombinant hTRPV1 has not been expressed in a neuronal cell-line.

Differences in the pharmacology of recombinant rTRPV1 compared to that of the endogenous vanilloid receptor in rat DRG neurones have been reported. The expression profile of cloned hTRPV1 is similar to that of rTRPV1 and was elevated, relative to other tissues, in DRG (Hayes *et al.*, 2000). However, preparation of primary DRG cultures in sufficient quantities for structure activity and mechanistic studies is problematic.

Recombinant TRPV1 expressed in cloned cells offers several advantages over cultured neurones expressing hTRPV1 in that a homogeneous population of cells is obtained. Also cloned cells are easier to maintain and grow in contrast to cultured neurones. However, the clonal population will only serve as a model which is not necessarily a faithful representation of the *in vivo* situation.

Derived from the SK-N-SH cell-line, the SH-SY5Y human neuroblastoma cell is often used as a model of sympathetic ganglia and has been extensively used in the study of neuronal function. SK-N-SH, was itself derived from human metastatic neuroblastoma tissue and originally cultured for cancer research. SH-SY5Y cells have small cell bodies with "neurite-like" cell processes and contain tyrosine hydroxylase and dopamine β hydroxalase, unique to catecholamine neurones. In addition, μ and δ opioid receptors are expressed and functionally coupled to cAMP inhibition *via* $G_i$. $M_3$ muscarinic α2 adrenergic receptors are also present. It has been reported that SH-SY5Y cells are capable of both uptake and subsequent release of [$^3$H]NA in response to $K^+$-depolarisation, the cholinergic agonist carbachol, the calcium ionophore ionomycin and nicotinic receptor stimulation. In addition to a muscarinic receptor population, SH-SY5Y cells also express

$B_2$ bradykinin receptors, the activation of which stimulates release of [$^3$H]NA. For further information, the reader is referred to a review by Vaughan (Vaughan *et al.*, 1995).

## 4.2 Aims

- To transfect recombinant human TRPV1 DNA into SH-SY5Y cells as these have specific cellular characteristics:
  - neurones that are easy to culture (and can be differentiated)
  - electrically excitable membranes that express L and N voltage-sensitive calcium channels (VSCCs)
  - well characterised with respect to other receptors (opioids, muscarinic α2, nociceptin/orphanin FQ (N/OFQ) peptide (NOP))
  - capable of uptake and release of NA
- To produce a cloned neuronal expression system by antibiotic selection pressure and verifying TRPV1 expression *via* $[Ca^{2+}]_i$ measurements

## 4.3 Cloning and Transfection methodology

### *4.3.1 Cloning of human TRPV1*

The cloning of human TRPV1 was performed at GlaxoSmithKline, Harlow, UK. Briefly, human TRPV1 cDNA was identified using the published rat TRPV1 sequence (GenBank accession AF029310) to search public nucleotide databases. Expressed sequence tag T48002 was identified and its sequence extended by rapid amplification of the cDNA ends using cDNA templates from a number of tissue sources. A complete 2517 bp open reading frame of the gene was amplified by PCR from brain cDNA and separated from shorter non-specific products by agarose gel electrophoresis. The DNA was inserted into the expression vector pcDNA3.1/V5/His-TOPO and double strand sequenced. The 2556 bp insert includes 4 nucleotides (an ACC Kozak consensus) before the ATG start codon and 33 following the TGA stop codon (Hayes *et al.*, 2000).

### *4.3.2 Luria-Bertani (LB) medium preparation*

LB medium was used for the growth of bacteria. 10 g tryptone, 5 g yeast extract and 10 g NaCl were dissolved in 1 l distilled $H_2O$. The pH was adjusted to 7.5 with NaOH. If Bacto-agar was required, 15 g of this was added and the medium was autoclaved. Once cooled to approximately 50°C, aseptic techniques were utilised for pouring onto sterile plates or into flasks. If antibiotics such as ampicillin were needed, 200 µl of a 100 mg/ml sterile ampicillin stock (previously dissolved in sterile $H_2O$) was added to 200 ml LB agar, cooled to approximately 50°C, before pouring onto sterile plates. The plates were left to cool until the LB media had set and were subsequently stored at 4°C until required.

### *4.3.3 Super optimal broth (SOB)*

2% tryptone, 0.5% yeast extract, 10 mM NaCl, 2.5 mM KCl, 10 mM $MgCl_2$ and 10 mM $MgSO_4$ were dissolved in 1 l distilled $H_2O$. The pH was adjusted to 7.0 with KOH and the solution was autoclaved.

### *4.3.4 Transformation buffer (TB)*

10 mM Pipes, 15 mM $CaCl_2$ and 250 mM KCl were dissolved in 1 l distilled $H_2O$. The pH was adjusted to 6.7 with KOH, 55 mM $MnCl_2$ was added and the solution was filter sterilised.

### *4.3.5 Agarose gel preparation*

To visualise DNA, ethidium bromide is used as it chelates $Mg^{2+}$ within the DNA. (As a precaution, nitrile gloves were worn when handling the gel as ethidium bromide is a strong mutagen). A 1% (w/v) agarose gel was prepared by using microwave heating to dissolve agarose powder in 1 x TAE buffer in a conical flask and 0.02% (v/v) ethidium bromide was added. The gel apparatus was set up with gel ends, gel combs and a gel tray. The gel was left to cool to 50°C, gently poured into the gel tray and allowed to set. Subsequently, running buffer was poured onto the gel to an approximate depth of 1 cm. The gel comb was carefully removed from the set gel to prevent damage to the newly formed wells. Appropriate volumes of loading dye were added to each DNA sample and a 500 bp DNA ladder (1 µg/ml). The DNA samples and the DNA ladder were loaded into the wells. The voltage supply was connected and ran at 100 mV until the dye front had reached the end of the gel. The gel was observed using a UV transilluminator, which displays the presence of DNA and a photograph of the gel was taken as appropriate.

### *4.3.6 Restriction enzyme digestion*

DNA that is intentionally made from different exogenous sources is called recombinant DNA. To produce separate DNA segments, restriction enzymes are used to cut up DNA at specific sites. To join the DNA parts, DNA ligase is used to ligate DNA into a bacterial plasmid. A typical restriction enzyme digest was performed by setting up the following:

| | **Volume (µl)** |
|---|---|
| DNA | 5 |
| Enzyme buffer | 2 |
| Restriction enzyme | 1 |
| Sterile distilled $H_2O$ | 12 |

The correct enzyme buffer was selected for optimum activity. When performing double enzyme digests, the buffer that offered the optimum activity for both enzymes was chosen. The total volume was 20 µl and the constituents were mixed thoroughly in an eppendorf tube. The digests were incubated at the enzymes' optimum temperature. Generally, 1 unit of restriction enzyme will completely digest 1 µg of DNA in a 50 µl reaction volume in 1 h.

### *4.3.7 DNA extraction from agarose gel*

To check that the DNA had been digested and that the correct fragments were present, restriction enzyme digests were run on a 1% (v/v) agarose gel with a 500 bp DNA ladder (1 µg/ml). The DNA can be extracted from the gel easily by excision and centrifugation ready for ligation.

The DNA fragments were observed under a UV transilluminator and those fragments of interest were quickly excised with a scalpel blade to minimise DNA degradation from UV light. The DNA was extracted from the agarose gel by centrifugation in Ultrafree-DA Amicon tubes. A 5 µl volume of DNA with an appropriate volume of loading dye was loaded on a 1% agarose (v/v) gel. A 500 bp DNA ladder (3 ng) was simultaneously run alongside the DNA sample. The DNA was observed under a UV transilluminator and the amount extracted was estimated by comparing the relative brightness of the sample band to the DNA ladder.

### *4.3.8 DNA ligation*

To synthesise recombinant DNA, linear plasmid and the DNA fragments of interest are ligated with DNA ligase. A range of insert:vector ratios were included in DNA ligation reactions. A ligation mix consisted of:

| | **Volume (µl)** |
|---|---|
| 10 mM ATP | 1 |
| Plasmid vector (30 ng) | 3 |
| 10 x T4 Ligase buffer | 2 |
| T4 Ligase (400000 u/ml) | 1 |
| hTRPV1 insert | |
| Sterile distilled $H_2O$ | |

The amount of vector was kept constant while the amount of insert was appropriately altered for the following insert:vector ratios – 1:1, 2:1 and 3:1. Sterile distilled $H_2O$ was added to make a final volume of 20 µl. A control was included in which the hTRPV1 DNA insert was excluded. The ligations were mixed thoroughly and incubated at 16°C overnight.

### *4.3.9 Preparation of competent Escherichia coli cells*

10-12 large *Escherichia coli* DH5α colonies were used to inoculate 250 ml SOB in a shakeflask. The culture was grown for 2-3 days until the cells reached an $OD_{600}$ of 0.6. The culture was incubated on ice for 10 min followed by centrifugation at 4000 x g for 10 min at 4°C. The supernatant was discarded and the pellet resuspended in 20 ml ice-cold TB, then incubated on ice for 10 min. This was centrifuged as previously described. The supernatant was discarded and the pellet resuspended in 20 ml ice-cold TB. The cells were shaken gently while DMSO was slowly added to the cells until a final concentration of 7% (v/v) was reached. The cells were incubated on ice for 10 min and were finally dispensed in aliquots into pre-cooled eppendorfs. The cells were stored at -80°C until required.

### *4.3.10 Transformation*

The ligation reactions were placed in ice. 10 µl of each ligation was added to a 100 µl aliquot of *E. coli* DH5α cells, mixed gently by pipetting and incubated on ice for 30 min. The cells were heat-shocked at 42°C in a water bath for 45 s and quickly returned onto ice for 2 min. 200 µl of SOC media was added to each ligation and the cells were placed in a shaker at 250 rpm for 1 h at 37°C. Each ligation mix was pipetted and spread aseptically onto an LB plate and left until the liquid had soaked completely into the agar surface. The plates were inverted to prevent condensation on the agar layer and incubated at 37°C overnight.

### *4.3.11 Mini plasmid preparation*

3 ml of LB media (supplemented with ampicillin to a final concentration of 100 µg/ml) was inoculated with a colony and incubated at 37°C in an orbital incubator overnight. The mini plasmid preparation was performed using a GFX Micro Plasmid Prep Kit. Briefly, 1.0-1.5 ml of the overnight culture was centrifuged to produce a pellet and the supernatant removed. The pellet was completely resuspended in 150 µl of Solution I (isotonic solution containing RNase) with vigorous vortexing. Cells were lysed by alkali treatment and chromosomal DNA and proteins denatured by adding 150 µl of Solution II (NaOH, sodium dodecyl sulphate) and was mixed by inverting the tube gently. The lysate was neutralised by adding 300 µl of Solution III (acetate solution) and mixed by inverting the tube gently until a flocculate appeared which was evenly dispersed. The mixture was centrifuged to pellet the cell debris and the supernatant was run through a column where the plasmid

DNA becomes isolated in the glass fibre matrix. The DNA was washed with an ethanolic buffer to remove salts and other residual contaminants. DNA was finally eluted and dissolved in 100 µl sterile $H_2O$.

### *4.3.12 Maxi plasmid preparation*

20 µl of the remaining bacterial culture (from the mini plasmid preparation) was used to inoculate a shakeflask of 500 ml LB media supplemented with ampicillin (final concentration 100 µg/ml). The flask was incubated overnight at 37°C in an orbital incubator. A maxi plasmid preparation was performed using a NucleoBond plasmid purification kit. Briefly, the bacterial culture was centrifuged at 6000 x g for 15 min at 4°C and the pellet resuspended in Buffer S1 and RNase A provided in the kit. Buffer S2 (for lysis) was added and this was mixed gently for up to 5 min. Then Buffer S3 (neutralisation) was added and this was mixed gently and incubated in ice for 5 min. The lysate was centrifuged at ≥10000 x g at 4°C. The supernatant was loaded into the NucleoBond cartridge and the cartridge washed. The plasmid DNA was eluted with a provided buffer and precipitated with isopropanol. The DNA was dissolved in 500 µl sterile $H_2O$.

**Transfection Methodology**

Initially, the plasmid used during chemical transfection of human TRPV1 was pcDNA3.1/V5-His-TOPO (see Section 4.3.1) as displayed in Figure 4.1. However, due to technical reasons, explained in Section 4.6, another plasmid pIREShyg2 (Figure 4.2) was utilised instead in an electroporation-type transfection.

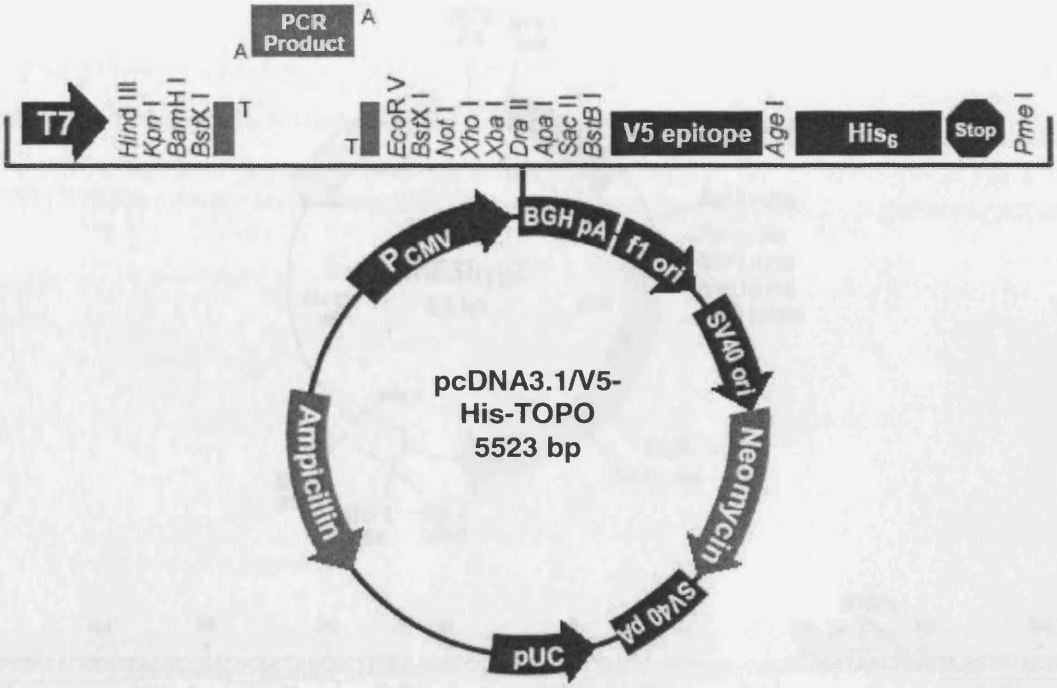


**Figure 4.1 The plasmid pcDNA3.1/V5-His-TOPO used for transfecting human TRPV1**

*The multiple cloning site is shown and the plasmid contains a human cytomegalovirus (CMV) promoter and ampicillin and neomycin resistance genes, SV40 promotor (SV40 pA) and origin (SV40 ori), BGH polyadenylation site (BGH pA) and a pUC origin.*

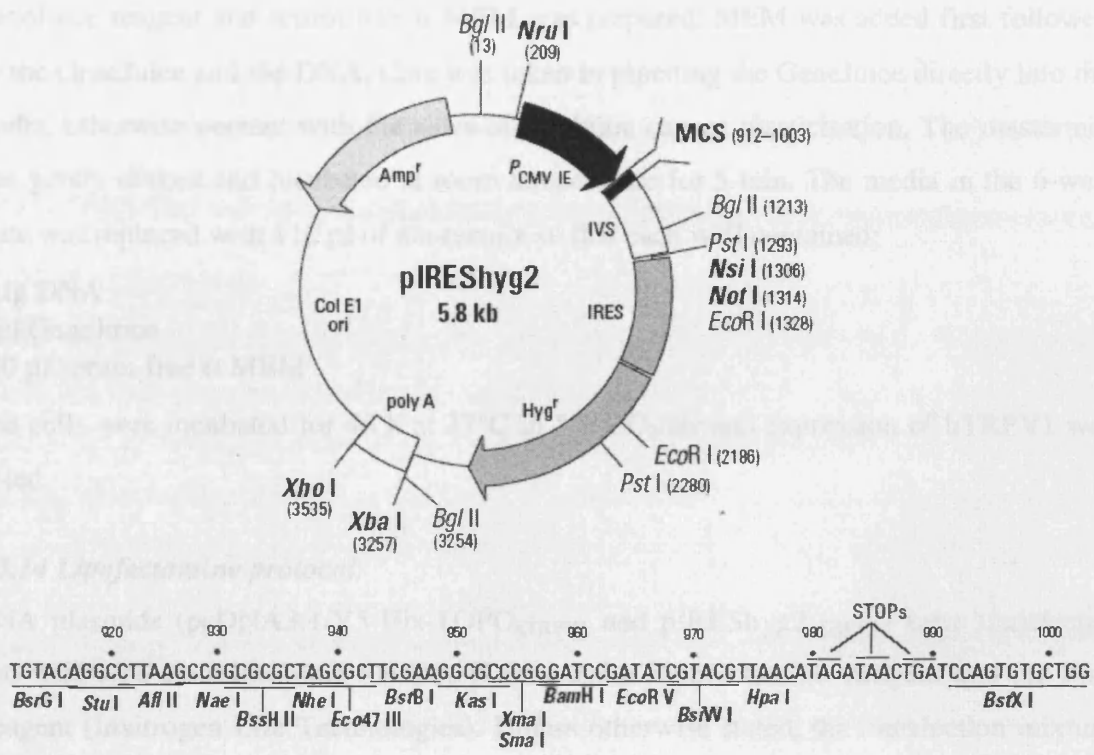


**Figure 4.2 The plasmid pIREShyg2 used for transfecting human TRPV1**
*A restriction map and multiple cloning site (MCS) of pIREShyg2 vector is shown with unique restriction sites in bold. The plasmid includes a human cytomegalovirus (CMV) major immediate early promoter, a synthetic intron (IVS), an internal ribosome entry site (IRES) from encephalomyocarditis virus, an origin of replication (Col E1 ori), hygromycin B phosphotransferase and ampicillin genes as selectable markers.*

### *4.3.13 GeneJuice protocol*

A transient transfection of pIREShyg2$_{hTRPV1}$ plasmid was performed using GeneJuice transfection reagent (Novagen) on CHO cells. CHO cells were grown to approximately 40% confluency in a 6-well plate at 37°C in 5% $CO_2$/air. A mastermix of plasmid DNA, GeneJuice reagent and serum-free α MEM was prepared. MEM was added first followed by the GeneJuice and the DNA. Care was taken in pipetting the GeneJuice directly into the media, otherwise contact with the sides of the bijou causes plasticisation. The mastermix was gently shaken and incubated at room temperature for 5 min. The media in the 6-well plate was replaced with 110 µl of mastermix so that each well contained:

3 µg DNA
8 µl GeneJuice
100 µl serum-free α MEM

The cells were incubated for 48 h at 37°C in 5% $CO_2$/air and expression of hTRPV1 was tested.

### *4.3.14 Lipofectamine protocol*

DNA plasmids (pcDNA3.1/V5-His-TOPO$_{hTRPV1}$ and pIREShyg2$_{hTRPV1}$) were transfected into wild-type neuroblastoma SH-SY5Y cells using Lipofectamine Reagent and the Plus Reagent (Invitrogen Life Technologies). Unless otherwise stated, the transfection mixture was split in half and GFP (green fluorescent protein) plasmid was added to one half of the transfection mix while the other half was left alone. GFP acts as a fluorescence indicator of successful transfection. GFP is a protein produced by a jellyfish *Aequorea* which fluoresces in the lower green portion of the visible spectrum. The gene for GFP has been isolated and has become a useful tool for making expressed proteins fluorescent (Chalfie *et al.*, 1994; Cubitt *et al.*, 1995). After the GFP-transfected cells were observed for successful transfection, these cells were discarded and the other set of cells left to grow (as it was inferred that the transfection of hTRPV1 was successful). Cell culture media (MEM), supplemented with antibiotics, was added to the cells in order to select only for SH-SY5Y cells transfected with hTRPV1. Clones were selected and grown in selection media to increase cell numbers.

### *4.3.15 Fugene protocol*

One day prior to transfection, cell culture flasks (80 $cm^2$) were seeded with cells to acheive no more than 50% confluency. One hour before transfection, the cell culture medium was

replaced with fresh unsupplemented MEM or with MEM supplemented with 10% foetal calf serum. For each transfection sample, 9 µl Fugene 6 was pipetted gently into 600 µl of unsupplemented media and gently mixed. The mixture was incubated at room temperature for 5 min. The pIREShyg2 plasmid incorporating the hTRPV1 insert was added and the contents mixed gently. The mixture was incubated at room temperature for 15 min. The DNA/Fugene mixture was added directly to the media of the flask. The flask was gently agitated to ensure complete mixing and covering of the cells. hTRPV1 expression was tested 48 h after transfection.

### *4.3.16 RNA extraction*

RNA extraction was performed with Invitrogen's TRIZOL reagent. Simultaneous extraction was also performed on GlaxoSmithKline's own $HEK293_{hTRPV1}$ stable cells in order to act as a positive control. RNA precipitation was performed with isopropyl alcohol and the RNA was spun down as a pellet. The pellets were washed with 70% (v/v) ethanol, dissolved in RNase-free water and stored at -20°C. The RNA was quantified using RNA 6000 Nano LabChip Kit (Agilent technologies) and analysed on an Agilent Technologies 2100 Bioanalyzer.

### *4.3.17 Reverse Transcription*

Those clones with sufficient RNA were grown up to a sufficient number for reverse transcription. The reverse transcription kit used was Omniscript RT kit (200) from Qiagen, RNaseOUT Ribonuclease inhibitor (Invitrogen Life technologies) and Oligo(dT) 12-18 Primer (Invitrogen Life Technologies). See Figure 4.3 for an illustrated description of cDNA synthesis. DNase I was used to remove genomic DNA. A negative control was included per sample without RNA polymerase in order to check whether the DNase I treatment was effective. Forward and reverse primers, both used at a concentration of 10 µM, were designed using Primer Express software:

5′ PCR primer: 5′ AAC CAT GAA GAA ATG GAG CAG CAC AG 3′

3′ PCR primer: 5′ AAG GCC CAG TGT TGA CAG TG 3′

Quantitative PCR product accumulation was measured by fluorescence increase by 5′-nuclease activity of Amplitaq polymerase in the Taqman machine (ABI 7700) using the sequence detector version 7.1 program and a SYBR green PCR kit (Applied Biosciences).

SYBR green PCR was repeated to investigate further into whether cDNA synthesis was successful by amplification of the house keeping genes: GAPDH and beta-actin as well as hTRPV1.

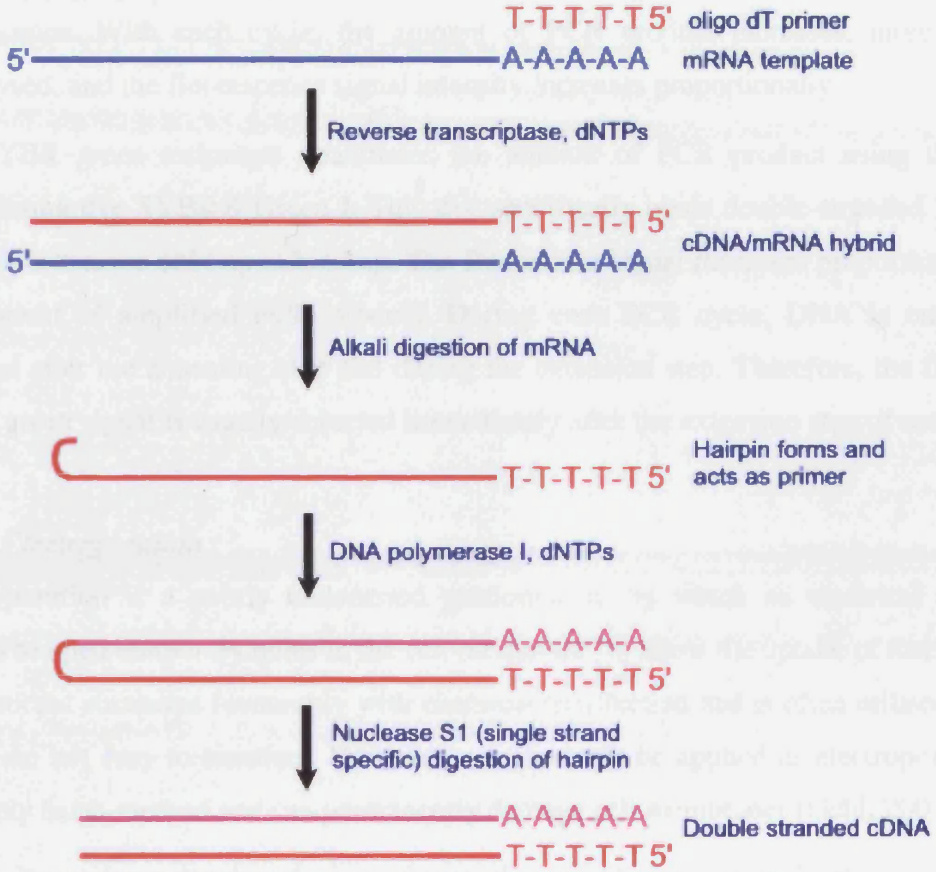


**Figure 4.3 cDNA synthesis**
*Image taken from website: http://www.bch.bris.ac.uk/staff/pfdg/teaching/genes.htm*
*Initially mRNA is extracted and a small oligonucleotide (oligo dT) is attached. The enzyme reverse transcriptase produces complementary DNA (cDNA) by transcribing the mRNA template, forming a cDNA/mRNA hybrid. Alkali digestion will selectively degrade the RNA strand into nucleotides. A hairpin loop is formed at the 3' end of cDNA which acts as a primer for DNA polymerase, producing a complementary strand of DNA. Nuclease S1 digests the hairpin to produce a double stranded cDNA copy of the original mRNA template.*

The TaqMan technique takes advantage of Taq DNA polymerase's 5'-nuclease activity to hydrolyze a fluorogenic probe bound to the single-stranded target DNA during the extension step. The fluorogenic probe is an oligonucleotide containing a fluorescent dye at its 5'-end and quenching dye at its 3'-end. The close proximity of the reporter and quencher prevents emission of fluorescence while the probe is intact. During PCR, the reporter dye is cleaved from the probe by the 5'-nuclease activity of the polymerase and starts to emit fluorescence. With each cycle, the amount of PCR product increases, more probe is hydrolysed, and the fluorescence signal intensity increases proportionally.

The SYBR green technique quantitates the amount of PCR product using the DNA-intercalating dye SYBR® Green I. This dye specifically binds double-stranded DNA and emits fluorescence only upon binding. The fluorescent signal increases proportionally with the amount of amplified PCR product. During each PCR cycle, DNA is only double stranded after the annealing step and during the extension step. Therefore, the fluorescent SYBR green signal is usually detected immediately after the extension step of each cycle.

### *4.3.18 Electroporation*

Electroporation is a poorly understood phenomenon, by which an electrical current is applied to open temporary holes in the cell membrane, to allow the uptake of foreign DNA. This process compares favourably with chemical transfection and is often utilised for cells which are not easy to transfect. However, caution must be applied as electroporation is a relatively harsh method and can permanently damage cell membranes (Gehl, 2003).

Amaxa Biosystems developed a set of special protocols for neuronal cell-lines including SH-SY5Y and neuronal primary cells as neuronal cells are among the most difficult to transfect. The Nucleofector technology, based on electroporation, is a highly efficient non-viral method for transfection. In addition, the Nucleofector is used in conjunction with a specialised kit containing cell-specific solutions which ensure a cell-friendly environment during the "nucleofection" procedure and support the DNA delivery into the nucleus of the cell.

Electroporation was performed using a Nucleofector (Amaxa Biosystems) with the Optimized Protocol Cell Line Nucleofector Kit V and the optimum program was selected for that cell-line. Briefly, 2 x $10^6$ cells were centrifuged to form a pellet at 200 x g for 10 min. The supernatant was discarded and the pellet resuspended in the Nucleofector specialised solution. 100 µl of cell suspension was mixed with 5 µg plasmid DNA and

pipetted into an Amaxa cuvette. The cuvette was placed in the Nucleofector and the optimum program chosen. The electrical settings on the Nucleofector were pre-programmed for a particular cell type, of which the details were proprietary information. Program A24 was selected for transfecting hTRPV1 DNA into the SH-SY5Y cell-line. Program Q-01 was selected to transfect human TRPV1 DNA into the HEK293 cell-line.

The combination of the Nucleofector solution and optimised program is believed to produce an optimised transfection efficiency combined with reduced cell mortality. A control using GFP (green fluorescent protein)-plasmid was included. 500 µl pre-warmed cell culture medium was added to the transfected cells. The cells were transferred to cell culture flasks and grown at 37°C overnight.

### *4.3.19 Immunocytochemistry*

The following were prepared in advance:

*Staining Medium*

500 ml Hanks balanced salt solution was supplemented with 5% foetal calf serum

*Antibody Diluent*

50 ml staining medium was supplemented with 0.1% NPA detergent

*2% Paraformaldehyde*

5 ml 8% paraformaldehyde was added to 15 ml sodium phosphate buffer

1-2 x $10^5$ cells were plated onto Labtek chamber slides (previously coated with poly-L-lysine) and grown overnight in a cell incubator at 37°C. The medium was aspirated off each slide and washed with 500 µl staining medium and the wash was repeated. Then 250 µl 2% paraformaldehyde was added to each chamber to fix the cells for 20 min at room temperature. The paraformaldehyde was aspirated off and the cells were washed with 500 µl staining medium three times. The primary antibody, C22 (α hTRPV1), was raised in rabbits at Research Genetics (Invitrogen) against the peptide CKPEDAEVEKSPAASGEK, then column purified against the peptide. This antibody was diluted 1:5000 in antibody diluent. 20 µl of the diluted primary antibody was added to each chamber and incubated overnight at 4°C. The liquid was aspirated from each chamber and washed in staining medium four times. Staining medium was added to cover the bottom of the slides. The

secondary antibody, Alexa Fluor 488 goat anti-rabbit IgG (2 mg/ml) was diluted 1:750 in antibody diluent. 200 µl of diluted antibody was added to each chamber and incubated for 30 min at room temperature in the dark as the antibody fluorophore is sensitive to light. The liquid was aspirated off the slides, washed three times in staining medium and finally washed in PBS. Antifade was spotted onto specially designed coverslips, which can fit onto the chamber slides, to minimise dye leakage. After the coverslips were placed over the slides, they were visualised with a laser scanning confocal Leica TCS SP microscope.

### *4.3.20 Antibiotic death curves*

### *4.3.21 Visual method (non-trypan blue)*

Hygromycin B is an aminocyclitol antibiotic produced by *Streptomyces hygroscopicus* which inhibits protein synthesis in both prokaryotes and eukaryotes. The antibiotic interferes with ribosomal translocation and with aminoacyltRNA recognition (Gonzalez *et al.*, 1978). Wild-type SH-SY5Y cells were cultured in 6-well sterile plates to approximately 50% confluency. Antibiotic (hygromycin B) was serially diluted in cell culture media to produce final concentrations ranging from 50 µg/ml to 800 µg/ml. 1 ml diluted antibiotic was added to each well and appropriate controls were included. Details of the concentration of antibiotic added were noted separate from the plate. The cells were grown for several days in a 37°C cell culture incubator. The cells were observed in a blind test by independent persons to estimate the proportion of dead cells relative to live cells.

### *4.3.22 CEDEX cell counting*

Trypan blue dye is commonly used to measure cell viability. The dye contains two azo chromophores which are negatively charged and will not interact with the cell unless the membrane is damaged. Hence, the dye will stain those cells which are not viable. Cell density and viability were determined with a CEDEX counter (Innovatis) and carried out according to the manufacturer's instructions. Briefly, wild-type SH-SY5Y cells were harvested and resuspended in cell culture media. The number of cells were counted using CEDEX and cells (500000/ml) were grown in 6-well plates at 37°C for 4 h. Then hygromycin B was added to wells at final concentrations of 0, 100, 200, 300, 400, 500, 600 and 700 µg/ml. Cells were incubated at 37°C for several days. Cells from each well were trypsinised, centrifuged and resuspended in phosphate buffered saline (PBS). 1 ml suspensions were placed in the CEDEX counter. CEDEX has an automated sample handler

and stains 1 ml cell suspensions with trypan blue. The trypan blue was a 0.2 % solution which was supplied with the CEDEX counter. CEDEX contains a CEDEX flow cell which is equivalent to a haemocytometer and uses a transmitted light microscope to "view" the cells. The counter automatically uses a CCD camera to photograph images of the samples. CEDEX contains image recognition software which is able to differentiate between live and dead cells as well as air-bubbles based on the trypan blue principle. CEDEX is then able to record, analyse and display the results for the user. All liquid handling was automated including elimination of waste products.

Data for two transfection strategies are presented.

1. transfection of pcDNA3.1/V5/His-TOPO$_{hTRPV1}$ plasmid into SH-SY5Y cells.
2. subcloning hTRPV1 DNA and ligating this into a pIREShyg2 plasmid followed by transfection into SH-SY5Y cells.

### 4.4 Results from transfection strategy 1

The cloning of the hTRPV1 receptor into a pcDNA3.1/V5/His-TOPO plasmid vector was conducted before the start of this research project at GlaxoSmithKline, Harlow, UK (Hayes *et al.*, 2000) as briefly described in Section 4.3.1.

A pcDNA3.1/V5/His-TOPO plasmid containing a SV40 poly A tail, the G418 gene for selection with geneticin and the hTRPV1 insert was transfected into wild-type neuroblastoma SH-SY5Y cells with Lipofectamine Reagent and the Plus Reagent according to the manufacturer's instructions (Section 4.3.14). In addition, GFP plasmid was added to half of the transfection mixture while the other half was left alone. Using a microscope, fluorescence was observed in those cells with added GFP, which indicated that transfection had occurred successfully. These cells were discarded and the other set of cells (no added GFP) were allowed to grow as it was assumed that transfection of hTRPV1 was successful according to the GFP fluorescence. Using CEDEX technology (Section 4.3.22), a geneticin death curve was constructed to calculate the minimum concentration of geneticin required to kill wild-type SH-SY5Y cells (results not shown). Geneticin was added to the transfected cells at a final concentration of 400 µg/ml to select only for SH-SY5Y transfected cells containing hTRPV1. Notably, the growth of the transfected cells was relatively slow in comparison to wild-type SH-SY5Y cells. Five clones were selected and each was grown in MEM media (including 400 µg/ml geneticin) to increase cell numbers.

RNA extraction was performed with Invitrogen's TRIZOL reagent (Section 4.3.16). Simultaneous extraction was also performed on GlaxoSmithKline's own HEK293 cells previously transfected with hTRPV1 to act as a positive control. The RNA was quantified using an RNA 6000 Nano LabChip Kit (Agilent technologies) and analysed on an Agilent Technologies 2100 Bioanalyzer. Notably, the RNA concentrations of the clones were considerably lower (ranged from 3-474 ng/µl) relative to HEK293$_{hTRPV1}$ (622 ng/µl). Those clones with sufficient RNA were grown up to an adequate number for future use.

Reverse transcription was performed on the quantified RNA samples, from the three clones with the highest RNA concentrations, using RNA polymerase and DNase I for Taqman PCR. Genomic DNA was eliminated with DNase I. A negative control excluding RNA polymerase was included per sample to confirm whether the DNase I treatment had worked. Quantitative PCR product accumulation was measured by fluorescence release by 5′-nuclease activity of Amplitaq polymerase in the taqman machine (ABI 7700) using the sequence detector vs 7.1 program. In addition, SBYR green PCR was performed with hTRPV1 primers. Both Taqman and SBYR green revealed no hTRPV1 cDNA was produced for the SH-SY5Y transfected clones, in contrast to the $HEK293_{hTRPV1}$ clone where a relatively high level of cDNA was observed.

To investigate further into whether cDNA synthesis was successful, amplification of specific house keeping genes (GAPDH and β-actin) was performed using SBYR green PCR. GAPDH was present in the positive controls and no GAPDH was present in the negative controls, this suggests that cDNA synthesis was successful despite the absence of hTRPV1 cDNA in the SH-SY5Y transfected clones. SBYR green PCR with GAPDH was repeated with the addition of β-actin. The cDNA synthesis of β-actin was present in the SH-SY5Y clones but this level was relatively lower than for wild-type SH-SY5Y and $HEK293_{hTRPV1}$ cells. Also GAPDH was only present in some of the transfected SH-SY5Y clones which contradicted the earlier GAPDH results. The combination of the GAPDH and β-actin cDNA synthesis results implied that the transfection process was unsuccessful or the expression of hTRPV1 was extremely low and hence this level was not detected during quantitive PCR and SBYR green analysis.

### 4.5 Results from transfection strategy 2

This strategy involved two stages (i) to subclone the hTRPV1 DNA insert from pcDNA3.1/V5/His-TOPO into a pIREShyg2 plasmid vector (ii) to transfect pIREShyg2/hTRPV1 plasmid construct into SH-SY5Y WT cells.

The process of cloning and transfecting hTRPV1, is summarised in Figure 4.4. The pIREShyg2 plasmid was chosen because transfection of $pcDNA3.1/V5/His\text{-}TOPO_{hTRPV1}$ plasmid construct was poor and the relatively slow growth of SH-SY5Y cells in cell culture media supplemented with geneticin was observed.

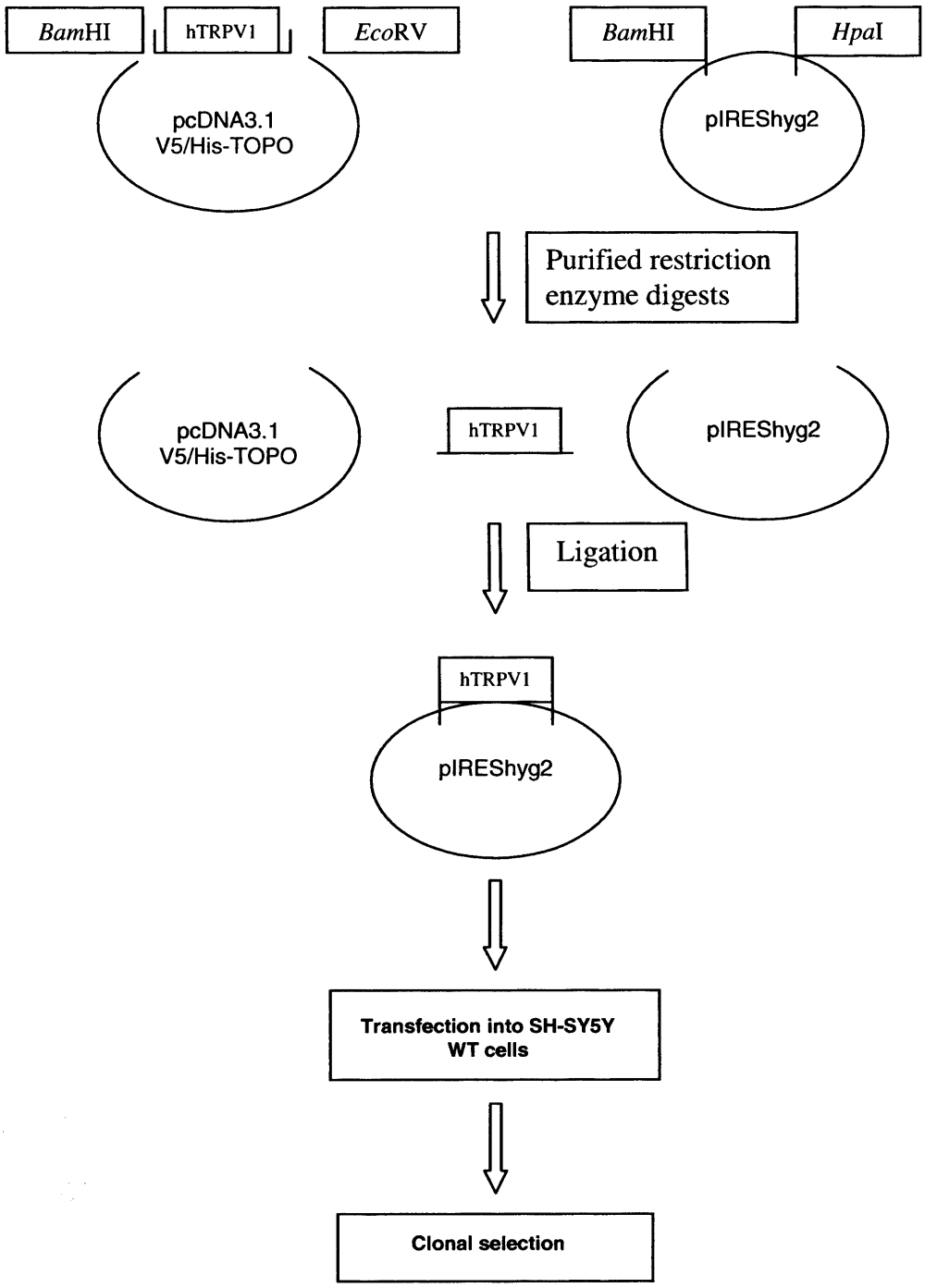


**Figure 4.4 Cloning and transfection strategy**
*Summary of procedure in subcloning hTRPV1 from the original construct, pcDNA3.1/V5/His-TOPO into plasmid pIREShyg2. The new plasmid construct was transfected into SH-SY5Y wild-type cells followed by clonal selection using the antibiotic hygromycin B as the selective agent.*

### *4.5.1 Cloning hTRPV1*

The pcDNA3.1/V5-His-TOPO$_{hTRPV1}$ plasmid construct was linearised with *Bam*HI and *Eco*RV restriction enzymes. In addition, these restriction enzymes separated the hTRPV1 DNA insert from the multiple cloning site of the plasmid. The pIREShyg2 plasmid was linearised with *Bam*HI and *Hpa*I restriction enzymes. The DNA digests were run on a 1% (w/v) agarose gel relative to a 500 bp marker (Invitrogen) to confirm the sizes of the DNA fragments (result not shown). DNA fragment sizes of approximately 2.6 kb and 6 kb from the digested pcDNA3.1/V5-His-TOPO$_{hTRPV1}$ plasmid construct showed that the hTRPV1 DNA insert was separated from the plasmid. Also, the linearised pIREShy2 plasmid appeared as a single DNA band of approximately 6 kb on the gel.

Subsequently, DNA of the hTRPV1 insert and pIREShyg2 vector (linear form) were extracted from the agarose gel (Section 4.3.7). The hTRPV1 DNA insert and pIREShyg2 plasmid were ligated together overnight with (Section 4.3.8). Competent *Esherichia coli* DH5α cells were transformed with ligated hTRPV1 and pIREShyg2 (Section 4.3.9). Next, these transformed *E. coli* cells were cultured on agar plates (supplemented with 100 μg/ml ampicillin). Nine bacterial colonies were selected to inoculate 15 ml Falcon tubes filled with 3 ml LB media (supplemented with 100 μg/ml ampicillin) and grown overnight. Subsequently, plasmid mini-preparations were performed on the colonies (Section 4.3.11). The ligation of hTRPV1 DNA insert and pIREShyg2 plasmid was checked by linearisation with a *Bam*HI restriction enzyme digest of each plasmid mini-preparation. The digests were run on a 1% (w/v) agarose gel and a single band of approximately 8.4 kb was observed for each plasmid except for plasmid 1b (Lane 3) which displayed a band of 5.8 kb (Figure 4.5). This suggested that ligation was successful for all the mini-plasmid preparations except for plasmid 1b. Further verification was obtained with restriction enzyme digests using *Bam*HI and *Bst*XI. For all the mini-plasmid preparations except 1b (Lane 3), four bands of approximately 8.4 kb, 1000 bp, 800 bp and 700 bp were seen on a 1% (w/v) agarose gel which corresponded correctly to known restriction enzyme sites for the ligated construct (Figure 4.6). Plasmid 1b produced two DNA fragments of approximately 1.3 kb and 2.5 kb which were not the expected sizes for correct ligation of hTRPV1 DNA insert and pIREShyg2 plasmid (Figure 4.6).

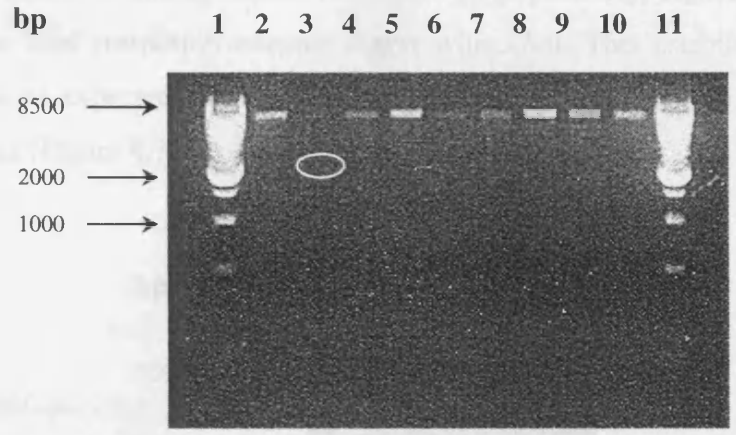


**Figure 4.5 Restriction enzyme (*Bam*HI) analysis of plasmid mini-preparations for the presence of hTRPV1 insert**

*BamHI digests for 9 plasmid mini-preparations on a 1% agarose gel. A 500 bp DNA ladder marker was included in Lanes 1 and 11. Lanes 2 to 10 display linearised pIREShyg2 plasmids ligated with the hTRPV1 insert displayed as a single band of approximately 8 kb. The only exception was in Lane 3, which shows a smaller band of approximately 3 kb (circled). This suggests the presence of unligated hTRPV1 insert only.*

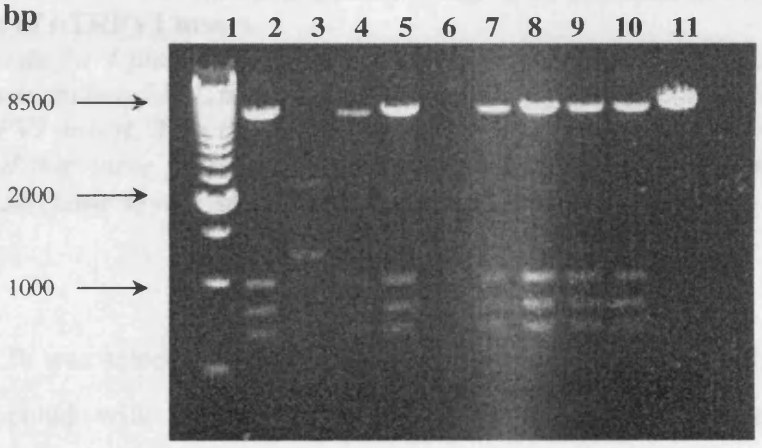


**Figure 4.6 Restriction enzyme (*Bam*HI and *Bst*XI) analysis of plasmid mini-preparations for the presence of hTRPV1 insert**

*BamHI and BstXI digests for 9 plasmid mini-preparations on a 1% agarose gel. A 500 bp DNA ladder marker was included in Lane 1. Lane 11 included digested pIREShyg2 plasmid which should have produced 2 fragments: 6 kb and 40 bp, however the latter fragment is too small to be observed on the gel. Lanes 2 to 10 display digested pIREShyg2 plasmids resulting in four bands of approximately 8 kb, 1 kb, 0.8 kb and 0.7 kb. This suggested that there were other BamHI and BstXI restriction sites present in the ligated hTRPV1 insert. Lane 3 showed two bands only of approximately 2.5 kb and 1.3 kb. Also, no bands were visualised in Lane 6, contrary to the BamHI digest in which DNA was present.*

Plasmids 2c, 3a, 3b and 3c (Lanes 7, 8, 9 and 10 respectively, Figure 4.6) were subjected to a separate final restriction enzyme digest with *Xho*I. This established that ligation was successful as expected band sizes of 5.7 kb and 2.7 kb were observed on a 1% (w/v) agarose gel (Figure 4.7).

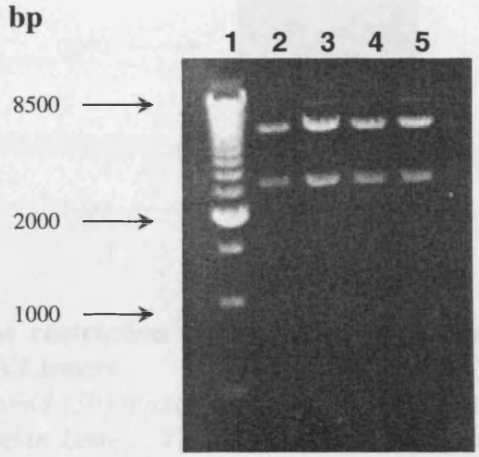


**Figure 4.7 Enzyme restriction (*Xho*I) analysis of plasmid mini-preparations for the presence of hTRPV1 insert**
*XhoI digests for 4 plasmid mini-preparations on a 1% agarose gel. A 500 bp DNA ladder marker was included in Lane 1. The XhoI site is unique to both the pIREShyg2 plasmid and the hTRPV1 insert. Two bands of approximately 6 kb and 2.7 kb were observed which confirmed that these plasmids were ligated with hTRPV1 and in the correct orientation. Plasmid 3b (Lane 4) was selected for plasmid maxi-preparation.*

Plasmid 3b was selected for further analysis and was used to inoculate 500 ml LB media (supplemented with 100 µg/ml ampicillin) and grown overnight. A maxi-plasmid preparation was performed (Section 4.3.12) and a restriction enzyme digest with *Xho*I confirmed again that the ligation was successful (Figure 4.8).

The DNA concentration of the maxi-plasmid preparation was determined with a SANYO SPB10 spectrophotometer at 260 nm. 50 µg/ml DNA produces an optical density (OD) of 1. An absorbance reading of 0.363 was obtained from the maxi-plasmid preparation, which equates to a concentration of 1.815 mg/ml DNA.

The hTRPV1 DNA was double strand sequenced at GlaxoSmithKline and compared to GlaxoSmithKline's original cloned hTRPV1 DNA for sequence errors. None were found in the newly transfected hTRPV1 DNA insert.

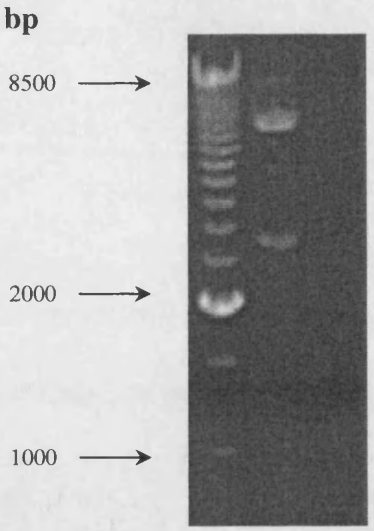


**Figure 4.8 Enzyme restriction (*Xho*I) analysis of plasmid maxi-preparation for the presence of hTRPV1 insert**
*XhoI digest for plasmid (3b) maxi-preparation on a 1% agarose gel. A 500 bp DNA ladder marker was included in Lane 1. The XhoI site is unique to both the pIREShyg2 plasmid and the hTRPV1 insert. Two bands of approximately 6 kb and 2.7 kb were observed which confirmed that plasmid 3b was ligated with hTRPV1 and in the correct orientation.*

### *4.5.2 Hygromycin B cell death (non-Trypan blue method)*

A death curve was constructed in wild-type SH-SY5Y cells with the antibiotic hygromycin B. The results (Figure 4.9) indicated that a minimum of 400 µg/ml hygromycin B was required to ensure 100% cell death in wild-type SH-SY5Y cells.

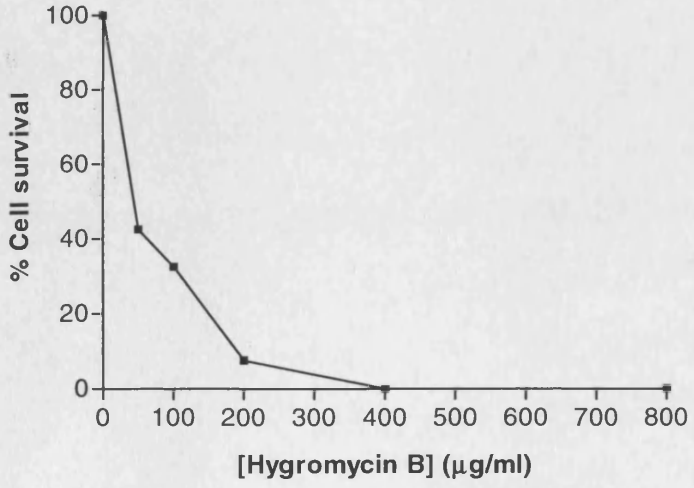


**Figure 4.9 Wild-type SH-SY5Y hygromycin B death curve**

### *4.5.3 Chemical transfections*

A transient test transfection of pIREShyg2$_{hTRPV1}$ plasmid into CHO cells was performed with Genejuice (Section 4.3.13). Cuvette-based fluorimetric tests were performed to measure the $[Ca^{2+}]_i$ response by applying 20 µl 100 µM capsaicin (final concentration) to harvested and fura-2AM loaded CHO cells. A total of three capsaicin tests were carried out with DMSO controls included (Figure 4.10). No calibrations were required as only the capsaicin response was being observed. The change in the fluorimetric ratio (ΔR) was calculated and there was a significant increase in $[Ca^{2+}]_i$ response in the transfected cells.

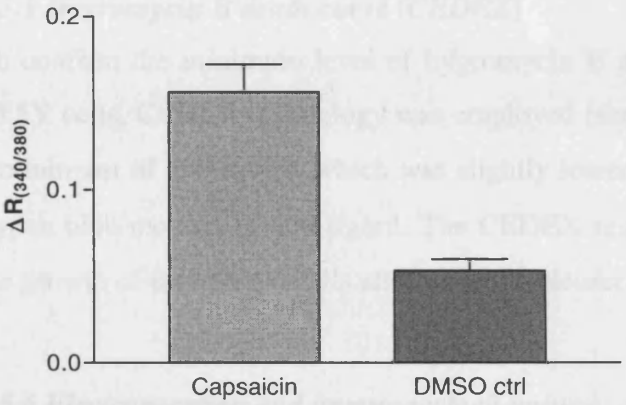


**Figure 4.10 $[Ca^{2+}]_i$ response of transient transfections**
*The pIREShyg2$_{hTRPV1}$ plasmid was transfected into CHO cells using GeneJuice. Expression of hTRPV1 was tested with 100 µM capsaicin and the response was statistically significant which was confirmed with a paired t-test (p=0.0451). Ctrl=control*

### *4.5.4 Attempts to stably transfect hTRPV1 into neuroblastoma cells*

An initial attempt to transfect the pIREShyg2$_{hTRPV1}$ construct into SH-SY5Y cells utilised lipid-mediated Fugene reagent. The ratio of Fugene 6:DNA used was 3:1 and the medium was replaced 3-4 h post-transfection with unsupplemented MEM. However cell death occurred several days post-transfection. Replacing the medium with MEM supplemented with 10% foetal calf serum and plating the cells 2 days post-transfection with selection antibiotic 600 µg/ml hygromycin B did not deter cell death. The latter process was repeated except 400 µg/ml hygromycin B was added but there was no cell survival. The ratio of F6:DNA was also varied to 3:2 and 6:1 and the medium was replaced 3-4 h post-transfection with unsupplemented MEM and capsaicin response was tested in fura-2AM loaded cells at 37°C. However, no change in $[Ca^{2+}]_i$ occurred after the addition of capsaicin.

Lipofectamine was also used to transfect the pIREShyg2$_{hTRPV1}$ construct into both wild-type SH-SY5Y and HEK293 cells. Capsaicin response was tested several days post-transfection in fura-2AM loaded cells. A significant increase in $[Ca^{2+}]_i$ was observed after the addition of 100 μM capsaicin only in transfected HEK293 cells but not in SH-SY5Y cells. Cell toxicity occurred after plating the transfected cells in selection media with 400 μg/ml hygromycin B which suggested that the transfection was not successful in SH-SY5Y cells.

### *4.5.5 Hygromycin B death curve (CEDEX)*

To confirm the minimum level of hygromycin B antibiotic to select for transfected SH-SY5Y cells, CEDEX technology was employed (see Section 4.3.22). The results indicated a minimum of 300 μg/ml, which was slightly lower than the value obtained with the non-trypan blue method of 400 μg/ml. The CEDEX result of 300 μg/ml was incorporated for the growth of transfected cells after using Nucleofection technology.

### *4.5.6 Electroporation and immunocytochemistry*

An initial successful transient test transfection with GFP plasmid in SH-SY5Y neuroblastoma cells by electroporation was performed using program A24 on the Nucleofector. Transfection was confirmed by visualising the cells with a microscope (Figure 4.11), in which transfected cells were fluorescent caused by GFP transfection. Subsequently, transfection of pIREShyg2$_{hTRPV1}$ plasmid was performed by electroporation into SH-SY5Y cells using program A24 on the Nucleofector device. As a comparison, transfection of pIREShyg2$_{hTRPV1}$ plasmid into HEK293 cells was carried out by selecting program Q-01 on the Nucleofector. However, the details of the Nucleofector technology are of proprietary information. Sub-cellular localisation of hTRPV1 DNA in SH-SY5Y cells was visualised using immunocytochemistry (Section 4.3.19). The primary antibody binds to the DNA relating to the C-terminus tail of hTRPV1. After the cells were stained with the secondary fluorophore-labelled goat anti-rabbit IgG antibody, the cells were prepared for fluorescence microscopy. Fluorescent staining revealed that hTRPV1 DNA was primarily located in the endoplasmic reticulum (Figure 4.12) of the cells.

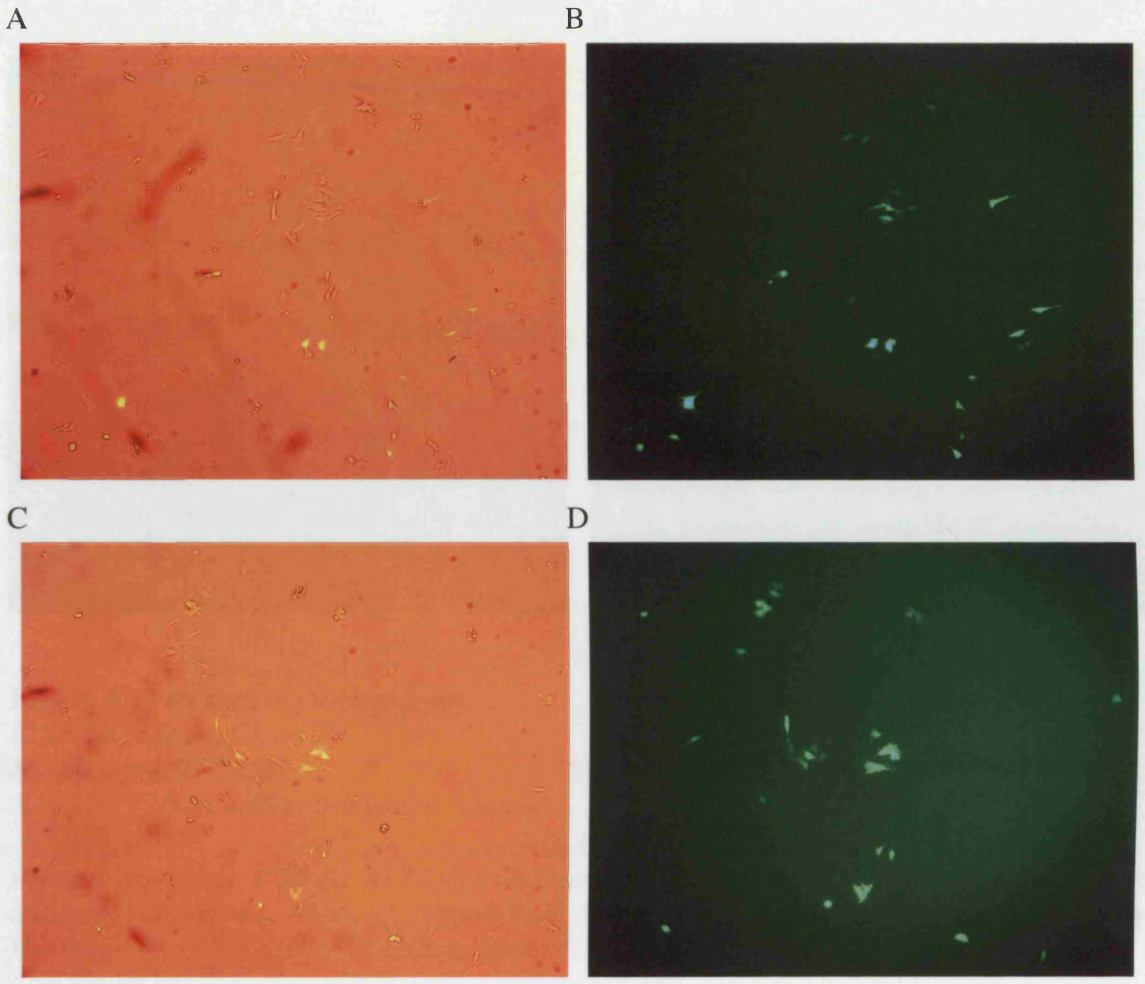


**Figure 4.11 GFP control transfection**

*Photos taken of SH-SY5Y cells transfected with GFP. Approximately 50% of the cells became transfected with GFP as observed under different coloured views by a Leica DM IRBG inverted microscope (x10 magnification). Photos A and B are of identical cells viewed in different lighting. Photo A displays transfected and non-GFP transfected cells while B only shows cells' fluorescence due to transfection of GFP and hence, hTRPV1. Likewise, photos C and D were taken of another set of cells. Photo C displays transfected and non-GFP transfected cells while photo D shows the fluorescence of corresponding transfected cells only.*

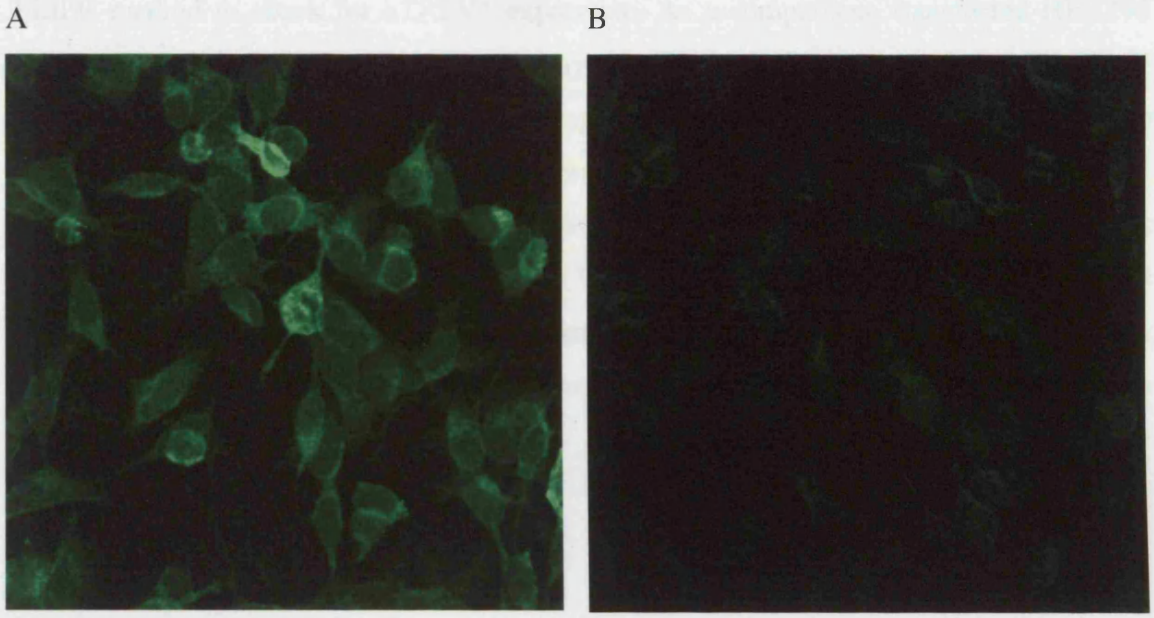


**Figure 4.12 Immunocytochemistry**
*A:SH-SY5Y$_{hTRPV1}$ Clone 7*
*B:Wild-type SH-SY5Y*
*Anti TRPV1/Alexa 488 (x40 magnification)*

*Primary antibody C22 ($\alpha$ hTRPV1) was used to bind to hTRPV1 protein. Secondary antibody, anti-rabbit Alexa 488, contained a fluorophore conjugation and consequently fluorescently stains SH-SY5Y cells to display the location of hTRPV1.*

### *4.5.7 Initial Pharmacological characterisation of transfected clones*

After electroporation, the transfected cells were tested for capsaicin response using the FLIPR method to check for hTRPV1 expression. As a comparison, transfected HEK293 cells were included and the results are displayed in Figure 4.13. Non-transfected SH-SY5Y cells produced a concentration-dependent response to the addition of carbachol but none to capsaicin. However, the transfected cells generally displayed a sigmoidal concentration-dependent response to both capsaicin and carbachol. Saturation occurred for capsaicin but not always so for carbachol. Capsazepine (300 nM) competitively inhibited capsaicin as indicated by a rightward shift in the sigmoidal curves as well as achieving similar saturation levels compared to capsaicin alone. Capsazepine displayed no inhibition effects against carbachol.

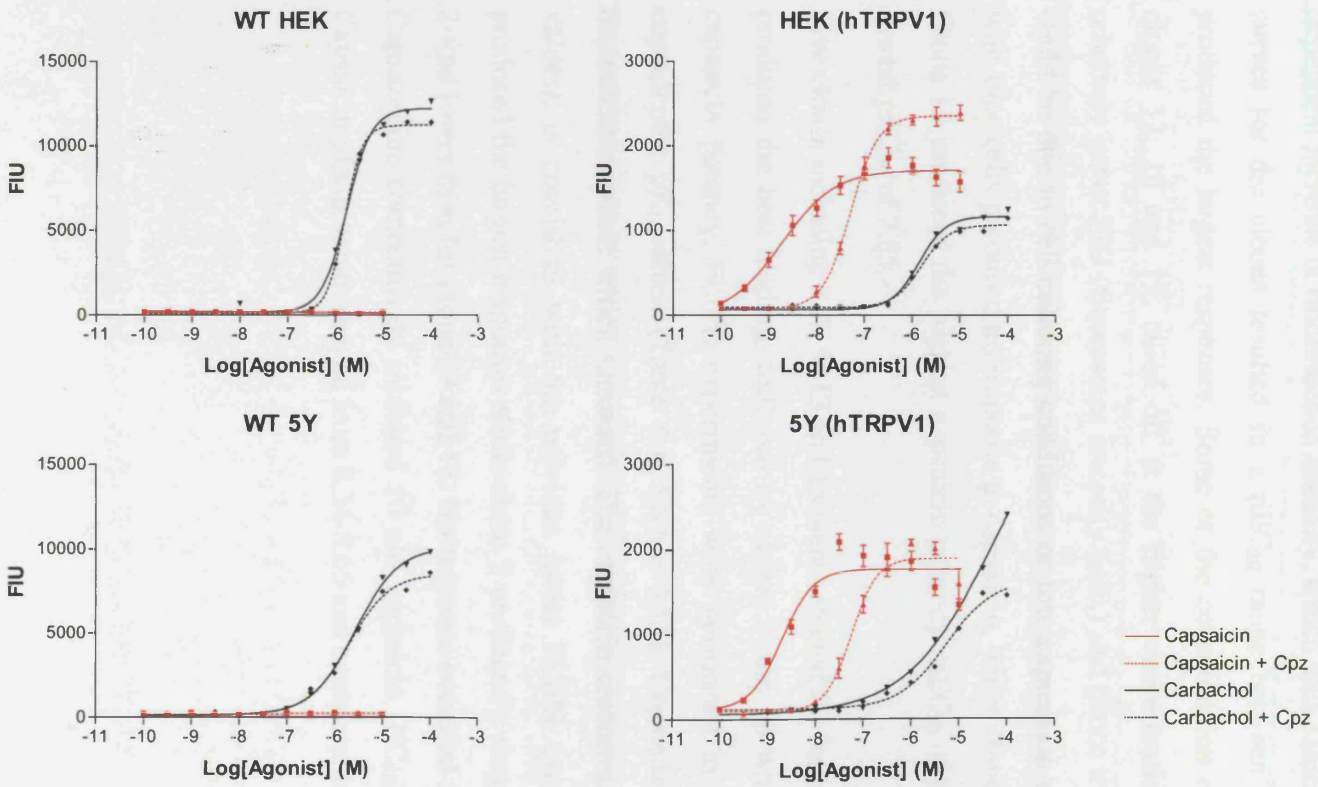


**Figure 4.13 Initial FLIPR testing of fluo-3AM loaded SH-SY5Y and HEK293 cells, both transfected and non-transfected with pIREShyg2$_{hTRPV1}$**

*(WT=wild-type, 5Y=SH-SY5Y). As expected, the non-transfected cells (wild-type) produced a concentration-dependent response to the addition of carbachol (n=1) but none to capsaicin (n=3). However, the transfected cells displayed an increase in fluoresence intensity which was concentration-dependent to both capsaicin (n=6) and carbachol (n=2). Also, the sigmoidal capsaicin curves saturated. Capsazepine (Cpz) competitively inhibited the capsaicin response (n=6) but did not antagonise carbachol (n=2). Capsazepine had no effect on capsaicin (n=3) or carbachol (n=1) in the wild-type cells.*

Sixteen transfected SH-SY5Y$_{hTRPV1}$ clones were selected and cultured separately for further FLIPR analysis. Response to increasing capsaicin concentration was analysed with $pEC_{50}$ values shown in Figure 4.14. Most of the clones produced a concentration-dependent increase in fluorescence intensity, which then saturated. Concentration response curves for the clones resulted in a $pEC_{50}$ range between 7.85-8.72. Clones 7 and 9 produced the largest responses. Some of the concentration response curves, such as for clones 12, 18 and 19, tailed off at the higher concentration of capsaicin and have a relatively lower FIU (fluorescent intensity units) and hence a lower $[Ca^{2+}]_i$ response. This could be due to cell culturing conditions or low expression of the receptor. Clone 6 and wild-type cells produced no response to capsaicin, which shows no expression of hTRPV1. Clone 13 produced the highest capsaicin potency ($pEC_{50}$ of 8.72) while clone 8 gave the lowest $pEC_{50}$ of 7.85.

Five clones including 3, 7, 9, 13 and 18 were selected for further analysis as clones 7 and 9 produced the best loading, followed by clones 3 and 18 while clone 13 had the highest capsaicin potency. FLIPR experiments were performed to obtain capsaicin $pEC_{50}$ and capsazepine $pK_i$ values (Table 4.1, Figure 4.15). Capsaicin produced a concentration-dependent response which saturated. The capsaicin response, in terms of potency ($pEC_{50}$ values), is consistent with the previous initial FLIPR experiments. Clones 9 and 13 produced the largest responses while clone 3 produced a response that was approximately 2-fold lower than for clones 9 and 13. No response occurred in wild-type SH-SY5Y cells. Capsazepine competitively inhibited 10 nM capsaicin ($EC_{80}$) response in all the clones. Capsaicin $pEC_{50}$ values ranged from 8.34-8.65 and capsazepine $pK_i$ values from 7.06-7.42.

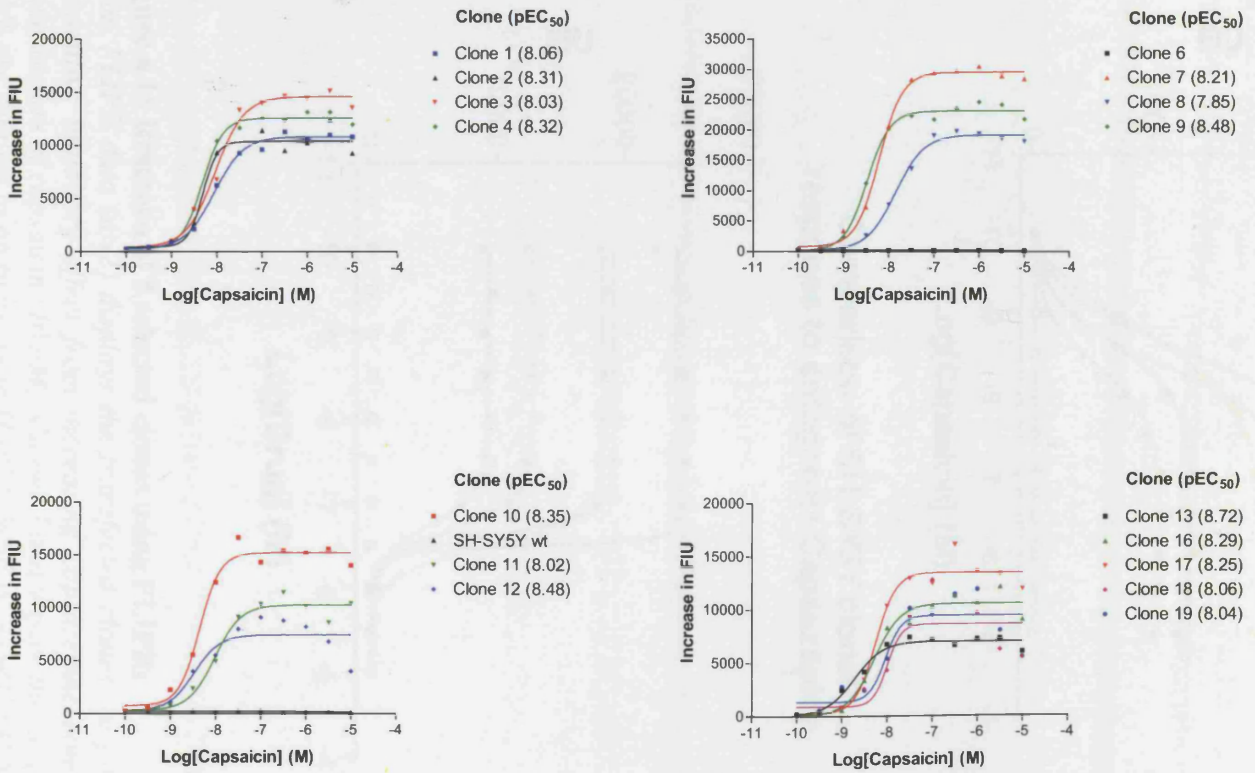


**Figure 4.14 FLIPR analysis of transfected SH-SY5Y clones**

*Response to capsaicin was analysed with $pEC_{50}$ values displayed as the mean (n=2) for each clone. Most of the clones produced a concentration-dependent increase in fluorescence intensity which then saturated. Clone 6 and wild-type (wt) cells produced no response to capsaicin.*

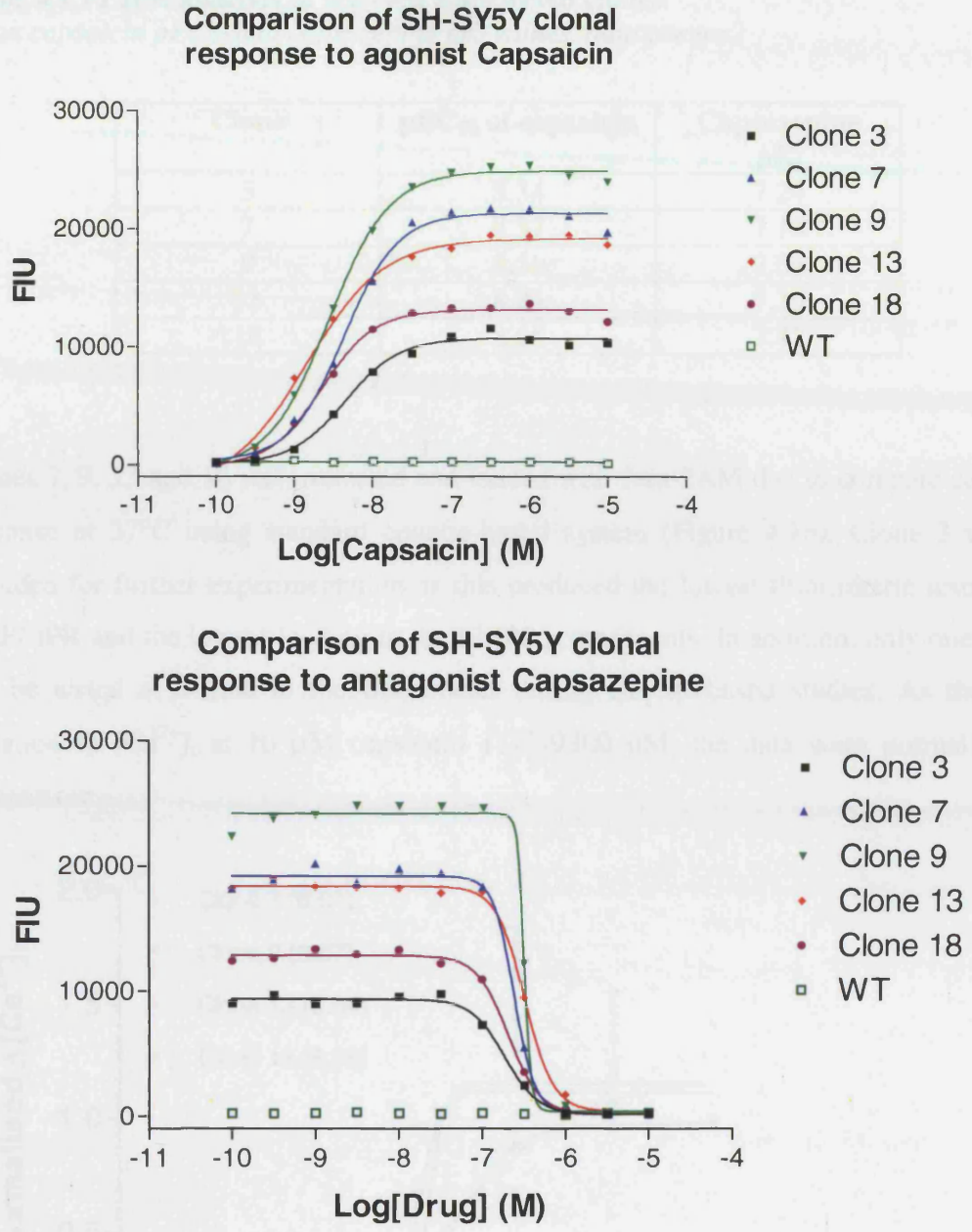


**Figure 4.15 Rescreen of 5 selected clones using FLIPR**

*Mean FLIPR data (n=2) displays the transfected clones' response to capsaicin and the competitive inhibitory effect from increasing capsazepine concentration versus a fixed concentration of capsaicin (10 nM). Clones 7 and 9 gave the largest fluorimetric responses which are relative to an increase in $[Ca^{2+}]_i$. Wild-type (WT) SH-SY5Y cells did not respond to capsaicin and capsazepine.*

**Table 4.1 FLIPR analysis of selected transfected clones**
*Mean capsaicin $pEC_{50}$ and capsazepine $pK_i$ values, data are n=2*

| Clone | $pEC_{50}$ of capsaicin | Capsazepine $pK_i$ |
|---|---|---|
| 3 | 8.34 | 7.24 |
| 7 | 8.37 | 7.14 |
| 9 | 8.56 | 7.06 |
| 13 | 8.84 | 7.39 |
| 18 | 8.65 | 7.42 |

Clones 7, 9, 13 and 18 were selected and loaded with fura-2AM dye to compare capsaicin response at 37°C using standard cuvette-based system (Figure 4.16). Clone 3 was not included for further experimentation as this produced the lowest fluorimetric response in the FLIPR and the lowest loading in the FLIPR experiments. In addition, only one sample can be tested at a time in the fluorimeter during cuvette-based studies. As there was variation in $[Ca^{2+}]_i$ at 10 μM capsaicin 1140-9300 nM, the data were normalised for comparison.

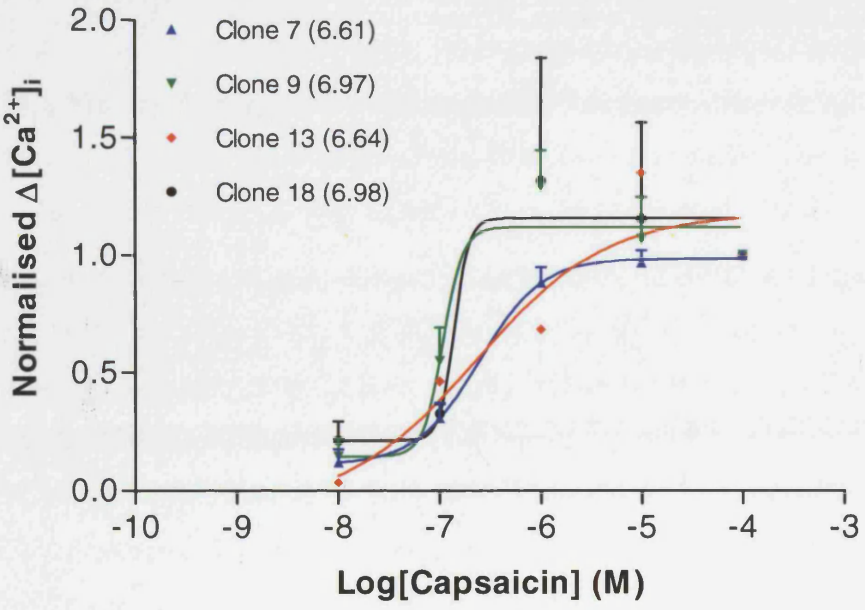


**Figure 4.16 Normalised fluorimetric data from fura-2AM loaded cells at 37°C**
*Clones 7, 9, 13 and 18 were selected and tested for capsaicin response and was shown to be concentration-dependent. Clones 7 and 9 (n=4), clone 13 (n=2) and clone 18 (n=3) were normalised for comparison, $pEC_{50}$ values are displayed on the graph.*

Each clone produced a concentration-dependent response to capsaicin. The error bars for clone 13 were relatively large compared to the other clones because one set of cells produced an unusually large response. However, as the number of experiments for clone 13 was only 2, this could not be compared to the other clones. Clone 7 produced a sigmoidal shaped curve with relatively small error bars. Hence it was decided that clone 7 alone should be selected for further detailed pharmacological analysis. The potency was generally at least 1 log lower than those obtained in the FLIPR experiments.

## 4.6 Discussion

*Summary*

This chapter has described the process of producing a stable neuronal model expressing hTRPV1 (SH-SY5Y$_{hTRPV1}$) and to date, this is the first such model. FLIPR and cuvette-based studies of the cloned cells have confirmed expression of hTRPV1 by a concentration-dependent response to the TRPV1 agonist capsaicin, which was antagonised competitively by capsazepine at 25°C and 37°C.

*Comparison with HEK293*

The capsaicin response was examined at recombinant hTRPV1 expressed in SH-SY5Y cells at 25°C with FLIPR technology. The potency ($pEC_{50}$) of the selected clone (number 7) was slightly higher than other reported FLIPR values in HEK293$_{hTRPV1}$ (Smart *et al.*, 2000a) and HEK293$_{rTRPV1}$ (Jerman *et al.*, 2000) but matched a reported FLIPR result in HEK293$_{rTRPV1}$ (Jerman *et al.*, 2002). In addition, the potency was higher than the capsaicin $pEC_{50}$ (Chapter 3, Section 3.3.2) at 22°C from HEK293$_{hTRPV1}$ cells in cuvette-based studies.

It is worth noting that FLIPR capsaicin potency ($pEC_{50}$) for the initial sixteen clones was higher relative to the cuvette-based experiments in HEK293 cells (6.88) (Chapter 3, Section 3.3.2). In the cuvette-based studies, the $pEC_{50}$ of clone 7 from normalised data (at 37°C) was in agreement with earlier results (Chapter 3, Section 3.3.2), from previously published data for HEK293$_{hTRPV1}$ cells from our laboratories (Sprague *et al.*, 2001) and CHO cells expressing rat and human TRPV1 (McIntyre *et al.*, 2001).

The antagonist capsazepine competitively inhibited hTRPV1 response to capsaicin in the short-listed five clones – 3, 7, 9, 13 and 18. The $pK_i$ varied by up to 0.5 log between the clones. As commented in Chapter 3, $pK_B$ values for this antagonist have proved highly variable. The $pK_i$ of clone 7 was slightly higher than the $pK_B$ obtained from HEK293$_{hTRPV1}$ (6.76) and HEK293$_{rTRPV1}$ (5.98) in previous experiments (Chapter 3, Section 3.3.4) at 22°C. However, the $pK_i$ of clone 7 matched other FLIPR results in the literature in HEK293$_{hTRPV1}$ cells of 7.31 (Smart *et al.*, 2000a), 6.58 (Smart *et al.*, 2001) and 7.52 in HEK293$_{rTRPV1}$ (Jerman *et al.*, 2000).

*Problems and solutions*

The initial transfection strategy involved chemically transfecting pcDNA3.1/V5/His-TOPO$_{hTRPV1}$ plasmid into SH-SY5Y cells. However, despite the initial co-transfection with GFP, which implied that hTRPV1 transfection was successful, unexpected problems appeared. The growth of the transfected cells, in media supplemented with geneticin, was relatively slow in comparison to wild-type SH-SY5Y cells, possibly caused by minimal expression of hTRPV1. High cytotoxicity occurred probably resulting from poor transfection efficiency, hence the number of successfully transfected cells was too low for detection.

Quantitative PCR employing both Taqman and SBYR green detection revealed that no hTRPV1 cDNA was present in the tested clones. However, conflicting results occurred when investigating cDNA synthesis by amplification of house-keeping genes (GAPDH and β-actin). The Taqman analysis is more sensitive than the SBYR green analysis because the PCR is relatively more specific due to the probe. Also, the SBYR green method does not distinguish between sequence-specific DNA and non-sequence specific DNA products such as primer dimers and amplification of non-specific priming events.

A different strategy of transfecting hTRPV1 DNA into the SH-SY5Y cell-line incorporated a subcloning step prior to transfection. The plasmid pIREShyg2 was chosen for a different antibiotic selection gene – hygromycin B, to minimise cytotoxicity observed with the original pcDNA3.1 plasmid. Cloning was relatively straightforward in contrast to transfection. The test transfection performed in CHO cells was successful, however chemical transfection in SH-SY5Y cells was attempted using a number of kits (Lipofectamine and Fugene) resulting in no expression and/or cytotoxicity.

Historically, it is generally difficult to transfect DNA into both cultured and primary neural cell types. Chemical transfection kits always recommend optimising the transfection protocol. The efficiency of establishing stably transfected cell-lines is dependent upon the efficiency of gene transfer into a given cell-line and upon the survival of successfully transfected cells when a selective pressure is applied. Since the efficiency of gene transfer into a given cell-line can be easily determined using reporter plasmids whose gene products can be quantified enzymatically or visualised at the single cell level, some transfection protocols have attempted to improve the efficiency of transfection by employing such methods as electroporation.

Nucleofector technology, which incorporates the principle of electroporation, was used successfully to transfect recombinant hTRPV1 DNA into the SH-SY5Y cell-line. An optimum program is available for various cell-types, however, the details of the actual settings are proprietary information (Amaxa Biosystems). In addition, the minimum level of hygromycin B antibiotic to select for transfected SH-SY5Y cells, was verified with CEDEX technology to ensure a relatively high transfection efficiency was maintained. The CEDEX technology indicated a minimum of 300 µg/ml, which was slightly lower than the value obtained with the non-trypan blue method. Whether the original level of hygromycin B used was a factor in observed cytotoxicity remains unknown. The CEDEX value (300 µg/ml) was incorporated for the growth of transfected cells after using Nucleofection technology.

In summary, immunocytochemistry confirmed the sub-cellular location of hTRPV1 in transfected SH-SY5Y cells. DNA sequencing verified that the hTRPV1 was complete without errors. An initial pharmacological screen has confirmed capsaicin activity, which can be competitively antagonised with capsazepine. This novel neuronal model is a more relevant pharmacological tool than recombinant human and rat TRPV1 expressed in HEK293 cells. Thus, a broader pharmacological characterisation will be investigated with a variety of agonists and antagonists for comparison to earlier results (Chapter 3) and the literature.

# 5 PHARMACOLOGICAL CHARACTERISATION OF HUMAN TRPV1 EXPRESSED IN SH-SY5Y CELLS

## 5.1 Introduction

The presence of vanilloid-sensitive nerves in humans is well-established (see Introduction, Section 1.6.2). Clearly, it is difficult to study TRPV1 in freshly acquired human sensory ganglia or spinal cord. However, a number of studies have been conducted in cultured adult human DRG neurones in which RTX binding sites have been found (Acs *et al.*, 1994; Szallasi *et al.*, 1994). The limitations can be overcome by utilising a cell-line stably transfected with recombinant hTRPV1. The preceding chapter described the validation and initial pharmacological characterisation of a selected clone which is a potential neuronal *in vitro* model expressing hTRPV1.

There have been a few reports of cloned recombinant hTRPV1 expressed in various cell-lines that have been pharmacologically characterised (Cortright *et al.*, 2001; Hayes *et al.*, 2000; McIntyre *et al.*, 2001). As discussed in Chapter 3, comparison of rat and human isoforms show that they compare favourably but with subtle differences. Interestingly, variation in potencies could lie in the selected methodology such as FLIPR employed at GlaxoSmithKline and the cuvette-based fluorimetry used in Chapter 3.

Since Caterina and co-workers cloned rTRPV1 from rat DRG (Caterina *et al.*, 1997), activity has been characterised using a variety of vanilloid ligands including capsaicin, AEA and olvanil, and the antagonists ruthenium red and capsazepine, see Introduction and Chapter 3. However, the search for an endogenous ligand (endovanilloid) remains unresolved. Several compounds including AEA, NADA and arachidonic acid metabolites have emerged as putative ligands and all have been reported to activate TRPV1 (Van Der Stelt *et al.*, 2004). NADA is an endogenous capsaicin-like substance with high potency at recombinant and native rTRPV1 (Huang *et al.*, 2002). Arachidonic acid metabolites are highly unstable and thus, vanilloid-mediated effects are difficult to obtain. Further clarification of the physiological processes relating to these potential endovanilloids is required and may lead to novel drug development for neuropathic pain syndromes (Van Der Stelt *et al.*, 2004).

Capsazepine is the only vanilloid antagonist to have been studied extensively. Another antagonist is ruthenium red, a pore-blocker (Amann *et al.*, 1991) use of which has declined because of its non-competitive nature. Consequently, synthetic antagonists, including iodo-RTX, KJM429 and JYL1421, have been designed to display a higher affinity relative to

capsazepine (Wahl *et al.*, 2001; Wang *et al.*, 2002). Interestingly, it has been proposed that new, high affinity vanilloid-specific antagonists could also be used therapeutically in the pain clinic. Iodo-RTX application produced a decrease in licking time, induced by capsaicin injection in mice, which was more potent than morphine and capsaicin. As new vanilloid antagonists could inhibit nociceptive transmission, side-effects currently caused by capsaicin pungency could be avoided (Wahl *et al.*, 2001).

## 5.2 Aims

To perform a detailed pharmacological characterisation on clone 7 selected from the previous chapter and compare with:

- previous data in HEK293 cells (Chapter 3)
- reported pharmacological data on recombinant and native TRPV1 in the literature

## 5.3 Results

### *5.3.1 Temporal profiles*

*Capsaicin*: the methods employed to perform these studies are described in Section 2.7.1. Figure 5.1 displays typical traces in response to increasing concentrations of capsaicin in SH-SY5Y$_{hTRPV1}$ cells at 37°C. Capsaicin produced a time- (Figure 5.1) and concentration- (Figure 5.2, Table 5.1) dependent increase in $[Ca^{2+}]_i$. Addition of capsaicin at 60 s caused a rapid (~20 s) elevation in $[Ca^{2+}]_i$ and this reached a maximum at around 10 μM capsaicin. In general, after the maximum increase in $[Ca^{2+}]_i$ was achieved, a plateau in response was maintained until the end. This contrasted with observations in the HEK293$_{hTRPV1}$ and HEK293$_{rTRPV1}$ cells (Chapter 3), in which there was a gradual decrease once the maximal $[Ca^{2+}]_i$ response was attained. Overall, there was some variability in $[Ca^{2+}]_i$ responses in SH-SY5Y$_{hTRPV1}$ cells, $[Ca^{2+}]_i$ ranged from 1457-2224 nM with 10 μM capsaicin. It was interesting to note that the level of response was relatively higher compared to that in both HEK293$_{rTRPV1}$ and HEK293$_{hTRPV1}$ cells at 37°C, which suggests that there is a higher level of receptor expression in the neuronal transfects.

*AEA*: the methods performed to carry out these experiments are described in Section 2.7.1. Figure 5.1 displays typical traces in response to varying concentrations of AEA in SH-SY5Y$_{hTRPV1}$ cells at 37°C. AEA produced a concentration- (Figure 5.2, Table 5.1) and time-dependent increase in $[Ca^{2+}]_i$ (Figure 5.1). Addition of AEA at 60 s caused a rapid (~25 s) elevation in $[Ca^{2+}]_i$ and this reached a maximum at approximately 3 μM AEA. Like capsaicin, AEA's maximum $[Ca^{2+}]_i$ response in SH-SY5Y$_{hTRPV1}$ cells was greater than in HEK293$_{hTRPV1}$ and HEK293$_{rTRPV1}$ cells and this could be attributed to higher expression in the former cell-line. In the SH-SY5Y$_{hTRPV1}$ cells the response was mostly biphasic in nature in which once the maximal $[Ca^{2+}]_i$ response was achieved, there was a gradual decrease or a plateau was maintained. In addition, variability in $[Ca^{2+}]_i$ responses ranged from 1751-3145 nM at 3 μM AEA.

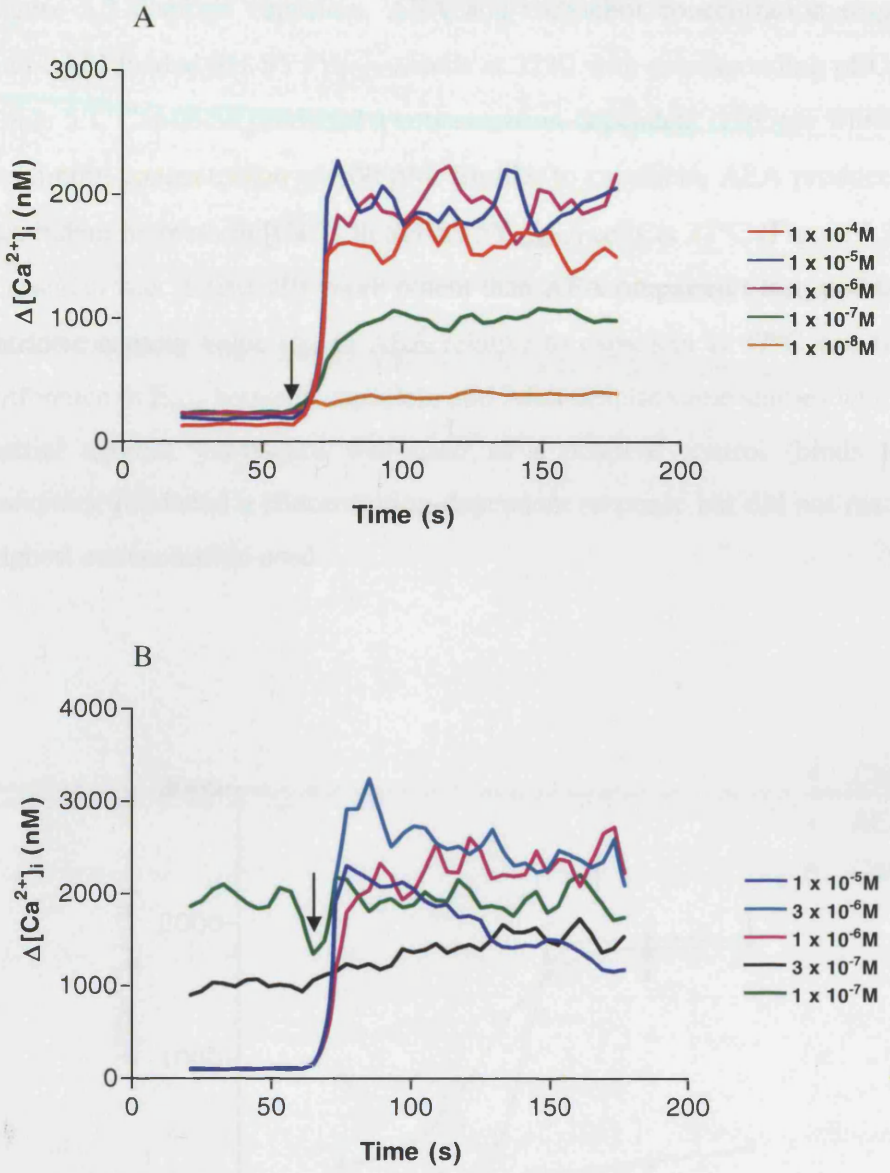


**Figure 5.1 Typical temporal profiles of capsaicin and AEA at 37°C**
*Addition of (A)capsaicin and (B)AEA occurred at 60 s (indicated by arrows) in fura-2AM loaded cells.*

### *5.3.2 Comparison of agonists at TRPV1*

*Cuvette agonist studies*

Figure 5.2 displays capsaicin, AEA and carbachol concentration response curves from fura-2AM loaded SH-SY5Y$_{hTRPV1}$ cells at 37°C with corresponding $pEC_{50}$ values shown in Table 5.1. Capsaicin produced a concentration-dependent response which saturated using a maximum concentration of 100 μM. Similar to capsaicin, AEA produced a concentration-dependent increase in $[Ca^{2+}]_i$ in SH-SY5Y$_{hTRPV1}$ cells at 37°C (Figure 5.2) which saturated. Capsaicin was statistically more potent than AEA (unpaired t-test, p=0.04) and the relative intrinsic activity value (α) of AEA relative to capsaicin at 37°C was 0.89. There was no difference in $E_{max}$ between capsaicin and AEA despite some studies which report AEA as a partial agonist. Carbachol was used as a positive control (binds to muscarinic M3 receptor), produced a concentration-dependent response but did not reach saturation at the highest concentration used.

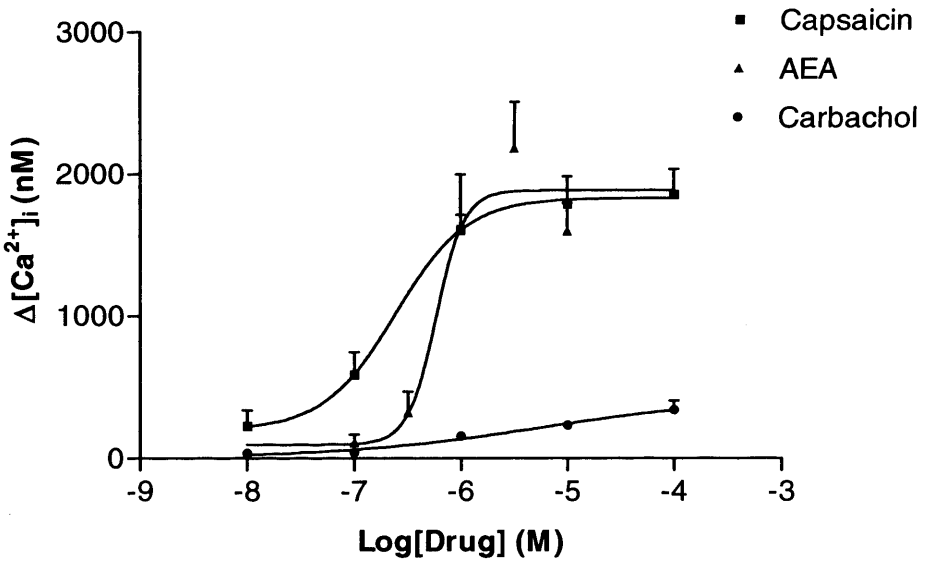


**Figure 5.2 Concentration response curves for capsaicin and AEA at 37°C**
*Data are mean±SEM: capsaicin (n=4), AEA (n=4) and carbachol (n=3) in cuvette-based studies.*

**Table 5.1 Corresponding potency values from cuvette-based studies in at 37°C**
*Data are mean±SEM, capsaicin and AEA n=4; carbachol $pEC_{50}$ was estimated, n=3*

| Compound | $pEC_{50}$ | $EC_{50}$ (nM) | $E_{max}$ (nM) |
|---|---|---|---|
| Capsaicin | 6.63±0.14 | 234.4 | 1854±182 |
| AEA | 6.20±0.10 | 631.0 | 1891±250 |
| Carbachol | 5.92±0.10 | 1202.3 | - |

*FLIPR agonist studies*

FLIPR technology was then employed to characterise a variety of agonists in fluo-3AM loaded SH-SY5$Y_{hTRPV1}$ cells at 25°C (Table 5.2). In addition, carbachol was included as a control as this acts on muscarinic receptors typically found in SH-SY5Y cells. The agonists produced no response while carbachol caused a concentration-dependent response in wild-type SH-SY5Y cells (Figure 5.3).

**Table 5.2 Corresponding potency values from FLIPR agonist experiments**
*Data are mean±SEM, n=3.*

| Compound | $pEC_{50}$ | $EC_{50}$ |
|---|---|---|
| Capsaicin | 8.54±0.06 | 2.9 nM |
| AEA | 5.34±0.02 | 4.6 µM |
| Olvanil | 7.46±0.11 | 34.7 nM |
| RTX | 9.03±0.10 | 0.9 nM |
| Carbachol | 5.83±0.02 | 1.5 µM |
| AM404 | Did not saturate | |
| NADA | Did not saturate | |

Similar to the response in fura-2AM loaded cells, capsaicin produced a concentration-dependent increase in response which saturated during FLIPR experimentation. RTX also caused a very similar response in terms of $pEC_{50}$ and also saturated with a similar $E_{max}$. NADA, a compound structurally similar to capsaicin, also produced a concentration-dependent response that did not saturate. AEA resulted in a concentration-dependent response curve, which was positioned to the far right relative to capsaicin, RTX and

olvanil. The potency of AEA was significantly lower compared to capsaicin and RTX. In addition, AEA revealed a relatively lower $E_{max}$ compared to capsaicin and RTX, which is indicative of partial agonism. Olvanil produced a concentration-dependent increase in response which saturated, was relatively less potent than capsaicin and RTX but had a higher $pEC_{50}$ than AEA. Like AEA, a significant reduction in maximum response relative to capsaicin and RTX was observed. All the test compounds produced a concentration-dependent increase in response that saturated except for AM404 and NADA in SH-$SY5Y_{hTRPV1}$ cells (Figure 5.3). The rank order of potency, in terms of $pEC_{50}$, was RTX>capsaicin>olvanil>AEA (Table 5.2).

A

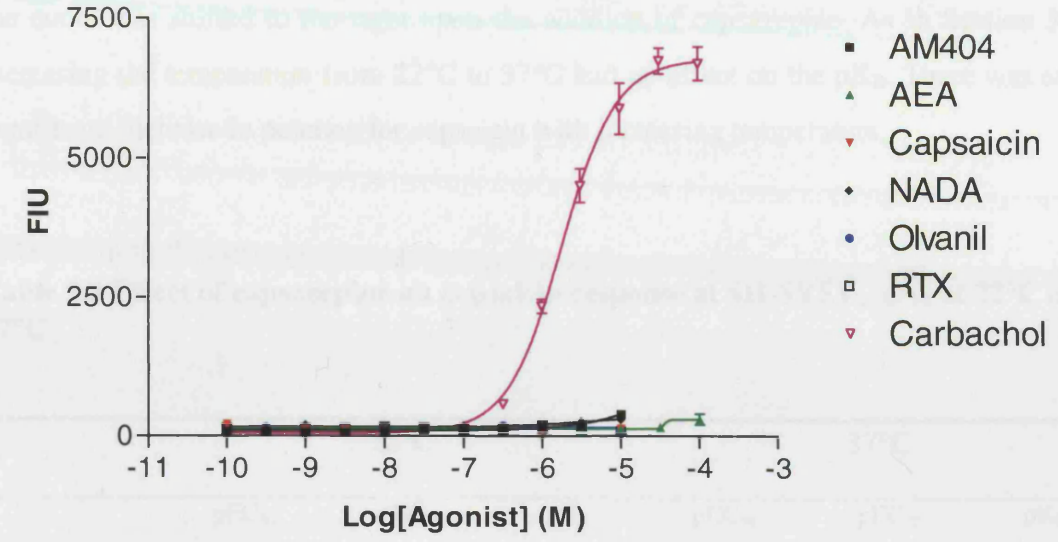


B

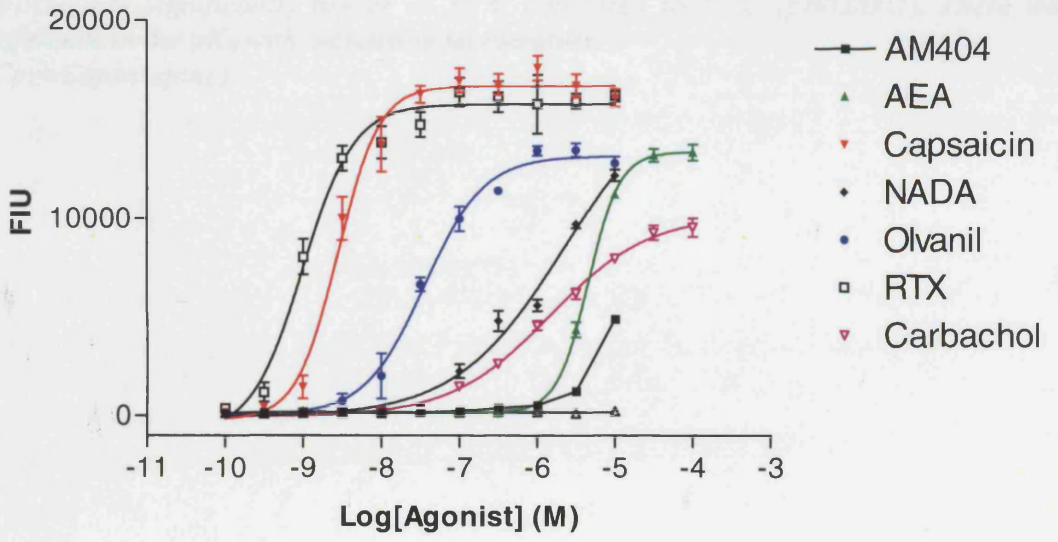


**Figure 5.3 Agonist response in wild-type SH-SY5Y and transfected SHSY5Y$_{hTRPV1}$ cells using FLIPR at 25°C**

*(A)Wild-type SH-SY5Y (B)transfected SH-SY5Y$_{hTRPV1}$, data presented as mean±SEM, n=3.*

### *5.3.3 Cuvette inhibition studies*

Capsazepine (0.3-1 μM) competitively antagonised the capsaicin-induced increase in $[Ca^{2+}]_i$ in fura-2AM loaded SH-SY5Y$_{hTRPV1}$ cells, Figure 5.4, yielding $pK_B$ values of 7.43±0.10 and 7.44±0.07 at 22°C and 37°C respectively (Table 5.3). At both temperatures, the curve was shifted to the right upon the addition of capsazepine. As in Section 3.3.4, increasing the temperature from 22°C to 37°C had no effect on the $pK_B$. There was also a significant increase in potency for capsaicin with increasing temperature.

**Table 5.3 Effect of capsazepine on capsaicin response at SH-SY5Y$_{hTRPV1}$ at 22°C and 37°C**

| | 22°C | | | 37°C | | |
|---|---|---|---|---|---|---|
| | $pEC_{50}$ (Control) | $pEC_{50}$ (+Cpz) | $pK_B$ | $pEC_{50}$ (Control) | $pEC_{50}$ (+Cpz) | $pK_B$ |
| hTRPV1 | 6.54± 0.07 | 5.65± 0.05 | 7.43± 0.10 | 7.40± 0.14* | 5.95± 0.12* | 7.44± 0.07 |

*Data are mean±SEM (n=6-7) at 22℃ and 37℃ and compared with unpaired t-test. *$pEC_{50}$ was significantly higher at 37℃ compared to 22℃ (p=0.0002). There was no difference in the $pK_B$ with increasing temperature.*
*(Cpz=Capsazepine)*

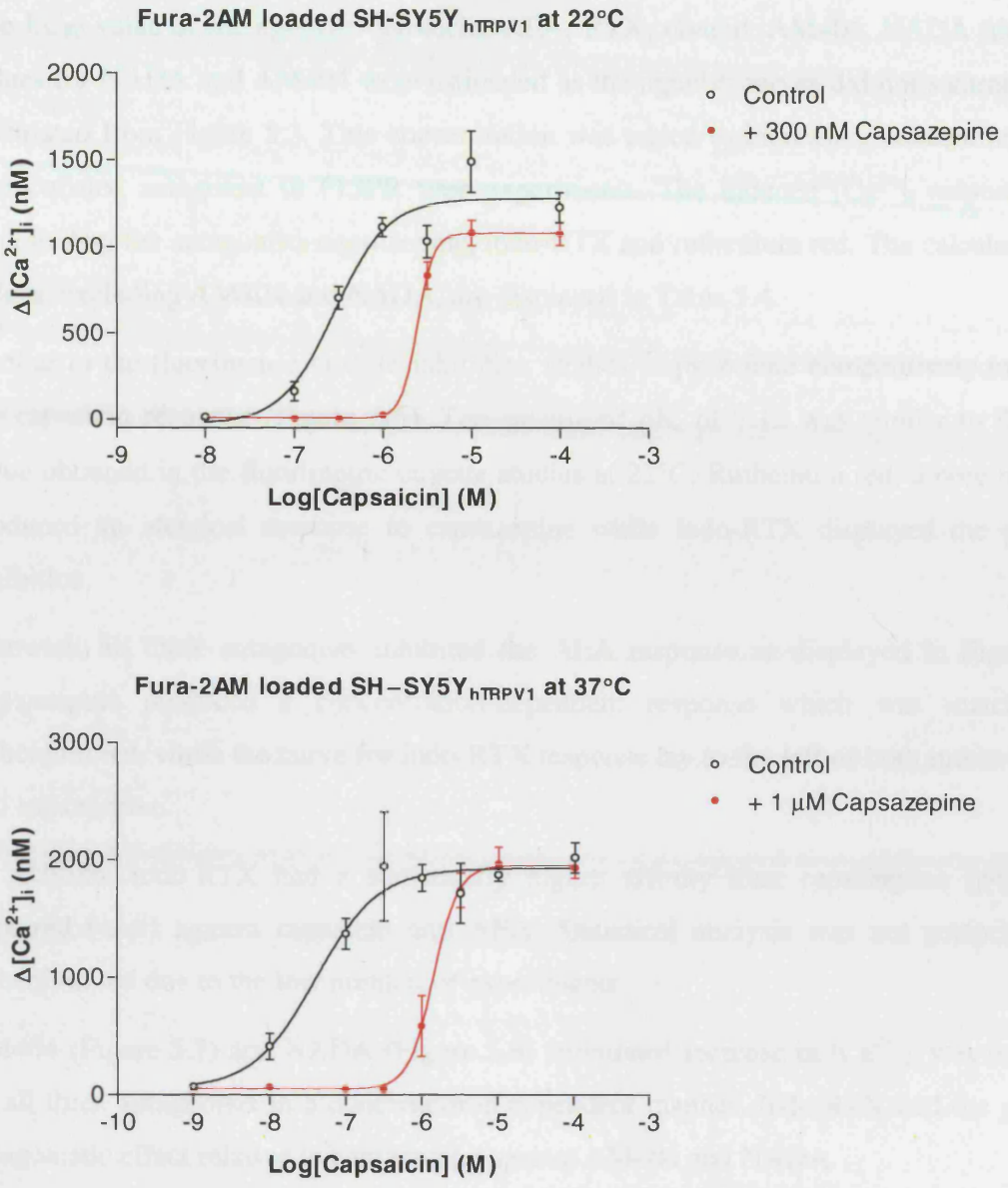


**Figure 5.4 Capsazepine inhibition studies (cuvette-based experiments)**
*Capsazepine produced a rightward shift in the concentration response curve to capsaicin indicative of competitive antagonism. Data (mean±SEM) are n=7 at 22℃ and n=6 at 37℃.*

### *5.3.4 FLIPR inhibition studies*

The $EC_{80}$ value of the agonists capsaicin, AEA, RTX, olvanil, AM404, NADA (the $EC_{80}$ values for NADA and AM404 were estimated as the agonist curves did not saturate), was calculated from Figure 5.3. This concentration was added to increasing concentrations of preincubated antagonist in FLIPR type experiments. The induced $[Ca^{2+}]_i$ response was inhibited by the antagonists capsazepine, iodo-RTX and ruthenium red. The calculated $pK_i$ values, excluding AM404 and NADA, are displayed in Table 5.4.

Similar to the fluorimetric cuvette inhibition studies, capsazepine competitively inhibited the capsaicin response (Figure 5.5). The calculated $pK_i$ of 7.12 was similar to the $pK_B$ value obtained in the fluorimetric cuvette studies at 22°C. Ruthenium red, a pore blocker, produced an identical response to capsazepine while iodo-RTX displayed the greatest inhibition.

Likewise, all three antagonists inhibited the AEA response as displayed in Figure 5.6. Capsazepine produced a concentration-dependent response which was matched by ruthenium red, while the curve for iodo-RTX response lay to the left of both ruthenium red and capsazepine.

In addition, iodo-RTX had a statistically higher affinity than capsazepine ($p<0.0001$, unpaired t-test) against capsaicin and AEA. Statistical analysis was not performed on ruthenium red due to the low number of experiments.

AM404 (Figure 5.7) and NADA (Figure 5.8) stimulated increase in $[Ca^{2+}]_i$, was inhibited by all three antagonists in a concentration-dependent manner. Iodo-RTX had the greatest antagonistic effect relative to capsazepine against AM404 and NADA.

Olvanil (Figure 5.9) and RTX (Figure 5.10) were also inhibited by the three antagonists. Capsazepine, ruthenium red and iodo-RTX inhibited olvanil in a concentration-dependent manner. Similar to capsaicin, AEA, NADA and AM404, iodo-RTX had the highest inhibition relative to capsazepine against olvanil and RTX. For olvanil, the rank order of affinity was iodo-RTX>ruthenium red=capsazepine.

In addition, the rank order of capsazepine affinity at the agonists was AEA>capsaicin=olvanil>RTX. Similarly, the rank order of affinity for iodo-RTX was AEA>capsaicin>olvanil and RTX.

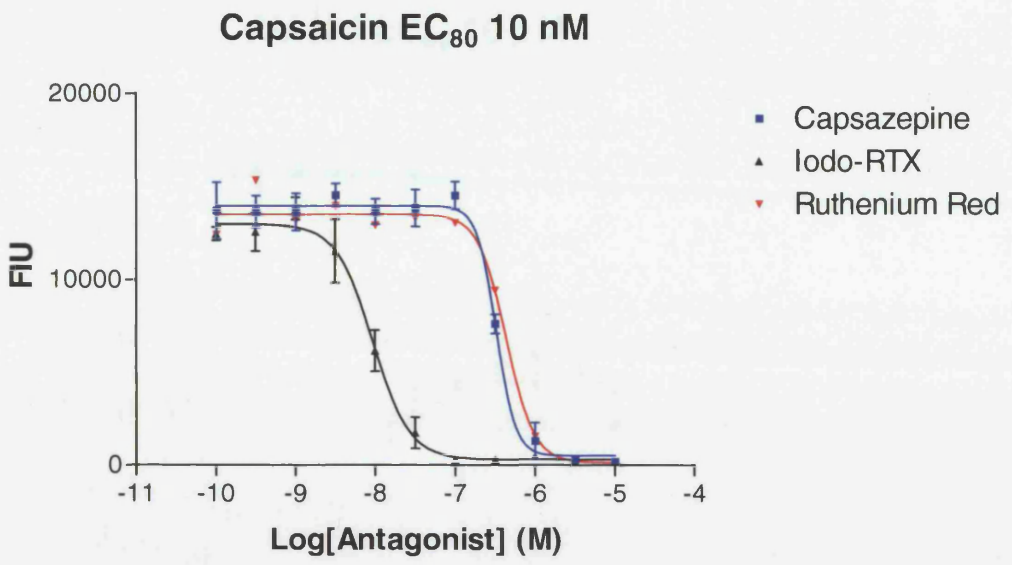


**Figure 5.5 FLIPR data – capsaicin response inhibited by vanilloid antagonists**
*Fluo-3 transfected vanilloid SH-SY5Y cells were preincubated with Tyrodes's buffer (control), capsazepine, iodo-RTX and ruthenium red. The fluorescence was monitored before and after the addition of capsaicin. Data are mean±SEM, n=3 for all except for ruthenium red where n=2.*

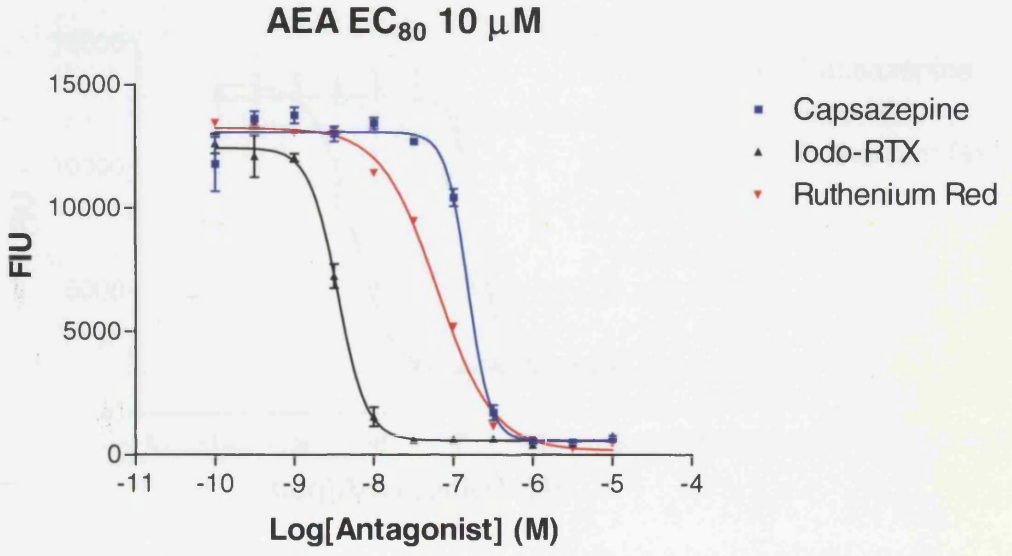


**Figure 5.6 FLIPR data – AEA response inhibited by vanilloid antagonists**
*Fluo-3 loaded transfected SH-SY5Y cells were preincubated with Tyrodes's buffer (control), capsazepine, iodo-RTX and ruthenium red. The fluorescence was monitored before and after the addition of AEA. Data are mean±SEM, n=3 except for ruthenium red where n=2.*

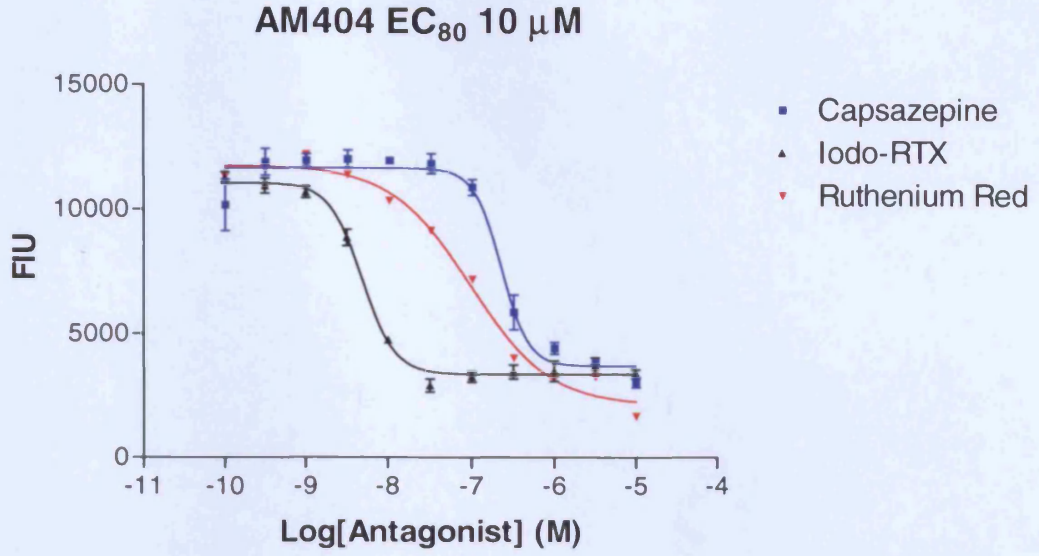


**Figure 5.7 FLIPR data – AM404 response inhibited by vanilloid antagonists**
*Fluo-3 loaded transfected SH-SY5Y cells were preincubated with Tyrodes's buffer (control), capsazepine, iodo-RTX and ruthenium red. The fluorescence was monitored before and after the addition of AM404 ($EC_{80}$ was estimated). Data are mean±SEM, n=3, except for ruthenium red where n=2.*

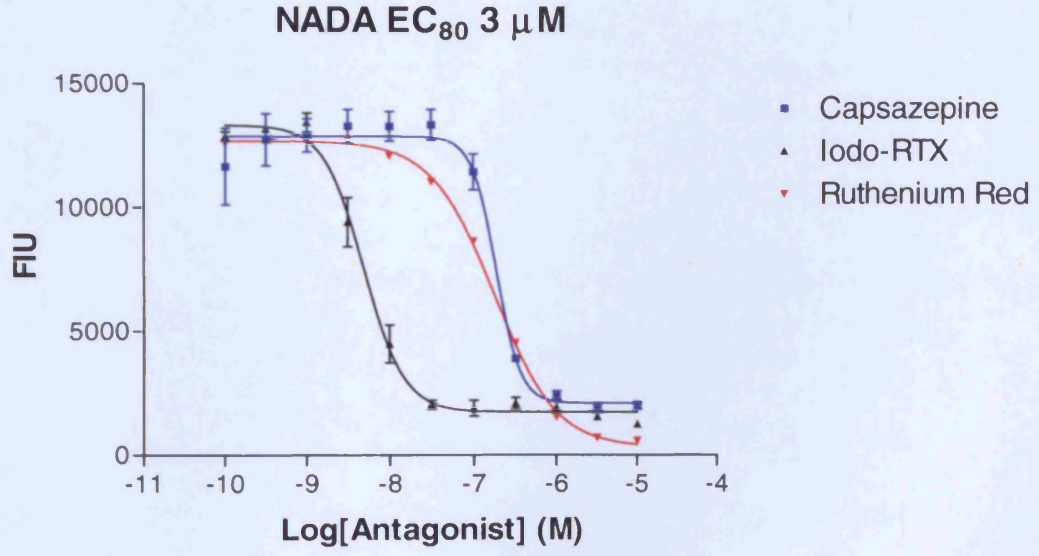


**Figure 5.8 FLIPR data – NADA response inhibited by vanilloid antagonists**
*Fluo-3 loaded transfected SH-SY5Y cells were preincubated with Tyrodes's buffer (control), capsazepine, iodo-RTX and ruthenium red. The fluorescence was monitored before and after the addition of NADA ($EC_{80}$ was estimated). Data are mean±SEM, n=3, except for ruthenium red where n=2.*

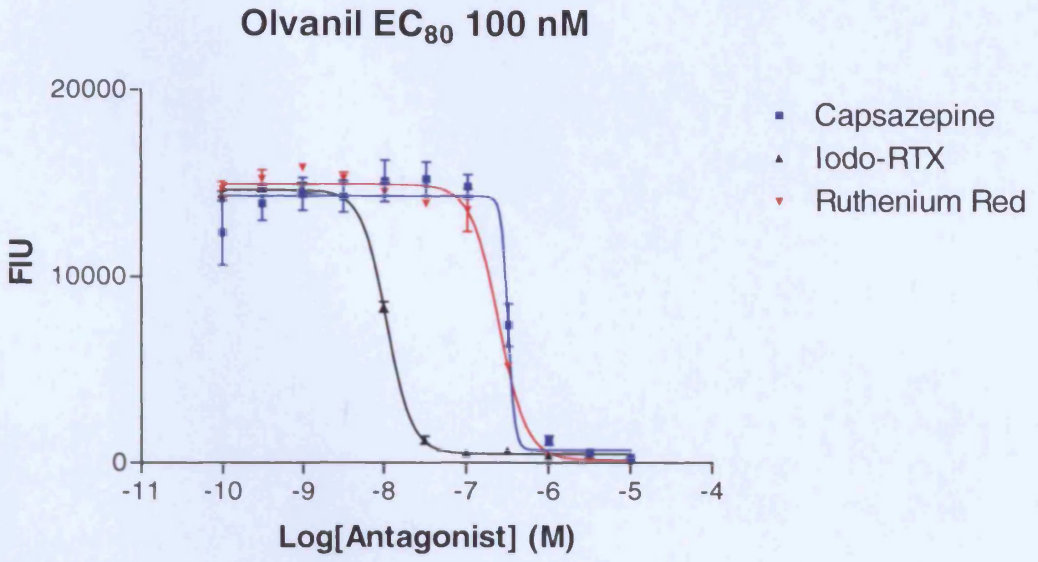


**Figure 5.9 FLIPR data – Olvanil response inhibited by vanilloid antagonists**
*Fluo-3 loaded transfected SH-SY5Y cells were preincubated with Tyrodes's buffer (control), capsazepine, iodo-RTX and ruthenium red. The fluorescence was monitored before and after the addition of olvanil. Data are mean±SEM, n=3.*

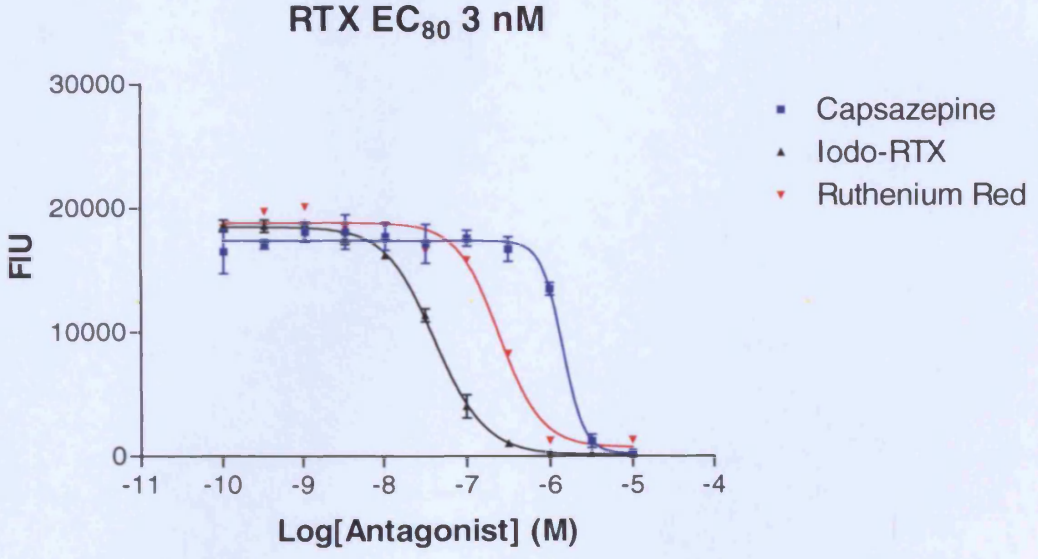


**Figure 5.10 FLIPR data – RTX response inhibited by vanilloid antagonists**
*Fluo-3 loaded transfected SH-SY5Y cells were preincubated with Tyrodes's buffer (control), capsazepine, iodo-RTX and ruthenium red. The fluorescence was monitored before and after the addition of RTX. Data are mean±SEM, n=3 for all except for ruthenium red where n=2.*

**Table 5.4 Inhibition of agonists by vanilloid antagonists obtained from FLIPR**

| | Capsazepine | Iodo-RTX | Ruthenium red |
|---|---|---|---|
| vs. capsaicin | 7.12±0.02 | 8.66±0.05 | 7.08 |
| vs. AEA | 7.32±0.03 | 8.95±0.04 | 7.71 |
| vs. RTX | 6.45±0.04 | 7.98±0.03 | 7.22 |
| vs. Olvanil | 7.05±0.03 | 8.53±0.01 | 7.19±0.04 |

*Data are displayed as $pK_i$ values (mean±SEM, n=3, except for ruthenium red against capsaicin, AEA and RTX where n=2)*

## 5.4 Discussion

This unique neuronal model is a homogeneous population of neuroblastoma cells which express recombinant human TRPV1. These cells have been shown to exhibit typical vanilloid responses from data obtained in cuvette- and FLIPR-based assays.

*Agonists*

*Cuvette-based studies*

The response of capsaicin, the archetypal vanilloid, was examined in SH-SY5Y$_{hTRPV1}$ cells at 37°C. Capsaicin produced a typical concentration response with a $pEC_{50}$ of 6.63 that matches the $pEC_{50}$ in HEK293$_{hTRPV1}$ cells at the same temperature (Chapter 3, Section 3.3.2). Capsaicin potency was also in good agreement with published data in recombinant rat and human TRPV1 receptors (McIntyre *et al.*, 2001; Ralevic *et al.*, 2001; Smart *et al.*, 2000a; Sprague *et al.*, 2001). In addition, the $E_{max}$ in the neuronal cells was three-fold higher compared to the HEK293$_{hTRPV1}$ cells, which could be due to an increase in receptor expression.

AEA was also studied in SH-SY5Y$_{hTRPV1}$ cells at 37°C and the potency ($pEC_{50}$ of 6.20) was similar to the result in HEK293$_{hTRPV1}$ cells at the same temperature (Chapter 3, Section 3.3.2) and is consistent with published values of 5.95 (Smart *et al.*, 2000a) and 5.69 (Sprague *et al.*, 2001). No difference in potency was observed for AEA relative to capsaicin which indicates that AEA is a full agonist in this assay. This corresponds with the findings in HEK293$_{hTRPV1}$ cells, contrary to some reports inferring that AEA is a partial agonist, discussed earlier (Chapter 3).

*FLIPR*

Generally, agonist potencies in the FLIPR assays were higher in comparison to cuvette-based studies in SH-SY5Y$_{hTRPV1}$, as seen in previous data relating to HEK293$_{rTRPV1}$ and HEK293$_{hTRPV1}$ cells (Chapter 3). Capsaicin with a $pEC_{50}$ of 8.54, is at least an order of magnitude higher compared to published FLIPR values and results from HEK293$_{hTRPV1}$ cells at 22°C (Chapter 3, Section 3.3.2) (Smart *et al.*, 2000a; Smart *et al.*, 2001). The potency of AEA was in good agreement with the result in HEK293$_{hTRPV1}$ cells (Chapter 3, Section 3.3.2) and other FLIPR reports (Smart *et al.*, 2000a; Smart *et al.*, 2001). Likewise, olvanil was similar to published FLIPR results (Smart *et al.*, 2000a; Smart *et al.*, 2001) but differed by an order of magnitude by comparison to HEK293$_{hTRPV1}$ cells at 37°C (Chapter

3, Section 3.3.3). Compared to the cuvette-based studies where AEA appeared to be a full agonist, this was not so in the FLIPR assay where the $E_{max}$ was significantly reduced relative to those of capsaicin and RTX. Partial agonism was also observed for olvanil, contrary to the literature where olvanil has been reported as a full agonist at both rat and human TRPV1 (Jerman *et al.*, 2000; Smart *et al.*, 2001). However, both of these compounds are highly lipophilic with low aqueous solubility.

The endogenous compound NADA, which is structurally similar to capsaicin, was found to be less potent than capsaicin but more potent than AEA. This corroborates other data that revealed the same rank order (Huang *et al.*, 2002). Also, it was inferred that NADA displayed partial agonism, however NADA pharmacology was found to vary in the literature. NADA was found to be a full agonist ($K_d$ of 5-10 μM in binding assays) in heterologous or native expression systems (Di Marzo *et al.*, 2002; Toth *et al.*, 2003). Reported NADA potencies seem to depend upon the cell and assay type, for example, rat DRG neurones ($Ca^{2+}$ imaging), HEK293 (rat and human TRPV1, $Ca^{2+}$ uptake) and rat $CHO_{rTRPV1}$ cells ($Ca^{2+}$ uptake), NADA potencies were 0.8 μM, 30 nM and 5 μM respectively (Huang *et al.*, 2002; Toth *et al.*, 2003). Similar to AEA, NADA has been classed as a putative endogenous TRPV1 ligand, however, investigations into the biosynthetic pathway and regulation are warranted (Van Der Stelt *et al.*, 2004).

AM404 is an AEA transport inhibitor and was thought to be a useful pharmacological tool for investigating the role of transport in endocannabinoid inactivation. However AM404 has displayed agonist activity at TRPV1, thus limiting its potential use in endocannabinoid inactivation studies (Piomelli, 2003).

RTX was approximately three-fold more potent than capsaicin which matches FLIPR results in $HEK293_{rTRPV1}$ cells (Jerman *et al.*, 2000). This was also in good agreement with that at hTRPV1 in another study (Smart *et al.*, 2000a).

The rank order of potency was RTX>capsaicin>olvanil>AEA, which was similar to a reported FLIPR study at hTRPV1 except olvanil was more potent than capsaicin (Smart *et al.*, 2001). However, the order matched that at rTRPV1 (Jerman *et al.*, 2000).

*Inhibition studies*

*Cuvette-based studies*

The antagonistic effect of capsazepine on capsaicin was studied at 22°C and 37°C. The effect was competitive in nature and not temperature-dependent, which is identical to the result in $HEK293_{rTRPV1}$ and $HEK293_{hTRPV1}$ cells (Chapter 3). However, $pK_B$ in the neuronal transfects was higher than that in $HEK293_{rTRPV1}$ and $HEK293_{hTRPV1}$ cells. Also, capsaicin control potency was significantly temperature-dependent where an increase in $pEC_{50}$ was noted with increasing temperature.

*FLIPR*

Capsazepine, iodo-RTX and ruthenium red antagonised capsaicin and RTX in a concentration-dependent manner, similar to other reports with the endogenous vanilloid receptor (Acs *et al.*, 1997; Bevan *et al.*, 1992; Wardle *et al.*, 1997). Capsazepine inhibited capsaicin with a $pK_i$ similiar to $pK_B$ values in cuvette-based studies in $SH\text{-}SY5Y_{hTRPV1}$ cells and was slightly higher than the value of 6.58 reported by Smart and colleagues (Smart *et al.*, 2001). Inhibition was also observed at hTRPV1 in the literature, but the concentration-dependency was not investigated (Hayes *et al.*, 2000).

Iodo-RTX had a higher affinity than capsazepine against the agonists tested matching other data at recombinant hTRPV1 (Smart *et al.*, 2001). Both capsazepine and iodo-RTX produced the highest affinity against AEA. However, a full capsazepine $pK_B$ analysis against AEA in the $HEK293_{hTRPV1}$ and $HEK293_{rTRPV1}$ cells (Chapter 3) was not determined. This was due to the low solubility of AEA, thus, a comparison could not be made.

The $pK_i$ data displayed in Table 5.4 may be theorectically invalid using the Cheng-Prusoff equation as shown by Lazareno and Birdsall. A modified Cheng-Prusoff equation was applied to the capsaicin versus capsazepine FLIPR data according to Lazareno and Birdsall (Lazareno *et al.*, 1993). This produced a $K_i$, which was 2-fold lower than the original $K_i$ obtained and 4-fold lower compared to the $K_B$ found in the cuvette inhibition studies. Despite these differences, the rank order of affinity for these antagonists will remain unchanged regardless of using the Cheng-Prusoff equation or another analysis.

Utilising FLIPR technology is advantageous due to a high level of automation where high throughput screening is required. In contrast, the cuvette-based studies involve only a single sample at one time; hence the process is labour-intensive. Nevertheless, the

temperature can be varied accordingly while FLIPR studies could only be performed at 25°C. Hence, FLIPR is only appropriate for laboratories and commercial facilities, which perform a high number of sample screenings.

*Further comments on AEA*

The principle action of AEA on vanilloid receptors could be to potentiate responses to other stimuli, especially heat or protons. Under conditions of elevated temperatures or decreased pH, the potency of AEA as a TRPV1 agonist may be significantly increased. Hence, pro-algesic agents such as ATP, bradykinin, serotonin, leukotrienes and prostanoids may sensitise the primary afferent neurone, in part, by stimulating the production of lipid-derived second messengers that sensitise TRPV1 and consequently enhance nociceptor excitability.

Also, AEA produced by non-neuronal cells may synergise with these agents by modulating the activity of TRPV1 channels on neighbouring sensory nerve terminals. Fatty acid amide hydrolase (FAAH) inactivates AEA *via* hydrolysis (Di Marzo *et al.*, 2001). If FAAH is blocked, AEA potency could increase at TRPV1 (De Petrocellis *et al.*, 2001; Ross *et al.*, 2001). The AEA membrane transporter (AMT) is thought to play a role in TRPV1 activation by AEA as it facilitates uptake of extracellular AEA. Furthermore, this supports the view that AEA binds to an intracellular site at TRPV1. Nitric oxide (NO) donors can activate AMT, which consequently enhances the apparent activity of AEA at hTRPV1. In contrast, AMT inhibitors decrease AEA activity at hTRPV1 (De Petrocellis *et al.*, 2001). In summary, the mechanism for TRPV1 channel gating and the location of TRPV1 binding for vanilloids and cannabinoids remains unclear (Caterina *et al.*, 2001).

*Summary*

Pharmacological characterisation, using FLIPR and cuvette-based studies, have provided additional evidence that SH-SY5Y$_{hTRPV1}$ cells compare well with other expression systems. A summary comparing these cells with other models expressing recombinant hTRPV1 is displayed in Table 5.5. These findings have revealed that this neuronal transfect is a reliable model, suitable for further examination.

**Table 5.5 Comparison of SH-SY5Y$_{hTRPV1}$ with other models**

| | Methodology | $pEC_{50}$ Cap | $pEC_{50}$ AEA | $pK_B$ (Cap vs. Cpz) | Reference |
|---|---|---|---|---|---|
| SH-SY5Y$_{hTRPV1}$ | cuvette-based | 6.63±0.14 (37) | 6.20±0.10 (37) | 7.43±0.10 (22)<br>7.44±0.07 (37) | |
| | FLIPR | 8.54±0.06 (25) | 5.34±0.02 (25) | 7.12±0.02 (25) | |
| HEK293$_{hTRPV1}$ | cuvette-based | 6.88±0.05 (22)<br>6.77±0.11 (37) | 5.82±0.08 (22)<br>5.84±0.09 (37) | 6.76±0.25 (22)<br>6.75±0.04 (37) | Chapter 3 |
| | FLIPR | 7.13±0.11 (25) | 5.94±0.06 (25) | | (Smart *et al.*, 2000a) |
| | FLIPR | 7.29±0.04 (25) | 5.60±0.10 (25) | 6.58±0.02 (25) | (Smart *et al.*, 2001) |
| | aequorin luminescence | 6.25 (RT) | | $IC_{50}$ 39 nM (RT) | (McIntyre *et al.*, 2001) |
| | cuvette-based | 7.58 (25) | 6.25 (25) | | (Huang *et al.*, 2002) |

*Key: Cap – capsaicin, Cpz – capsazepine, RT – room temperature. Experimental temperature is displayed in brackets*

# 6 NORADRENALINE RELEASE STUDIES

## 6.1 Introduction

Capsaicin treatment releases a variety of transmitters from primary sensory neurones including calcitonin gene related peptide (CGRP) and tachykinins such as substance P, thereby interrupting sensory transmission, essentially resulting in a chemical denervation and, hence, analgesia.

Neurotransmitter secretion involves several stages including movement of vesicles to docking sites at the plasma membrane, followed by fusion and retrieval of vesicular and membrane components by endocytosis. The fusion of vesicular and plasma membranes is initiated by a sudden rise in $[Ca^{2+}]_i$ largely confined to the plasma membrane, followed by release of vesicular contents into the extracellular space. This process is referred to as exocytosis. For further information on neurotransmitter release, the reader is referred to a publication by Sudhof (Sudhof, 2004).

Noradrenaline (NA) is released from noradrenergic neurones during synaptic transmission and acts as a neurotransmitter. NA activates the adrenergic receptors which consist of α- and β-subtypes. Also, NA has been shown to elevate hyperalgesia to heat in human skin sensitised by capsaicin and Drummond suggested that sympathetic neural activity might increase pain associated with skin damage (Drummond, 1995). The role of TRPV1 in hyperalgesia, as observed in knock-out mice studies, displayed reduced responsiveness to noxious heat and the mice did not show thermal hyperalgesia in response to inflammation (Caterina *et al.*, 2000). The latter observation may be the key mechanism by which primary hyperalgesia is produced as TRPV1 expression is known to be increased by inflammation.

The regulation of NA secretion is fundamental to the control of the sympathetic nervous system. Secretion is dependent upon an increase in $[Ca^{2+}]_i$ following activation of voltage gated or receptor regulated calcium channels and is regulated by receptors situated on nerve endings. The biochemical mechanisms underlying these processes include phosphorylation of specific proteins which play a key role. For example, PKC, calcium/calmodulin kinase II and protein kinase A (PKA) have all been implicated in the regulation of NA secretion. Control of movement of synaptic vesicles is very precise, being regulated by 'trafficking proteins' involved in docking and fusion and located both in the synaptic vesicle itself. These proteins include the plasma membrane soluble NSF attachment proteins (SNAPs) and SNAP receptors (SNAREs). For information on synaptic vesicle trafficking the reader is referred to a review by Augustine (Augustine *et al.*, 1999).

## 6.2 Aims

As the TRPV1 channel is $Ca^{2+}$-permeable, it was hypothesised that the increase in $[Ca^{2+}]_i$ produced by activation of TRPV1 in SH-SY5Y cells could be sufficient to sustain NA release. Initially, static monolayer cultures were utilised to establish a correlation between capsaicin application and [$^3$H]NA release. Subsequently, a unique perfusion chamber was employed to study the effects of capsaicin addition by simultaneous measurements of $[Ca^{2+}]_i$ and NA release.

## 6.3 Results

### *6.3.1 Static Cultures*

Monolayers of wild-type SH-SY5Y and SH-SY5Y$_{hTRPV1}$ cells were treated with capsaicin as described in Section 2.9.1. In addition, $K^+$-evoked release of [$^3$H]NA as a positive control was incorporated in the SH-SY5Y$_{hTRPV1}$ cells (Figure 6.1). In wild-type cells, 10 μM capsaicin stimulation (7%) did not evoke the release of [$^3$H]NA relative to basal (6%). In contrast, the opposite occurred where capsaicin produced a release of 22%, 3.5 fold higher relative to basal in SH-SY5Y$_{hTRPV1}$ cells. Also, $K^+$-evoked release was 2.5 fold higher relative to basal in SH-SY5Y$_{hTRPV1}$ cells.

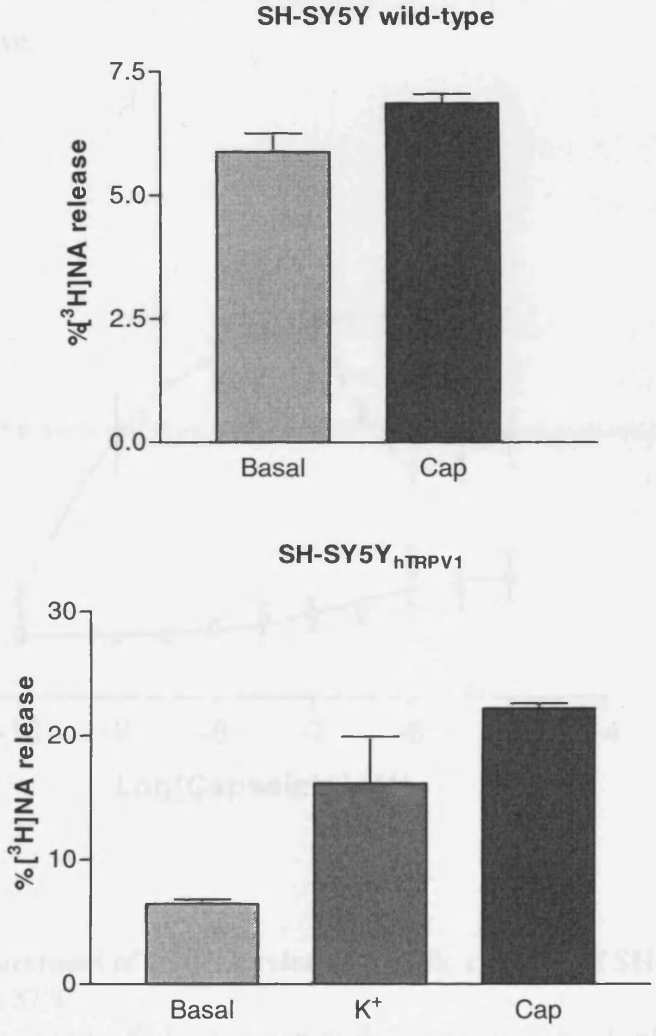


**Figure 6.1 Comparison of [$^3$H]NA release in various cell-types**
*Key: Cap – capsaicin. Monolayers of wild-type SH-SY5Y and SH-SY5Y$_{hTRPV1}$ cells were treated 10 μM capsaicin, the latter cells were treated with 100 mM $K^+$, at 37°C. [$^3$H]NA release is expressed as a fraction of the total. Data are mean±SEM, n=3.*

### *6.3.2 Capsaicin concentration response curves*

[$^3$H]NA release was measured after applying an increasing concentration of capsaicin in static monolayer SH-SY5Y$_{hTRPV1}$ and wild-type SH-SY5Y cultures as described in Section 2.9.1 and results are displayed in Figure 6.2. There was concentration-dependent increase in [$^3$H]NA release with a $pEC_{50}$ of 9.21±0.29, calculated using a fixed maxima at 100 nM capsaicin stimulation. Stimulating with capsaicin concentrations above 100 nM capsaicin caused [$^3$H]NA release to gradually decrease to approximately 25% (shown by the red dashed line). This figure matches the earlier experiments after stimulating with 10 µM capsaicin (Figure 6.1). Wild-type cells did not display a concentration-dependent increase in [$^3$H]NA release. However, there was a small increase with a concentration of 100 nM capsaicin and above.

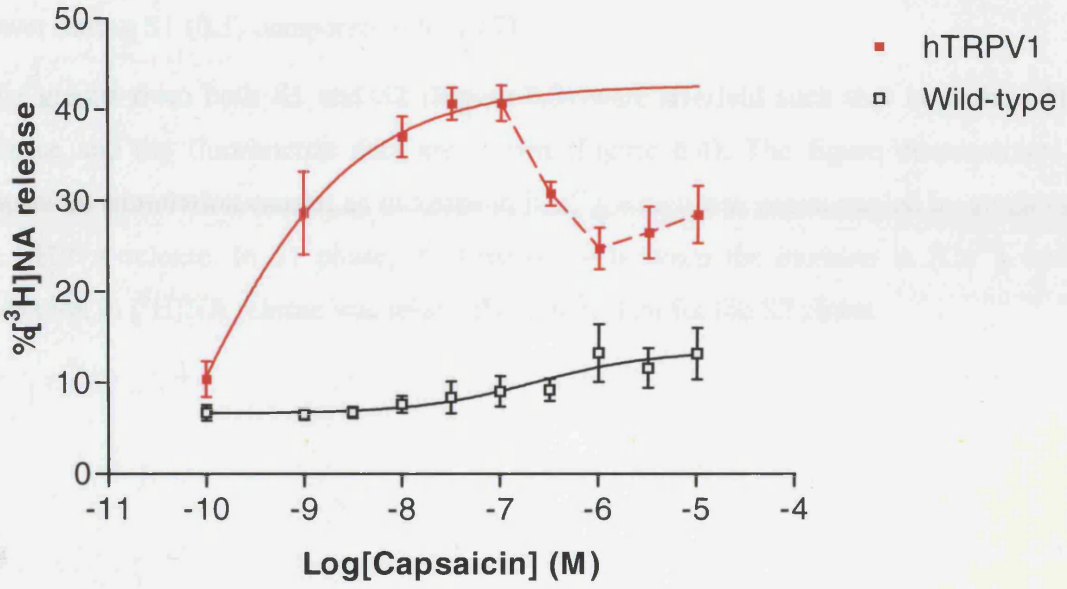


**Figure 6.2 Measurement of [$^3$H]NA release in static cultures of SH-SY5Y$_{hTRPV1}$ and wild-type cells at 37°C**

*[$^3$H]NA release is expressed as a fraction of the total. Data are displayed as mean±SEM, n=6.*

### *6.3.3 Perfusion chamber studies*

Using a perfusion chamber (Section 2.9.2), simultaneous measurements of $[Ca^{2+}]_i$ and [$^3$H]NA release (dpm) were made. 1 ml 100 nM capsaicin was perfused onto monolayers of SH-SY5Y$_{hTRPV1}$ cells, at 60 s at a perfusion rate of 22 µl/s during the first stimulation (S1) period. As displayed in Figure 6.3, a washout effect was also observed prior to the increase in [$^3$H]NA release during S1. A peak in the fluorimetric ratio 340/380 nm occurred at approximately 200 s and then gradually decreased over time. In addition, a peak in the corresponding [$^3$H]NA release was observed around 200 s. After a break of 10 min during which Krebs/HEPES buffer was continuously perfused into the perfusion chamber, the second application (S2 phase) of 1 ml 100 nM capsaicin also produced a peak in the fluorimetric ratio 340/380 nm at approximately 1350 s which gradually decreased over time. The corresponding [$^3$H]NA release increased to a peak at approximately 1400 s. The change in peak height (basal as a minimum) for normalised [$^3$H]NA release during both phases was approximately 0.2. While the change in normalised 340/380 ratio was lower during S1 (0.3) compared to S2 (0.7).

The graphs from both S1 and S2 (Figure 6.3) were overlaid such that both the [$^3$H]NA release and the fluorimetric data are shown (Figure 6.4). The figure demonstrates that capsaicin stimulation caused an increase in $[Ca^{2+}]_i$ which was accompanied by an elevation in [$^3$H]NA release. In S1 phase, the time delay between the increase in $[Ca^{2+}]_i$ and the elevation in [$^3$H]NA release was relatively shorter than for the S2 phase.

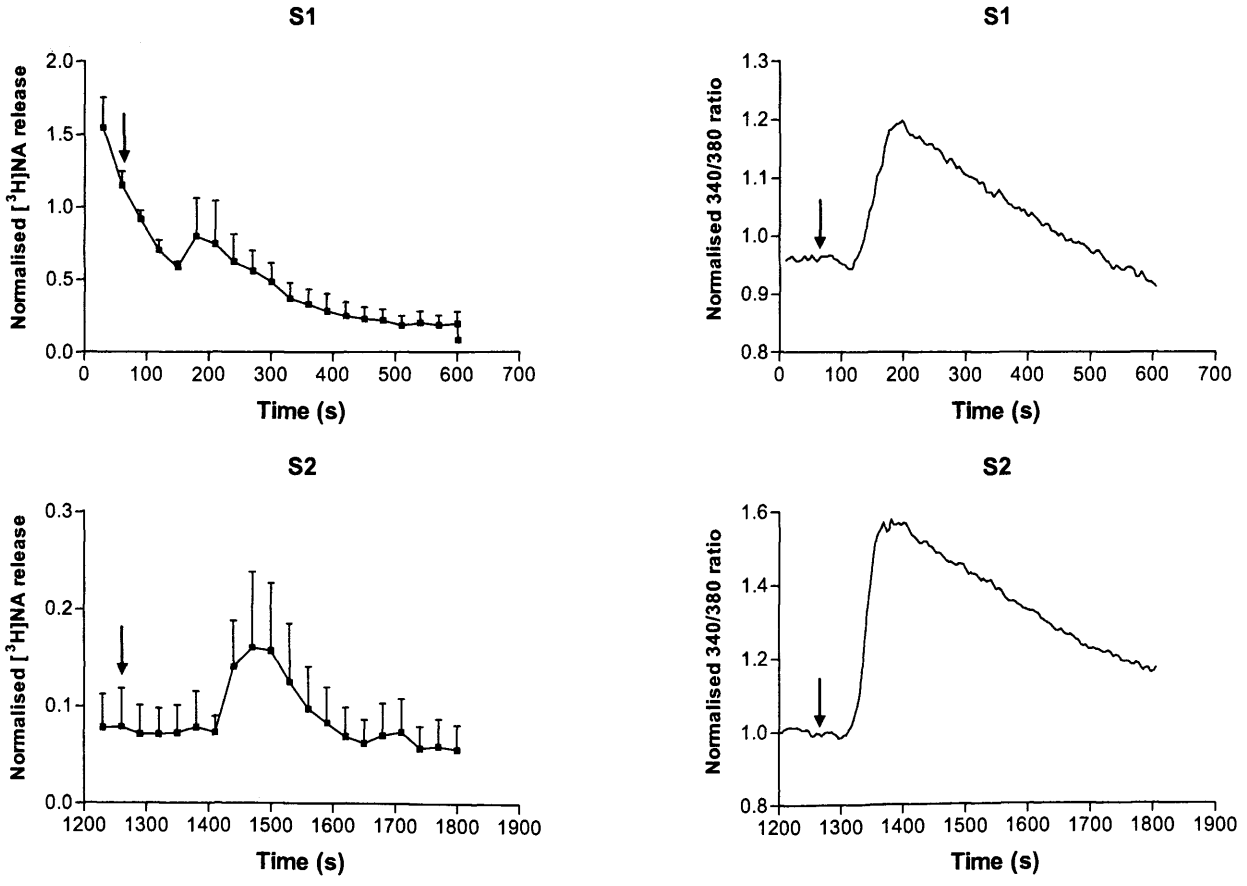


**Figure 6.3 Simultaneous measurement of $[Ca^{2+}]_i$ and [$^3$H]NA release in perfused SH-SY5Y$_{hTRPV1}$ cells at 37°C (n=4)**
*S1: Addition of 1 ml 100 nM Capsaicin at 60 s; S2: Addition of 1 ml 100 nM Capsaicin at 60 s. 10 min break between S1 and S2 during which Krebs/HEPES buffer was perfused through the chamber. Arrows indicate addition of capsaicin. Data (n=4) were normalised to the basal; [$^3$H]NA release displayed as mean±SEM and fluorimetric data as mean only.*

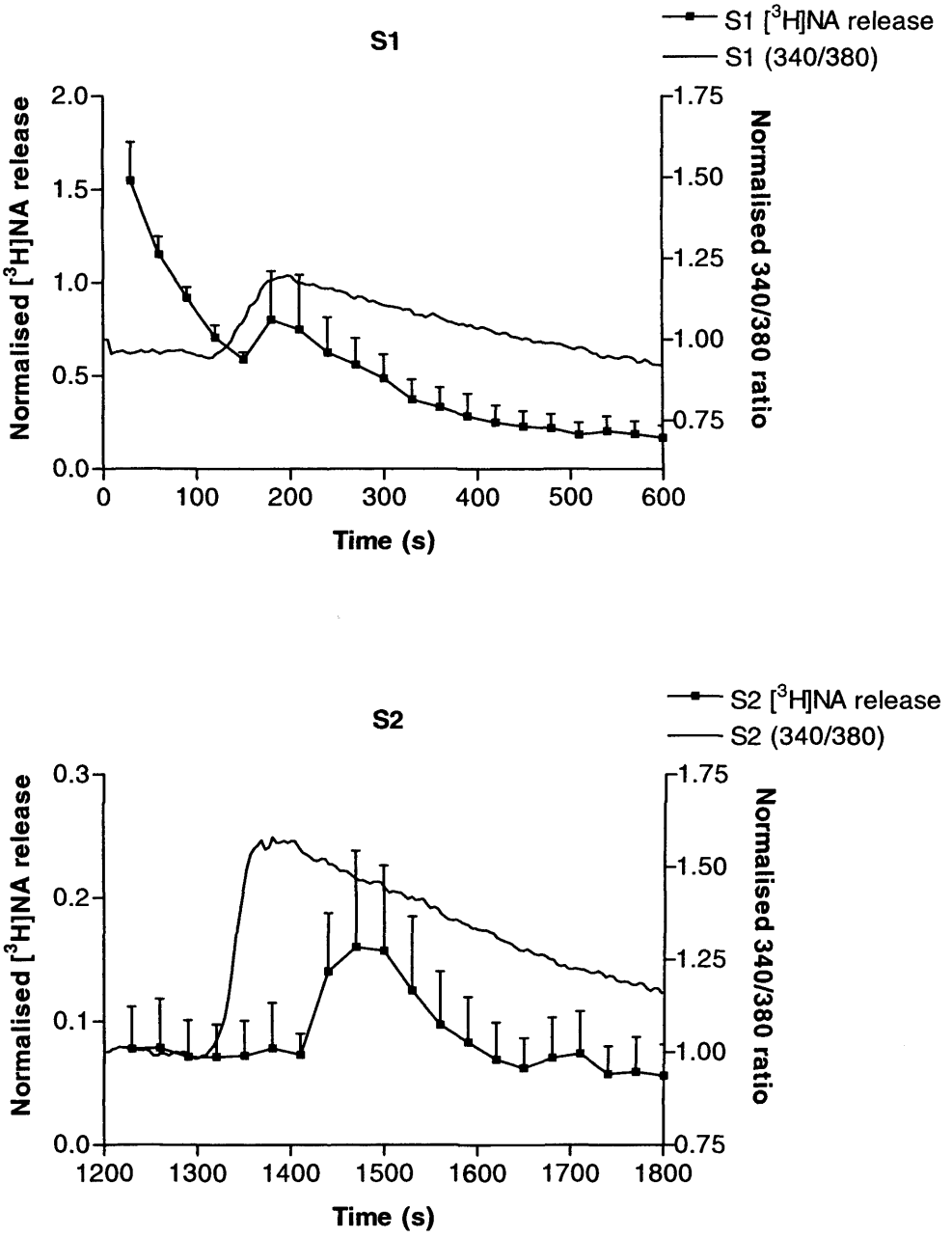


**Figure 6.4 Overlaid graphs of normalised [$^3$H]NA release and normalised fluorescence ratio in perfused SH-SY5Y$_{hTRPV1}$ cells at 37°C**

*S1: Addition of 1 ml 100 nM capsaicin at 60 s; S2: Addition of 1 ml 100 nM Capsaicin at 60 s. 10 min break between S1 and S2 during which SH-SY5Y$_{hTRPV1}$ cells were perfused with Krebs/HEPES buffer. Data (n=4) were normalised to the basal; fluorimetric data displayed as mean and [$^3$H]NA release as mean±SEM.*

### *6.3.4 Control experiments*

To exclude simple perfusion artefacts, cells were perfused with Krebs/HEPES buffer during the S1 phase (10 min period) while cells were perfused with capsaicin in S2 (Figure 6.5). As before during the previous capsaicin experiments (Figure 6.3), a washout effect was observed in relation to [$^3$H]NA release during S1. After 1 ml 100 nM capsaicin was applied during S2 phase, a biphasic response occurred where a relatively rapid elevation in $[Ca^{2+}]_i$ resulted in a peak at approximately 1350 s and gradually decreased. The corresponding [$^3$H]NA release during S2 also caused an elevation reaching a peak at 1400 s and gradually decreased to basal. The change in peak height for normalised 340/380 ratio during S2 was approximately 1.2, three-fold larger than during capsaicin application in S1 (Figure 6.3). The change in peak height for normalised [$^3$H]NA release was 0.35, slightly higher than for the S1 phase in Figure 6.3 when capsaicin was applied.

The data relating to phase S1 and S2 from the control experiments were overlaid such that the [$^3$H]NA release matched with the fluorimetric data (Figure 6.6). It is clear that there was a delay between $[Ca^{2+}]_i$ release and the induction of [$^3$H]NA release.

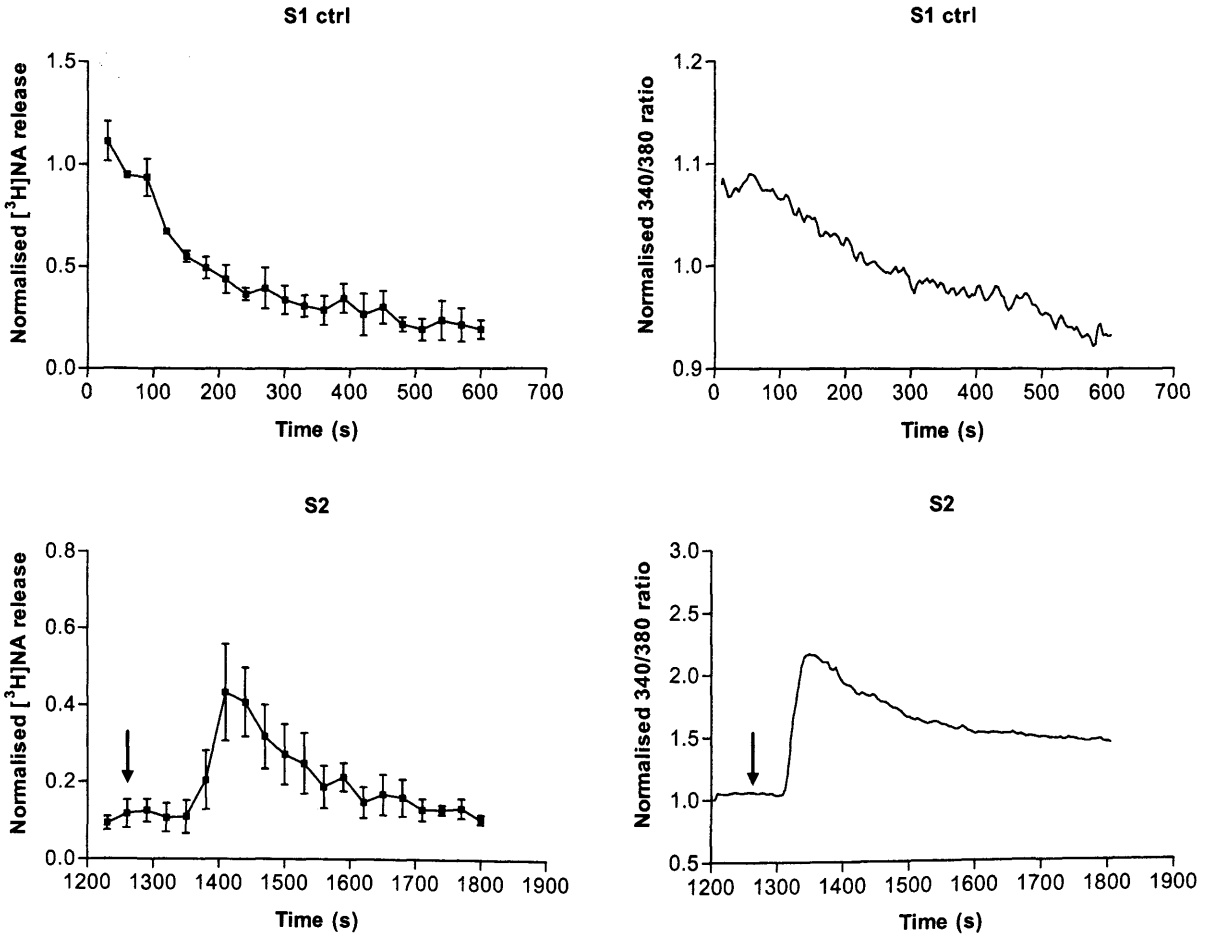


**Figure 6.5 Simultaneous measurement of $[Ca^{2+}]_i$ and [$^3$H]NA release in perfused SH-SY5Y$_{hTRPV1}$ cells at 37°C**

*S1:Perfusion of Krebs/HEPES buffer (ctrl=control); S2:Addition of 1 ml 100 nM capsaicin at 60 s. 10 min break between S1 and S2 during which Krebs/HEPES buffer was perfused through the chamber. Arrows indicate addition of capsaicin. Data (n=3) are displayed as mean±SEM. Error bars not shown on fluorimetric data. Data were normalised to the basal.*

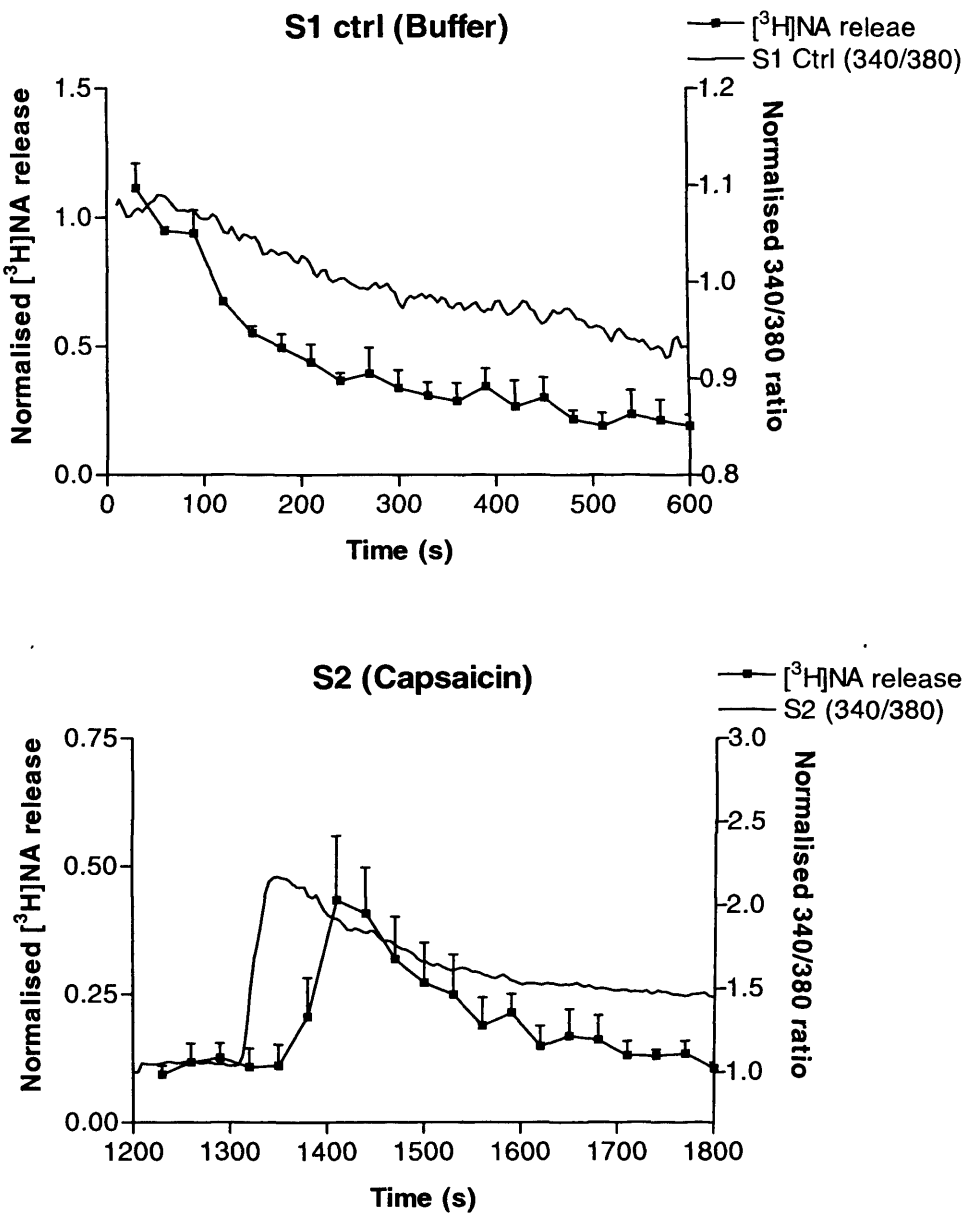


**Figure 6.6 Overlaid graphs of normalised [$^3$H]NA release and normalised fluorescence ratio in perfused SH-SY5Y$_{hTRPV1}$ cells at 37°C**

*S1: Only Krebs/HEPES buffer was perfused through the chamber (ctrl=control). S2: Addition of 1 ml 100 nM capsaicin at 60 s. Data (n=3) are displayed as mean±SEM. Error bars not shown on fluorimetric data. Data were normalised to the basal.*

## 6.4 Discussion

These investigations have demonstrated that TRPV1, a ligand-gated ion channel permeable to $Ca^{2+}$, produced an increase in [$^3$H]NA release after stimulating the transfected cells with capsaicin. Initially, static monolayer cultures established a correlation between capsaicin application and [$^3$H]NA release. Perfusion chamber studies corroborated the results from the static cultures by revealing $[Ca^{2+}]_i$ influx and [$^3$H]NA release were linked and evoked by capsaicin.

*Static cultures*

Experiments using $K^+$ stimulation as a positive control in SH-SY5Y$_{hTRPV1}$ cells confirmed that [$^3$H]NA release was as described in the literature (Vaughan *et al.*, 1995). Indeed, reported SH-SY5Y cellular characteristics include uptake and subsequent release of [$^3$H]NA in response to $K^+$ depolarisarisation as well as carbachol but not in the absence of extracellular calcium (Murphy *et al.*, 1991). Also, these cells possess L- and N-type VSCC which can be opened under $K^+$ depolarising conditions to increase $[Ca^{2+}]_i$ (Lambert *et al.*, 1990).

Release of [$^3$H]NA in the static cultures was concentration-dependent up to 100 nM capsaicin. However, the release decreased with higher concentrations of capsaicin. Interestingly, the opposite effect occurred in the wild-type cells. Neurotransmitter release requires an increase in $[Ca^{2+}]_i$ as a signal for vesicle fusion with the synaptic membrane. Calcium increase occurs through VSCCs activated by membrane depolarisation. Such channels are not equally distributed but are grouped near release sites and open, forming "microdomains" (Robitaille *et al.*, 1990). The $Ca^{2+}$ thresholds have been reported to reach high levels of 200-300 μM and calcium microdomains have since been implicated in regulating the kinetics of transmitter release (Llinas *et al.*, 1992).

However, a study on the Calyx of Held, a large axon terminal in the vertebrate brainstem, was shown to have a low $Ca^{2+}$ threshold at micromolar concentration for transmitter release. Here, the rate of exocytosis was thought to depend upon $Ca^{2+}$ cooperativity. This activity, first described at the neuromuscular junction, is thought to occur at other action potential synapses where it enhances the on and off regulation of transmission and also renders the synapse highly sensitive to small changes in $Ca^{2+}$ (Bollmann *et al.*, 2000). Nonetheless, it is unknown whether these microdomains participate with TRPV1 to regulate NA release but it is a possibility.

Capsaicin $pEC_{50}$ of 9.21, based on the extrapolated curve for [$^3$H]NA release, is at least a logarithm higher than values found in capsaicin concentration response curves at transfected TRPV1 in other cell-types (Caterina *et al.*, 1997; Jerman *et al.*, 2000; McIntyre *et al.*, 2001; Smart *et al.*, 2001; Sprague *et al.*, 2001). Further analysis of this effect is displayed in Figure 6.7, where changes in $[Ca^{2+}]_i$ were compared with [$^3$H]NA release after stimulation with increasing capsaicin concentrations using clone 7. The graphs were overlaid revealing that a small increase in $[Ca^{2+}]_i$ consequently produced a relatively large increase in [$^3$H]NA release at 10-100 nM capsaicin. This figure also apparently showed release without an elevation of $[Ca^{2+}]_i$ (for example, at 1 nM capsaicin) which maybe explained by local subplasma membrane increases in $Ca^{2+}$. These would not be detected in population-based fluorimetry but would be sufficient to support release as the local increase close to the release vesicles maybe high. In addition, the reason for the decrease in [$^3$H]NA release, from 100 nM capsaicin onwards (depicted by the dashed line), or how this is mediated remains unclear. However, calcium inhibition has been noted in the literature, including that of adenylyl cyclase (Colvin *et al.*, 1991). The reduced release may also result from capsaicin-induced toxicity at higher doses.

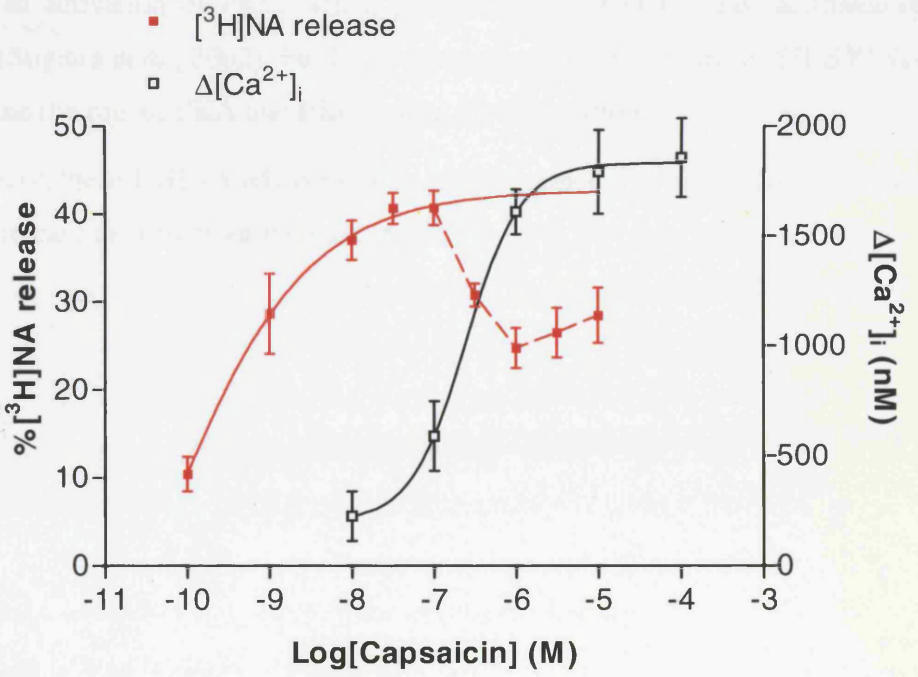


**Figure 6.7 Amplification of $[Ca^{2+}]_i$ by [$^3$H]NA release**
*[$^3$H]NA release data obtained from Figure 6.2 and $[Ca^{2+}]_i$ data from Figure 5.2.*

*Perfusion chamber studies*

$[Ca^{2+}]_i$ and [$^3$H]NA release were simultaneously measured in a perfusion system. The biphasic shape relating to $[Ca^{2+}]_i$ response after capsaicin stimulation matched some of the temporal profiles seen in previous chapters. Following the initial capsaicin application, the $[Ca^{2+}]_i$ response was reduced after a second application of capsaicin. However, this contrasted with [$^3$H]NA release in which no change occurred. In comparison, the control experiments displayed a relatively higher increase in $[Ca^{2+}]_i$ and [$^3$H]NA release during the S2 phase compared to the S1 phase in the previous capsaicin studies for reasons that are unclear. As before, calcium microdomains may have a role to play, as regulated exocytosis of neurotransmitters after activation by G-protein-linked receptors is not fully understood.

*Future studies*

TRPV1 activity is known to be modulated by phosphorylation/dephosphorylation and the receptor has modulatory sites for PKA, PKC and the protein phosphatase 2B (calcineurin) (Kress *et al.*, 1999). Premkumar and Ahern reported the induction of the TRPV1 activity by PKC when expressed in *Xenopus* oocytes (Premkumar *et al.*, 2000). Therefore, the activity of the TRPV1 may be modified by other cellular signal transduction pathways resulting in desensitisation. Bradykinin is also thought to sensitise TRPV1 as they are coupled to activation of PKC, which phosphorylates TRPV1 and facilitates opening of TRPV1 (Sugiura *et al.*, 2002). Further studies should be performed in SH-SY5Y$_{hTRPV1}$ cells to examine the role of PKA and PKC during desensitisation.

In summary, these [$^3$H]NA release studies have revealed that capsaicin stimulation induces [$^3$H]NA release as well as an increase in $[Ca^{2+}]_i$.

# 7 DISCUSSION

Pain is often difficult to treat, especially for neuropathic conditions, despite the large number of treatments and analgesics currently available. One potential therapeutic lead is the vanilloid receptor TRPV1, which is thought to play a role in neuropathic and inflammatory pain. TRPV1 has a complex pharmacology by acting as a polymodal detector of noxious stimuli and is also activated by the endocannabinoid AEA. Despite various studies in animals and investigations of recombinant TRPV1, the pharmacology - particularly the desensitisation process which causes analgesia, is incomplete.

## 7.1 Summary of findings

### *7.1.1 Pharmacological characterisation of rat and human TRPV1 (non-neuronal cells)*

Generally between receptor species and temperatures, there was no difference in capsaicin and AEA potency. The pharmacology of the TRPV1 antagonist capsazepine was not termperature-dependent but capsazepine had a higher $pK_B$ in $HEK293_{hTRPV1}$ cells relative to $HEK293_{rTRPV1}$. The exocannabinoid $\Delta^9$-THC was originally thought to activate TRPV1 but subsequent studies with an ethanol control attributed this effect to ethanol only. Also, ethanol has subsequently been shown to activate TRPV1 (Trevisani *et al.*, 2002).

### *7.1.2 Cloning hTRPV1*

The process of producing a novel stable neuronal model expressing hTRPV1 involved two strategies. Initially $pcDNA3.1/V5/His\text{-}TOPO_{hTRPV1}$ plasmid was chemically transfected into SH-SY5Y cells. However, there were unexpected problems despite the initial co-transfection with GFP which implied that transfection was successful. A different approach involved cloning hTRPV1 DNA and ligating this into another plasmid (pIREShyg2). Transfection was attempted *via* chemical means but the results were unsuccessful. Transfection employing the principle of electroporation, albeit a relatively harsher method, was used to transfer hTRPV1 DNA successfully into the SH-SY5Y cell-line. To date, this is the first neuronal model which expresses recombinant human TRPV1.

### *7.1.3 Pharmacological screening of the neuronal transfect*

Utilising FLIPR technology allowed rapid screening of the cloned hTRPV1 transfect with a number of common agonists including capsaicin and AEA. The rank order of potency from the highest to the lowest was RTX>capsaicin>olvanil>AEA. In general, cannabinoid

agonists were less potent than the archetypal vanilloid agonist capsaicin. By comparison, a smaller number of agonists: capsaicin and AEA, were chosen for fluorimetric cuvette-based experiments at 37°C. Similar to the FLIPR results, capsaicin potency was also higher relative to AEA. In addition, inhibition studies with three antagonists (capsazepine, iodo-RTX and ruthenium red) were undertaken against agonists including capsaicin, AEA, RTX and olvanil. All the antagonists inhibited the responses of each agonist. In summary, for capsaicin, AEA, RTX and olvanil, the affinity of IRTX was greater relative to that of capsazepine. Capsazepine was employed in determining inhibition effects against capsaicin and AEA at 22°C and 37°C in cuvette-based studies. Capsazepine did not produce a temperature-dependent effect which matched earlier data in HEK293 cells.

### *7.1.4 Neurotransmitter release studies*

These investigations have demonstrated that TRPV1, a ligand gated ion channel permeable to $Ca^{2+}$, produced a simultaneous increase in [$^3$H]NA release and $[Ca^{2+}]_i$ after stimulating the transfected cells with capsaicin. Initially, static monolayer cultures were used to establish a capsaicin concentration response curve for [$^3$H]NA release. Novel perfusion chamber studies successfully measured $[Ca^{2+}]_i$ and [$^3$H]NA release simultaneously. An illustration summarising NA release is displayed in Figure 7.1.

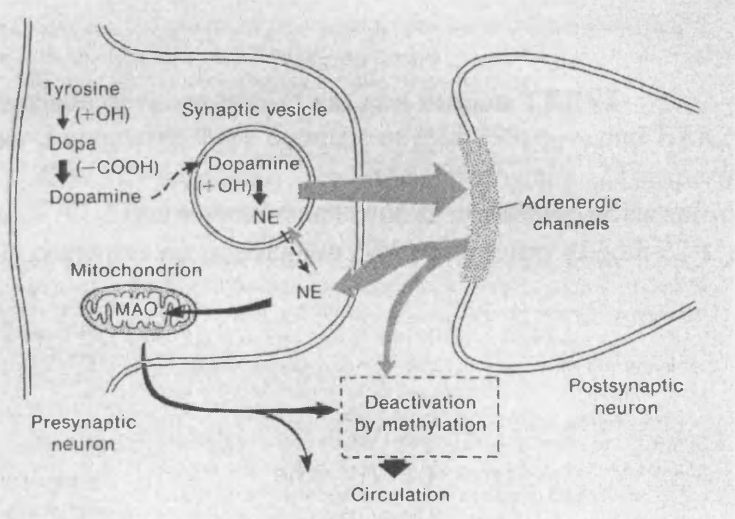


**Figure 7.1 NA release**
*NE (norepinephrine or NA) is released at adrenergic channels. Following release, some NA is taken back up into the presynaptic terminal and some is deactivated by methylation and carried away in the blood. Cytoplasmic NA is either taken up into a synaptic vesicle or degraded by monoamine oxidase (MAO). Figure from Eckert and co-authors (Eckert et al., 1988).*

## 7.2 Comparision of rat and human TRPV1

In $HEK293_{rTRPV1}$ and $HEK293_{hTRPV1}$ cells, there were no significant species differences in potency at both 22°C and 37°C (Figure 7.2, Table 7.1). Agonist activity at rTRPV1 displayed the same rank order as hTRPV1: capsaicin>olvanil>AEA.

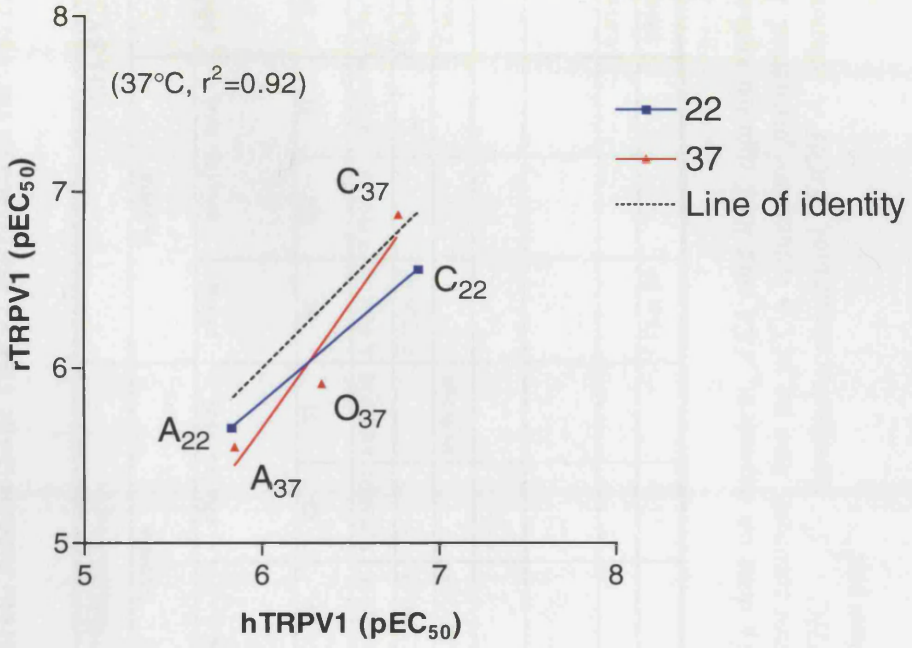


**Figure 7.2 Comparison of recombinant rat and human TRPV1**
*Data from Chapter 3 compares three agonists in $HEK293_{hTRPV1}$ and $HEK293_{rTRPV1}$ cells at 22℃ and 37℃. Key: C=capsaicin; A=AEA; O=olvanil; 22=experiment at 22℃; 37=experiment at 37℃. Experimental temperatures are displayed as subscript characters. The line of identity compares rat and human TRPV1 isoforms at both 22℃ and 37℃.*

**Table 7.1 Summary of pharmacological data obtained from recombinant TRPV1 expressed in various cell-types**

| | $HEK293_{hTRPV1}$ | | | | | $HEK293_{rTRPV1}$ | | | | $SH\text{-}SY5Y_{hTRPV1}$ | | | | | | |
|---|---|---|---|---|---|---|---|---|---|---|---|---|---|---|---|---|
| | Cuvette | | | | $CB_1$ $GTP\gamma[^{35}S]$ | Cuvette | | | | Cuvette | | | FLIPR | | | |
| | $pEC_{50}$ | | $pK_B$ (vs. cpz) | | $pEC_{50}$ | $pEC_{50}$ | | $pK_B$ (vs. cpz) | | $pEC_{50}$ | $pK_B$ (vs. cpz) | | $pEC_{50}$ | $pK_B$ (vs. cpz) | $pK_B$ (vs. I-RTX | $pK_B$ (vs. RR) |
| Temp (°C) | 22 | 37 | 22 | 37 | | 22 | 37 | 22 | 37 | 37 | 22 | 37 | 25 | 25 | 25 | 25 |
| Cap | 6.88±0.05 | 6.77±0.11 | 6.76±0.25 | 6.75±0.04 | None | 6.56±0.11 | 6.87±0.08 | 5.98±0.09 | 6.02±0.10 | 6.63±0.14 | 7.43±0.10 | 7.44±0.07 | 8.54±0.06 | 7.12±0.02 | 8.66±0.05 | 7.08±0.13 |
| AEA | 5.82±0.08 | 5.84±0.09 | inhibition | inhibition | 5.79±0.09 | 5.66±0.04 | 5.55±0.05 | | | 6.13±0.10 | | | 5.34±0.02 | 7.32±0.03 | 8.95±0.04 | 7.71±0.11 |
| Olv | | 6.33±0.22 | | inhibition | None | | 5.91±0.10 | | inhibition | | | | 7.46±0.11 | 7.05±0.03 | 8.53±0.01 | 7.19±0.04 |
| $\Delta^9$-THC | | | | | 7.10±0.13 | | | | | | | | | | | |
| EtOH | Did not saturate | Did not saturate | | | | | | | | | | | | | | |
| RTX | | | | | | | | | | | | | 9.03±0.10 | 6.45±0.04 | 7.98±0.03 | 7.22±0.04 |
| CC | | | | | | | | | | 5.92±0.29 | | | 5.83±0.02 | | | |

*Data are presented as mean±SEM except for FLIPR $pK_B$ data on capsaicin, AEA and RTX against ruthenium red. The concentration response curves for compounds AM404 and NADA did not saturate, thus no $pEC_{50}$ values are presented. Key: Cap – capsaicin, Olv – olvanil, Cpz – capsazepine, AEA – anandamide, $\Delta^9$-THC - $\Delta^9$- tetrahydrocannabinol, EtOH – ethanol, CC – carbachol, RTX – resiniferatoxin, I-RTX – iodo-resiniferatoxin, RR – ruthenium red*

## 7.3 The TRPV family

TRP channels are a superfamily of ion channels that function in sensory transduction cascades in both vertebrates and invertebrates. An extensive body of research has consequently revealed five additional members comprising the TRPV family since the cloning of TRPV1. Reports have suggested that the functions of TRPV ion channels are multiple including thermosensation, osmoregulation and nociception.

### *7.3.1 The bigger picture: the $CB_1$ and TRPV1 link*

Speculation exists over whether AEA or other similar unidentified lipid compounds are endogenous ligands at TRPV1. An illustration summarising TRPV1 and $CB_1$ interactions is displayed in Figure 7.3. It has been clearly demonstrated that AEA is active at both TRPV1 and $CB_1$. It has been known for some time that TRPV1 receptors mediate vasodilation in arterial vessels in response to AEA (Zygmunt *et al.*, 1999).

The endocannabinoid AEA has been proposed as the "endovanilloid", a description attributed by agonist properties at TRPV1 as well as $CB_1$. AEA behaved as a full agonist relative to capsaicin at hTRPV1 expressed in HEK293 cells. In contrast, AEA acted as a partial agonist relative to capsaicin at rat hTRPV1. In the literature, differences in the efficacy of AEA have been reported, thus resulting in conflicting arguments on whether AEA is the endogenous ligand at hTRPV1.

Recently, the compound NADA, found endogenously in human nervous tissue, has been hypothesised to be the endogenous ligand at TRPV1. However, the FLIPR data on NADA revealed TRPV1 agonist activity but the compound did not appear to be as potent in comparison to capsaicin.

In summary, capsaicin activates TRPV1, $\Delta^9$-THC activates $CB_1$ and AEA activates both receptors. It is therefore tempting to suggest that $CB_1$ and TRPV1 maybe respectively metabotropic and ionotropic members of a superfamily of receptors.

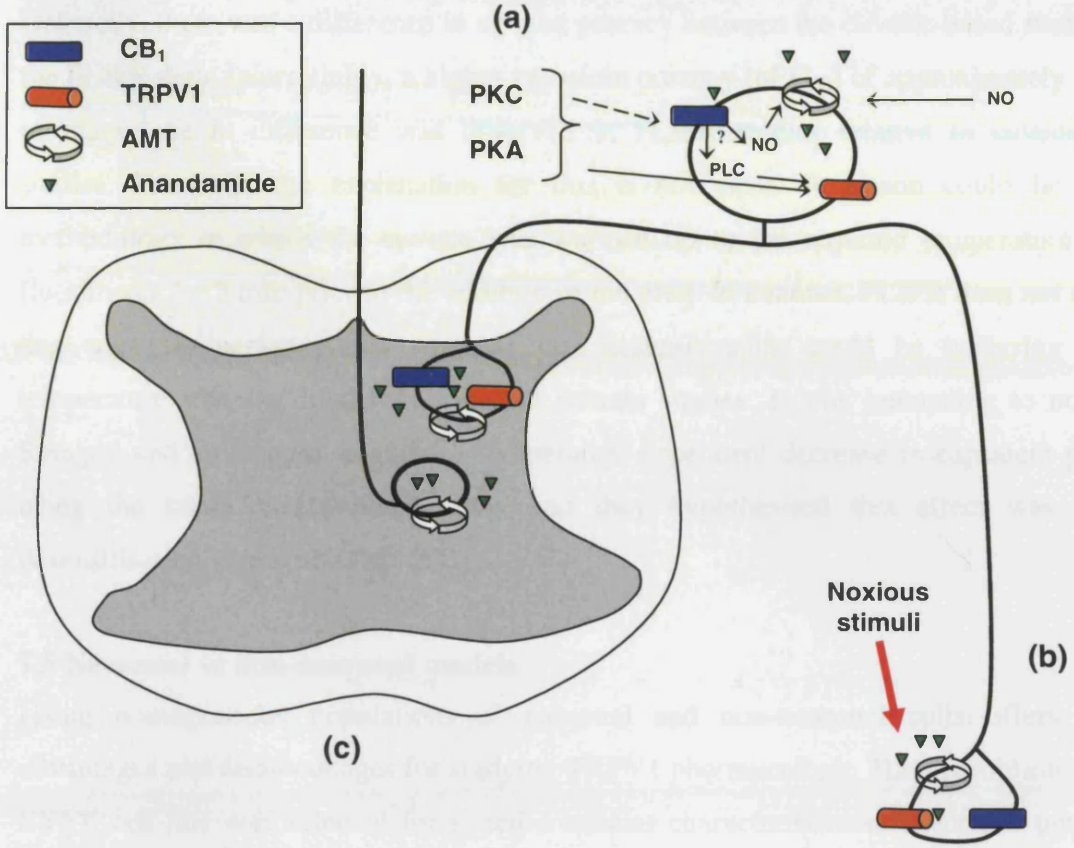


**Figure 7.3 Simplified scheme of vanilloid (TRPV1) and cannabinoid ($CB_1$) receptor interactions in nociception control**
*(a)TRPV1 expression in bipolar DRG neurones.*
*(b)The peripheral fibre of these neurones collects nociceptive information.*
*(c)The central fibre of these neurones transmits to the dorsal horn of the spinal cord.*

*TRPV1 is expressed along the entire length of these neurones. TRPV1 integrates the effects of noxious heat, protons, AEA and other fatty acid metabolites produced by inflammatory cells. The majority of TRPV1-expressing DRG neurones express $CB_1$. AEA mediates opposing effects; TRPV1 (excitation), $CB_1$ (inhibition). TRPV1 and $CB_1$ represent ionotrophic and metabotropic receptors respectively and it is likely that they represent subgroups of an unknown superfamily. The AEA binding site is thought to be intracellular for TRPV1 but extracellular for $CB_1$. Hence, the AMT (AEA membrane transporter) must determine the net effect of AEA on DRG neurones. If AEA is stimulated by NO, AEA will be transported intracellularly and neuronal excitation via TRPV1 will dominate. In comparison, if AEA is produced by other non-TRPV1-expressing neurones or inflammatory cells, neuroinhibition via $CB_1$ is expected to occur. TRPV1 and $CB_1$ receptors that are co-expressed may interact during intracellular signal transduction. For example, stimulation of $CB_1$ could result in the release of TRPV1 under the inhibitory control of phosphotidylinositol 4,5-bisphosphate ($PIP_2$) via PLC-mediated hydrolysis of $PIP_2$. (Solid lines – activation, broken lines – inhibition). Figure adapted from a publication by Di Marzo and colleagues (Di Marzo et al., 2002).*

## 7.4 Differences in results from cuvette-based studies and FLIPR

Generally, there was a difference in agonist potency between the cuvette-based studies and the FLIPR data. Interestingly, a higher capsaicin potency ($pEC_{50}$) of approximately 1 order of magnitude in difference was observed in FLIPR studies relative to cuvette-based studies. However, the explanation for this is not clear. A reason could lie in the methodology in which the cuvette was warmed up to the required temperature in the fluorimeter for 3 min prior to the addition of the drug. In contrast, FLIPR does not involve this warm-up period which suggests that desensitisation could be occurring during temperature ramping in the fluorimetric cuvette studies. It was interesting to note that Sprague and colleagues reported a temperature-dependent decrease in capsaicin potency using the same cuvette-based assay and they hypothesised this effect was due to desensitisation (Sprague *et al.*, 2001).

## 7.5 Neuronal vs non-neuronal models

Using homogeneous populations of neuronal and non-neuronal cells offers several advantages and disadvantages for studying TRPV1 pharmacology. The neuroblastoma SH-SY5Y cell-line was selected for specific cellular characteristics as described previously (Vaughan *et al.*, 1995) and is physiologically more relevant for study as TRPV1 is expressed in DRG. In particular, SH-SY5Y cells are capable of uptake and release of NA, which is advantageous for future studies on desensitisation. The disadvantage encountered was the difficulty in transfecting human TRPV1 into a neuronal cell-line although this was eventually resolved.

In addition, SH-SY5Y$_{hTRPV1}$ cells compare favourably in comparison to other non-neuronal models expressing recombinant hTRPV1. The potency ($pEC_{50}$) values of common TRPV1 agonists from the FLIPR studies were compared to published FLIPR results from non-neuronal models (Figure 7.4). The SH-SY5Y$_{hTRPV1}$ cells displayed similar agonist potencies to other models including HEK293$_{hTRPV1}$ and HEK293$_{rTRPV1}$ (Jerman *et al.*, 2002; Smart *et al.*, 2001). This comparison is encouraging in supporting SH-SY5Y$_{hTRPV1}$ cells as a suitable, comparable model for further study of TRPV1.

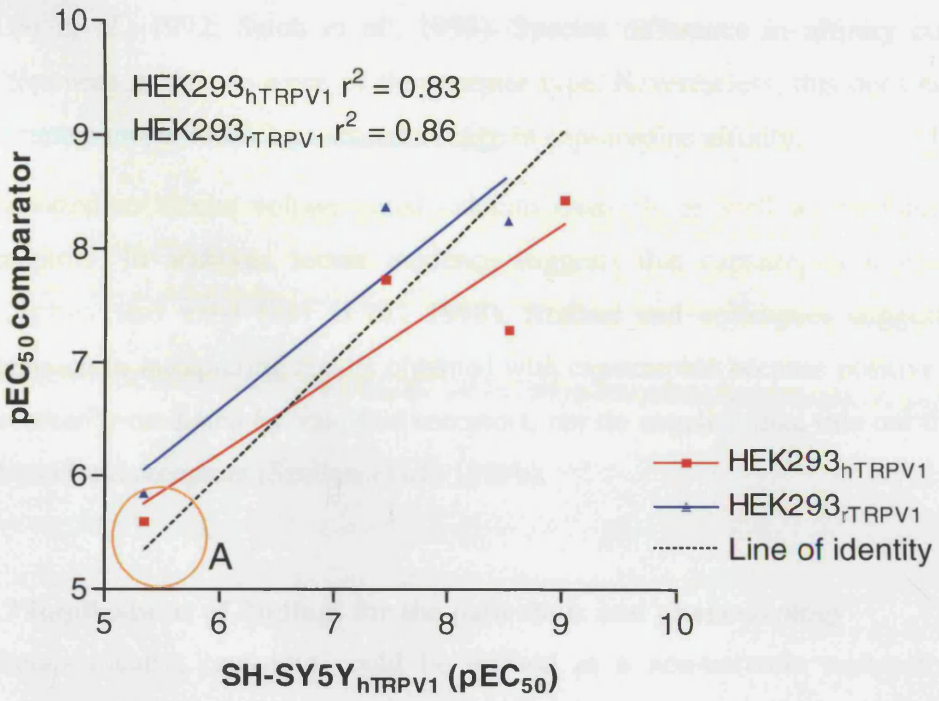


**Figure 7.4 Comparison of SH-SY5Y$_{hTRPV1}$ cells with other recombinant TRPV1 models**

*Data was from FLIPR experiments (Chapter 5) and from published FLIPR data in HEK293$_{hTRPV1}$ and HEK293$_{rTRPV1}$ cells (Jerman et al., 2002; Smart et al., 2001). The SH-SY5Y$_{hTRPV1}$ cells displayed similar correlation with HEK293$_{rTRPV1}$ cells in terms of potency. There were differences in comparison with HEK293$_{hTRPV1}$ cells with some of the agonists including capsaicin and olvanil in which the rank order of potency varied. In all the models, AEA had the lowest relative potency (A on the graph) and RTX produced the highest potency in both SH-SY5Y$_{hTRPV1}$ and HEK293$_{hTRPV1}$ cells.*

## 7.6 Further comments on antagonists

Capsazepine, a non-selective antagonist, acts with moderate potency at TRPV1 produced a highly variable range in capsazepine affinities versus capsaicin. Affinity values for this antagonist have proved highly inconsistent, this varied from 5.12 in guinea-pig bronchi (sensory neurones) (Ellis *et al.*, 1994) to 7.52 in HEK293$_{rTRPV1}$ (Jerman *et al.*, 2000). Some of the differences in capsazepine affinity could be due to species selectivity as observed in the experiments where there was a six-fold higher affinity in human than in rat TRPV1 cells. An identical result was also reported in recombinant TRPV1 expressed in CHO cells (McIntyre *et al.*, 2001). Interestingly, factors including pH and temperature affect capsazepine affinity in that this antagonist is unable to inhibit low pH-evoked

depolarisation in rat DRG neurones (Habelt *et al.*, 2000) but did so in guinea pig airways (Lou *et al.*, 1992; Satoh *et al.*, 1993). Species difference in affinity could be due to differences in the sequence of the receptor type. Nevertheless, this does not explain why recombinant rat TRPV1 produced a range in capsazepine affinity.

Capsazepine blocks voltage-gated calcium channels as well as nicotinic acetylcholine receptors. In addition, recent evidence suggests that capsazepine-insensitive vanilloid receptors also exist (Liu *et al.*, 1998). Szallasi and colleagues suggested a cautious approach to interpreting results obtained with capsazepine because positive effects are not necessarily mediated by vanilloid receptors, nor do negative data rule out the involvement of vanilloid receptors (Szallasi *et al.*, 1999b).

## 7.7 Implications of findings for the pain clinic and pharmacology

Therapeutically, capsaicin could be utilised as a non-narcotic analgesic, especially in neuropathic pain syndromes and cancer pain. However, capsaicin use is limited for reasons described in the introduction and are briefly summarised:

1. Capsaicin irritancy from topical application limits sufficient dose for desensitisation.
2. Extrapolation of data from animal to human should be approached with caution as capsaicin-sensitive neurones mediate different biological responses in humans and animals.

Currently, capsaicin solutions and creams can be applied topically for a variety of human pain disorders and are beneficial. Their rationale is based on the principle of desensitisation caused by repeated application of capsaicin. The efficacy of capsaicin in treating pain seems to be related to its ability to deplete substance P from local sensory terminals. Minimal systemic absorption occurs after topical application (single or repeated) of effective local concentrations of the drug and no permanent damage to tissues is known to occur in the adult. Diseases treated include non-allergic (vasomotor) rhinitis, urinary bladder hyperreflexia and notalgia paresthetica (Szallasi *et al.*, 1999b).

## 7.8 Desensitisation, design and synthesis of new vanilloid ligands and antagonists

Vanilloids, with a greater potency than capsaicin, could benefit conditions including neuropathic pain in diabetes, postherpetic neuralgia, chronic distal painful polyneurothapy, post-mastectomy pain syndrome, Guillain-Barré syndrome, reflex sympathetic dystrophy and vulvar vestibulitis. The ultrapotent capsaicin analog RTX is undergoing clinical trials and holds several advantages over capsaicin. However, as RTX activates PKC and is structurally similar to phorbol esters, well-known tumour promotors, there is an increased risk of developing cancer with the use of RTX.

Vanilloid-like and vanilloid/cannabinoid hybrid compounds have been chemically synthesised in anticipation that new capsaicin-like substances can activate TRPV1 without the burning side-effect. Capsazepine is the only vanilloid antagonist to have been studied extensively. Besides desensitisation, it has been hypothesised that vanilloid-specific antagonists could also be used therapeutically in the pain clinic. Consequently, antagonists, including iodo-RTX, KJM429 and JYL1421, have been designed to display a higher affinity relative to capsazepine (Wahl *et al.*, 2001; Wang *et al.*, 2002).

Previous studies have shown that capsazepine is unable to reverse the hyperalgesia associated with inflammatory and neuropathic pain models in the rat, whereas strong activity has been demonstrated using similar models in the guinea pig (Walker *et al.*, 2003). These results correlate with the finding that capsazepine is able to block acid-induced activation of guinea pig TRPV1 *in vitro* (Fox *et al.*, 1995; Lou *et al.*, 1992; Satoh *et al.*, 1993; Savidge *et al.*, 2002), a property shared with human TRPV1 but absent from rat TRPV1 (McIntyre *et al.*, 2001). Together, these data raise the possibility that blockade of TRPV1 responses activated by low pH, or dual blockade of capsaicin site and pH site-mediated responses, may be important for antihyperalgesic efficacy *in vivo* (Valenzano *et al.*, 2003).

## 7.9 Future investigations

As capsaicin can evoke NA release in SH-SY5Y$_{hTRPV1}$ cells, it could be hypothesised that AEA may also act to stimulate neurotransmitter release. In addition, the antagonistic effect of capsazepine on NA release can be investigated and confirm that this effect is TRPV1-related. However, as AEA is a highly lipophilic compound, it may be technically difficult to evoke release at a high enough concentration.

There are few studies on the desensitisation of vanilloid responses and this is clearly of great importance. Studies of this nature are complex as TRPV1 responds by increasing $Ca^{2+}$ to pH, temperature and AEA. TRPV1 activity is known to be modulated by phosphorylation/dephosphorylation and the receptor has modulatory sites for protein kinase A, protein kinase C and the protein phosphatase 2B (calcineurin) (Kress *et al.*, 1999). Premkumar and Ahern reported the induction of the TRPV1 activity by PKC when expressed in *Xenopus* oocytes (Premkumar *et al.*, 2000). Therefore, other cellular signal transduction pathways resulting in desensitisation may modify the activity of TRPV1.

Examination of the desensitisation profile of human TRPV1 is warranted to elucidate the mechanism involved using the novel perfusion system. SH-SY5Y$_{hTRPV1}$ desensitisation can be initiated by capsaicin pre-treatment with subsequent challenge with capsaicin and a concentration response curve constructed. TRPV1 activation can be confirmed with capsazepine.

Prolonged activation of TRPV1 in mammalian expression systems leads to cell death. The mechanism of TRPV1-mediated toxicity may have relevance to pathophysiological processes that can occur in neurones. Thus, capsaicin neurotoxicity is another facet which could be explored using the neuronal transfects.

### 7.10 Contributions of findings to further the elucidation of pain

In conclusion, TRPV1 is a molecular integrator of painful stimuli and plays a role in inflammation and nociception, especially neuropathic pain. This thesis has contributed to and expanded recombinant TRPV1 pharmacology by utilising different species and models. This project describes the first neuronal model to express recombinant human TRPV1 and will be a valuable research tool in unravelling the TRPV1 desensitisation process. Using this model may possibly gain new insights into this interesting receptor, contributing to the future development of novel, non-narcotic analgesics.

# 8 APPENDICES

## 8.1 Amino acids and their abbreviations

A = alanine

C = cysteine

D = aspartate

E = glutamate

F = phenylalanine

G = glycine

H = histidine

I = isoleucine

K = lysine

L = leucine

M = methionine

N = asparagine

P = proline

Q = glutamine

R = arginine

S = serine

T = threonine

V = valine

W = tryptophan

Y = tyrosine

## 8.2 Publications arising from this thesis

### *8.2.1 Papers*

- Lam PMW, Hainsworth AH & Lambert DG. Pharmacological characterisation of human TRPV1 expressed in SH-SY5Y human neuroblastoma cells
  *Manuscript in preparation for the Journal of Biological Chemistry*
- Lam PMW, McDonald J & Lambert DG. Characterization and comparison of recombinant human and rat TRPV1 receptors: effects of exo- and endocannabinoids *Br J Anaesth* 2005; **94**, 649-56

### *8.2.2 Abstracts*

- Ahmad F, Lam PMW, Smart D, Lambert DG. Comparisons of the effects of olvanil and capsaicin at recombinant rat and human vanilloid (TRPV1) receptors. *Br J Anaesth* 2004; **93**, 168P
- Lam PMW, Smart D, Lambert DG. Differences in the affinity of capsazepine at recombinant rat and human VR1 receptors. *Br J Pharmacol* 2003; **138**, 220P
- Lam PMW, Smart D, Lambert DG. Anandamide but not $\Delta^9$-tetrahydrocannabinol activates recombinant human vanilloid receptors. *Br J Anaesth* 2003; **90**, 418P

### *8.2.3 Conference presentations*

- **Anaesthetic Research Society Meeting, Aberdeen, UK (Apr 2004)**: "Comparisons of the effects of olvanil and capsaicin at recombinant rat and human vanilloid (TRPV1) receptors". *Talk.*
- **British Pharmacological Society Meeting, Brighton, UK (Jan 2003)**: "Differences in the affinity of capsazepine at recombinant rat and human VR1 receptors". *Poster.*
- **Leicestershire UHL Research Prize Day, Leicester, UK (Sep 2003)**: "Effects of the endocannabinoid, anandamide and the exocannabinoid, $\Delta^9$-tetrahydrocannabinol at VR1-vanilloid and $CB_1$ receptors". *Poster.*
- **Anaesthetic Research Society Meeting, London, UK (Dec 2002)**: "Anandamide but not $\Delta^9$-tetrahydrocannabinol activates recombinant human vanilloid receptors". *Talk.*

# 9 REFERENCES


ACS, G., BIRO, T., ACS, P., MODARRES, S. & BLUMBERG, P.M. (1997). Differential activation and desensitization of sensory neurons by resiniferatoxin. *J Neurosci*, 17, 5622-8.

ACS, G., LEE, J., MARQUEZ, V.E. & BLUMBERG, P.M. (1996). Distinct structure-activity relations for stimulation of 45Ca uptake and for high affinity binding in cultured rat dorsal root ganglion neurons and dorsal root ganglion membranes. *Brain Res Mol Brain Res*, 35, 173-82.

ACS, G., PALKOVITS, M. & BLUMBERG, P.M. (1994). [3H]resiniferatoxin binding by the human vanilloid (capsaicin) receptor. *Brain Res Mol Brain Res*, 23, 185-90.

ADRIAN, E.D. (1931). The messages in sensory nerve fibres and their interpretation. *Proceedings of the Royal Society Series B*, 109, 1-18.

ALBERTS, B., BRAY, D., LEWIS, J., RAFF, M., ROBERTS, K. & WATSON, J.D. (1994). *Molecular biology of the cell.* New York: Garland Publishing.

AMANN, R. & MAGGI, C.A. (1991). Ruthenium red as a capsaicin antagonist. *Life Sci*, 49, 849-56.

APPENDINO, G., CRAVOTTO, G., PALMISANO, G., ANNUNZIATA, R. & SZALLASI, A. (1996). Synthesis and evaluation of phorboid 20-homovanillates: discovery of a class of ligands binding to the vanilloid (capsaicin) receptor with different degrees of cooperativity. *J Med Chem*, 39, 3123-31.

ARUNLAKSHANA, O. & SCHILD, H.O. (1959). Some quantitative uses of drug antagonists. *Br J Pharmacol Chemother*, 14, 48-58.

AUGUSTINE, G.J., BURNS, M.E., DEBELLO, W.M., HILFIKER, S., MORGAN, J.R., SCHWEIZER, F.E., TOKUMARU, H. & UMAYAHARA, K. (1999). Proteins involved in synaptic vesicle trafficking. *J Physiol*, 520 Pt 1, 33-41.

BALDWIN, J.M. (1994). Structure and function of receptors coupled to G proteins. *Curr Opin Cell Biol*, 6, 180-90.

BANDELL, M., STORY, G.M., HWANG, S.W., VISWANATH, V., EID, S.R., PETRUS, M.J., EARLEY, T.J. & PATAPOUTIAN, A. (2004). Noxious cold ion channel TRPA1 is activated by pungent compounds and bradykinin. *Neuron*, 41, 849-57.

BAUMANN, T.K. & MARTENSON, M.E. (2000). Extracellular protons both increase the activity and reduce the conductance of capsaicin- gated channels. *J Neurosci*, 20, 80.

BEAR, M.F., CONNERS, B.W. & PARADISO, M.A. (2001). *Neuroscience: Exploring the brain.* Baltimore: Lippincott Williams & Wilkins.

BELTRAMO, M. & PIOMELLI, D. (1999). Anandamide transport inhibition by the vanilloid agonist olvanil. *Eur J Pharmacol*, 364, 75-8.

BELVISI, M.G., MIURA, M., STRETTON, D. & BARNES, P.J. (1992). Capsazepine as a selective antagonist of capsaicin-induced activation of C-fibres in guinea-pig bronchi. *Eur J Pharmacol*, 215, 341-4.

BERGER, H., CALO, G., ALBRECHT, E., GUERRINI, R. & BIENERT, M. (2000). [Nphe(1)]NC(1-13)NH(2) selectively antagonizes nociceptin/orphanin FQ-stimulated G-protein activation in rat brain. *J Pharmacol Exp Ther*, 294, 428-33.

BERNSTEIN, J.E., KORMAN, N.J., BICKERS, D.R., DAHL, M.V. & MILLIKAN, L.E. (1989). Topical capsaicin treatment of chronic postherpetic neuralgia. *J Am Acad Dermatol*, 21, 265-70.

BESSOU, P. & PERL, E.R. (1969). Response of cutaneous sensory units with unmyelinated fibers to noxious stimuli. *J Neurophysiol*, 32, 1025-43.

BEVAN, S. & GEPPETTI, P. (1994). Protons: small stimulants of capsaicin-sensitive sensory nerves. *Trends Neurosci*, 17, 509-12.

BEVAN, S., HOTHI, S., HUGHES, G., JAMES, I.F., RANG, H.P., SHAH, K., WALPOLE, C.S. & YEATS, J.C. (1992). Capsazepine: a competitive antagonist of the sensory neurone excitant capsaicin. *Br J Pharmacol*, 107, 544-52.

BOLLMANN, J.H., SAKMANN, B. & BORST, J.G. (2000). Calcium sensitivity of glutamate release in a calyx-type terminal. *Science*, 289, 953-7.

BONICA, J. (1990). *The Management of Pain*. Philadephia: Lea & Febiger.

BURGESS, P.R. & PERL, E.R. (1967). Myelinated afferent fibres responding specifically to noxious stimulation of the skin. *J Physiol*, 190, 541-62.

CABRAL, G.A., HARMON, K.N. & CARLISLE, S.J. (2001). Cannabinoid-mediated inhibition of inducible nitric oxide production by rat microglial cells: evidence for CB1 receptor participation. *Adv Exp Med Biol*, 493, 207-14.

CALIGNANO, A., LA RANA, G., GIUFFRIDA, A. & PIOMELLI, D. (1998). Control of pain initiation by endogenous cannabinoids. *Nature*, 394, 277-81.

CAMPERO, M., SERRA, J. & OCHOA, J.L. (1996). C-polymodal nociceptors activated by noxious low temperature in human skin. *J Physiol*, 497 (Pt 2), 565-72.

CATERINA, M.J. & JULIUS, D. (2001). The vanilloid receptor: a molecular gateway to the pain pathway. *Annu Rev Neurosci*, 24, 487-517.

CATERINA, M.J., LEFFLER, A., MALMBERG, A.B., MARTIN, W.J., TRAFTON, J., PETERSEN-ZEITZ, K.R., KOLTZENBURG, M., BASBAUM, A.I. & JULIUS, D. (2000). Impaired nociception and pain sensation in mice lacking the capsaicin receptor. *Science*, 288, 306-13.

CATERINA, M.J., ROSEN, T.A., TOMINAGA, M., BRAKE, A.J. & JULIUS, D. (1999). A capsaicin-receptor homologue with a high threshold for noxious heat. *Nature*, 398, 436-41.

CATERINA, M.J., SCHUMACHER, M.A., TOMINAGA, M., ROSEN, T.A., LEVINE, J.D. & JULIUS, D. (1997). The capsaicin receptor: a heat-activated ion channel in the pain pathway. *Nature*, 389, 816-24.

CATTERALL, W.A., GOLDIN, A.L. & WAXMAN, S.G. (2003a). International Union of Pharmacology. XXXIX. Compendium of voltage-gated ion channels: sodium channels. *Pharmacol Rev*, 55, 575-8.

CATTERALL, W.A., STRIESSNIG, J., SNUTCH, T.P. & PEREZ-REYES, E. (2003b). International Union of Pharmacology. XL. Compendium of voltage-gated ion channels: calcium channels. *Pharmacol Rev*, 55, 579-81.

CESARE, P. & MCNAUGHTON, P. (1996). A novel heat-activated current in nociceptive neurons and its sensitization by bradykinin. *Proc Natl Acad Sci USA*, 93, 15435-9.

CHAD, D.A., ARONIN, N., LUNDSTROM, R., MCKEON, P., ROSS, D., MOLITCH, M., SCHIPPER, H.M., STALL, G., DYESS, E. & TARSY, D. (1990). Does capsaicin relieve the pain of diabetic neuropathy? *Pain*, 42, 387-8.

CHALFIE, M., TU, Y., EUSKIRCHEN, G., WARD, W.W. & PRASHER, D.C. (1994). Green fluorescent protein as a marker for gene expression. *Science*, 263, 802-5.

CHEN, C.C., ENGLAND, S., AKOPIAN, A.N. & WOOD, J.N. (1998). A sensory neuron-specific, proton-gated ion channel. *Proc Natl Acad Sci USA*, 95, 10240-5.

CHENG, Y. & PRUSOFF, W.H. (1973). Relationship between the inhibition constant (K1) and the concentration of inhibitor which causes 50 per cent inhibition (I50) of an enzymatic reaction. *Biochem Pharmacol*, 22, 3099-108.

CHYB, S., RAGHU, P. & HARDIE, R.C. (1999). Polyunsaturated fatty acids activate the Drosophila light-sensitive channels TRP and TRPL. *Nature*, 397, 255-9.

CLAPHAM, D.E., MONTELL, C., SCHULTZ, G. & JULIUS, D. (2003). International Union of Pharmacology. XLIII. Compendium of voltage-gated ion channels: transient receptor potential channels. *Pharmacol Rev*, 55, 591-6.

CLAPHAM, D.E., RUNNELS, L.W. & STRUBING, C. (2001). The TRP ion channel family. *Nat Rev Neurosci*, 2, 387-96.

COLQUHOUN, D. (1998). Binding, gating, affinity and efficacy: the interpretation of structure-activity relationships for agonists and of the effects of mutating receptors. *Br J Pharmacol*, 125, 924-47.

COLVIN, R.A., OIBO, J.A. & ALLEN, R.A. (1991). Calcium inhibition of cardiac adenylyl cyclase. Evidence for two distinct sites of inhibition. *Cell Calcium*, 12, 19-27.

CORTRIGHT, D.N., CRANDALL, M., SANCHEZ, J.F., ZOU, T., KRAUSE, J.E. & WHITE, G. (2001). The tissue distribution and functional characterization of human VR1. *Biochem Biophys Res Commun*, 281, 1183-9.

CORTRIGHT, D.N. & SZALLASI, A. (2004). Biochemical pharmacology of the vanilloid receptor TRPV1. An update. *Eur J Biochem*, 271, 1814-9.

CRAIG, K.D. (1994). Emotional aspects of pain. In *Textbook of Pain*. eds Wall, P.D. & Melzack, R. pp. 261-274. Edinburgh: Churchill Livingstone.

CUBITT, A.B., HEIM, R., ADAMS, S.R., BOYD, A.E., GROSS, L.A. & TSIEN, R.Y. (1995). Understanding, improving and using green fluorescent proteins. *Trends Biochem Sci*, 20, 448-55.

DASGUPTA, P. & FOWLER, C.J. (1997). Chillies: from antiquity to urology. *Br J Urol*, 80, 845-52.

DAVIS, J.B., GRAY, J., GUNTHORPE, M.J., HATCHER, J.P., DAVEY, P.T., OVEREND, P., HARRIES, M.H., LATCHAM, J., CLAPHAM, C., ATKINSON, K., HUGHES, S.A., RANCE, K., GRAU, E., HARPER, A.J., PUGH, P.L., ROGERS, D.C., BINGHAM, S., RANDALL, A. & SHEARDOWN, S.A. (2000). Vanilloid receptor-1 is essential for inflammatory thermal hyperalgesia. *Nature*, 405, 183-7.

DE PETROCELLIS, L., BISOGNO, T., MACCARRONE, M., DAVIS, J.B., FINAZZI-AGRO, A. & DI MARZO, V. (2001). The activity of anandamide at vanilloid VR1 receptors requires facilitated transport across the cell membrane and is limited by intracellular metabolism. *J Biol Chem*, 276, 12856-63.

DI MARZO, V., BISOGNO, T. & DE PETROCELLIS, L. (2001). Anandamide: some like it hot. *Trends Pharmacol Sci*, 22, 346-9.

DI MARZO, V., BISOGNO, T., MELCK, D., ROSS, R., BROCKIE, H., STEVENSON, L., PERTWEE, R. & DE PETROCELLIS, L. (1998). Interactions between synthetic vanilloids and the endogenous cannabinoid system. *FEBS Lett*, 436, 449-54.

DI MARZO, V., BLUMBERG, P.M. & SZALLASI, A. (2002). Endovanilloid signaling in pain. *Curr Opin Neurobiol*, 12, 372-9.

DI MARZO, V., BREIVOGEL, C.S., TAO, Q., BRIDGEN, D.T., RAZDAN, R.K., ZIMMER, A.M., ZIMMER, A. & MARTIN, B.R. (2000). Levels, metabolism, and pharmacological activity of anandamide in CB(1) cannabinoid receptor knockout mice: evidence for non-CB(1), non-CB(2) receptor-mediated actions of anandamide in mouse brain. *J Neurochem*, 75, 2434-44.

DICKENSON, A.H. (2002). Gate control theory of pain stands the test of time. *Br J Anaesth*, 88, 755-7.

DOCHERTY, R.J., YEATS, J.C. & PIPER, A.S. (1997). Capsazepine block of voltage-activated calcium channels in adult rat dorsal root ganglion neurones in culture. *Br J Pharmacol*, 121, 1461-7.

DRUMMOND, P.D. (1995). Noradrenaline increases hyperalgesia to heat in skin sensitized by capsaicin. *Pain*, 60, 311-5.

ECKERT, R., RANDALL, A. & AUGUSTINE, G. (1988). *Animal physiology*. New York: Freeman.

ELLIS, J.L. & UNDEM, B.J. (1994). Inhibition by capsazepine of resiniferatoxin- and capsaicin-induced contractions of guinea pig trachea. *J Pharmacol Exp Ther*, 268, 85-9.

ERLANGER, J. & GASSER, H.S. (1937). In *Electrical signs of nervous activity*. Philadelphia: University of Pennsylvania Press.

FIELDS, H.L. & BASBAUM, A.I. (1994). Central nervous system mechanisms of pain modulation. In *Textbook of pain*. eds Wall, P.D. & Melzack, R. pp. 243-257. Edinburgh: Churchill Livingstone.

FINE, P.G. & ASHBURN, M.A. (1998). Functional neuroanatomy and nociception. In *The management of pain*. eds Ashburn, M.A. & Rice, L.J. pp. 1-16. New York: Churchill Livingstone.

FOX, A.J., URBAN, L., BARNES, P.J. & DRAY, A. (1995). Effects of capsazepine against capsaicin- and proton-evoked excitation of single airway C-fibres and vagus nerve from the guinea-pig. *Neuroscience*, 67, 741-52.

GEHL, J. (2003). Electroporation: theory and methods, perspectives for drug delivery, gene therapy and research. *Acta Physiol Scand*, 177, 437-47.

GLINSUKON, T., STITMUNNAITHUM, V., TOSKULKAO, C., BURANAWUTI, T. & TANGKRISANAVINONT, V. (1980). Acute toxicity of capsaicin in several animal species. *Toxicon*, 18, 215-20.

GONZALEZ, A., JIMENEZ, A., VAZQUEZ, D., DAVIES, J.E. & SCHINDLER, D. (1978). Studies on the mode of action of hygromycin B, an inhibitor of translocation in eukaryotes. *Biochim Biophys Acta*, 521, 459-69.

GRYNKIEWICZ, G., POENIE, M. & TSIEN, R.Y. (1985). A new generation of Ca2+ indicators with greatly improved fluorescence properties. *J Biol Chem*, 260, 3440-50.

GUNTHORPE, M.J., BENHAM, C.D., RANDALL, A. & DAVIS, J.B. (2002). The diversity in the vanilloid (TRPV) receptor family of ion channels. *Trends Pharmacol Sci*, 23, 183-91.

GUNTHORPE, M.J., HARRIES, M.H., PRINJHA, R.K., DAVIS, J.B. & RANDALL, A. (2000). Voltage- and time-dependent properties of the recombinant rat vanilloid receptor (rVR1). *J Physiol*, 525 Pt 3, 747-59.

GUTMAN, G.A., CHANDY, K.G., ADELMAN, J.P., AIYAR, J., BAYLISS, D.A., CLAPHAM, D.E., COVARRIUBIAS, M., DESIR, G.V., FURUICHI, K., GANETZKY, B., GARCIA, M.L., GRISSMER, S., JAN, L.Y., KARSCHIN, A., KIM, D., KUPERSCHMIDT, S., KURACHI, Y., LAZDUNSKI, M., LESAGE, F., LESTER, H.A., MCKINNON, D., NICHOLS, C.G., O'KELLY, I., ROBBINS, J., ROBERTSON, G.A., RUDY, B., SANGUINETTI, M., SEINO, S., STUEHMER, W., TAMKUN, M.M., VANDENBERG, C.A., WEI, A., WULFF, H. & WYMORE, R.S. (2003). International Union of Pharmacology. XLI. Compendium of voltage-gated ion channels: potassium channels. *Pharmacol Rev*, 55, 583-6.

HABELT, C., KESSLER, F., DISTLER, C., KRESS, M. & REEH, P.W. (2000). Interactions of inflammatory mediators and low pH not influenced by capsazepine in rat cutaneous nociceptors. *Neuroreport*, 11, 973-6.

HANDWERKER, H. & REEH, P.W. (1991). Pain and inflammation. In *Proceedings of the 6th World Congress on Pain*. ed Bond, M.R., Charlton, J.E. & Woolf, C.J. pp. 59-70. Amsterdam: Elsevier.

HARPER, A.A. & LAWSON, S.N. (1985). Conduction velocity is related to morphological cell type in rat dorsal root ganglion neurones. *J Physiol*, 359, 31-46.

HAWTHORN, J. & REDMOND, K. (1999). Pain: causes and management. London: Blackwell Science.

HAYES, P., MEADOWS, H.J., GUNTHORPE, M.J., HARRIES, M.H., DUCKWORTH, D.M., CAIRNS, W., HARRISON, D.C., CLARKE, C.E., ELLINGTON, K., PRINJHA, R.K., BARTON, A.J., MEDHURST, A.D., SMITH, G.D., TOPP, S., MURDOCK, P., SANGER, G.J., TERRETT, J., JENKINS, O., BENHAM, C.D., RANDALL, A.D., GLOGER, I.S. & DAVIS, J.B. (2000). Cloning and functional expression of a human orthologue of rat vanilloid receptor-1. *Pain*, 88, 205-15.

HERGENHAHN, M., ADOLF, M. & HECKER, E. (1975). Resiniferatoxin and other esters of novel polyfunctional diterpenes from Euphorbia resinifera and unispina. *Tetrahedron Lett*, 19, 1595-1598.

HOFMANN, T., OBUKHOV, A.G., SCHAEFER, M., HARTENECK, C., GUDERMANN, T. & SCHULTZ, G. (1999). Direct activation of human TRPC6 and TRPC3 channels by diacylglycerol. *Nature*, 397, 259-63.

HOLZER, P. (1991). Capsaicin: cellular targets, mechanisms of action, and selectivity for thin sensory neurons. *Pharmacol Rev*, 43, 143-201.

HORI, T. (1984). Capsaicin and central control of thermoregulation. *Pharmacol Ther*, 26, 389-416.

HUANG, S.M., BISOGNO, T., TREVISANI, M., AL-HAYANI, A., DE PETROCELLIS, L., FEZZA, F., TOGNETTO, M., PETROS, T.J., KREY, J.F., CHU, C.J., MILLER, J.D., DAVIES, S.N., GEPPETTI, P., WALKER, J.M. & DI MARZO, V. (2002). An endogenous capsaicin-like substance with high potency at recombinant and native vanilloid VR1 receptors. *Proc Natl Acad Sci USA*, 99, 8400-5.

HWANG, S.W., CHO, H., KWAK, J., LEE, S.Y., KANG, C.J., JUNG, J., CHO, S., MIN, K.H., SUH, Y.G., KIM, D. & OH, U. (2000). Direct activation of capsaicin receptors by products of lipoxygenases: endogenous capsaicin-like substances. *Proc Natl Acad Sci USA*, 97, 6155-60.

JANCSO, G., KIRALY, E. & JANCSO-GABOR, A. (1977). Pharmacologically induced selective degeneration of chemosensitive primary sensory neurones. *Nature*, 270, 741-3.

JANCSO, G., KIRALY, E., JOO, F., SUCH, G. & NAGY, A. (1985). Selective degeneration by capsaicin of a subpopulation of primary sensory neurons in the adult rat. *Neurosci Lett*, 59, 209-14.

JANCSO, N., JANCSO-GABOR, A. & SZOLCSANYI, J. (1967). Direct evidence for neurogenic inflammation and its prevention by denervation and by pretreatment with capsaicin. *Br J Pharmacol*, 31, 138-51.

JANCSO, N., JANCSO-GABOR, A. & SZOLCSANYI, J. (1968). The role of sensory nerve endings in neurogenic inflammation induced in human skin and in the eye and paw of the rat. *Br J Pharmacol*, 33, 32-41.

JANCSO-GABOR, A., SZOLCSANYI, J. & JANCSO, N. (1970). Stimulation and desensitization of the hypothalamic heat-sensitive structures by capsaicin in rats. *J Physiol*, 208, 449-59.

JANUSZ, J.M., BUCKWALTER, B.L., YOUNG, P.A., LAHANN, T.R., FARMER, R.W., KASTING, G.B., LOOMANS, M.E., KERCKAERT, G.A., MADDIN, C.S., BERMAN, E.F. & ET AL. (1993). Vanilloids. 1. Analogs of capsaicin with antinociceptive and antiinflammatory activity. *J Med Chem*, 36, 2595-604.

JERMAN, J.C., BROUGH, S.J., PRINJHA, R., HARRIES, M.H., DAVIS, J.B. & SMART, D. (2000). Characterization using FLIPR of rat vanilloid receptor (rVR1) pharmacology. *Br J Pharmacol*, 130, 916-22.

JERMAN, J.C., GRAY, J., BROUGH, S.J., OOI, L., OWEN, D., DAVIS, J.B. & SMART, D. (2002). Comparison of effects of anandamide at recombinant and endogenous rat vanilloid receptors. *Br J Anaesth*, 89, 882-7.

JORDT, S.E., BAUTISTA, D.M., CHUANG, H.H., MCKEMY, D.D., ZYGMUNT, P.M., HOGESTATT, E.D., MENG, I.D. & JULIUS, D. (2004). Mustard oils and cannabinoids excite sensory nerve fibres through the TRP channel ANKTM1. *Nature*, 427, 260-5.

JORDT, S.E. & JULIUS, D. (2002). Molecular basis for species-specific sensitivity to "hot" chili peppers. *Cell*, 108, 421-30.

JORDT, S.E., MCKEMY, D.D. & JULIUS, D. (2003). Lessons from peppers and peppermint: the molecular logic of thermosensation. *Curr Opin Neurobiol*, 13, 487-92.

JORDT, S.E., TOMINAGA, M. & JULIUS, D. (2000). Acid potentiation of the capsaicin receptor determined by a key extracellular site. *Proc Natl Acad Sci USA*, 97, 8134-9.

JUNG, J., HWANG, S.W., KWAK, J., LEE, S.Y., KANG, C.J., KIM, W.B., KIM, D. & OH, U. (1999). Capsaicin binds to the intracellular domain of the capsaicin-activated ion channel. *J Neurosci*, 19, 529-38.

KANDEL, E.R. (1991). Nerve cells and behavior. In *Principles of Neural Science*. eds Kandel, E.R., Schwartz, J.H. & Jessel, T.M. pp. 18-32. London: Prentice Hall International Limited.

KEARN, C.S., GREENBERG, M.J., DICAMELLI, R., KURZAWA, K. & HILLARD, C.J. (1999). Relationships between ligand affinities for the cerebellar cannabinoid receptor CB1 and the induction of GDP/GTP exchange. *J Neurochem*, 72, 2379-87.

KEDEI, N., SZABO, T., LILE, J.D., TREANOR, J.J., OLAH, Z., IADAROLA, M.J. & BLUMBERG, P.M. (2001). Analysis of the native quaternary structure of vanilloid receptor 1. *J Biol Chem*, 276, 28613-9.

KELLENBERGER, S. & SCHILD, L. (2002). Epithelial sodium channel/degenerin family of ion channels: a variety of functions for a shared structure. *Physiol Rev*, 82, 735-67.

KIRSCHSTEIN, T., GREFFRATH, W., BUSSELBERG, D. & TREEDE, R.D. (1999). Inhibition of rapid heat responses in nociceptive primary sensory neurons of rats by vanilloid receptor antagonists. *J Neurophysiol*, 82, 2853-60.

KLEMENT, W. & ARNDT, J.O. (1992). The role of nociceptors of cutaneous veins in the mediation of cold pain in man. *J Physiol*, 449, 73-83.

KRESS, M. & ZEILHOFER, H.U. (1999). Capsaicin, protons and heat: new excitement about nociceptors. *Trends Pharmacol Sci*, 20, 112-8.

LAMBERT, D.G., WHITHAM, E.M., BAIRD, J.G. & NAHORSKI, S.R. (1990). Different mechanisms of Ca2+ entry induced by depolarization and muscarinic receptor stimulation in SH-SY5Y human neuroblastoma cells. *Brain Res Mol Brain Res*, 8, 263-6.

LAMOTTE, R.H. & CAMPBELL, J.N. (1978). Comparison of responses of warm and nociceptive C-fiber afferents in monkey with human judgments of thermal pain. *J Neurophysiol*, 41, 509-28.

LAMOTTE, R.H. & THALHAMMER, J.G. (1982). Response properties of high-threshold cutaneous cold receptors in the primate. *Brain Res*, 244, 279-87.

LAZARENO, S. & BIRDSALL, N.J. (1993). Estimation of competitive antagonist affinity from functional inhibition curves using the Gaddum, Schild and Cheng-Prusoff equations. *Br J Pharmacol*, 109, 1110-9.

LEVINE, J. & TAIWO, Y. (1994). Inflammatory pain. In *Textbook of pain*. eds Wall, P.D. & Melzack, R. pp. 45-56. Edinburgh: Churchill Livingstone.

LI, C., PEOPLES, R.W. & WEIGHT, F.F. (1997). Enhancement of ATP-activated current by protons in dorsal root ganglion neurons. *Pflugers Arch*, 433, 446-54.

LINGUEGLIA, E., DE WEILLE, J.R., BASSILANA, F., HEURTEAUX, C., SAKAI, H., WALDMANN, R. & LAZDUNSKI, M. (1997). A modulatory subunit of acid sensing ion channels in brain and dorsal root ganglion cells. *J Biol Chem*, 272, 29778-83.

LIU, L. & SIMON, S.A. (1997). Capsazepine, a vanilloid receptor antagonist, inhibits nicotinic acetylcholine receptors in rat trigeminal ganglia. *Neurosci Lett*, 228, 29-32.

LIU, L. & SIMON, S.A. (1998). The influence of removing extracellular Ca2+ in the desensitization responses to capsaicin, zingerone and olvanil in rat trigeminal ganglion neurons. *Brain Res*, 809, 246-52.

LLINAS, R., SUGIMORI, M. & SILVER, R.B. (1992). Microdomains of high calcium concentration in a presynaptic terminal. *Science*, 256, 677-9.

LLOYD, D.P.C. (1943). Neuron patterns controlling transmission of ipsilateral hindlimb reflexes in cat. *J Neurophysiol*, 6, 293-315.

LOU, Y.P. & LUNDBERG, J.M. (1992). Inhibition of low pH evoked activation of airway sensory nerves by capsazepine, a novel capsaicin-receptor antagonist. *Biochem Biophys Res Commun*, 189, 537-44.

LOW, P.A., OPFER-GEHRKING, T.L., DYCK, P.J., LITCHY, W.J. & O'BRIEN, P.C. (1995). Double-blind, placebo-controlled study of the application of capsaicin cream in chronic distal painful polyneuropathy. *Pain*, 62, 163-8.

LOWRY, O.H., NIRA, J., ROSENBROUGH, A., FARR, L. & RANDALL, R.J. (1951). Protein measurements with the Folin phenol reagent. *J Biol Chem*, 193, 265-275.

MACLENNAN, S.J., REYNEN, P.H., KWAN, J. & BONHAUS, D.W. (1998). Evidence for inverse agonism of SR141716A at human recombinant cannabinoid CB1 and CB2 receptors. *Br J Pharmacol*, 124, 619-22.

MAIN, C.J. & SPANSWICK, C.C. (2000). *Pain management: an interdisciplinary approach*. London: Churchill Livingstone.

MASON, L., MOORE, R.A., DERRY, S., EDWARDS, J.E. & MCQUAY, H.J. (2004). Systematic review of topical capsaicin for the treatment of chronic pain. *BMJ*, 328, 991.

MCINTYRE, P., MCLATCHIE, L.M., CHAMBERS, A., PHILLIPS, E., CLARKE, M., SAVIDGE, J., TOMS, C., PEACOCK, M., SHAH, K., WINTER, J., WEERASAKERA, N., WEBB, M., RANG, H.P., BEVAN, S. & JAMES, I.F. (2001). Pharmacological differences between the human and rat vanilloid receptor 1 (VR1). *Br J Pharmacol*, 132, 1084-94.

MCKEMY, D.D. (2005). How cold is it? TRPM8 and TRPA1 in the molecular logic of cold sensation. *Mol Pain*, 1, 16.

MELCK, D., BISOGNO, T., DE PETROCELLIS, L., CHUANG, H., JULIUS, D., BIFULCO, M. & DI MARZO, V. (1999). Unsaturated long-chain N-acyl-vanillyl-amides (N-AVAMs): vanilloid receptor ligands that inhibit anandamide-facilitated transport and bind to CB1 cannabinoid receptors. *Biochem Biophys Res Commun*, 262, 275-84.

MELZACK, R. & WALL, P.D. (1965). Pain mechanisms: a new theory. *Science*, 150, 971-9.

MERSKEY, H. (1986). Classification of chronic pain: description of chronic pain syndromes and definition of pain terms. *Pain*, S1-S225.

MERSKEY, H. & BOGDUK, N. (1994). *Classification of Chronic Pain Syndromes and Definitions of Pain Terms*. Seattle, WA: IASP Press.

MEYER, R.A., CAMPBELL, J.N. & RAJA, S.N. (1994). Peripheral neural mechanisms of nociception. In *Textbook of Pain*. eds Wall, P.D. & Melzack, R. pp. 13-44. Edinburgh: Churchill Livingstone.

MINKE, B. & COOK, B. (2002). TRP channel proteins and signal transduction. *Physiol Rev*, 82, 429-72.

MONTELL, C., BIRNBAUMER, L. & FLOCKERZI, V. (2002). The TRP channels, a remarkably functional family. *Cell*, 108, 595-8.

MURPHY, N.P., BALL, S.G. & VAUGHAN, P.F. (1991). Potassium- and carbachol-evoked release of [3H]noradrenaline from human neuroblastoma cells, SH-SY5Y. *J Neurochem*, 56, 1810-5.

NAGY, I. & RANG, H. (1999a). Noxious heat activates all capsaicin-sensitive and also a sub-population of capsaicin-insensitive dorsal root ganglion neurons. *Neuroscience*, 88, 995-7.

NAGY, I. & RANG, H.P. (1999b). Similarities and differences between the responses of rat sensory neurons to noxious heat and capsaicin. *J Neurosci*, 19, 10647-55.

NAGY, J.I., IVERSEN, L.L., GOEDERT, M., CHAPMAN, D. & HUNT, S.P. (1983). Dose-dependent effects of capsaicin on primary sensory neurons in the neonatal rat. *J Neurosci*, 3, 399-406.

NEER, E.J. (1995). Heterotrimeric G proteins: organizers of transmembrane signals. *Cell*, 80, 249-57.

NELSON, E.K. (1919). The constitution of capsaicin - the pungent principle of capsicum. *J Am Chem Soc*, 41, 1115-1117.

NESS, T.J. & GEBHART, G.F. (1990). Visceral pain: a review of experimental studies. *Pain*, 41, 167-234.

NILIUS, B. & VOETS, T. (2005). TRP channels: a TR(I)P through a world of multifunctional cation channels. *Pflugers Arch*.

NILIUS, B., VRIENS, J., PRENEN, J., DROOGMANS, G. & VOETS, T. (2004). TRPV4 calcium entry channel: a paradigm for gating diversity. *Am J Physiol Cell Physiol*, 286, C195-205.

PEIER, A.M., MOQRICH, A., HERGARDEN, A.C., REEVE, A.J., ANDERSSON, D.A., STORY, G.M., EARLEY, T.J., DRAGONI, I., MCINTYRE, P., BEVAN, S. & PATAPOUTIAN, A. (2002). A TRP channel that senses cold stimuli and menthol. *Cell*, 108, 705-15.

PERTWEE, R.G. (2001). Cannabinoid receptors and pain. *Prog Neurobiol*, 63, 569-611.

PIOMELLI, D. (2003). The molecular logic of endocannabinoid signalling. *Nat Rev Neurosci*, 4, 873-84.

PREMKUMAR, L.S. & AHERN, G.P. (2000). Induction of vanilloid receptor channel activity by protein kinase C. *Nature*, 408, 985-90.

RAJA, S.N., MEYER, R.A., RINGKAMP, M. & CAMPBELL, J.N. (1999). Peripheral neural mechanisms of nociception. In *Textbook of Pain*. eds Wall, P.D. & Melzack, R. pp. 11-57. Edinburgh: Churchill Livingstone.

RALEVIC, V., KENDALL, D.A., JERMAN, J.C., MIDDLEMISS, D.N. & SMART, D. (2001). Cannabinoid activation of recombinant and endogenous vanilloid receptors. *Eur J Pharmacol*, 424, 211-9.

RANG, H., DALE, M.M., RITTER, J.M. & MOORE, P.K. (2003). *Pharmacology*. Edinburgh: Churchill Livingstone.

RANG, H.P., BEVAN, S. & DRAY, A. (1991). Chemical activation of nociceptive peripheral neurones. *Br Med Bull*, 47, 534-48.

RANG, H.P., DALE, M.M. & RITTER, J.M. (2000). *Pharmacology*. Edinburgh: Churchill Livingstone.

REICHLING, D.B. & LEVINE, J.D. (1997). Heat transduction in rat sensory neurons by calcium-dependent activation of a cation channel. *Proc Natl Acad Sci USA*, 94, 7006-11.

REYNOLDS, D.V. (1969). Surgery in the rat during electrical analgesia induced by focal brain stimulation. *Science*, 164, 444-5.

ROBERTS, J.C., DAVIS, J.B. & BENHAM, C.D. (2004). [3H]Resiniferatoxin autoradiography in the CNS of wild-type and TRPV1 null mice defines TRPV1 (VR-1) protein distribution. *Brain Res*, 995, 176-83.

ROBITAILLE, R., ADLER, E.M. & CHARLTON, M.P. (1990). Strategic location of calcium channels at transmitter release sites of frog neuromuscular synapses. *Neuron*, 5, 773-9.

ROSS, R.A., COUTTS, A.A., MCFARLANE, S.M., ANAVI-GOFFER, S., IRVING, A.J., PERTWEE, R.G., MACEWAN, D.J. & SCOTT, R.H. (2001). Actions of cannabinoid receptor ligands on rat cultured sensory neurones: implications for antinociception. *Neuropharmacology*, 40, 221-32.

SANCHEZ, J.F., KRAUSE, J.E. & CORTRIGHT, D.N. (2001). The distribution and regulation of vanilloid receptor VR1 and VR1 5' splice variant RNA expression in rat. *Neuroscience*, 107, 373-81.

SATOH, H., LOU, Y.P. & LUNDBERG, J.M. (1993). Inhibitory effects of capsazepine and SR 48968 on citric acid-induced bronchoconstriction in guinea-pigs. *Eur J Pharmacol*, 236, 367-72.

SAVIDGE, J., DAVIS, C., SHAH, K., COLLEY, S., PHILLIPS, E., RANASINGHE, S., WINTER, J., KOTSONIS, P., RANG, H. & MCINTYRE, P. (2002). Cloning and functional characterization of the guinea pig vanilloid receptor 1. *Neuropharmacology*, 43, 450-6.

SCADDING, J.W. (1980). The permanent anatomical effects of neonatal capsaicin on somatosensory nerves. *J Anat*, 131, 471-82.

SCHROEDER, K.S. & NEAGLE, B.D. (1996). FLIPR: A New Instrument for Accurate, High Throughput Optical Screening. *J Biomol Screen*, 1, 75-80.

SCHUMACHER, M.A., MOFF, I., SUDANAGUNTA, S.P. & LEVINE, J.D. (2000). Molecular cloning of an N-terminal splice variant of the capsaicin receptor. Loss of N-terminal domain suggests functional divergence among capsaicin receptor subtypes. *J Biol Chem*, 275, 2756-62.

SHIN, J., CHO, H., HWANG, S.W., JUNG, J., SHIN, C.Y., LEE, S.Y., KIM, S.H., LEE, M.G., CHOI, Y.H., KIM, J., HABER, N.A., REICHLING, D.B., KHASAR, S., LEVINE, J.D. & OH, U. (2002). Bradykinin-12-lipoxygenase-VR1 signaling pathway for inflammatory hyperalgesia. *Proc Natl Acad Sci USA*, 99, 10150-5.

SIMONE, D.A. & KAJANDER, K.C. (1997). Responses of cutaneous A-fiber nociceptors to noxious cold. *J Neurophysiol*, 77, 2049-60.

SIMPSON, A.W.M. (1999). Fluorescent measurement of [Ca2+]c: basic practical considerations. In *Calcium signalling protocols*. ed Lambert, D.G. pp. 3-30. USA: Totowa, NJ: Humana Press.

SMART, D., GUNTHORPE, M.J., JERMAN, J.C., NASIR, S., GRAY, J., MUIR, A.I., CHAMBERS, J.K., RANDALL, A.D. & DAVIS, J.B. (2000a). The endogenous lipid

anandamide is a full agonist at the human vanilloid receptor (hVR1). *Br J Pharmacol*, 129, 227-30.

SMART, D. & JERMAN, J.C. (2000b). Anandamide: an endogenous activator of the vanilloid receptor. *Trends Pharmacol Sci*, 21, 134.

SMART, D., JERMAN, J.C., GUNTHORPE, M.J., BROUGH, S.J., RANSON, J., CAIRNS, W., HAYES, P.D., RANDALL, A.D. & DAVIS, J.B. (2001). Characterisation using FLIPR of human vanilloid VR1 receptor pharmacology. *Eur J Pharmacol*, 417, 51-8.

SMITH, G.D., GUNTHORPE, M.J., KELSELL, R.E., HAYES, P.D., REILLY, P., FACER, P., WRIGHT, J.E., JERMAN, J.C., WALHIN, J.P., OOI, L., EGERTON, J., CHARLES, K.J., SMART, D., RANDALL, A.D., ANAND, P. & DAVIS, J.B. (2002). TRPV3 is a temperature-sensitive vanilloid receptor-like protein. *Nature*, 418, 186-90.

SNIDER, W.D. & MCMAHON, S.B. (1998). Tackling pain at the source: new ideas about nociceptors. *Neuron*, 20, 629-32.

SPRAGUE, J., HARRISON, C., ROWBOTHAM, D.J., SMART, D. & LAMBERT, D.G. (2001). Temperature-dependent activation of recombinant rat vanilloid VR1 receptors expressed in HEK293 cells by capsaicin and anandamide. *Eur J Pharmacol*, 423, 121-5.

STEPHENSON, R.P. (1956). A modification of receptor theory. *Br J Pharmacol*, 11, 379-93.

STERNER, O. & SZALLASI, A. (1999). Novel natural vanilloid receptor agonists: new therapeutic targets for drug development. *Trends Pharmacol Sci*, 20, 459-65.

STUCKY, C.L., GOLD, M.S. & ZHANG, X. (2001). Mechanisms of pain. *Proc Natl Acad Sci USA*, 98, 11845-6.

SUDHOF, T.C. (2004). The synaptic vesicle cycle. *Annu Rev Neurosci*, 27, 509-47.

SUGIURA, T., TOMINAGA, M., KATSUYA, H. & MIZUMURA, K. (2002). Bradykinin lowers the threshold temperature for heat activation of vanilloid receptor 1. *J Neurophysiol*, 88, 544-8.

SULLIVAN, E., TUCKER, E.M. & DALE, I. (1999). Measurement of [Ca2+] using the fluorimetric imaging plate reader (FLIPR). In *Calcium Signalling Protocols*. ed Lambert, D.G. pp. 125-133. USA: Totowa, NJ: Humana Press.

SZALLASI, A., BIRO, T., SZABO, T., MODARRES, S., PETERSEN, M., KLUSCH, A., BLUMBERG, P.M., KRAUSE, J.E. & STERNER, O. (1999a). A non-pungent triprenyl phenol of fungal origin, scutigeral, stimulates rat dorsal root ganglion neurons via interaction at vanilloid receptors. *Br J Pharmacol*, 126, 1351-8.

SZALLASI, A. & BLUMBERG, P.M. (1990). Specific binding of resiniferatoxin, an ultrapotent capsaicin analog, by dorsal root ganglion membranes. *Brain Res*, 524, 106-11.

SZALLASI, A. & BLUMBERG, P.M. (1999b). Vanilloid (Capsaicin) receptors and mechanisms. *Pharmacol Rev*, 51, 159-212.

SZALLASI, A. & BLUMBERG, P.M. (1996a). Vanilloid receptors: new insights enhance potential as a therapeutic target. *Pain*, 68, 195-208.

SZALLASI, A. & GOSO, C. (1994). Characterization by [3H]resiniferatoxin binding of a human vanilloid (capsaicin) receptor in post-mortem spinal cord. *Neurosci Lett*, 165, 101-4.

SZALLASI, A., JONASSOHN, M., ACS, G., BIRO, T., ACS, P., BLUMBERG, P.M. & STERNER, O. (1996b). The stimulation of capsaicin-sensitive neurones in a vanilloid receptor- mediated fashion by pungent terpenoids possessing an unsaturated 1,4- dialdehyde moiety. *Br J Pharmacol*, 119, 283-90.

SZOLCSANYI, J. (2000). Anandamide and the question of its functional role for activation of capsaicin receptors. *Trends Pharmacol Sci*, 21, 203-4.

SZOLCSANYI, J. (1977). A pharmacological approach to elucidation of the role of different nerve fibres and receptor endings in mediation of pain. *J Physiol (Paris)*, 73, 251-9.

TAKAHASHI, A., CAMACHO, P., LECHLEITER, J.D. & HERMAN, B. (1999). Measurement of intracellular calcium. *Physiol Rev*, 79, 1089-125.

THE CAPSAICIN STUDY GROUP (1991). Treatment of painful diabetic neuropathy with topical capsaicin. A multicenter, double-blind, vehicle-controlled study. The Capsaicin Study Group. *Arch Intern Med*, 151, 2225-9.

TOMINAGA, M., CATERINA, M.J., MALMBERG, A.B., ROSEN, T.A., GILBERT, H., SKINNER, K., RAUMANN, B.E., BASBAUM, A.I. & JULIUS, D. (1998). The cloned capsaicin receptor integrates multiple pain-producing stimuli. *Neuron*, 21, 531-43.

TOTH, A., KEDEI, N., WANG, Y. & BLUMBERG, P.M. (2003). Arachidonyl dopamine as a ligand for the vanilloid receptor VR1 of the rat. *Life Sci*, 73, 487-98.

TRATSK, K.S., CAMPOS, M.M., VAZ, Z.R., FILHO, V.C., SCHLEMPER, V., YUNES, R.A. & CALIXTO, J.B. (1997). Anti-allergic effects and oedema inhibition caused by the extract of Drymis winteri. *Inflamm Res*, 46, 509-14.

TREVISANI, M., SMART, D., GUNTHORPE, M.J., TOGNETTO, M., BARBIERI, M., CAMPI, B., AMADESI, S., GRAY, J., JERMAN, J.C., BROUGH, S.J., OWEN, D., SMITH, G.D., RANDALL, A.D., HARRISON, S., BIANCHI, A., DAVIS, J.B. & GEPPETTI, P. (2002). Ethanol elicits and potentiates nociceptor responses via the vanilloid receptor-1. *Nat Neurosci*, 5, 546-51.

VALENZANO, K.J., GRANT, E.R., WU, G., HACHICHA, M., SCHMID, L., TAFESSE, L., SUN, Q., ROTSHTEYN, Y., FRANCIS, J., LIMBERIS, J., MALIK, S., WHITTEMORE, E.R. & HODGES, D. (2003). N-(4-tertiarybutylphenyl)-4-(3-chloropyridin-2-yl)tetrahydropyrazine -1(2H)-carbox-amide (BCTC), a novel, orally effective vanilloid receptor 1 antagonist with analgesic properties: I. in vitro characterization and pharmacokinetic properties. *J Pharmacol Exp Ther*, 306, 377-86.

VAN DER STELT, M. & DI MARZO, V. (2004). Endovanilloids. Putative endogenous ligands of transient receptor potential vanilloid 1 channels. *Eur J Biochem*, 271, 1827-34.

VAUGHAN, P.F., PEERS, C. & WALKER, J.H. (1995). The use of the human neuroblastoma SH-SY5Y to study the effect of second messengers on noradrenaline release. *Gen Pharmacol*, 26, 1191-201.

VAUQUELIN, G., VAN LIEFDE, I., BIRZBIER, B.B. & VANDERHEYDEN, P.M. (2002). New insights in insurmountable antagonism. *Fundam Clin Pharmacol*, 16, 263-72.

VYKLICKY, L., LYFENKO, A., KUFFLER, D.P. & VLACHOVA, V. (2003). Vanilloid receptor TRPV1 is not activated by vanilloids applied intracellularly. *Neuroreport*, 14, 1061-5.

WAHL, P., FOGED, C., TULLIN, S. & THOMSEN, C. (2001). Iodo-resiniferatoxin, a new potent vanilloid receptor antagonist. *Mol Pharmacol*, 59, 9-15.

WALDMANN, R., BASSILANA, F., DE WEILLE, J., CHAMPIGNY, G., HEURTEAUX, C. & LAZDUNSKI, M. (1997a). Molecular cloning of a non-inactivating proton-gated Na+ channel specific for sensory neurons. *J Biol Chem*, 272, 20975-8.

WALDMANN, R., CHAMPIGNY, G., BASSILANA, F., HEURTEAUX, C. & LAZDUNSKI, M. (1997b). A proton-gated cation channel involved in acid-sensing. *Nature*, 386, 173-7.

WALKER, K.M., URBAN, L., MEDHURST, S.J., PATEL, S., PANESAR, M., FOX, A.J. & MCINTYRE, P. (2003). The VR1 antagonist capsazepine reverses mechanical hyperalgesia in models of inflammatory and neuropathic pain. *Journal of Pharmacology and Experimental Therapeutics*, 304, 56-62.

WALKER, R.G., WILLINGHAM, A.T. & ZUKER, C.S. (2000). A Drosophila mechanosensory transduction channel. *Science*, 287, 2229-34.

WALPOLE, C.S., BEVAN, S., BOVERMANN, G., BOELSTERLI, J.J., BRECKENRIDGE, R., DAVIES, J.W., HUGHES, G.A., JAMES, I., OBERER, L., WINTER, J. & WRIGGLESWORTH, R. (1994). The discovery of capsazepine, the first competitive antagonist of the sensory neuron excitants capsaicin and resiniferatoxin. *J Med Chem*, 37, 1942-54.

WANG, Y., SZABO, T., WELTER, J.D., TOTH, A., TRAN, R., LEE, J., KANG, S.U., SUH, Y.G. & BLUMBERG, P.M. (2002). High affinity antagonists of the vanilloid receptor. *Mol Pharmacol*, 62, 947-56.

WARDLE, K.A., RANSON, J. & SANGER, G.J. (1997). Pharmacological characterization of the vanilloid receptor in the rat dorsal spinal cord. *Br J Pharmacol*, 121, 1012-6.

WATSON, C.P., TYLER, K.L., BICKERS, D.R., MILLIKAN, L.E., SMITH, S. & COLEMAN, E. (1993). A randomized vehicle-controlled trial of topical capsaicin in the treatment of postherpetic neuralgia. *Clin Ther*, 15, 510-26.

WEISENBERG, M. (1994). Cognitive aspects of pain. In *Textbook of pain*. eds Wall, P.D. & Melzack, R. pp. 275-289. Edinburgh: Churchill Livingstone.

WINTER, J., BEVAN, S. & CAMPBELL, E.A. (1995). Capsaicin and pain mechanisms. *Br J Anaesth*, 75, 157-68.

WOOLF, C.J. (1991). Generation of acute pain: central mechanisms. *Br Med Bull*, 47, 523-33.

XU, H., RAMSEY, I.S., KOTECHA, S.A., MORAN, M.M., CHONG, J.A., LAWSON, D., GE, P., LILLY, J., SILOS-SANTIAGO, I., XIE, Y., DISTEFANO, P.S., CURTIS, R. & CLAPHAM, D.E. (2002). TRPV3 is a calcium-permeable temperature-sensitive cation channel. *Nature*, 418, 181-6.

ZYGMUNT, P.M., CHUANG, H., MOVAHED, P., JULIUS, D. & HOGESTATT, E.D. (2000). The anandamide transport inhibitor AM404 activates vanilloid receptors. *Eur J Pharmacol*, 396, 39-42.

ZYGMUNT, P.M., PETERSSON, J., ANDERSSON, D.A., CHUANG, H., SORGARD, M., DI MARZO, V., JULIUS, D. & HOGESTATT, E.D. (1999). Vanilloid receptors on sensory nerves mediate the vasodilator action of anandamide. *Nature*, 400, 452-7.

## Website links

http://www.algorx.com
http://www.neurogesx.com
http://www.bch.bris.ac.uk/staff/pfdg/teaching/genes.htm